ABSTRACT

THERMOCHEMISTRY AND KINETICS IN PYROLYSIS AND OXIDATION REACTIONS OF OXYGENATED CHLOROCARBONS, NEOPENTANE AND ORTHO-XYLENE

by
Hongyan Sun

Thermochemical properties of chlorinated alcohols, chlorinated hydroperoxides and corresponding alkoxy, hydroxy alkyl radicals, peroxy and hydroperoxy alkyl radicals are determined by *ab initio* and density functional calculations for modeling and optimization of complex chemical processes for combustion or incineration of chlorinated hydrocarbons. The entropy and heat capacities from vibrational, translational, and external rotational contributions are calculated by statistical mechanics, and the hindered rotational contributions to S^o_{298} and $C_p(T)$'s are calculated by using direct integration over energy levels of the internal rotational potentials. The values of ΔH^o_{f298} are determined using isodesmic reactions with group balance. Groups for use in Benson type additivity estimations are determined for the carbon bonded to oxygen and chlorine(s). Hydrogen bond increment groups for the chloroalkoxy, hydroxy chloroalkyl radicals and interaction terms for peroxy group with chlorine(s) are developed for group additivity approach.

The reactions of alkyl radical with oxygen are important rate controlling processes in the low and intermediate temperature chemistry of hydrocarbon oxidation, especially the chemistry which occurs prior to ignition in internal combustion engines and in cool flames. Thermochemical properties for reactants, intermediates, products and transition states in neopentyl radical + O_2 reaction system are analyzed with *ab initio* and density functional calculations to evaluate reaction paths and oxidation kinetics. Rate

constants to products and stabilized adducts of the chemically activated neopentyl-peroxy are calculated as function of pressure and temperature using Quantum Rice-Ramsperger-Kassel analysis for $k(E)$ and a master equation analysis for pressure fall-off. An elementary reaction mechanism is constructed to model experimental OH and HO_2 formation profiles.

Aromatic compounds are an important component of higher-octane automotive fuels and consequently they are present in emissions from incomplete combustion and other evaporation from solvents and fuels handling and storage. Oxidation reactions of ortho-xylene are studied to identify the important reaction channels of this class of high-octane aromatics. Elementary reactions, energy well depths, and absolute rate constants of benzylic radical derived from ortho-xylene, 2-methylbenzyl radical with O_2, are determined with computational chemistry at density functional levels.

THERMOCHEMISTRY AND KINETICS IN PYROLYSIS AND OXIDATION REACTIONS OF OXYGENATED CHLOROCARBONS, NEOPENTANE AND ORTHO-XYLENE

by
Hongyan Sun

A Dissertation
Submitted to the Faculty of
New Jersey Institute of Technology
in Partial Fulfillment of the Requirement for the Degree of
Doctor of Philosophy

Department of
Chemistry and Environmental Science

August 2003

THERMOCHEMISTRY AND KINETICS IN PYROLYSIS AND OXIDATION REACTIONS OF OXYGENATED CHLOROCARBONS, NEOPENTANE AND ORTHO-XYLENE

Hongyan Sun

Dr. Joseph W. Bozzelli, Dissertation Advisor   Date
Distinguished Professor of Chemistry, NJIT

Dr. Lev N. Krasnoperov, Committee Member   Date
Professor of Chemistry, NJIT

Dr. Tamara M. Gund, Committee Member   Date
Professor of Chemistry, NJIT

Dr. Sanjay V. Malhotra, Committee Member   Date
Assistant Professor of Chemistry, NJIT

Dr. Edward R. Ritter, Committee Member   Date
Associate Professor of Chemical Engineering, Villanova University

BIOGRAPHICAL SKETCH

Author: Hongyan Sun

Degree: Doctor of Philosophy

Date: August 2003

Undergraduate and Graduate Education:

- Doctor of Philosophy in Chemistry,
  New Jersey Institute of Technology, Newark, NJ, 2003

- Master of Science in Applied Chemistry,
  New Jersey Institute of Technology, Newark, NJ, 2000

- Bachelor of Science in Chemical Engineering,
  Tianjin University, Tianjin, P. R. China, 1987

Major: Chemistry

Journal Publications:

Sun, H.; Bozzelli, J. W. "Thermochemical and Kinetic Analysis on the Reactions of Neopentyl and Hydroperoxy-Neopentyl Radicals with Oxygen: Part I OH Product Formation" Submitted to *J. Phys. Chem. A* 2003.

Sun, H.; Bozzelli, J. W. "Structures, Rotational Barriers, and Thermochemical Properties of β-Chlorinated Ethyl Hydroperoxides" *J. Phys. Chem. A* (2003),107(7), 1018 - 1024.

Sun, H.; Bozzelli, J. W. "Structures, Rotational Barriers, Thermochemical Properties, and Additivity Groups for 2-Propanol, 2-Chloro-2-Propanol and the Corresponding Alkoxy and Hydroxy-Alkyl Radical" *J. Phys. Chem. A* (2002), 106(15), 3947-3956.

Sun, H.; Bozzelli, J. W. "Structures, Intramolecular Rotation Barriers, and Thermochemical Properties: Ethanol, α-Monoethanols, Dichloroethanols, and Corresponding Radicals Derived from H Atom Loss" *J. Phys. Chem. A* (2001), 105(41), 9543-9552

Sun, H.; Bozzelli, J. W. "Structures, Intramolecular Rotation Barriers, and Thermo-chemical Properties of Radicals Derived from H Atom Loss in Mono-, Di-and Trichloromethanol and Parent Chloromethanols" *J. Phys. Chem. A* (2001), 105(18), 4504-4516.

Sun, H.; Chen, C.-J.; Bozzelli, J. W. "Structures, Intramolecular Rotation Barriers, and Thermodynamic Properties (Enthalpies, Entropies and Heat Capacities) of Chlorinated Methyl Hydroperoxides (CH_2ClOOH, $CHCl_2OOH$, and CCl_3OOH)" *J. Phys. Chem. A* (2000), 104(35), 8270-8282.

Sun, H.; Tian, W. "Analysis of Main Impurity in Coupler COY-5," Liaoning Chemical Industry (1997), 26(1), 53-56.

Sun, H.; Ma, Y. "Separation and Identification of 1,3,4-trichloro-2-ethyl-5-nitrobenzene by HPLC," Image Science and Practice (1993), 2, 32-33, 62.

Conference Proceedings and Presentations:

Sun, H.; Bozzelli, J. W. "Kinetics and Thermochemistry for Dissociation of Chloromethanols and Chemical Activation Reactions of OH and Cl With Chloromethyl Radicals" Accepted by *the 226th ACS National Meeting*, Sep 7-11, 2003, New York, NY, USA

Sun, H.; Bozzelli, J. W. "Kinetic Analysis on the Reactions of Neopentyl Radical With Oxygen" *Third Joint Meeting of The U.S. Sections of the Combustion Institute*, March, 16-19, 2003, Kinetics Section, University of Illinois at Chicago, Chicago, Illinois, USA

Sun, H.; Bozzelli, J. W. "Thermochemical Properties, Reaction Pathways and Kinetics of Neopentyl + O_2 Reaction System" *AIChE Annual Meeting*, Nov 3-8, 2002, Detailed Reaction and Reactor Modeling II Session, Indiana Convention Center, Indianapolis, Indiana, USA

Sun, H.; Bozzelli, J. W. "Determination of Thermochemical Parameters on β-Chlorinated Ethyl Hydroperoxides" *AIChE Annual Meeting*, Nov 3-8, 2002, Obtaining Physical and Chemical Properties for Process Design by Computational Chemistry Session, Indiana Convention Center, Indianapolis, Indiana, USA

Sun, H.; Chen, C.-J.; Bozzelli, J. W. "Thermochemical Properties, Reaction Pathways and Kinetic Analysis of Ortho-Xylene Oxidation Reactions" *AIChE Annual Meeting*, Nov 3-8, 2002, Understanding Reactivity Session, Indiana Convention Center, Indianapolis, Indiana, USA

Bozzelli, J. W.; Sun, H. "Thermochemical Properties, Reaction Pathways and Kinetics of Neopentyl + O_2 Reaction System" *17th Internatinal Symposium on Gas Kinetics*, Aug 24-29, 2002, Essen, Germany

Bozzelli, J. W.; Sun, H. "Thermochemical Properties and Internal Rotational Barriers of Chlorinated Alcohols" *17th IUPAC Conference on Chemical Thermodymics*, July 28-Aug 02, 2002, University of Rostock, Postock, Germany

Sun, H.; Bozzelli, J. W. "Structures, Intramolecular Rotation Barriers, and Thermochemical Properties: Ethanol, α-Monoethanols, Dichloroethanols, and Corresponding Radicals Derived from H Atom Loss" *5th International Conference on Chemical Kinetics*, July 16-20, 2001, National Institute of Standards and Technology, Gaithersburg, MD 20899, USA.

Bozzelli, J. W. Sheng, C.; Sun, H. "Comparison of Chemical Activation Association Reactions: Chloromethyl and Methyl Radicals with OH" *16th International Symposiun on Gas Kinetics*, July 23-27, 2000, University of Cambridge, Cambridge, England.

Sheng, C.; Thipse, S.; Sun, H.; Bozzelli, J. W.; Booty, M. R.; Magee, R. S.; Hoecke, D. "A Pilot-Scale Incinerator for Evaluating the Combustion of Co-fired Plastics" *Proc. Int. Conf. Incineration Therm. Treat. Technol.* (1999), 83-88. Publisher: University of California, Irvine, California, USA.

Jung, D; Sun, H.; Chen, C.-J.; Bozzelli, J. W."Thermochemical Properties $\Delta H_f°_{298}$, ΔS_{298}, and $C_p(T)$ of Chloro-Methyl oxychlorides and Chloromethanols: CH_3OX, CH_2ClOX, $CHCl_2OX$ and CCl_3OX (X=H or Cl), Density Functional and Ab Initio Calculations" *32nd Middle Atlantic ACS Regional meeting.* May 17-19, 1999, Fairleigh Dicknsion University, Madison, NJ 07940, USA.

Thipse, S.; Sheng, C., Sun, H.; Bozzelli, J. W.; Booty, M. R.; Magee, R. S. "A Pilot-Scale Incinerator for Evaluating the Combustion of Co-fired Plastics" *First Joint Meeting of the U. S. Sections of the Combustion Institute: Western States, Central States, Eastern States.* March 14-17, 1999, The George Washington University, Washington DC, USA.

To

Dr. Joseph W. Bozzelli

who introduced me to the field of thermochemical kinetics
during my graduate study at New Jersey Institute of Technology

ACKNOWLEDGEMENT

TABLE OF CONTENTS

TABLE OF CONTENTS
(Continued)

Chapter   **Page**

TABLE OF CONTENTS
(Continued)

LIST OF TABLES

LIST OF TABLES
(Continued)

LIST OF FIGURES

CHAPTER 1

THERMOCHEMICAL KINETICS

1.1 Introduction

Detail kinetic models using reaction mechanisms comprised of many elementary chemical reaction steps, based upon fundamental thermochemical and kinetic principles, are presently used and being developed by researchers attempting to optimize or more fully understand a number of chemical complex systems. These systems include combustion, flame inhibition, ignition, atmospheric smog formation, stratospheric ozone depletion, municipal and hazardous wastes incineration, chemical vapor deposition, semiconductor etching, rocket propulsion and other related fields.

One important requirement for modeling and simulation of these systems is accurate thermochemical property data such as enthalpies of formation ($\Delta H_f^o{}_{298}$), entropy ($S^o{}_{298}$), and heat capacities as functions of temperature ($C_p(T)$'s) for reactants, intermediates, final products, and reaction transition states. These data allow determination of equilibrium, and reverse rate constants from the forward rate constant and the equilibrium constant. *Ab initio* and density functional calculations provide an opportunity to accurately calculate these thermochemical properties data which are often difficult or impossible to obtain through experiment.

1.2 Computational Chemistry

Ab initio molecular orbital theory is concerned with predicting the properties of atomic and molecular systems. It is based upon the fundamental laws of quantum mechanics and a variety of mathematical transformation and approximation techniques to solve the fundamental equations, i.e. Schrödinger equation,

$$\hat{H}\Psi = E\Psi$$

Here $\hat{H}$ is the *Hamiltonian*, a differential operator representing the total energy. E is the numerical value of the energy of the state, i.e., the energy relative to a state in which the constituent particles (nuclei and electrons) are infinitely separated and at rest. Ψ is a many-electron wavefunction, and it depends on the Cartesian coordinates of all particles and also on the spin coordinates. The square of the wavefunction, Ψ^2, is the probability distribution of the particles within the molecule.

The many-electron Schrödinger equation cannot be solved exactly, and approximations need to be introduced to provide practical methods. The approximation of separating electronic and nuclear motions is Born-Oppenheimer approximation that is basic to quantum chemistry. The Hartree-Fock (HF) approximation treats electron interactions between individual electrons by interactions between a particular electron and the average field created by all the other electrons. The HF model does not include a full treatment of the effects of instantaneous electron correction, i.e. it does not include the energy contributions arising from electrons interacting with one another. This leads to overestimation of the electron-electron repulsion energy and to too high a total energy.[1] Electron correction accounts for coupling or correction of electron motions, and leads to a lessening of the electron-repulsion energy and also leads to a lowering of the total energy.

The correction energy is defined as the difference between the Hartree-Fock energy and the experimental energy. A variety of theoretical methods, such as density functional, configuration interaction, and Møller-Plesset perturbation have been developed which include some effects of electron correction. Density functional models introduce an "approximate" correction term in an explicit manner, and they reduce computational cost than Hartree-Fork models. Configuration interaction models and Møller-Plesset models extend the flexibility of Hartree-Fock models by mixing ground-state and excited-state wavefunctions. They are significantly more costly than Hartree-Fock models. Traditionally, such methods are referred as post-SCF methods because they add this electron correlation correction to the basic Hartree-Fock model.

The density functional theory (DFT) is based on the fact that the sum of the exchange and correlation energies of a uniform electron gas can be calculated exactly knowing only its electron density. These DFT functionals partition the ground state electronic energy into several components: the kinetic energy, the electron-nuclear interaction, the Coulomb repulsion, and an exchange-correlation term, which accounts for the remainder of the electron-electron interactions.[2] A variety of functionals have been defined, generally distinguished by the way that they treat exchange and correlation components: (1) Local exchange and correlation functions based on the local spin density approximation. (2) Gradient-corrected functionals based on the generalized gradient approximation or Hartree-Fock exchange functional.[3]

Any exchange functional can be combined with any correlation functional. A commonly used gradient-corrected exchange functional is proposed by Becke,[4] and gradient-corrected correlation functional is the Lee, Yang and Parr (LYP) correlation

functional. The combination of the two functionals forms the B-LYP method. The notation B3LYP denotes a DFT calculation with the Becke functional and the Lee-Yang-Parr correlation functional.

Configuration Interaction (CI) models calculate the correlation energy by mixing the ground-state (Hartree-Fock) wavefunction with "excited-state" wavefunctions. The configuration functions in a CI calculation are classified as singly excited, doubly excited, triply excited, …, according to whether 1, 2, 3, … electron are excited from occupied to unoccupied orbitals. It is reported that the first-order correction to the unperturbed (Hartree-Fock) wavefunction of a closed-shell state contains only double excited configuration functions, and the second-order correction to the Hartree-Fock function includes single, double, triple, and quadruple excitations.[1] The singly excited configuration functions are less important than double excitations in affecting the wave function, but single excitations have a significant effect on one-electron properties. Therefore single excitations are usually included in a CI calculation, and the most common type is CISD calculation which includes the singly and doubly excited configuration functions.[5] The CISD(T) method also includes the triple excited functions.

Another correction energy scheme is the second-order Møller-Plesset (MP2) model proposed by Møller-Plesset in 1934. The MP2 is a perturbation treatment of atoms and molecules in which the unperturbed wave function is the Hartree-Fock function. The perturbation is the difference between the true interelectronic repulsions and the Hartree-Fock interelectronic potential, and the molecular energy is taken as Hartree-Fock energy plus MP2 energy correction. The MP2 calculation are much fast than the CI calculations, but for species involving open-shell ground states, unrestricted SCF wave functions are

not eigenfunction of the total spin operator $\hat{S}^2$, and this "spin contamination" can sometimes produce serious errors in UMP-calculated quantities.

Currently available functionals in DFT can not compute a thermodynamic energy such as heat of atomization and the enthalpy of formation with accuracy of 1 kcal/mol. High level configuration interaction methods with large basis sets can do this but too costly to be feasible except for small molecules. The composite CBS method[6] is reported to achieve 1 kcal/mol accuracy with a computational time that allows calculation on molecules containing several nonhydrogen atoms.[7] The CBS methods use special procedures designed to extrapolate calculated energies to the complete-basis-set limit. The CBS methods include several corrected calculations done at a geometry optimized at a lower level of theory. The highest-level calculation used is the QCISD(T)/6-31+G(d,p) in the CBS-Q method.

Model chemistry is characterized by the combination of theoretical procedure and a basis set. A basis set is a mathematical representation of the molecular orbitals within a molecule. The basis set can be interpreted as restricting each electron to a particular region of space. Large basis sets impose fewer constraints on electrons to particular accurately approximate exact molecular orbitals. However, the computation of atomic or molecular properties with large basis sets requires correspondingly more and more computational resources.

Standard basis sets for electronic structure calculation use linear combinations of Gaussian functions to form the orbitals. Basis sets assign a group of basis functions to each atom within a molecule to approximate its orbitals. These basis functions themselves are composed of a linear combination of Gaussian functions. The linear

combined basis functions are refereed to as contracted functions, and the component Gaussian functions are referred to as primitives. A basis function consisting of a single Gaussian function is termed uncontracted. In the nomenclature of 6-31G basis set, "6" stands for using 6-component type d function, "31" stands for using two sets of function in the valence region (one function consisting of 3 primitive Gaussian, one consisting of 1 primitive Gaussian).

The 6-31G(d,p) indicates that it is the polarized 6-31G basis set with one d function added to the heavy atoms and one p function added to hydrogen atoms. The 6-311+G(3df,2p) is the basis set with diffuse functions added to heavy atoms, as well as three d functions and one f function added to heavy atoms, and 2 p functions added to the hydrogen atoms. If 6-311++G(3df,2p), then it also adds diffuse functions to hydrogen atoms.[2]

1.3 Kinetics

Several important aspects are needed in order to understand the kinetics of unimolecular reactions. These include: (1) the formation of an energized molecule with energy E, (2) the intramolecular vibrational / rotational motion of high energized molecules; (3) unimolecular rate constants for dissociation of the energized molecules as a function of their energy $k(E)$; (4) intramolecular energy transfer to and from highly energized molecules; and (5) energy partitioning between unimolecular dissociation fragments.

There are a number of different theories to present these topics such as Lindemann-Hinshelwood theory, Slater theory, RRK theory, RRKM theory, and Quantum RRK theory. This section will focus on unimolecular reactions, and also discuss chemical activation reactions, which is of great importance to unimolecular reactions.

1.3.1 Lindemann-Hinshelwood Mechanism for Unimolecular Reactions

In 1922, Lindemann[8] proposed a general theory for the thermal unimolecular reaction, which forms the basis for the current theory of thermal unimolecular rates. He proposed that a certain fraction of molecules become energized by bimolecular collisions, i.e. gain energy in excess of a critical quantity E_0; the rate of the energy transfer depends upon the rate of bimolecular collisions, and the energized molecules are also de-energized by collision; there is a time lag between the moment of collision energy transfer and the time the molecule decomposes, and an energized molecule can undergo deactivating collisions before decomposition occurs in this time period; this unimolecular dissociation occurs with a rate constant independent of the energy content of the energized molecules, i.e., all molecules with energy above threshold E_0 dissociate with the same energy. The mechanism in Lindemann theory is written as:

$$A + M \xrightarrow{k1} A* + M$$

$$A* + M \xrightarrow{k-1} A + M$$

$$A* \xrightarrow{k2} \text{Products}$$
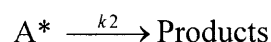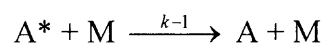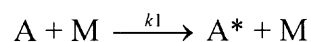
The asterisk represents that a molecule A contains sufficient energy to react with collider M. It is assumed that each A* + M collision is "strong" and thus leads to de-energizing of A; this is known as "strong collision assumption" for de-energizing collisions. Therefore, this de-energized rate is taken to be energy-independent and is equated with the collision number Z_1 by assuming that every collision of A^* leads to a de-energized state.

The overall concept can be expressed by the equations below, where M can represent a generic bath gas molecule ("inert" gas molecule); it may also represent a

second molecule of reactant or product. In the simple Lindemann theory k_1, along with k_{-1} and k_2 are taken to be energy-independent and are calculated from the simple collision theory equation.

Application of the steady-state hypothesis to the concentration of A^*, allows the unimolecular rate constant and the high- and low-pressure limit rate and rate constants to be determined as follows:

$$\text{Rate} = k_{\text{uni}} [A] = k_2 [A^*] = \frac{k_1 k_2 [A][M]}{k_{-1}[M] + k_2}$$

$$k_{\text{uni}} = k_1 k_2 \ \frac{k_1 k_2 [M]}{k_{-1}[M] + k_2}$$

High-pressure limit rate, $[M] \rightarrow \infty$, $k_{\text{uni}} = k_\infty = \dfrac{k_1 k_2}{k_{-1}}$

Low-pressure limit rate, $[M] \rightarrow 0$, $k_{\text{uni}} = k_0 = k_1 [M]$

The unimolecular rate constant is then written as: $k_{\text{uni}} = \dfrac{k_\infty}{1 + k_\infty / k_1 [M]}$

One can expect the Lindemann theory to predict a linear change in the initial rate of a unimolecular reaction with respect to concentration of M at low pressure. The transition from high-pressure rate constant to low pressure is called "fall-off region". The k_1 in the original Lindemann theory is taken from collision theory:

$$k_1 = Z_1 \, exp(-\frac{E_0}{k_B T})$$

where $Z_1 = \left(\dfrac{\sigma_d^2 \, N_A}{R} \right) \left(\dfrac{8 \pi N_A k_B}{\mu} \right)^{1/2} \left(\dfrac{1}{T} \right)^{1/2}$. The unit for Z_1 is in Torr^{-1}-s^{-1} (consistent with [M] in Torr and k_2 in s^{-1}). σ_d is collision diameter in cm; μ is reduced molar mass in

g-mol^{-1}, $\mu = \left(\dfrac{1}{M_A} + \dfrac{1}{M_B} \right)^{-1}$; T is temperature in Kelvin; N_A is Avogadro's number 6.022

$\times 10^{23}$ mol^{-1}; R is gas constant 6.2326×10^4 cm^3-Torr-K^{-1}-mol^{-1}; k_B is Bolzmann constant

1.3805×10^{-16} erg-K^{-1}.

A major achievement of Lindemann's theory is its ability to explain the experimental finding that the unimolecular dissociation rate can be pressure dependent. However, it predicts the fall-off in k_{uni} to occur at much higher pressure than what is observed experimentally. In 1926 Hinshelwood[9] proposed that the internal degree of freedom can contribute to the threshold energy E_0. The probability that a molecule contains energy great than or equal to E_0 increases with the number of internal degree of freedom, and such the energization rate constant k_1 is larger for a complex reactant than for a simple one. Hinshelwood increases k_1 by using a much higher probability of a molecule possessing total energy $\geq E_0$ in s classical degrees of freedom, $(E_0/k_BT)^{s-1}\exp(-E_0/k_BT)/(s-1)!$, rather than the simpler $\exp(-E_0/k_BT)$ that Lindemann used. The result is

$$k_1 = \frac{Z_1}{(s-1)!} \left(\frac{E_0}{k_B T} \right)^{s-1} exp\left(\frac{-E_0}{k_B T} \right)$$

Based on the Lindemann's suggestion that k_1 could be increased by assuming that the required energy for energized molecules could be drawn in part from the internal degrees of freedom (mainly vibration) of the reactant molecule. Since k_1 increases with s classical degrees of freedom in the Lindemann-Hinshelwood theory, then $k_2 = k_\infty k_{-1}/k_1$ should decrease with s. Thus the lifetime of the energized molecule t $\approx 1/k_2$ increases when the molecule can store energy among a large number of degrees of freedom. Then k_2 is

expected to depend on the energy of A*. Making k_2 energy-dependent, expressed as $k(E)$, the energy interval from E to E+dE is considered:

$$A + M \xrightarrow{dk1} A^* (E, E+dE) + M$$

$$A^*(E, E+dE) + M \xrightarrow{k-1} A + M$$

$$A^*(E, E+dE) \xrightarrow{k(E)} Products$$
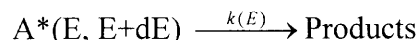
Applying the steady-state approximation to energized intermediate A*(E, E+dE) leads to the differential unimolecular rate constant:

$$dk_{uni} (E, E+dE) = \frac{k(E)(dk_1/k_{-1})}{1 + k(E)/k_{-1}[M]}$$

It is assumed that for all pressure dk_1/k_{-1} represents the equilibrium probability and that the A* has energy between E and E+dE. This probability may be denoted $P(E)dE$. Also k_{-1} [M] is the collision frequency ω between an A* molecular and collider M, this leads to the thermal unimolecular rate constant:

$$k_{uni} = \omega \int_{E_0}^{\infty} \frac{k(E)P(E)dE}{k(E) + \omega}$$

In order to make accurate quantitative predictions of the fall-off behavior of a unimolecular reaction, it is essential to take into account the energy dependence of the rate constant $k(E)$ for the conversion of energized molecules into activated complexes where products result from decomposition or reaction of the energized complex.

Two different approaches may be taken to determine $k(E)$. One is to consider the explicit nature of the intramolecular motion of highly energized molecules, such as Slater theory. The other approach is based on statistical assumptions, such as RRK theory and its extension, RRKM theory. Most modern theories of unimolecular reaction rates,

including the Slater theory, the RRK theory and the RRKM theory, are based on the fundamental Lindemann mechanism involving collision energy transfer of the reactant molecules, and more specifically on Hinshelwood's development.

1.3.2 RRK Theory of Unimolecular Reactions

The RRK theory was developed independently and nearly simultaneously by Rice and Ramsperger[10] and by Kassel.[11] in 1927 and 1928. Both Rice and Ramsperger theory and Kassel theory consider that a critical energy E_0 must become concentrated in one part (a specific vibration) of the molecule for reaction to occur. They used the basic Lindemann-Hinshelwood mechanism of collision energy transfer and de-energization, but assumed more realistically that the rate constant for conversion of an energized molecule into products is proportional to a specific probability. This is a finite statistical probability that energy, E_0, is found in the relevant part of the energized molecule which contains total energy, E, is greater than E_0 since E of the molecule under consideration is assumed to be rapidly redistributed around the molecule. This probability will increase with E and make k(E) a function of its energy content.

The difference between the Rice and Ramsperger model and Kassel model is two-fold. First, Rice and Ramsperger used classical statistical mechanics throughout, while Kassel used classical methods and also developed a quantum treatment. The quantum method turns out to be much more realistic and accurate. Second, different assumptions were made about the part of the molecule into which the critical energy E_0 has to be concentrated. The Kassel's model seems slightly more realistic by assuming the energy had to be concentrated into one oscillator. The quantum version of the Kassel theory serves as a theoretical basis for the most of calculations performed in this thesis.

The classical RRK theory is based on the notion that the probability that a molecule of s classical oscillators with total energy E has energy greater than E_0 in one chosen oscillator, which is the critical mode leading to reaction. The assumptions used to derive the quantum RRK rate constant are similar to those for classical theory. In the single frequency quantum Kassel theory it is assumed there are s identical oscillators in the molecule, all having frequency ν. The energized molecule has total n quanta, so $E = nh\nu$. The critical oscillator must have m quanta for dissociation to occur, $m = E_0/h\nu$.

The probability that one oscillator contains at least m quanta (probability of energy $\geq$ m quanta in one chosen oscillator) from probability theory[12] is

$$\text{Probability} = \frac{n!(n-m+s-1)!}{(n-m)!(n+s-1)!}$$

Hence, rate constant $k_a(E)$ for conversion of energized molecules to product is

$$k_a(nh\upsilon) = A\frac{n!(n-m+s-1)!}{(n-m)!(n+s-1)!}$$

where A is Arrhenius pre-exponential parameter. The corresponding $k_1(E)$ of the Hinshelwood expression is now derived. It refers to energy transfer into a specific quantum state rather than into an energy range E to E+dE, as

$$k_1(nh\upsilon) = k_2\alpha^n (1-\alpha)^s \frac{(n+s-1)!}{n!(s-1)!}$$

where $\alpha = \exp(-h\nu/k_B T)$. Both classical and quantum versions of RRK theory were developed, and in the limit of a large excitation energy E the two versions become identical.

In RRK theory the assumption is made that the rate of conversion of energized molecules into products is related to the probability that the critical energy E_0 is

concentrated in one part of the molecule, e.g. in one oscillator (Kassel theory) or in one squared term (Rice-Ramsperger theory). This probability is a function of the total energy E of the energized molecule, and the total vibrations among which the vibration energy quanta can be distributed.

1.3.3 RRKM Theory of Unimolecular Reactions

The RRKM theory was developed using the RRK model and was extended to consider explicit vibration and rotational energies and also include zero point energies.[13] Several minor modifications of the theory have been made, primarily as a result of improved treatments of external degrees of freedom.[14,15]

RRKM theory is a microcanonical transition state theory, and it provides the connection between statistical unimolecular rate theory and the transition state theory of thermal chemical reaction rates. Isomerization or dissociation of an energized molecule A* is assumed to occur via the mechanism

$$A^* \xrightarrow{\ k(E)\ } A^{\neq} \rightarrow \text{Products}$$

where $A^{\neq}$ is the transition state. The energized molecule A* contains both vibrational and external rotational energies by E_v and E_r, respectively. The sum of E_v and E_r is E. To treat the external rotational energy of a nonlinear molecule quantum mechanically, the specific rotational energy levels must be considered. The RRKM rate constant k_{EJ} is the microcanonical transition state theory rate constant, and is given by

$$k_{EJ} = \frac{N^{\dagger}_{EJ}}{h\rho_{EJ}}$$

where N_{EJ} is the sum of states for the active degrees of freedom in the transition states and ρ_{EJ} is the density of states for the active degrees of freedom in the reactants. To

determine an RRKM rate constant requires evaluating the sum of states for the transition state and the density of states for the reactants. The information needed for calculating the sum and density of states includes the total reactant energy E, rotational energy E_r, the unimolecular threshold E_0. One also needs harmonic vibrational frequencies and moments of inertia for both the reactant and the transition states. This information can be obtained by either experimental data or ab initio calculations.

Different experimental techniques, including static pyrolysis, carrier (flow) techniques, shock tube methods, and very-low-pressure-pyrolysis, have been used to measure k_{uni} as a function of temperature and pressure. One of the most significant achievements of RRKM theory is its ability to match measurements of k_{uni} with pressure.

1.3.4 Chemical Activation Reactions

The energization methods other than by molecular collision, such as photoactivation and chemical activation, may produce a non-equilibrium situation in which molecules acquire energies far in excess of the average thermal energy. This presence of excess energy in the energized adduct makes chemical activation reactions much more important in these systems. A treatment for the rate of conversion, which includes decomposition of energized adduct to product(s) (including reverse back to reactants) and the competing rate of its collision stabilization, is needed.

An example of a chemically activated reaction system is neopentyl radical $(C_3CC\bullet) + O_2$ system. As is discussed in Chapter 3, $C_3CC\bullet$ radical reacts with O_2 to form a chemically activated, energized adduct $[C_3CCOO\bullet]^*$, this process of forming adduct is much more efficient than that by thermal molecular collision, and adduct contains excess energy from the new bond formed in this chemical reaction. The energized adduct

$[C_3CCOO\bullet]^*$ could go back to reactant $C_3CC\bullet$ + O_2, or could go to products 3,3-dimethyloxetane + OH via an intramolecular H shift. The QRRK analysis (A + BC $\rightarrow$ ABC*) shows that the chemical activation process is more important than thermal dissociation process.

The basic idea of the treatment of a chemical activation system is that a vibration excited molecule ABC^* formed by an association of reactants can reform reactants A + BC with a rate constant $k'(E)$, form decomposition products, AB + C, with a rate constant $k_a(E)$ or be de-energized to stable molecules ABC.

In the strong collision assumption the first order rate constant for de-energization is equal to the collision frequency, $\omega = Zp$ where p is the total pressure and Z is collision number. This assumes that stabilization occurs at energy collision.

Suppose that the fraction of molecules which are energized per unit time into the energy range between E and E+dE is f(E)dE. To simplify, one can consider decomposition path (back to reactant, A + BC, as the decomposition path), then the fraction of ABC^* decomposing (path A + BC) compared with those stabilized (path ABC) is k(E)/ [k(E)+ω]. The fraction of molecules in the energy range between E and E+dE decomposing to products is therefore {k(E)/[k(E)+ω]}f(E)dE, and the total number of molecules decomposing per unit time (D), at all energies above the critical energy E_0, is:[16]

$$D = \int_{E_0}^{\infty} \frac{k(E)}{k(E) + \omega} f(E)dE$$

Corresponding, the total rate of stabilization (S) is:

$$S = \int_{E_0}^{\infty} \frac{\omega}{k(E) + \omega} f(E)dE$$

Considering an average rate constant <k> for all energies above E_0, one would have:

$$\frac{<k>}{\omega} = \frac{D}{S} = \frac{No.\,molecules\,decomposing\,per\,unit\,time}{No.\,of\,molecules\,being\,stabilized\,per\,unit\,time}$$

So,

$$<k> = \omega \cdot \frac{\int_{E_0}^{\infty} \{k(E)/[k(E)+\omega]\} f(E) dE}{\int_{E_0}^{\infty} \{\omega/[k(E)+\omega]\} f(E) dE}$$

The f(E) is the distribution function of energized molecules in the energy range between E and E+dE. In the thermal energy transfer systems, this distribution function is simply the thermal quantum Boltzmann distribution $K(E)$ and the rate of energy transfer into the energy range between E and E+dE is $K(E)dE = dk_1/k_2$. For the chemically activated system described here, the distribution function can be derived by applying the principle of detailed balancing to the reverse process to reactants. Consider a situation in which other processes can be ignored and equilibrium is established between A^* and reactants. Then the fraction of molecules with energy between E and E+dE is Boltzmann distribution $K(E)dE$, so the rate of dissociation to reactants is then $k'(E)K(E)dE$, and by the principle of detailed balancing this also gives the rate of combination of reactants to give A^* in this energy range. The total rate of energy transfer to all levels above the minimum energy E_{min} (the minimum energy of A^*) is:

$$Total\,rate\,of\,energization = \int_{E_0}^{\infty} k'(E)K(E) dE$$

Therefore, the distribution function is given by:

$$f(E)\delta E = \frac{k'(E)K(E)dE}{\int_{E_0}^{\infty} k'(E)K(E) dE}$$

The $f(E)$dE can be incorporated into QRRK theory for k(E) and k$_1$(E) serves as a basis for the calculations for chemical activation reaction systems.

1.3.5 QRRK Analysis for Chemical Activation and Unimolecular Dissociation

1.3.5.1 Input Information Requirements for QRRK Calculation.   Quantum Rice-Ramsperger-Kassel (QRRK) analysis, as initially presented by Dean[17-19] combined with the modified strong collision approach of Gilbert et al.,[20,21] to compute rate constants for both chemical activation and unimolecular reactions, over a range of temperature and pressure. The computer program CHEMDIS is designed to calculate unimolecular and chemical activation reactions based on the QRRK theory and unimolecular dissociation and chemical activation formalism. The input parameters for CHEMDIS are: (1) High-pressure limit rate constants (Arrhenius A factor and activation energy E_a) for each reaction included for analysis; (2) A reduced set of three vibration frequencies and their associated degeneracy; (3) Lennard-Jones transport parameters, (s (Angstroms) and e/k (Kelvin)), and (4) molecular weight of well species.

High pressure limit rate constants k_∞'s are fitted by three parameters A_∞, n, and E_a over temperature range from 298 to 2000K, $k_\infty = A_\infty(T)^n \exp(-E_a/RT)$. Entropy differences between reactant and transition state are used to determine the pre-exponential factor, A, via canonical Transition State Theory (TST):

$$A = (k_B T/h_p)\exp(\Delta S^{\neq}/R), \quad E_a = \Delta H^{\neq}$$

where h_p is the Planck constant and k$_B$ is the Boltzmann constant. $\Delta S^{\neq}$ = S(TST) − S(reactants) and $\Delta H^{\neq}$ = H(TST) − H(reactants). Treatment of the internal rotors for S and $C_p(T)$ of reactants and the TST's is important here because these internal rotors are often lost in the cyclic transition state structures. Pre-exponential factors (A_∞), are calculated

from structures determined by DFT or estimated from the literature and from trends in homologous series of reactions. Activation energies come from ab initio calculations plus evaluated endothermicity of reaction ΔU_{rxn}, and from analogy to similar reactions with known energies.

Reduced sets of three vibration frequencies and their associated degeneracies are computed from fits to heat capacity data, as described by Ritter and Bozzelli et al.[22,23] These have been shown by Ritter to accurately reproduce molecular heat capacities, $Cp(T)$, and by Bozzelli et al.[23] to yield accurate ratios of density of states to partition coefficient, $\rho(E)/Q$.

Lennard-Jones parameters, sigma (angstroms) and ε/k (Kelvin's), are obtained from tabulations[24] and from a calculation method based on molar volumes and compressibility.[25]

1.3.5.2 Quantum RRK / Master Equation Calculation. The Quantum RRK / Master equation analysis is described by Chang et al.[17,26] The QRRK code utilizes a reduced set of three vibration frequencies which accurately reproduce the molecule's (adduct) heat capacity; the code includes contribution from one external rotation in calculation of the ratio of the density of states to the partition coefficient $\rho(E)/Q$.

Comparisons of ratios of these $\rho(E)/Q$ with direct count $\rho(E)/Q$'s are shown to be in good agreement.[23] Rate constant results from the QRRK/Master equation analysis are shown to accurately reproduce experimental data on several complex systems. They also provide a reasonable method to estimate rate constants for numerical integration codes by which the effects of temperature and pressure can be evaluated in complex reaction systems.

Multifrequency QRRK analysis is used to calculate k(E) with a master equation analysis[26] for fall-off. A 500 cal. energy grain interval is used for the energy intervals. Rate constants are obtained as a function of temperature and pressure for the chemical activation and dissociation reactions. The master equation analysis[26] uses an exponential-down model for the energy transfer function. Troe et al.[27] reported that $(\Delta E)^\circ_{down}$ is independent of temperature (293 – 866 K) for the rare and diatomic bath gases, and Hann et al.[28] recently determined a value of $(\Delta E)^\circ_{down} = 500$ cm^{-1} for matching the two-dimensional master equation solutions to the experimental fall-off behavior in the C_3H_3 + O_2 system with N_2 bath gas. Knyazev and Slagle[29] reported that $(\Delta E)^\circ_{down}$ changes with temperature; they compared three models, two of which are $(\Delta E)^\circ_{down} = \alpha T$ and $(\Delta E)^\circ_{down}$ = constant, in reaction of n-$C_4H_9 \Leftrightarrow C_2H_5$ + C_2H_4 with Helium as bath gas. The energy difference between the values of the barrier height needed to fit the experimental data with these two $(\Delta E)^\circ_{down}$ models is only 0.4 kJ mol^{-1} over a relatively narrow temperature range (560 – 620 K). Constant values of 1000 cal mol^{-1} (N_2 as bath gas) and 570 cal mol^{-1} (He as bath gas) for $(\Delta E)^\circ_{down}$ are used in this study.

CHAPTER 2

THERMOCHEMICAL PROPERTIES OF CHLORINATED ALCOHOLS, HYDROPEROXIDES AND CORRESPONDING RADICALS

2.1 Background

The incineration and atmospheric oxidation processes of chlorine-containing organic compounds are of major interest since such compounds can contribute to the transport of chlorine species to atmosphere and stratosphere. The oxidation of chlorinated hydrocarbon is initiated mainly by the reaction with OH radical to produce chloroalkyl radicals that will react with O_2 to generate peroxy radicals. Chlorinated alkyl peroxy species are also formed in the atmosphere where chlorine atom can add to olefins and then react with O_2. Chloro-alkyl hydroperoxides are produced in the further reactions of alkylperoxy radicals with the hydroperoxy radical, HO_2, and are also formed via H-atom abstraction from other hydrocarbon species with weakly bonded hydrogen atoms. Chloroalkyl peroxy radicals are important intermediates in low-temperature oxidation such as in the initial stages of combustion and in the atmospheric photochemical oxidation of chlorohydrocarbons because peroxy radical reactions are the first step in the oxidation processes, these radicals will subsequently react with NO or another organic peroxy radical to form the corresponding chlorinated alkoxy radicals.[30] The thermochemistry of the dissociation products of chlorinated alcohols and alkyl hydroperoxides are needed for understanding and predicting the reaction pathways, rate constants and equilibrium constants in order to assess the impact of chlorocarbon degradation products on the environment. Reliable thermochemical properties of these oxygenated chlorocarbon species are important in evaluation of kinetics or

20

thermodynamic equilibrium for both destruction and synthesis processes and in chemical engineering design.

2.2 Calculation Method

2.2.1 Computational Details

All of the density functional and *ab initio* calculations are performed using the Gaussian 94/98 program.[31,32] The geometry optimization, harmonic vibration frequencies and zero-point vibrational energies (ZPVE) are computed at the B3LYP/6-31G(d,p) level. Three calculation methods are proposed obtain single point total electronic energies:

1. B3LYP/6-311+G(3df,2p)

2. QCISD(T)/6-31G(d,p)

3. CBSQ//B3LYP/6-31G(d,p)

The DFT method computes electron correlation via general functionals of the electron density. The best DFT methods achieve significantly greater accuracy than Hartree-Fock theory at only a modest increase in cost, and this is achieved by including some of the effects of electron correlation much less expensively than traditional correlated methods.[1] The B3LYP with the basis set of 6-31G(d,p) is used for geometry optimization and frequency calculation. Curtiss et al.[33] reported that B3LYP/6-31G(d,p) provides highly accurate structures for compounds with elements up to atomic number ten. Durant[34,35] has compared density functional calculations B3LYP and hybrid (BH and H) with MP2 and Hartree-Fock methods for geometry and vibration frequencies. He reports that these density functional methods provide excellent geometries and vibration frequencies, relative to MP2 at a reduced computational expense. Petersson et al.[36]

recommended use of B3LYP for geometry and frequencies in several of his CBS calculation methods. B3LYP/6-311+G(3df,2p) is chosen to see if this larger basis set with diffuse functions results in any improvement to the above commonly used density functional calculation method.[37] QCISD(T)/6-31G(d,p) is a configuration interaction method; but with a small, economical basis set.[38,39] CBS-Q calculation is a high level composite method with an empirical correction reported compared with QCISD(T)/6-311+G(3df,2p).[40,41] CBS-Q[6] attempts to approximate the energy of a species at the infinite basis set limit by an extrapolation of the energies of pair natural orbital at the MP2 level. The effects of going from MP2 to QCISD(T) are accounted for with an additivity scheme. The geometry is obtained at the MP2/6-31G level of theory, while the ZPE used is the scaled (by 0.9135) HF/6-31G value. For the open-shell systems, there is also a correction for spin contamination in the unrestricted Hartree-Fock wave function. The CBS-Q method has been shown to yield reliable $\Delta H_f^{o}{}_{298}$ values for small molecules.[6] The CBSQ//B3LYP/6-31G(d,p) method differs from CBS-Q in that it employs improved geometry and ZPE at the B3LYP/6-31G(d,p) level with a correction for spin contamination for the open shell systems.

2.2.2 Enthalpies of Formation ($\Delta H_f^{o}{}_{298}$)

The $\Delta H_f^{o}{}_{298}$ are calculated using total energies and isodesmic reactions. Total energies are corrected by ZPVE, which are scaled by 0.9806 as recommended by Scott et al.[42] Thermal correction is taken into account using the B3LYP structure and vibrations. Isodesmic reactions are hypothetical reactions where the number of electron pairs and the bonds of the same type are conserved on both sides of the equation, only the relationship among the bonds are altered. Density functional and *ab initio* calculations with ZPVE and

thermal correction are performed for all four compounds in each reaction, and enthalpy of reaction $\Delta H^{o}_{rxn,298}$ is calculated. Since the enthalpies of formation of the three compounds, have been experimentally determined or theoretically calculated, the unknown enthalpy of the target compound is obtained.

Density functional and *ab initio* calculations at the B3LYP/6-31G(d,p), B3LYP/6-311+G(3df,2p), QCISD(T)/6-31G(d,p) and CBS-Q level of theory are performed on the most stable conformer of each compound, and the $\Delta H^{o}_{f\,298}$ of this conformer is calculated using isodesmic reactions. $\Delta H^{o}_{f\,298}$'s of other conformers, if present, are estimated with the same method. Final $\Delta H^{o}_{f\,298}$ values are calculated from a statistical distribution of rotational conformers.

2.2.3 Entropy and Heat Capacities

Contributions of vibration, translation, and external rotation to entropies and heat capacities are calculated from scaled vibrational frequencies and moments of inertia of the DFT optimized structures. Contributions from hindered rotors to S^{o}_{298} and $C_p(T)$'s are determined using direct integration over energy levels of the intramolecular rotational potential curves, which can be represented by a truncated Fourier series expansion.[43] Potential barriers for internal rotations are determined at the B3LYP/6-31G(d,p) calculation level. A technique for calculation of thermodynamic functions from hindered rotations with arbitrary potentials is used to calculate hindered internal contributions to S^{o}_{298} and $C_p(T)$'s.[43] This technique employs expansion of the hindrance potential in the Fourier series, calculation of the Hamiltonian matrix in the basis of wave functions of free internal rotation, and subsequent calculation of energy levels by direct diagonalization of the Hamiltonian matrix. The calculations are based on optimized

geometries, atom connectivity, and the coefficients of the Fourier expansion components from rotational potential curves. The torsional potential calculated at the discrete torsional angles is represented by a truncated Fourier series.

$$V(\Phi) = a_0 + \sum a_i \cos(i\,\Phi) + \sum b_i \sin(i\,\Phi) \qquad i = 1, 2, 3, 4, 5$$

Values of the coefficients a_i and b_i are calculated to provide the minimum and maxima of the torsional potentials with allowance of a shift of the theoretical extreme angular positions.

2.3 α-Chlorinated Ethanols and Radicals

2.3.1 Geometries

The lowest energy conformation for the two chloroethanols and three hydroxyl chloroethyl radicals consistently has the hydroxyl H atom gauche to the maximum number of chlorine atoms as illustrated in the Appendix Table A.1, despite an apparent steric penalty. These lowest energy conformations exhibit the anomeric effect as those of chloromethanols reported by Schneider[44], Omoto[45] and Sun et al.[46] This preference is ascribed to the delocalization of the lone pair e⁻ on the oxygen with the antibonding σ* orbital of the C—Cl bond; it is also supported by the electrostatic repulsion between the non-bonding e⁻ pair of oxygen and electronegative Cl atom(s) and intramolecular interaction between the hydroxyl H atom and the Cl atom.[47]

It can be seen from Table A.1 that the C—O bond length decreases significantly with chlorine substitution. This is due to the anomeric effect where the non-bonding e⁻ pair on oxygen is mixing with the antibonding orbital of the C—Cl bond.[44,45,48] In valence bond terminology, this would be described as:

$$\left[\text{CH}_3\text{—CH—}\overset{\bullet\bullet}{\underset{\bullet\bullet}{\text{O}}}\text{—H} \right] \longleftrightarrow \left[\text{CH}_3\text{—CH=}\overset{+}{\underset{\bullet\bullet}{\text{O}}}\text{—H} \right]$$
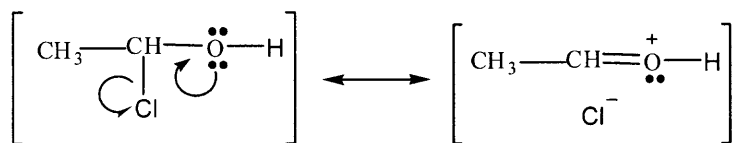
The anomeric effect can also be seen in the C—Cl bond length, which is longer than normal C—Cl bond. The O—H bond increases with increased chlorine substitution and bond strength gets stronger (see the bond energy discussion below).

The Density Functional structure predicts, planar (sp^2) vs tetrahedral (sp^3), on the hydroxyethyl and hydroxychloroethyl radicals. The $\angle H_c\text{-C-C-}H_c$ dihedral angle in $C^\bullet H_2CH_2OH$ and $C^\bullet H_2CHClOH$ are 170.1° and 168.0°, which suggests a non-planar structure. However, the $\angle H_c\text{-C-C-}H_c$ and the $\angle$C-C-O-H dihedral angle in $C^\bullet H_2CCl_2OH$ both are 180.0°, indicating there is a mirror plane between the two chlorine atoms, i.e. C_s symmetry in $C^\bullet H_2CCl_2OH$. The inversion frequencies for $C^\bullet H_2CH_2OH$, $C^\bullet H_2CHClOH$ and $C^\bullet H_2CCl_2OH$ are calculated in this work to be 458.2, 666.5 and 539.2 cm^{-1}, respectively. The symmetry number is assigned as 1 for $C^\bullet H_2CH_2OH$ and $C^\bullet H_2CHClOH$, and two for $C^\bullet H_2CCl_2OH$ on the basis of these data.

2.3.2 Rotational Barriers

Potential barriers for internal rotations of all the species are calculated at the B3LYP/6-31G(d,p) level. Potential energy as function of dihedral angle is determined by scanning the torsion angles from 0° to 360° at 15° intervals and allowing the remaining molecular structural parameters to be optimized. Each minimum and maximum on the torsional potential are fully optimized. The barriers for internal rotations are calculated from the differences between the total energy of each conformation and that of the most stable conformer.

The calculated rotational barriers about the C—C bond of CH_3CH_2OH, $CH_3CHClOH$, CH_3CCl_2OH, $CH_3CH_2O^\bullet$, $CH_3CHClO^\bullet$, $CH_3CCl_2O^\bullet$, $CH_3C^\bullet HOH$ and $CH_3C^\bullet ClOH$ are shown in Figure 2.1.
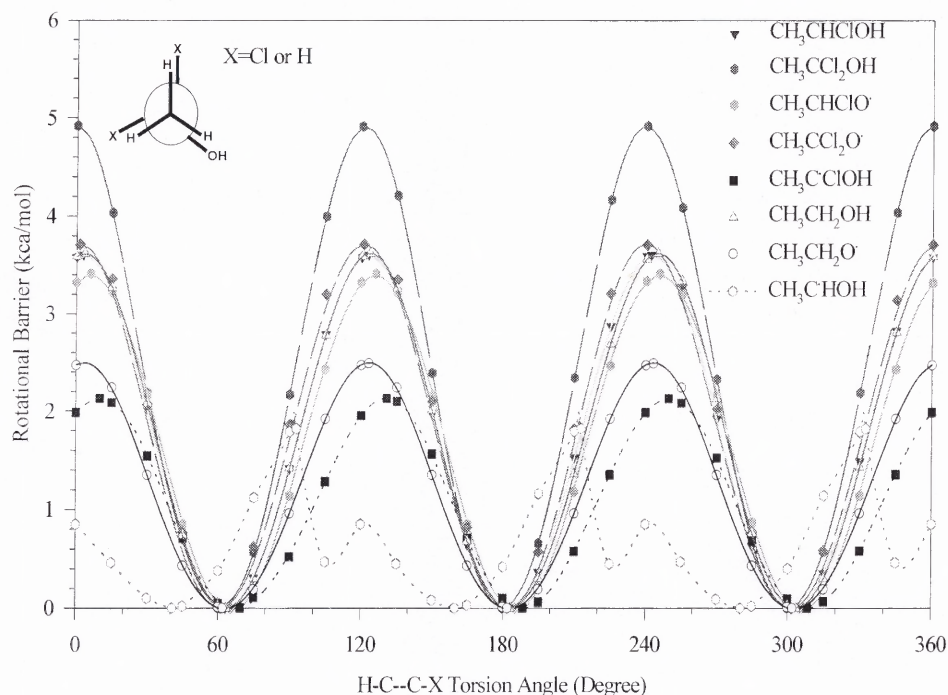
Figure 2.1 Potential barriers for internal rotation about the C—C bond of C_2H_5OH, $CH_3CHClOH$, CH_3CCl_2OH, $C_2H_5O^\bullet$, $CH_3CHClO^\bullet$, $CH_3CCl_2O^\bullet$, $CH_3C^\bullet HOH$, and $CH_3C^\bullet ClOH$.

All the curves for C–C torsion potential are symmetric and show a threefold barrier except $CH_3C^\bullet HOH$, which shows a sixfold barrier. The barrier heights for C–C torsion are: 3.62, 3.61, 4.91 kcal/mol for CH_3CH_2OH, $CH_3CHClOH$, CH_3CCl_2OH; 2.49, 3.41, 3.71 kcal/mol for $CH_3CH_2O^\bullet$, $CH_3CHClO^\bullet$, $CH_3CCl_2O^\bullet$; 1.82, and 2.13 kcal/mol for $CH_3C^\bullet HOH$ and $CH_3C^\bullet ClOH$. The above data show the barrier for the C–C torsion increases with increasing α-chlorine substitution on ethanol, ethoxy, and α-hydroxy-ethyl radical. The barriers for CH_3CH_2OH vs $CH_3CHClOH$, are, however, quite similar, 3.62

and 3.61 kcal/mol at the B3LYP level. These two barriers are furture evaluated by using MP2(FULL)/6-31G(d) level calculation; the values are slightly higher, and are 4.04 and 4.28 kcal/mol respectively. The reason for the similarity in barriers for CH_3CH_2OH and $CH_3CHClOH$ is likely due to the anomeric effect[45] in $CH_3CHClOH$. The data also show that C–C torsion barriers for (chloro)ethanols are higher than those of the corresponding (chloro)ethoxy radicals, which may in part be due to steric hindrance of the hydroxyl hydrogen.
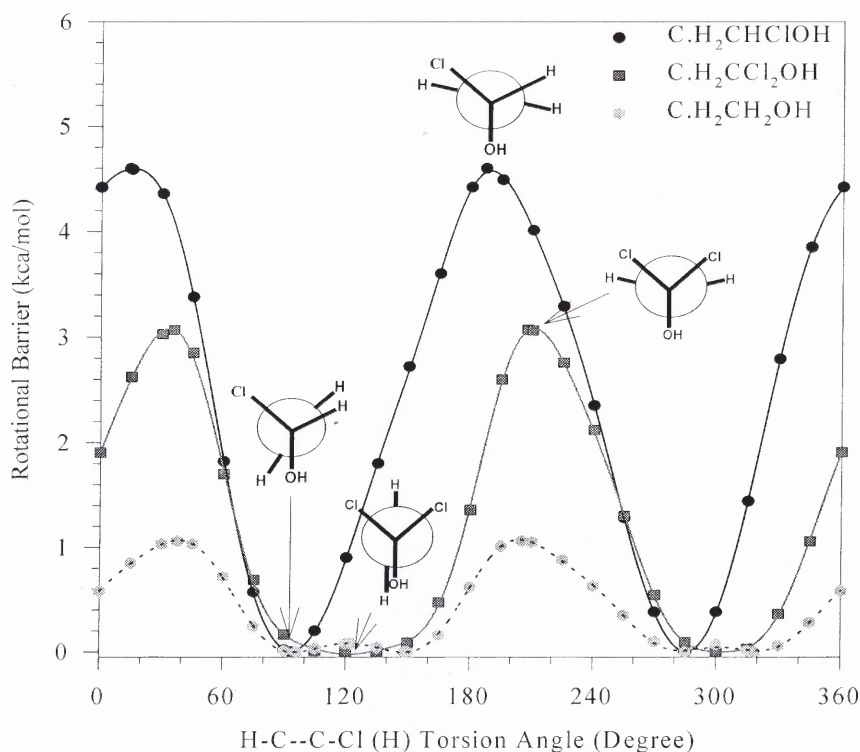
Figure 2.2 Potential barriers for internal rotation about the C—C bond of $C^•H_2CH_2OH$, $C^•H_2CHClOH$ and $C^•H_2CCl_2OH$.

Figure 2.2 shows the calculated rotational barriers about the C—C bond for $C^•H_2CH_2OH$, $C^•H_2CHClOH$ and $C^•H_2CCl_2OH$. These C–C torsion potentials show a twofold barrier for both of the chlorinated hydroxy ethyl radicals; but a fourfold barrier in

$C^\bullet H_2 CH_2 OH$. The H--OH eclipsed conformer is the most stable for the C–C torsion of $C^\bullet H_2 CCl_2 OH$ due to the interaction of H atom on the $-C^\bullet H_2$ group and the O atom (the interatomic distance 2.483 Å). In contrast, the H--OH gauche structure (the $\angle H_c$-C-C-Cl dihedral 207.56°) lacks the above interaction due to a longer interatomic distance, 2.930 Å. This gauche structure is 3.07 kcal/mol higher energy and corresponds to the maximum point on the potential curve. Similar maxima and minima structures exist in $C^\bullet H_2 CHClOH$ and $C^\bullet H_2 CH_2 OH$. The C—C rotation barrier in $C^\bullet H_2 CHClOH$ calculated at the B3LYP level is 4.60 kcal/mol, which is 1.53 kcal/mol higher than the barrier in $C^\bullet H_2 CCl_2 OH$. MP2/6-31G(d) calculations in this work also show a decrease in barrier in $C^\bullet H_2 CCl_2 OH$ relative to $C^\bullet H_2 CHClOH$ and they also predict partial sp^2 geometry for the $-CH_2^\bullet$ groups.
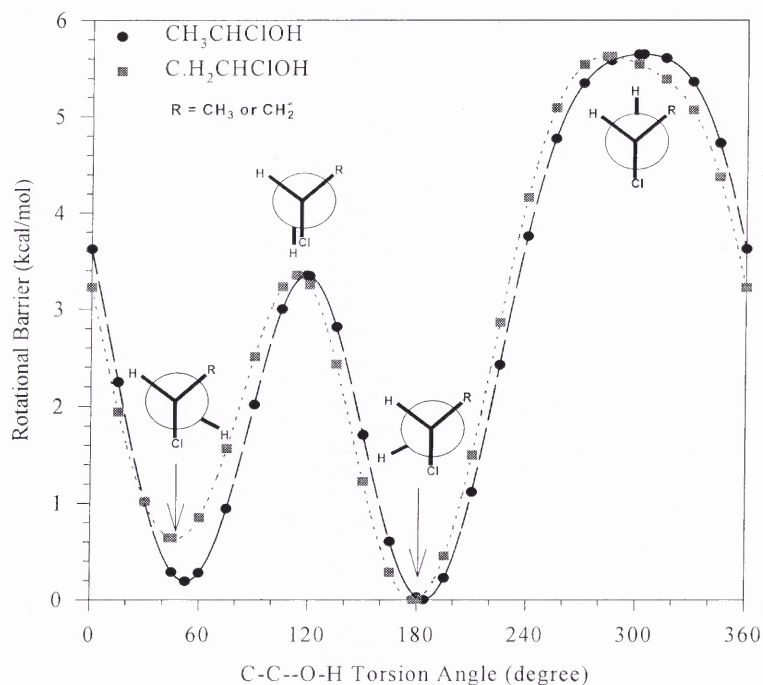
Figure 2.3 Potential barriers for internal rotation about the C—O bond of $CH_3 CHClOH$ and $C^\bullet H_2 CHClOH$.

The higher barrier for C$^\bullet$H$_2$CHClOH suggests that the H--OH eclipsed conformer of C$^\bullet$H$_2$CHClOH has extra stability. This C$^\bullet$H$_2$CCl$_2$OH radical exhibits hyperconjugation between the -CH$_2$$^\bullet$ center and the σ* (C-Cl) molecular orbital in its lowest energy conformer.[21] This effective orbital overlap is possible because the dihedral $\angle$H$_c$-C-C-H$_c$ and $\angle$H$_c$-C-C-O in the minimum energy conformer are 32.2° and –25.1° respectively, so the p orbital in the -CH$_2$$^\bullet$ center and the σ* (C-Cl) orbital are nearly parallel. This reduces the minima energy for C$^\bullet$H$_2$CHClOH and gives it a higher barrier than either the parent or C$^\bullet$H$_2$CCl$_2$OH.
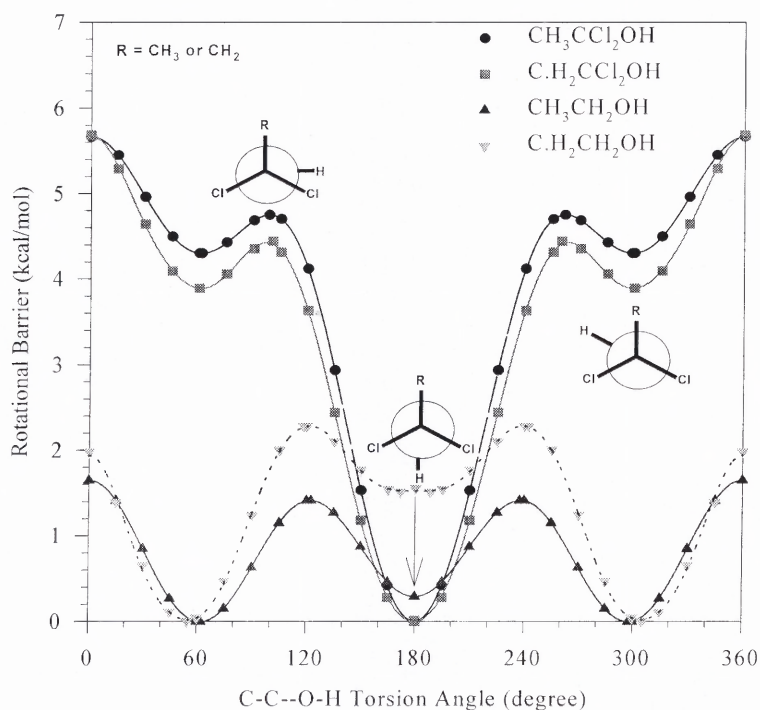
Figure 2.4 Potential barriers for internal rotation about the C—O bond of CH$_3$CH$_2$OH, C$^\bullet$H$_2$CH$_2$OH, CH$_3$CCl$_2$OH and C$^\bullet$H$_2$CCl$_2$OH.

The calculated rotational barriers about the C—O bond of CH$_3$CHClOH and C$^\bullet$H$_2$CHClOH are shown in Figure 2.3. The torsion potential curves for rotation about the

C—O bonds in $CH_3CHClOH$ and $C^•H_2CHClOH$ are similar. The most stable conformer is R--H (R = CH_3 or CH_2) anti conformer, and its energy is lower than that of the R--H gauche conformer. This is because an oxygen non-bonding e^- pair eclipsed to the H atom on the α-carbon in the R--H anti conformer, but eclipsed to the R group on the α-carbon in the R--H gauche conformer. The maxima points on the potential curves correspond to the structures that the hydroxyl H atom is anti to the Cl atom on α-carbon because the two non-bonding e^- pairs from oxygen are gauche to the Cl atom. This preference can also be ascribed to anomeric effect, the delocalization of the lone pair e^- on the oxygen with the antibonding σ^* orbital of the C—Cl bond. This phenomenon is similar to that in the chloromethanol, which is observed by our previous study.[46]

Figure 2.4 shows the calculated rotational barriers about the C—O bond of CH_3CH_2OH, $C^•H_2CH_2OH$, CH_3CCl_2OH and $C^•H_2CCl_2OH$. The C–O torsion potential curves for CH_3CCl_2OH and $C^•H_2CCl_2OH$ are similar and have the same maximum barrier of 5.68 kcal/mol. The R--H anti structure is the stable conformation with the two non-bonding e^- pairs from oxygen gauche to the two Cl atoms. The R--H gauche conformers have higher energies than those of the R--H anti conformers because of the three gauche interactions between two non-bonding e^- pairs and the Cl atom (only two of these interactions in the R--H anti conformers). The energy difference between the two conformers calculated at the CBS-Q level is: 3.27 kcal/mol for CH_3CCl_2OH, 2.68 kcal/mol for $C^•H_2CCl_2OH$. This is in agreement with the energy difference for similar conformers in $CHCl_2OH$, 2.94 kcal/mol at the same level of calculation. These values support that a gauche interaction between a Cl atom and an O atom non-bonding e^- pair increases energy in the molecule by ca. 3 kcal/mol.[46] The C–O torsion potential for

CH$_3$CH$_2$OH and C$^\bullet$H$_2$CH$_2$OH are also similar and they have lower barriers relative to CH$_3$CCl$_2$OH and C$^\bullet$H$_2$CCl$_2$OH.

Figure 2.5 Potential barriers for internal rotation about the C—O bond of CH$_3$C$^\bullet$HOH and CH$_3$C$^\bullet$ClOH.

The calculated rotational barriers about the C—O bond of CH$_3$C$^\bullet$HOH and CH$_3$C$^\bullet$ClOH are shown in Figure 2.5. The C–O torsion potential for CH$_3$C$^\bullet$ClOH has a maximum corresponding to the structure with a C-C-O-H dihedral of 91.30°. In this structure, the two non-bonding e$^-$ pairs from the O atom are eclipsed with the Cl atom and the -CH$_3$ group, with energy increased by 4.97 kcal/mol relative to that of the stable conformer, which has the two non-bonding e$^-$ pairs gauche to the Cl atom and methyl group. The C–O torsion potential for CH$_3$C$^\bullet$HOH also has a similar curve; however, the CH$_3$--H eclipsed structure for CH$_3$C$^\bullet$ClOH has energy 3.43 kcal/mol higher than that of

CH₃CH₂OH and C[•]H₂CH₂OH are also similar and they have lower barriers relative to CH₃CCl₂OH and C[•]H₂CCl₂OH.

Figure 2.5 Potential barriers for internal rotation about the C—O bond of CH₃C[•]HOH and CH₃C[•]ClOH.

The calculated rotational barriers about the C—O bond of CH₃C[•]HOH and CH₃C[•]ClOH are shown in Figure 2.5. The C–O torsion potential for CH₃C[•]ClOH has a maximum corresponding to the structure with a C-C-O-H dihedral of 91.30°. In this structure, the two non-bonding e⁻ pairs from the O atom are eclipsed with the Cl atom and the -CH₃ group, with energy increased by 4.97 kcal/mol relative to that of the stable conformer, which has the two non-bonding e⁻ pairs gauche to the Cl atom and methyl group. The C–O torsion potential for CH₃C[•]HOH also has a similar curve; however, the CH₃--H eclipsed structure for CH₃C[•]ClOH has energy 3.43 kcal/mol higher than that of

CH_3CH_2OH and $C^{\bullet}H_2CH_2OH$ are also similar and they have lower barriers relative to CH_3CCl_2OH and $C^{\bullet}H_2CCl_2OH$.

Figure 2.5 Potential barriers for internal rotation about the C—O bond of $CH_3C^{\bullet}HOH$ and $CH_3C^{\bullet}ClOH$.

The calculated rotational barriers about the C—O bond of $CH_3C^\bullet HOH$ and $CH_3C^\bullet ClOH$ are shown in Figure 2.5. The C–O torsion potential for $CH_3C^\bullet ClOH$ has a maximum corresponding to the structure with a C-C-O-H dihedral of 91.30°. In this structure, the two non-bonding e^- pairs from the O atom are eclipsed with the Cl atom and the $-CH_3$ group, with energy increased by 4.97 kcal/mol relative to that of the stable conformer, which has the two non-bonding e^- pairs gauche to the Cl atom and methyl group. The C–O torsion potential for $CH_3C^\bullet HOH$ also has a similar curve; however, the CH_3--H eclipsed structure for $CH_3C^\bullet ClOH$ has energy 3.43 kcal/mol higher than that of

the CH_3--H eclipsed structure for $CH_3C^\bullet HOH$. This is because the non-bonding e^- pair from the O atom is eclipsed to the H atom in $CH_3C^\bullet HOH$; but eclipsed to the Cl atom in $CH_3C^\bullet ClOH$.

2.3.3 Enthalpy of Formation

The total electronic energies are determined at the B3LYP/6-31G(d,p), B3LYP/6-311+G(3df,2p), QCISD(T)/6-31G(d,p) and CBSQ//B3LYP/6-31G(d,p) levels. The spin expectation values, $<S^2>$, range from 0.760 to 0.781 for the eight target radicals. The values are close to the correct value of 0.75 and suggest no significant error (due to spin contamination) for these radicals.

Table 2.1 $\Delta H_f^o{}_{298}$ for Standard Species in Reaction Schemes

species	$\Delta H_f^o{}_{298}$ (kcal/mol)	species	$\Delta H_f^o{}_{298}$ (kcal/mol)
CH_4	-17.89[49] ± 0.07	$C^\bullet Cl_2OH$	-20.54[46] ± 1.83
CH_3Cl	-19.60[50]± 0.12	$CH_3^\bullet$	34.82 ± 0.2[51]
CH_2Cl_2	-22.83[52] ± 0.29	$C_2H_5^\bullet$	28.80 ± 0.50[51]
CH_3OH	-48.08[52] ± 0.05	$CH_2Cl^\bullet$	27.7 ± 2.0[53]
C_2H_6	-20.24[52] ± 0.12	$C^\bullet H_2OH$	-3.97 ± 0.22[54]
CH_3CH_2Cl	-26.84[50] ± 0.26	$CH_3C^\bullet HOH$	-13.34 ± 0.84[46]
CH_3CHCl_2	-31.09[50] ± 0.29	$CH_3O^\bullet$	4.10 ± 1.0[55]
C_3H_8	-25.02 ± 0.12[56]	$C_2H_5O^\bullet$	-3.90 ± 1.27[46]
$CH_3CHClCH_3$	-35.00[52] ± 0.56	$CH_3CHCl^\bullet$	19.15 ± 2.0[57]
$CH_3CCl_2CH_3$	-42.23[58] ± 1.0	$CH_3CCl_2^\bullet$	12.43[57]
C_2H_5OH	-56.12[51] ± 0.2	$C^\bullet H_2CH_2OH$	-5.70 ± 0.85[59]
n-C_3H_7OH	-60.97 ± 0.12[52]	$Cl^\bullet$	28.92 ± 0.3[51]
CH_2ClOH	-58.07[46] ± 0.69	$H^\bullet$	52.10 ± 0.001[51]
$CHCl_2OH$	-65.88[46] ± 0.76	$OH^\bullet$	9.43 ± 0.3[51]
$C^\bullet HClOH$	-14.46[46] ± 1.75		

[a] The uncertainties without reference are evaluated from Pedley et al.[56] and Cox et al.[60]

The $\Delta H_f^o{}_{298}$'s for chloro-substituted species are estimated using total energies and isodesmic reactions. Density functional and *ab initio* calculations with ZPVE and thermal correction are performed for all four compounds in each reaction, and enthalpy of reaction $\Delta H^o{}_{rxn,298}$ is calculated. Since $\Delta H_f^o{}_{298}$ of three compounds, have been

experimentally determined or theoretical calculated, the unknown enthalpy of formation of target compound is obtained. The $\Delta H_f^{\circ}{}_{298}$ and their respective uncertainties for standard species used in the working reactions are listed in Table 2.1.

2.3.3.1 Mono- and Dichloroethanols.   The isodesmic reactions, reaction enthalpies, and $\Delta H_f^{\circ}{}_{298}$ values for the monochloroethanols and dichloroethanols are tabulated in Appendix Table A.2. The results for $\Delta H_f^{\circ}{}_{298}$'s in Table A.2 show very good consistency for $CH_3CHClOH$ over the seven reactions and all the calculation methods. The $\Delta H_f^{\circ}{}_{298}$ for CH_3CCl_2OH derived from the seven reaction series show consistency over all reactions for the higher level Density Functional calculation; but the $\Delta H_f^{\circ}{}_{298}$'s for dichloroethanol derived from reaction series 1, 2 and 3 in the CBSQ calculations result in values that are ca. 3 kcal/mol lower than values of reaction series 4, 5, 6 and 7. The density function results agree with CBSQ results in reactions 4 to 7. The difference in CBSQ values is suggested due to the changes to the environment of the di-chlorinated carbon in the different reactions schemes. Specifically, the methyl group is retained on the $-CCl_2-$ carbon in reaction series 4, 5, 6 and 7. The methyl group is substituted with a H atom on this $-CCl_2-$ carbon, in reactions 1, 2 and 3. The higher-level Density Functional calculations do not show this problem. This data suggests: (i.) substitution of a methyl group with a hydrogen atom does not lead to good cancellation of errors, and (ii.) reactions 4 to 7 are preferred.

The G3MP2 calculations with seven working reactions and MP2(FULL)/6-31G(d) geometries are used to further validate the enthalpy data. The results from G3MP2 calculation show good agreement in $\Delta H^{\circ}{}_{rxn,298}$ and $\Delta H_f^{\circ}{}_{298}$ vs reaction set, with

the CBSQ//B3 data. The CBSQ values from the reaction series 4 to 7 are recommended values on both $CH_3CHClOH$ and CH_3CCl_2OH. The enthalpy on the pure enantiomer of lowest energy for $CH_3CHClOH$ is -68.72 ± 1.24 kcal/mol and for CH_3CCl_2OH is -75.75 ± 1.31 kcal/mol.

2.3.3.2 Chloroethoxy and Hydroxy-Chloroethyl Radicals. The $\Delta H_f^{\circ}{}_{298}$ values of chloroethoxy and hydroxy-chloroethyl radicals are calculated based on the $\Delta H_f^{\circ}{}_{298}$'s for the chloroethanols and several isodesmic reaction series and are listed in Table 2.2. Reaction series 4, 5, 6, and 7 for the chloroethoxy radicals are isodesmic, while reactions 1, 2 and 3 are not. The $\Delta H_f^{\circ}{}_{298}$ for the two chloroethoxy radicals show remarkable consistency at the CBSQ//B3 level for isodesmic reactions, where the standard deviation is within 0.2 kcal/mol. The DFT and QCISD(T) calculations for the isodesmic reactions show deviation of ca. ± 1 kcal/mol with the CBSQ values.

The DFT and QCISD(T) calculations result in still larger variations for non-isodesmic reaction series 1, 2 and 3. CBSQ//B3 calculation results for non-isodesmic reactions are in satisfactory agreement with the isodesmic reactions; but consistently result in 0.5 kcal/mol higher values for the two chloromethoxy radicals.

The recommended $\Delta H_f^{\circ}{}_{298}$ for the two chloroethoxy radicals are an average of four isodesmic reactions at the CBSQ//B3 calculation level. The $\Delta H_f^{\circ}{}_{298}$ are -14.79 ± 2.90 and -21.85 ± 2.82 kcal/mol for $CH_3CHClO^{\bullet}$ and $CH_3CCl_2O^{\bullet}$ respectively.

The $\Delta H_f^{\circ}{}_{298}$ on the pure enantiomer of lowest energy for the three hydroxy-chloroethyl radicals are an average over the five isodesmic reactions at the CBSQ//B3 level: -25.92 ± 2.13, -17.62 ± 2.13 and 23.85 ± 2.13 kcal/mol for $CH_3C^{\bullet}ClOH$, $C^{\bullet}H_2CHClOH$, and $C^{\bullet}H_2CCl_2OH$, respectively. The CBSQ values show excellent agreement across the five

isodesmic reaction series with a standard deviation on the order of 0.01 kcal/mol. The
QCISD(T) also show very good agreement with CBSQ results.

Table 2.2 Reaction Enthalpies at 298K and Calculated $\Delta H_f^o{}_{298}$ [a]

Reaction Series	B3LYP /6-31G(d,p)		B3LYP/6- 311+G(3df,2p)		QCISD(T) /6-31G(d,p)		CBSQ//B3LYP /6-31G(d,p)	
	$\Delta H^o{}_{rxn}$	$\Delta H_f^o{}_{298}$	$\Delta H^o{}_{rxn}$	$\Delta H_f^o{}_{298}$	$\Delta H^o{}_{rxn}$	$\Delta H_f^o{}_{298}$	$\Delta H^o{}_{rxn}$	$\Delta H_f^o{}_{298}$
1. $CH_3CHClO^{\bullet}$+CH_4 —› $CH_3^{\bullet}$ + $CH_3CHClOH$	6.28	-22.20	2.65	-18.57	2.23	-18.15	-1.78	-14.14
2. $CH_3CHClO^{\bullet}$+C_2H_6 —› $C_2H_5^{\bullet}$+ $CH_3CHClOH$	1.52	-21.11	-2.05	-17.54	-0.75	-18.84	-5.44	-14.15
3. $CH_3CHClO^{\bullet}$+CH_3Cl —› $CH_2Cl^{\bullet}$ + $CH_3CHClOH$	0.24	-21.57	-3.44	-17.89	-2.82	-18.51	-7.16	-14.17
4. $CH_3CHClO^{\bullet}$+CH_3OH —› $CH_3O^{\bullet}$ + $CH_3CHClOH$	-1.19	-15.26	-0.74	-15.71	-2.33	-14.12	-1.83	**-14.62**
5. $CH_3CHClO^{\bullet}$+C_2H_5OH —› $C_2H_5O^{\bullet}$ + $CH_3CHClOH$	-1.38	-15.03	-1.15	-15.26	-2.24	-14.17	-1.78	**-14.63**
6. $CH_3CHClO^{\bullet}$+CH_4 —› $CH_3O^{\bullet}$ + CH_3CH_2Cl	11.14	-15.99	10.34	-15.19	9.77	-14.62	10.10	**-14.95**
7. $CH_3CHClO^{\bullet}$+C_2H_6 —› $C_2H_5O^{\bullet}$ + CH_3CH_2Cl	5.48	-15.98	4.94	-15.44	4.30	-14.80	4.44	**-14.94**
Average value and deviation[b]:								**-14.79±0.19**
1. $CH_3CCl_2O^{\bullet}$ +CH_4 —› $CH_3^{\bullet}$ + CH_3CCl_2OH	1.40	-24.41	-1.56	-21.45	-2.66	-20.35	-1.68	-21.33
2. $CH_3CCl_2O^{\bullet}$ + C_2H_6 —› $C_2H_5^{\bullet}$+ CH_3CCl_2OH	-3.36	-23.32	-6.26	-20.42	-5.64	-21.04	-5.34	-21.34
3. $CH_3CCl_2O^{\bullet}$ + CH_3Cl —› $CH_2Cl^{\bullet}$+ CH_3CCl_2OH	-4.64	-23.78	-7.65	-20.77	-7.71	-20.71	-7.06	-21.36
4. $CH_3CCl_2O^{\bullet}$ + CH_3OH —› $CH_3O^{\bullet}$+ CH_3CCl_2OH	-6.07	-17.47	-4.95	-18.59	-7.22	-16.32	-1.74	**-21.80**
5. $CH_3CCl_2O^{\bullet}$ + C_2H_5OH —› $C_2H_5O^{\bullet}$ + CH_3CCl_2OH	-6.26	-17.24	-5.36	-18.14	-7.13	-16.37	-1.68	**-21.82**
6. $CH_3CCl_2O^{\bullet}$ +CH_4 —› $CH_3O^{\bullet}$ + CH_3CHCl_2	9.07	-18.17	7.96	-17.06	8.16	-17.26	12.79	**-21.89**
7. $CH_3CCl_2O^{\bullet}$ + C_2H_6 —› $C_2H_5O^{\bullet}$ + CH_3CHCl_2	3.41	-18.16	2.57	-17.32	2.68	-17.43	7.13	**-21.88**
Average value and deviation[b]:								**-21.85±0.04**
1. $CH_3C^{\bullet}ClOH$ + CH_4 —› $CH_3^{\bullet}$ + $CH_3CHClOH$	12.83	-28.75	11.79	-27.71	10.02	-25.94	9.99	**-25.91**
2. $CH_3C^{\bullet}ClOH$ + C_2H_6 —› $C_2H_5^{\bullet}$+ $CH_3CHClOH$	8.07	-27.66	7.14	-26.73	7.04	-26.63	6.33	**-25.92**
3. $CH_3C^{\bullet}ClOH$+CH_3Cl —› $CH_2Cl^{\bullet}$ + $CH_3CHClOH$	6.79	-28.12	5.72	-27.05	4.97	-26.30	4.60	**-25.93**
4. $CH_3C^{\bullet}ClOH$+CH_3OH—›$C^{\bullet}H_2OH$+$CH_3CHClOH$	2.25	-26.77	2.23	-26.75	1.74	-26.26	1.42	**-25.94**
5. $CH_3C^{\bullet}ClOH$+C_2H_5OH—›$CH_3C^{\bullet}HOH$+$CH_3CHClOH$	0.23	-26.05	0.21	-26.03	0.75	-26.57	0.10	**-25.92**
Average value and deviation[b]:								**-25.92±0.01**
1. $C^{\bullet}H_2CHClOH$ + CH_4 —› $CH_3^{\bullet}$ + $CH_3CHClOH$	5.17	-21.09	4.42	-20.34	0.81	-16.73	1.69	**-17.61**
2. $C^{\bullet}H_2CHClOH$ + C_2H_6 —› $C_2H_5^{\bullet}$ + $CH_3CHClOH$	0.41	-20.00	-0.23	-19.36	-2.17	-17.42	-1.97	**-17.62**
3. $C^{\bullet}H_2CHClOH$ +CH_3Cl—›$CH_2Cl^{\bullet}$ + $CH_3CHClOH$	-0.87	-20.46	-1.66	-19.67	-4.24	-17.09	-3.70	**-17.63**
4.$C^{\bullet}H_2CHClOH$+CH_3OH›$C^{\bullet}H_2OH$+$CH_3CHClOH$	-5.41	-19.11	-5.15	-19.37	-7.47	-17.05	-6.88	**-17.64**
5.$C^{\bullet}H_2CHClOH$+C_2H_5OH›$CH_3C^{\bullet}HOH$+CH_3CHCH	-7.42	-18.40	-7.16	-18.66	-8.46	-17.36	-8.20	**-17.62**
Average value and deviation[b]:								**-17.62±0.01**
1. $C^{\bullet}H_2CCl_2OH$ + CH_4 —› $CH_3^{\bullet}$ + CH_3CCl_2OH	3.89	-26.90	3.31	-26.32	-0.11	-22.90	0.82	**-23.83**
2. $C^{\bullet}H_2CCl_2OH$ + C_2H_6 —› $C_2H_5^{\bullet}$+ CH_3CCl_2OH	-0.87	-25.81	-1.34	-25.34	-3.09	-23.59	-2.84	**-23.84**
3. $C^{\bullet}H_2CCl_2OH$ +CH_3Cl —› $CH_2Cl^{\bullet}$ + CH_3CCl_2OH	-2.14	-26.28	-2.77	-25.65	-5.17	-23.25	-4.56	**-23.86**
4. $C^{\bullet}H_2CCl_2OH$ +CH_3OH—›$C^{\bullet}H_2OH$ + CH_3CCl_2OH	-6.69	-24.92	-6.26	-25.35	-8.39	-23.22	-7.75	**-23.86**
5.$C^{\bullet}H_2CCl_2OH$+C_2H_5OH—›$CH_3C^{\bullet}HOH$+ CH_3CCl_2OH	-8.70	-24.21	-8.27	-24.64	-9.39	-23.52	-9.06	**-23.85**
								-23.85±0.01

[a] Reaction enthalpies include thermal correction and zero-point energy. Units in kcal/mol.
[b] Average value calculated at the CBSQ//B3 level, and the deviation are between the
isodesmic reactions.

The error limits of $\Delta H_f^o{}_{298}$ for above species are calculated by adding the deviations between the isodesmic reactions and the maximum uncertainties in the $\Delta H_f^o{}_{298}$ of reference species.

2.3.3.3 Comparison with Literature Enthalpies. The $\Delta H_f^o{}_{298}$ for monochloroethanol and the corresponding radicals are found in literature for comparisons. Sekušak et al.[61] estimated $\Delta H_f^o{}_{298}$ of $CH_3CHClOH$ to be −69.7 kcal/mol by Benson's group additivity method, and this is in agreement with our recommend value, −68.63 ± 1.24 kcal/mol. Sekušak et al. also calculated the $\Delta H_f^o{}_{298}$ of $C^•H_2CHClOH$ at the MP2/aug-cc-pVTZ level to be −23.0 kcal/mol by reaction $CH_2CHCl + OH^• \rightarrow C^•H_2CHClOH$, which is a non-isodesmic reaction. Wallington et al.[62] estimated the $\Delta H_f^o{}_{298}$ of $CH_3CHClO^•$ to be −18.9 kcal/mol by assuming that the difference in the $\Delta H_f^o{}_{298}$ between chloromethoxy and methoxy radicals is the same as that between α-chloroethoxy and ethoxy radicals. Hou et al.[63] calculated the $\Delta H_f^o{}_{298}$ for $CH_3CHClO^•$, $CH_3C^•ClOH$ and $C^•H_2CHClOH$ at the G2(MP2, SVP) level to be −17.8, −29.7, and −21.3 kcal/mol, respectively; however, they did not provide calculation details or indicate the method of analysis. The recommended $\Delta H_f^o{}_{298}$ values for $CH_3CHClO^•$, $CH_3C^•ClOH$ and $C^•H_2CHClOH$ are consistently 3 to 4 kcal/mol higher than data estimated by Hou et al.[9] The consistent difference between our values and those of Hou et. al. could result from the differences in $\Delta H_f^o{}_{298}$ of the parent $CH_3CHClOH$, which is used in each working reaction.

The G3MP2 calculations for the two saturated chloroethanols show excellent agreement with the other calculations. The precision of our calculated enthalpies on $CH_3CHClOH$ over a range of calculation methods and working reactions does not provide any support for a different value. The good agreement observed over the several

calculation levels for α-chloroethanol and the corresponding radicals provides support that our calculations are consistent across different calculation methods. The QCISD(T) results also indicate that our values are consistent with HF and MP2 calculations. The high level QCISD(T)/6-31G(d,p), CBSQ//B3, and G3MP2 calculations all predict very similar enthalpies. The recommended data are based on analysis of conformer energies from internal rotations and use of the lowest energy conformers.

2.3.3.4 Enthalpy of Rotational Conformers. Two conformers are present in chloro-ethanols and hydroxyl chloroethyl radicals (shown in Figures 2.3, 2.4 and 2.5); one is R--H (R = CH_3 or CH_2) anti conformer and the other is R--H gauche conformer. The total electronic energies of these conformers are calculated at the B3LYP/6-31G(d,p), B3LYP/6-311+G(3df,2p), QCISD(T)/6-31G(d,p) and CBSQ//B3LYP/6-31G(d,p) calculation levels. The energy differences between the conformers are listed in Table 2.3.

Table 2.3 $\Delta H_f^o{}_{298}$ of Conformers and Relative Fraction

	ΔE of conformers (kcal/mol)				$\Delta H_f^o{}_{298}{}^c$	relative	final $\Delta H_f^o{}_{298}$
	B3LYP /6-31G(d,p)	B3LYP/6-311+G(3df,2p)	QCISD(T) /6-31G(d,p)	CBSQ//B3LYP /6-31G(d,p)	(kcal/mol)	fraction (%)	(kcal/mol)
$CH_3CHClOH(1)^a$					−68.72	59.18	
$CH_3CHClOH(1)^b$	0.17	0.44	0.24	0.22	−68.50	40.82	−68.63
$CH_3CCl_2OH(1)^a$					−75.75	99.20	
$CH_3CCl_2OH(2)^b$	4.07	3.66	3.49	3.27	−72.48	0.40	−75.72
$CH_3C^•ClOH(1)^a$					−25.92	98.79	
$CH_3C^•ClOH(1)^b$	3.79	3.16	3.26	2.61	−23.32	1.21	-25.89
$C^•H_2CHClOH(1)^a$					−17.62	62.79	
$C^•H_2CHClOH(1)^b$	0.59	0.75	0.36	0.31	−17.32	37.21	−17.51
$C^•H_2CCl_2OH(1)^a$					−23.85	97.88	
$C^•H_2CCl_2OH(2)^b$	3.76	3.45	2.05	2.68	−21.17	1.06	−23.79

[a] The rotational conformer with the lowest energy. [b] The rotational conformer with higher energy. [c] Enthalpy of formation at 298 K calculated at the CBSQ//B3 level.

The $\Delta H_f^o{}_{298}$ of the rotational conformers are determined from values calculated at the CBSQ//B3 level using isodesmic reaction schemes. The statistical distribution and

overall $\Delta H_f^\circ{}_{298}$ of the chloroethanols and hydroxy-chloroethyl radicals are also listed in Table 2.3. It can be seen that energy difference between the conformers decreases for the higher level calculations. The energy differences at the CBSQ//B3 calculation level are used to calculate the statistical distribution of rotational conformers.

2.3.3.5 Bond Energies. The RO—H, R—OH, R—H, and R—Cl bonds dissociation energies are presented in Table 2.4. They are estimated using the $\Delta H_f^\circ{}_{298}$ of chloroethanols and the radicals from this work, plus reference radicals.

Table 2.4 Bond Energies

reaction series	bond energy (kcal/mol)
RO—H	
$CH_3CH_2OH \rightarrow CH_3CH_2O^\bullet + H^\bullet$	104.32
$CH_3CHClOH \rightarrow CH_3CHClO^\bullet + H^\bullet$	105.94
$CH_3CCl_2OH \rightarrow CH_3CCl_2O^\bullet + H^\bullet$	105.97
R—α-H	
$CH_3CH_2OH \rightarrow CH_3C^\bullet HOH + H^\bullet$	94.88
$CH_3CHClOH \rightarrow CH_3C^\bullet ClOH + H^\bullet$	94.84
R—β-H	
$CH_3CH_2OH \rightarrow C^\bullet H_2CH_2OH + H^\bullet$	102.52
$CH_3CHClOH \rightarrow C^\bullet H_2CHClOH + H^\bullet$	103.22
$CH_3CCl_2OH \rightarrow C^\bullet H_2CCl_2OH + H^\bullet$	104.03
R—Cl	
$CH_3CHClOH \rightarrow CH_3C^\bullet HOH + Cl^\bullet$	84.21
$CH_3CCl_2OH \rightarrow CH_3C^\bullet ClOH + Cl^\bullet$	78.75
R—ROH	
$CH_3CH_2OH \rightarrow CH_3^\bullet + C^\bullet H_2OH$	86.97
$CH_3CHClOH \rightarrow CH_3^\bullet + C^\bullet HClOH$	88.99
$CH_3CCl_2OH \rightarrow CH_3^\bullet + C^\bullet Cl_2OH$	90.00
R—OH	
$CH_3CH_2OH \rightarrow CH_3CH_2^\bullet + OH^\bullet$	94.35
$CH_3CHClOH \rightarrow CH_3CHCl^\bullet + OH^\bullet$	97.21
$CH_3CCl_2OH \rightarrow CH_3CCl_2^\bullet + OH^\bullet$	97.58

The R—OH bond energies increase from 94.35 kcal/mol in CH_3CH_2–OH to 97 kcal/mol in CH_3CHCl–OH and CH_3CCl_2–OH. The second chlorine does not appear to affect an increase on the R—OH bond energies. This can be explained by a negative

hyperconjugation effect. The hydroxyl group includes two nonbonding e⁻ pairs centered on oxygen, one pair can interact strongly with σ^* (C-Cl$_1$) orbital, however, the other pair cannot effectively overlap with σ^* (C-Cl$_2$) orbital. The RO—H bond energy for mono, and dichloroethanol increases 1.6 kcal/mol relative to that of ethanol; this is because the O—H bond is heterolytic rather than homolytic, and it is slightly stabilized by negative hyperconjugation even though the O—H bond is not directly perturbed by the chlorine(s).[44]

The C—Cl bond energies decrease from 84.21 to 78.75 kcal/mol with successive addition of chlorine. However, the C—COH bond energy increases from 86.97 in CH_3–CH_2OH to 88.99 in CH_3–$CHClOH$ and to 90.00 kcal/mol in CH_3–CCl_2OH. The C—α-H bond energies in ethanol and chloroethanol are quite similar; they show a very slight decrease from 94.88 to 94.84 with the mono-chlorine substitution. Normally it is expected a decrease in bond energy on the C—α-H bond in chloroethanol relative to ethanol using the trends of C—H bond energies in the series: CH_4, CH_3Cl, CH_2Cl_2, and $CHCl_3$, and CH_3OH, CH_2ClOH, and $CHCl_2OH$ studied previously.[46] But no indication of this trend is found in the C—α-H bond strength of CH_3CH_2OH and $CH_3CHClOH$. In contrast, the C—β-H bond energies in CH_3CH_2OH, $CH_3CHClOH$ and CH_3CCl_2OH show a consistent increase: 102.52, 103.22 and 104.03 kcal/mol, respectively.

2.3.4 Entropy and Heat Capacity

S^o_{298} and $C_p(T)$'s calculation results using the B3LYP/6-31G(d,p) determined geometries and harmonic frequencies are summarized in Table 2.5. Harmonic vibrational frequencies and moments of inertia are listed in Table 2.6.

Table 2.5 Ideal Gas-phase Thermodynamic Properties [a]

species		$\Delta H_{f\,298}^{\circ}$ [b]	S°_{298} [c]	C_p300 [c]	C_p400	C_p500	C_p600	C_p800	C_p1000	C_p1500
CH_3CH_2OH	TVR [d]		59.12	12.11	15.57	19.00	22.05	27.00	30.76	36.79
(3)*	I.R. [e]		3.66	2.17	2.26	2.21	2.08	1.81	1.60	1.31
	I.R. [f]		4.00	1.61	1.45	1.33	1.25	1.15	1.10	1.05
	Total [g]	−56.12 ± 0.2	66.78	15.89	19.29	22.54	25.38	29.97	33.47	39.15
$CH_3CHClOH$	TVR [d]		67.13	15.25	18.94	22.29	25.13	29.56	32.83	38.02
(3)*	I.R. [e]		4.22	2.07	2.17	2.12	2.01	1.76	1.57	1.30
(2)^	I.R. [f]		2.52	1.80	2.05	2.15	2.17	2.07	1.90	1.56
	Total [g]	-68.63±1.24	75.22	19.12	23.15	26.56	29.31	33.39	36.31	40.88
CH_3CCl_2OH	TVR [d]		71.64	19.14	22.91	26.03	28.56	32.36	35.09	39.36
(3)*	I.R. [e]		3.93	1.91	2.09	2.16	2.15	2.01	1.83	1.49
	I.R. [f]		1.10	1.95	2.76	3.32	3.52	3.23	2.71	1.84
	Total [g]	-75.72±1.31	76.77	23.00	27.75	31.51	34.23	37.60	39.63	42.68
$CH_3CH_2O^{\bullet}$	TVR [d]		61.74	13.44	16.54	19.52	22.16	26.41	29.63	34.67
(3)*	I.R. [e]		4.59	2.08	1.98	1.82	1.67	1.45	1.31	1.15
	Total [g]	−3.90±1.27	66.33	15.52	18.52	21.34	23.83	27.86	30.94	35.82
$CH_3CHClO^{\bullet}$	TVR [d]		69.42	16.06	19.51	22.52	25.01	28.80	31.56	35.80
(3)*	I.R. [e]		4.21	2.07	1.96	1.90	1.84	1.73	1.63	1.42
(2)^	Total [g]	-14.79±2.90	73.63	18.13	21.47	24.42	26.85	30.53	33.19	37.22
$CH_3CCl_2O^{\bullet}$	TVR [d]		74.74	20.14	23.37	26.02	28.14	31.32	33.58	37.00
(3)*	I.R. [e]		4.19	2.07	2.18	2.14	2.04	1.80	1.60	1.31
	Total [g]	-21.85±2.82	78.93	22.21	25.55	28.16	30.18	33.12	35.18	38.31
$CH_3C^{\bullet}HOH$	TVR [d]		60.39	12.30	15.28	18.11	20.58	24.54	27.55	32.42
(3)*	I.R. [e]		5.22	1.57	1.42	1.32	1.25	1.16	1.11	1.05
	I.R. [f]		3.31	1.52	1.66	1.70	1.69	1.60	1.49	1.30
	Total [g]	−13.34±0.84	68.92	15.39	18.36	21.13	23.52	27.30	30.15	34.77
$CH_3C^{\bullet}ClOH$	TVR [d]		67.03	15.00	18.14	20.91	23.23	26.80	29.43	33.57
(3)*	I.R. [e]		4.84	2.06	1.88	1.69	1.54	1.35	1.24	1.11
	I.R. [f]		1.25	2.18	2.99	3.41	3.45	2.98	2.45	1.68
	Total [g]	-25.89±2.13	73.26	19.24	23.01	26.02	28.22	31.13	33.12	36.36
$C^{\bullet}H_2CH_2OH$	TVR [d]		60.84	12.94	15.97	18.77	21.17	24.99	27.88	32.58
(1)*[a]	I.R. [e]		4.86	1.42	1.29	1.21	1.15	1.09	1.06	1.02
	I.R. [f]		3.36	2.28	2.09	1.84	1.65	1.40	1.27	1.12
	Total [g]	-5.70±0.85	69.06	16.64	19.35	21.82	23.97	27.48	30.21	34.72
$C^{\bullet}H_2CHClOH$	TVR [d]		71.40	16.06	19.26	21.94	24.10	27.37	29.78	33.67
(1)*[a]	I.R. [e]		3.21	2.05	2.27	2.34	2.30	2.09	1.86	1.48
(2)^	I.R. [f]		2.40	2.18	2.27	2.28	2.24	2.07	1.88	1.53
	Total [g]	-17.51±2.13	78.33	20.29	23.80	26.56	28.64	31.53	33.52	36.68
$C^{\bullet}H_2CCl_2OH$	TVR [d]		74.63	20.01	23.29	25.72	27.57	30.20	32.06	35.04
(2)*	I.R. [e]		4.13	1.79	1.82	1.76	1.68	1.52	1.39	1.21
	I.R. [f]		1.31	2.07	2.80	3.24	3.34	2.99	2.51	1.74
	Total [g]	-23.79±2.13	80.30	23.87	27.90	30.72	32.59	34.71	35.96	37.99

[a] Thermodynamic properties are referred to a standard state of an ideal gas of at 1 atm.
[b] Units in kcal/mol. [c] Units in cal/mol/K. [d] The sum of contributions from translations, external rotations, and vibrations. [e] Contribution from internal rotation about the C—C bond. [f] Contribution from internal rotation about the C—O bond. [g] Symmetry number is taken into account (–Rln(symmetry number)). * Symmetry number. *[a] –CH$_2$ group is not planar. ^ Optical isomer number.

Table 2.6 Harmonic Vibrational Frequencies (cm^{-1})

species	frequencies (based on B3LYP/6-31G(d,p) level)										moments of inertia amu-Bohr^2
CH$_3$CH$_2$OH	270.2	317.1	420.1	807.4	892.8	1066.5	1082.6	1144.9	1288.0	1387.9 1412.4	52.5
	1432.9	1504.1	1508.0	1532.7	2987.0	3035.4	3082.5	3106.5	3127.0	3830.3	197.4
											223.2
CH$_3$CHClOH	249.1	310.2	356.2	438.7	481.0	604.3	927.3	1033.5	1074.1	1182.5 1298.1	200.8
	1304.0	1411.5	1463.3	1495.9	1502.1	3064.6	3077.6	3143.2	3167.6	3809.2	407.2
											562.0
CH$_3$CCl$_2$OH	255.7	260.5	279.7	361.9	372.9	427.8	478.3	557.9	655.6	965.5 1055.4	484.3
	1099.7	1236.8	1373	1431.3	1494.2	1492.6	3077.5	3157.9	3186.6	3788.3	728.3
											861.3
CH$_3$CH$_2$O$^\bullet$	199.2	333.0	434.0	870.5	896.2	1084.7	1100.9	1244.1	1354.8	1398.6 1420.6	45.7
	1501.1	1511.2	2896.4	2926.9	3049.2	3123.0	3133.9				189.5
											213.0
CH$_3$CHClO$^\bullet$	234.7	312.0	345.6	374.7	597.4	903.8	917.9	1019.5	1151.1	1175.3 1204.7	186.5
	1400.3	1487.3	1499.3	2950.4	3075.2	3166.2	3180.3				407.2
											552.6
CH$_3$CCl$_2$O$^\bullet$	198.9	251.7	273.4	339.3	355.1	387.0	438.7	588.6	930.0	1023.3 1086.3	447.8
	1243.4	1409.0	1485.6	1489.6	3072.7	3158.3	3178.1				737.1
											861.6
CH$_3$C$^\bullet$HOH	200.7	355.0	407.4	603.1	920.4	1025.8	1064.8	1208.4	1319.8	1410.0 1448.5	40.7
	1482.5	1502.5	2952.4	3024.8	3114.6	3196.2	3801.4				192.6
											220.0
CH$_3$C$^\bullet$ClOH	193.0	318.1	378.5	391.0	472.5	587.4	961.2	1051.1	1057.2	1267.9 1358.1	192.1
	1424.1	1483	1492.9	3013.6	3103	3154.5	3793.4				388.7
											560.4
C$^\bullet$H$_2$CH$_2$OH	155.2	276.2	401.3	458.2	865.7	967.8	1071.6	1124.1	1221.4	1276.8 1430.8	45.0
	1475.6	1510.3	2876.7	2945.5	3173.4	3286.4	3822.8				180.6
											212.7
C$^\bullet$H$_2$CHClOH	246.8	266.0	314.4	425.1	448.3	508.5	666.5	938.4	1072.1	1163.4 1234.6	192.2
	1299.5	1436.1	1506.7	3113.3	3188.6	3306.9	3810.3				413.8
											560.9
C$^\bullet$H$_2$CCl$_2$OH	16.1	247.6	250.9	345.4	372.9	414.9	449.8	539.2	556.2	665.6 957.3	471.5
	1056.9	1241.6	1386.1	1458.0	3199.8	3330.3	3797.2				718.7
											854.6

The two lowest frequencies (one in CH$_3$CH$_2$O$^\bullet$, CH$_3$CHClO$^\bullet$ and CH$_3$CCl$_2$O$^\bullet$) are omitted in calculation of S^o_{298} and $C_p(T)$'s; but their contributions are placed by values from analysis of the internal rotations. TVR, represent the sum of the contributions from translation, vibration and external rotation for S^o_{298} and $C_p(T)$'s. I.R., represent the contributions from hindered internal rotations about C—C and C—O bonds for S^o_{298} and $C_p(T)$'s. The calculations are based on optimized geometries and rotational potential

curves from the B3LYP/6-31G(d,p) data. There are differences in barrier height calculated at the B3LYP/6-31G(d,p) and the MP2(FULL)/6-31G(d) levels of theory, as discussed in the rotation barrier section. The resulting differences in S^o_{298} and $C_p(T)$'s are however small. In the most extreme case, the barrier height varies by 2 kcal/mol for $C^\bullet H_2CCl_2OH$ in the two calculations.

The resulting difference in the contribution to S^o_{298} is ca. 0.7 cal/mol-K, and the maximum difference for the contribution to $C_p(T)$'s is ca. 0.5 cal/mol-K. This indicates that the maximum error for the contribution to S^o_{298} and $C_p(T)$'s from one internal rotor is less than 0.7 cal/mol-K.

2.3.5 Group Additivity Values

Group additivity[64] is a straightforward and reasonably accurate calculation method to estimate thermodynamic properties of hydrocarbons and oxygenated hydrocarbons; it is particularly useful for application to larger molecules and codes or databases for thermochemical properties and reaction mechanism generation. The C/C/Cl/H/O and C/C/Cl$_2$/O group values are derived from the thermodynamic property data of $CH_3CHClOH$ and CH_3CCl_2OH respectively. The group values for $\Delta H^o_{f\,298}$ and C_p's of C/C/Cl/H/O are calculated on the basis of:

$$(CH_3CHClOH) = (C/C/Cl/H/O) + (C/C/H_3) + (O/C/H)$$

and S^o_{298} of C/C/Cl/H/O is calculated on the basis of:

$$(CH_3CHClOH) = (C/C/Cl/H/O) + (C/C/H_3) + (O/C/H) + Rln(OI) - Rln(\sigma)$$

where R = 1.987 cal/mol K, OI stands for optical isomer number and σ symmetry number. The group values of C/C/Cl$_2$/O are estimated in the same manner. The

thermochemical properties on $C/C/H_3$ and $O/C/H$ group are taken from the existing literature value.[65] The two derived carbon-chlorine-oxygen group values are listed in Table 2.6, which shows that the group values for $\Delta H_f^{\circ}{}_{298}$ decrease with increased number of chlorine atom.

Table 2.7 Group Values

Groups	$\Delta H_f^{\circ}{}_{298}{}^a$	$S^{\circ}{}_{298}{}^b$	C_p300^b	C_p400	C_p500	C_p600	C_p800	C_p1000	C_p1500
$C/C/H_3{}^{65}$	-10.20	30.41	6.19	7.84	9.40	10.79	13.02	14.77	17.58
$O/C/H^{65}$	-37.90	29.07	4.30	4.50	4.82	5.23	6.02	6.61	7.44
$C/C/Cl/H/O$	-20.53	16.54	8.63	10.81	12.34	13.29	14.35	14.93	15.86
$C/C/Cl_2/O$	-27.62	19.47	12.51	15.41	17.29	18.21	18.56	18.25	17.66

^{a} Units in kcal/mol. ^{b} Units in cal/mol-K.

2.3.6 Hydrogen Bond Increment Group Values

A method to estimate thermochemical properties for radicals from the corresponding properties of the parent with a H atom bonded to the radical site using a single group to modify the parent properties (hydrogen bond increment (HBI) group) has been reported by Lay et al.[66] A HBI group for $\Delta H_f^{\circ}{}_{298}$ reflects the enthalpy change due to loss of a H atom[66] from a stable parent molecule in the form of the R—H bond energy. Hydrogen Bond Increment group values for the chloro-oxy-ethyl radicals are derived using the thermodynamic property data of chloroethoxy and hydroxy-chloroethyl radicals and parent chloroethanols.

As an example, the bond energy of CH_3CHClO—H is based on the $\Delta H^{\circ}{}_{rxn, 298}$ of the homolytic reaction: $(CH_3CHClOH) = (CH_3CHClO^{\bullet}) + H$

$\Delta S^{\circ}{}_{298}$ and ΔC_p are determined more directly, as the differences in respective properties of the molecule versus the radical in such a way that the HBI values for $S^{\circ}{}_{298}$ and $C_p(T)$ are added to the parent values to form the radical.

HBI $C_p(T_i)$ (CH$_3$CHClO$^\bullet$) = $C_p(T_i)$ CH$_3$CHClO$^\bullet$ – $C_p(T_i)$ (CH$_3$CHClOH)

HBI S°_{298}(CH$_3$CHClO$^\bullet$) = S°_{298} (CH$_3$CHClO$^\bullet$) –S°_{298}(CH$_3$CHClOH) + Rln($\sigma_{CH3CHClO}$/$\sigma_{CH3CHClOH}$)

Effects for changes in symmetry between the radical and parent are not included in the HBI group; but are included in evaluation of the entropy of each species separately. The following species have optical isomer number of two due to the different constituents on the carbon bonded with chlorine: CH$_3$CHClOH, CH$_3$CHClO$^\bullet$, and C$^\bullet$H$_2$CHClOH. The HBI values for other radical species are estimated in the same manner as CH$_3$CHClO$^\bullet$ above and they are listed in Table 2.7.

Table 2.8 Hydrogen Bond Increment (HBI) Group Values

Groups	bond energy[a]	S°_{298}[b]	C_p300[b]	C_p400	C_p500	C_p600	C_p800	C_p1000	C_p1500
CH$_3$CH$_2$O$^\bullet$	104.32	0.93	-0.37	-0.77	-1.20	-1.56	-2.11	-2.52	-3.33
CH$_3$CHClO$^\bullet$	105.94	-1.59	-0.99	-1.68	-2.14	-2.46	-2.86	-3.12	-3.66
CH$_3$CCl$_2$O$^\bullet$	105.97	2.16	-0.79	-2.20	-3.35	-4.05	-4.48	-4.45	-4.37
CH$_3$C$^\bullet$HOH	94.88	2.14	-0.50	-0.93	-1.41	-1.87	-2.67	-3.31	-4.38
CH$_3$C$^\bullet$ClOH	94.84	-1.96	0.12	-0.14	-0.54	-1.09	-2.26	-3.19	-4.52
C$^\bullet$H$_2$CH$_2$OH	102.52	0.09	0.75	0.06	-0.72	-1.41	-2.48	-3.26	-4.42
C$^\bullet$H$_2$CHClOH	103.22	0.93	1.17	0.65	0.00	-0.67	-1.86	-2.79	-4.20
C$^\bullet$H$_2$CCl$_2$OH	104.03	2.73	0.88	0.16	-0.78	-1.64	-2.89	-3.68	-4.69

[a] Units in kcal/mol. [b] Units in cal/mol-K.

The HBI group values for bond energy of CH$_3$CH$_2$O$^\bullet$ and CH$_3$CHClO$^\bullet$ are similar to the values of CH$_3$O$^\bullet$ and CH$_2$ClO$^\bullet$ derived from previous work,[46] ca. 105 kcal/mol. The HBI group values for the bond energy of CH$_3$C$^\bullet$HOH and CH$_3$C$^\bullet$ClOH are similar to those of C$^\bullet$H$_2$OH and C$^\bullet$HClOH,[46] ca. 95 kcal/mol. The HBI group values of entropy for CH$_3$O$^\bullet$ and CCl$_3$O$^\bullet$ are –4.18 and –0.58 cal/mol-K from the previous work,[46] these two values did not include electronic orbital degeneracy of 2 by C$_{3v}$ symmetry because the optimized geometries at the B3LYP/6-31G(d,p) level resulted in C$_s$ symmetry for the two molecules. The C$_s$ symmetry is due to the Jahn-Taller distortion and a vibronic coupling

where the asymmetric vibrational e modes couple to the degenerate E electronic states.[67] Barckholtz et al.[67] report that an effective electronic degeneracy of $CH_3O^\bullet$ is 2 because of the dynamic nature of the Jahn-Taller effect and the relatively larger zero-point vibration energy in $CH_3O^\bullet$ (degeneracy is in addition to the spin states). When the electronic orbital degeneracy for $CH_3O^\bullet$ and $CCl_3O^\bullet$ is 2, the S^o_{298} for $CCl_3O^\bullet$ is 80.41 cal/mol-K rather than 79.03 cal/mol-K, and the HBI group values for entropy of $CH_3O^\bullet$ and $CCl_3O^\bullet$ are – 2.80 and 0.80 cal/mol-K. For $CH_3CH_2O^\bullet$, the substitution of a hydrogen in $CH_3O^\bullet$ with a methyl group perturbs the C_{3v} geometry and thus slightly lifts the electronic degeneracy present in $CH_3O^\bullet$. At room temperature, the HBI group value of entropy for $CH_3CH_2O^\bullet$ is –0.45 cal/mol-K without the electronic orbital degeneracy. However, Ramond et al.[68] report that the splitting between the ground $\tilde{A}^2A''$ and the first $\tilde{X}^2A'$ excited states of $CH_3CH_2O^\bullet$ is very small, 355±10 cm⁻¹. The effective electronic degeneracy of $CH_3CH_2O^\bullet$ at room temperature can then be considered as 2, and this gives the HBI group values of entropy for $CH_3CH_2O^\bullet$ is 0.93 cal/mol-K. The electronic degeneracy present in $CH_3O^\bullet$ for $CH_3CHClO^\bullet$ and $CH_3CCl_2O^\bullet$ radicals will be removed by the orbital splitting.

2.4 α-Chlorinated Propanol and Radicals

2.4.1 Geometries

The optimized geometric parameters along with vibrational frequencies and moments of inertia for six target species are presented in the Appendix (Table A.3). The lowest energy conformations of $(CH_3)_2CClOH$, $(CH_3)_2CClO^\bullet$ and $C^\bullet H_2CCl(OH)CH_3$ exhibit the

anomeric effect, i.e., a delocalization of the lone pair electron on the oxygen with the antibonding σ^* orbital of the C—Cl bond. Due to the anomeric effect, the C—O bond length decreases significantly with chlorine substitution (1.4296 Å in $(CH_3)_2CHOH$, 1.3843 Å in $(CH_3)_2CClOH$; 1.3749 Å in $(CH_3)_2CHO^{\bullet}$, 1.3178 Å in $(CH_3)_2CClO^{\bullet}$; 1.4354 Å in $C^{\bullet}H_2CH(OH)CH_3$ and 1.3674 Å in $C^{\bullet}H_2CCl(OH)CH_3$). The anomeric effect can also be seen in the C—Cl bond length, which is longer than a normal C—Cl bond (1.8995 Å in $(CH_3)_2CClOH$, 1.9094 Å in $(CH_3)_2CClO^{\bullet}$, 2.0598 Å in $C^{\bullet}H_2CCl(OH)CH_3$) as predicted by the DFT calculations. The C—Cl bond in $C^{\bullet}H_2CCl(OH)CH_3$ is 0.1 Å longer than in the other two chloro species due to hyperconjugation between $-CH_2^{\bullet}$ center and the $\sigma^*(C—Cl)$ molecular orbital in its lowest energy conformer. Because p-π orbital overlap implies transfer of electron density, the C—Cl bond becomes weaker and longer, while the C—C bond gets stronger and shorter. The C—C bond length in $C^{\bullet}H_2CCl(OH)CH_3$ is 1.44 Å which shorter than the normal, 1.53 Å. The MP2(full)/6-31g(d,p) geometry optimization predicts tight structures for these species, and gives the C—Cl bond length 1.8299 Å, 1.8294 Å, and 1.8640 Å, respectively; these data also suggest that an anomeric effect and hyperconjugation exist in these species.

The DFT calculations predict a non-planar structure for $-C^{\bullet}H_2$ group in 2-hydroxy-propyl and 2-chloro-2-hydroxy-propyl radicals, where the inversion frequencies for the methylene group are 566.0 and 672.8 cm^{-1}, respectively. The density functional optimized geometry for $(CH_3)_2CHOH$ gives the $\angle H_c$-C-O-H_o dihedral angle 180.0°, indicating that there is a mirror plane between the two methyl groups, i.e., C_s symmetry in $(CH_3)_2CHOH$. The density functional structure also predicts C_s symmetry in

$(CH_3)_2CHO^\bullet$. The symmetry number is assigned as 18 for $(CH_3)_2CHOH$ and $(CH_3)_2CHO^\bullet$ on the basis of these data.

2.4.2 Rotational Barriers

Potential energy as a function of torsion angle was determined by scanning the dihedral angles from 0° to 360° at 15° increments and allowing the remaining molecular structural parameters to be optimized at the B3LYP/6-31G(d,p) level. The $C^\bullet H_2CCl(OH)CH_3$ is an exception, here the C-Cl bond length was constrained when scanning the H_c-C-C-O and C-C-O-H dihedral angles in $C^\bullet H_2CCl(OH)CH_3$. This is a result of the weak C-Cl bond in this radical; it requires only 18 kcal/mol for β-scission to form 2-hydroxy propene + Cl atom. The barrier of a given rotation was then calculated as the difference between the highest points on the potential energy surface and the corresponding most stable conformer. The geometries at the points of minima and maxima were fully optimized when possible.

The calculated rotational barriers about the CH_3–C_{sp3} bond of the six target species are shown in Figure 2.6. All the curves for C_{sp3}–C_{sp3} torsion potential are symmetric and show a 3-fold symmetry with barriers between 2.72 and 4.26 kcal/mol. The barriers for the CH_3–C_{sp3} torsion of chloro-substituted species are higher than those of nonchlorinated species and the barriers for stable parent are higher than those of the corresponding radicals probably due to reduced steric effect by the radical carbon groups. Two C_{sp3}–C_{sp3} rotational curves for $(CH_3)_2CClOH$ are shown in Figure 2.6, and one is 0.55 kcal/mol higher than the other because the hydroxyl H atom orients toward one methyl group resulting in a steric interaction.
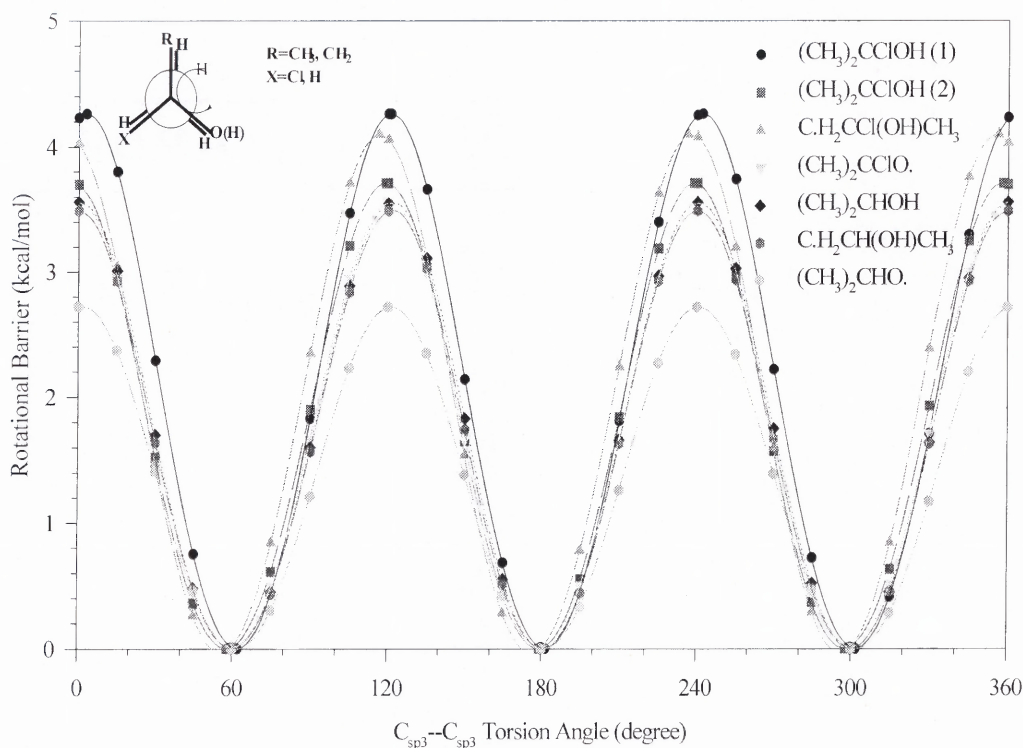
Figure 2.6 Potential barriers for internal rotation about the C—C bond of $(CH_3)_2CHOH$, $(CH_3)_2CClOH$, $(CH_3)_2CHO^\bullet$, $(CH_3)_2CClO^\bullet$, $C^\bullet H_2CH(OH)CH_3$ and $C^\bullet H_2CCl(OH)CH_3$.

Figure 2.7 shows the two-fold rotational barriers about the CH_2–C_{sp3} bond for the $C^\bullet H_2CCl(OH)CH_3$ and the $C^\bullet H_2CH(OH)CH_3$ radicals. The H--OH eclipsed conformer of $C^\bullet H_2CCl(OH)CH_3$ has the lowest energy due to the interaction between the H atom in --CH_2 group and the O atom (interatomic distance is 2.528 Å). The barrier height for $C^\bullet H_2CCl(OH)CH_3$ is 3.6 kcal/mol higher than that of $C^\bullet H_2CH(OH)CH_3$, probably still due to the electrostatic interaction between the Cl atom and the H atom on the -$C^\bullet H_2$ group (the interatomic distance 2.83 Å) on the barrier top.
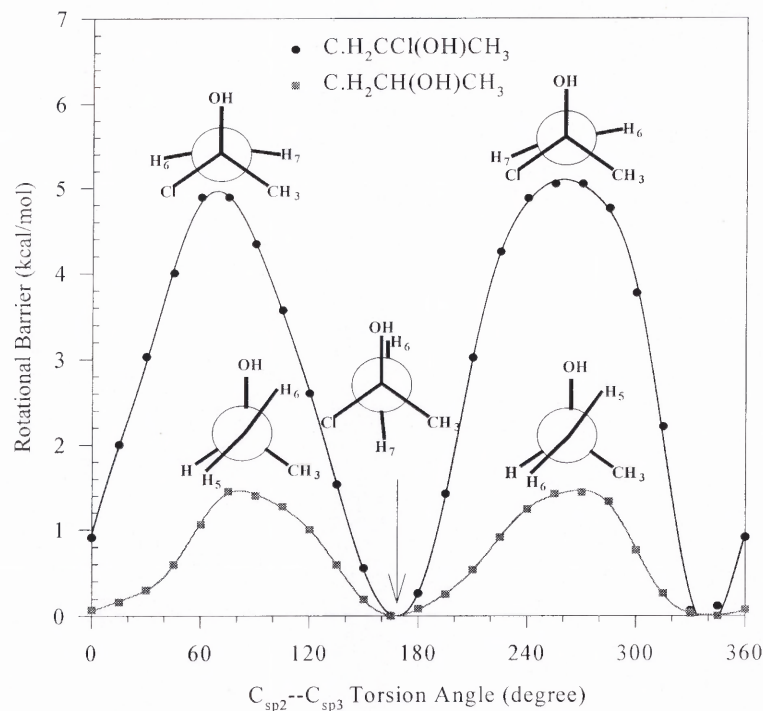
Figure 2.7 Potential barriers for internal rotation about the C—C bond of C·H₂CH(OH)CH₃ and C·H₂CCl(OH)CH₃.
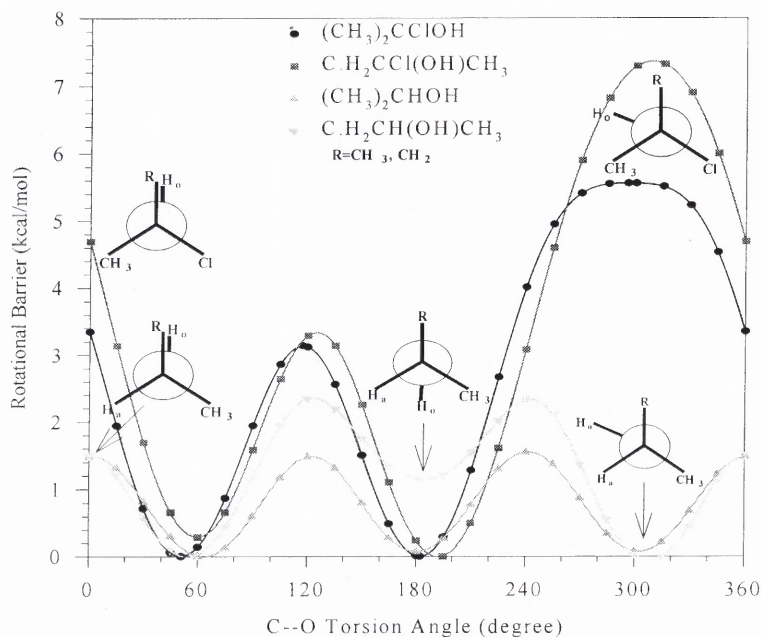
Figure 2.8 Potential barriers for internal rotation about the C—O bond of (CH₃)₂CClOH, (CH₃)₂CClOH, C·H₂CH(OH)CH₃ and C·H₂CCl(OH)CH₃.

The calculated rotational barriers about the C—O bond of $(CH_3)_2CClOH$, $C^\bullet H_2CCl(OH)CH_3$, $(CH_3)_2CHOH$, and $C^\bullet H_2CH(OH)CH_3$ are shown in Figure 2.8. There are three conformers in $(CH_3)_2CHOH$; two are the H_o-H_α gauche conformers (subscript "o" stands for oxygen atom), and one is the H_o-H_α anti conformer. The energy for the H_o-H_α anti conformer is only 0.08 kcal/mol lower than that of the H_o-H_α gauche conformer, so the three conformers should be equally populated at room temperature. For $C^\bullet H_2CH(OH)CH_3$, there are two H_o-CH_2 gauche conformers and one H_o-CH_2 anti conformer. The energy for the H_o-CH_2 anti conformer is 1.16 kcal/mol higher than that of H_o-CH_2 gauche conformer. For $C^\bullet H_2CCl(OH)CH_3$, the H_o-CH_2 gauche conformer is 0.29 kcal/mol higher than that of the H_o-CH_2 anti conformer. The maxima on the potential curves of $(CH_3)_2CClOH$ and $C^\bullet H_2CCl(OH)CH_3$ correspond to the structures where the hydroxyl H atom is anti to the Cl atom on the α-carbon due to anomeric effects. This phenomenon is similar to those in the chloromethanol and chloroethanol observed in the previous study.[46,59]

2.4.3 Enthalpy of Formation

The total electronic energies are determined at the B3LYP/6-31G(d,p), B3LYP/6-311+G(3df,2p) and CBSQ//B3LYP/6-31G(d,p) levels for chloropropanol and corresponding radicals. The spin expectation values, $<S^2>$, range from 0.760 to 0.786 for the target radicals, and suggest no significant error for pure doublet radicals due to spin contamination.

The $\Delta H_{f}^{o}{}_{298}$ values are estimated using total energies and isodesmic reactions. The accuracy of the enthalpies of formation obtained theoretically is controlled by several

factors: the level of sophistication applied to calculate the electronic energy, the reliability of the $\Delta H_f^o{}_{298}$ of the reference compounds, the uncertainty of the ZPVEs and the thermal corrections, and the choice of the isodesmic reactions. The uncertainty of ZPVEs and thermal correction are small relative to other errors. Scott and Radom[42] report rms errors $\pm$ 0.1 kcal/mol for ZPVE after scaling 0.9806 for B3LYP/6-31G(d) and rms errors of $\pm$ 0.01 kcal/mol for thermal correction from 0 to 298 K in DFT. We assume that the uncertainty from ZPVEs and the thermal correction in our calculation have the same error ranges and assign the cumulative ZPVEs and the thermal energy uncertainties to be 0.44 kcal/mol in an isodesmic reaction. The reaction enthalpies and $\Delta H_f^o{}_{298}$ values for 6 target species obtained from 8 isodesmic reactions are tabulated in Table A.4. The results for $\Delta H_f^o{}_{298}$ values in Table A.4 show good consistency for 6 target species over eight working reactions and the three calculation methods. DFT calculations show good agreement with the high level ab initio calculations, indicating the errors inherent in computations for different types of molecule are canceled to a significant extent and lead to reliable results. Ab initio calculations show remarkable consistency at the CBSQ//B3 level where the standard deviation is within 0.3 kcal/mol. The $\Delta H_f^o{}_{298}$ values for target radicals are based on the $\Delta H_f^o{}_{298}$ values of the parent molecules in this work. The calculated $\Delta H_f^o{}_{298}$ for $(CH_3)_2CHOH$ in this work is -69.19 kal/mol, which is similar to the results of Atkinson et al.,[69] -65.15; Frenkel et al.,[50] -65.18, Snelson et al.,[70] -65.19, and Cohen,[71] -65.20 kal/mol. The $\Delta H_f^o{}_{298}$ for $(CH_3)_2CHO^\bullet$ are calculated to be -11.87 kal/mol at the CBSQ//B3 level, which shows agreement with Ramond et al.'s value, -11.0 ± 1.2 kcal/mol,[68] which derived from the $\Delta H_f^o{}_{298}$ of $(CH_3)_2CHOH$ and electron affinities.

The recommended $\Delta H_f^{\circ}{}_{298}$ for $(CH_3)_2CHOH$, $(CH_3)_2CHO^{\bullet}$, $C^{\bullet}H_2(CH_3)CHOH$, $(CH_3)_2CClOH$, $(CH_3)_2CClO^{\bullet}$ and $C^{\bullet}H_2CCl(OH)CH_3$ are -69.19 ± 2.2, -11.85 ± 1.9, -14.95 ± 2.8, -79.83 ± 2.1, -25.88 ± 2.0, and -29.00 ± 2.8 kcal/mol, respectively, which are the average values from eight reactions for each species at the CBSQ//B3 calculation level, where the statistical distribution of rotational conformers is included.

The RO—H, R—OH, R—H and R—Cl bond dissociation energies in Table 2.8 were calculated using the $\Delta H_f^{\circ}{}_{298}$ values and the $\Delta H_f^{\circ}{}_{298}$ of reference radicals. These bond energies are very similar to those derived from chloromethanol and α-chloroethanol in previous work,[46,59] and a comparison for these bond energies derived from monochloro-alcohols is listed in Table 2.9. Bond energies on isopropanol for the methyl hydrogens are 102 kcal/mol, and the hydroxyl hydrogen bond energy is 105 kcal/mol. Bond energies in 2-chloro-2-propanol are 103 kcal/mol for the methyl hydrogens and 106 kcal/mol for the hydroxyl hydrogen.

Table 2.9 Bond Energies

reaction series	bond energy (kcal/mol)
RO—H	
$(CH_3)_2CHOH \longrightarrow (CH_3)_2CHO^{\bullet} + H^{\bullet}$	105.44
$(CH_3)_2CClOH \longrightarrow (CH_3)_2CClO^{\bullet} + H^{\bullet}$	106.05
R_{β}—H	
$(CH_3)_2CHOH \longrightarrow C^{\bullet}H_2CH(OH)CH_3 + H^{\bullet}$	102.34
$(CH_3)_2CClOH \longrightarrow C^{\bullet}H_2CCl(OH)CH_3 + H^{\bullet}$	102.93
R—Cl	
$(CH_3)_2CClOH \longrightarrow (CH_3)_2C^{\bullet}OH + Cl^{\bullet}$	83.15
R—ROH	
$(CH_3)_2CHOH \longrightarrow CH_3C^{\bullet}HOH + CH_3^{\bullet}$	86.67
$(CH_3)_2CClOH \longrightarrow CH_3C^{\bullet}ClOH + CH_3^{\bullet}$	88.76
R—OH	
$(CH_3)_2CHOH \longrightarrow (CH_3)_2C^{\bullet}H + OH^{\bullet}$	96.15
$(CH_3)_2CClOH \longrightarrow (CH_3)_2C^{\bullet}Cl + OH^{\bullet}$	95.94

Table 2.10 Bond Energy Derived from Monochloro-Alcohols

species	bond energy (kcal/mol)					
	RO—H	R—OH	R—Cl	R—ROH	R_α—H	R_β—H
CH_3OH	104.28	92.33	*	*	96.21	*
CH_2ClOH	105.04	95.20	83.02	*	95.71	*
CH_3CH_2OH	104.32	94.35	*	86.97	94.88	102.52
$CH_3CHClOH$	105.94	97.21	84.21	88.99	94.84	103.22
$(CH_3)_2CHOH$	105.44	96.15	*	86.67	91.69	102.34
$(CH_3)_2CClOH$	106.05	95.94	83.15	88.76	*	102.93

*Bond does not exist.

2.4.4 Entropy and Heat Capacity

The $S^o{}_{298}$ and $C_p(T)$'s (300 ≤ T/K ≤ 1500) calculation results using the B3LYP/6-31G(d,p) geometries and harmonic frequencies are summarized in Table 2.9. The torsion frequencies are omitted in the calculation of $S^o{}_{298}$ and $C_p(T)$; but we replace their contributions with values from analysis of the internal rotations. TVR, represents the sum of the contributions from translation, vibration and external rotation for $S^o{}_{298}$ and $C_p(T)$'s and was calculated using the program "SMCPS".[72] I. R., represents the contributions from hindered internal rotations about C—C and C—O bonds for $S^o{}_{298}$ and $C_p(T)$ and was calculated by the program "ROTATOR".[73]

This calculation is based on an optimized 3D atom coordinate for the lowest energy conformer, the respective connection to atoms of the bond about which rotation is occurring, and the coefficients of the Fourier expansion components from rotational potential curves.

The $C^\bullet H_2CH(OH)CH_3$ and $C^\bullet H_2CCl(OH)CH_3$ radicals have an optical isomer number of two due to the different constituents on the central carbon. The thermochemical properties of 2-propanol in Table 2.9 show agreement with the values

calculated by Chao[50] at TRC using the methods of statistical thermodynamics based on

spectral data.

Table 2.11 Ideal Gas-Phase Thermodynamic Properties [a]

species		$\Delta H^o_{f\,298}$ [b]	S^o_{298} [c]	C_p300 [c]	C_p400	C_p500	C_p600	C_p800	C_p1000	C_p1500
$(CH_3)_2CHOH$	TVR [d]		60.44	15.86	20.86	25.64	29.83	36.56	41.65	49.75
(18) [h]	I.R. [e]		4.21	2.23	2.25	2.16	2.02	1.69	1.40	0.89
	I.R. [e]		4.22	2.04	2.14	2.09	1.98	1.74	1.56	1.29
	I.R. [f]		4.02	1.58	1.45	1.34	1.26	1.16	1.11	1.05
	Total [g]	-65.19± 2.2	72.89	21.71	26.70	31.23	35.09	41.15	45.71	52.98
$(CH_3)_2CClOH$	TVR [d]		67.81	19.56	24.65	29.23	33.12	39.23	43.77	50.99
(9) [h]	I.R. [e]		4.16	2.04	2.14	2.11	2.01	1.78	1.59	1.31
	I.R. [e]		3.99	1.97	2.13	2.16	2.10	1.90	1.71	1.39
	I.R. [f]		2.46	1.71	1.98	2.10	2.13	2.04	1.89	1.56
	Total [g]	-79.83± 2.1	78.43	25.27	30.91	35.60	39.37	44.95	48.96	55.26
$(CH_3)_2CHO^{\bullet}$	TVR [d]		61.94	16.19	21.08	25.61	29.51	35.69	40.30	47.50
(18) [h]	I.R. [e]		4.52	2.23	2.13	1.96	1.79	1.53	1.36	1.08
	I.R. [f]		4.52	2.23	2.13	1.96	1.79	1.53	1.36	1.08
	Total [g]	-11.85± 1.9	70.98	20.66	25.34	29.52	33.09	38.75	43.02	49.66
$(CH_3)_2CClO^{\bullet}$	TVR [d]		70.57	20.45	25.19	29.37	32.88	38.33	42.36	48.66
(9) [h]	I.R. [e]		5.31	2.19	2.23	2.15	2.02	1.75	1.53	1.14
	I.R. [f]		5.31	2.19	2.23	2.15	2.02	1.75	1.53	1.14
	Total [g]	–25.88±2.0	81.18	24.84	29.65	33.67	36.92	41.84	45.42	50.93
$C^{\bullet}H_2CH(OH)CH_3$	TVR [d]		67.05	16.54	21.14	25.3	28.84	34.43	38.65	45.45
(3) [h]	I.R. [e]		4.64	1.74	1.54	1.39	1.29	1.18	1.12	1.05
(2) [i]	I.R. [e]		4.24	2.07	2.15	2.09	1.97	1.73	1.54	1.28
	I.R. [f]		3.49	2.19	1.97	1.75	1.58	1.36	1.24	1.11
	Total [g]	–14.95±2.8	81.19	22.54	26.79	30.53	33.69	38.70	42.55	48.90
$C^{\bullet}H_2CCl(OH)CH_3$	TVR [d]		73.44	20.21	24.81	28.72	31.95	36.94	40.65	46.61
(3) [h]	I.R. [e]		4.07	2.01	2.16	2.17	2.10	1.89	1.69	1.38
(2) [i]	I.R. [e]		2.89	2.00	2.33	2.49	2.51	2.33	2.08	1.61
	I.R. [f]		3.44	2.16	2.20	2.19	2.16	2.06	1.93	1.65
	Total [g]	–29.00±2.8	85.15	26.38	31.49	35.57	38.72	43.22	46.35	51.25

[a] Thermodynamic properties are referred to a standard state of an ideal gas of at 1 atm. [b] Units in kcal/mol. [c] Units in cal/mol/K. [d] The sum of contributions from translations, vibrations, and external rotations. [e] Contribution from internal rotation about the C—C bond. [f] Contribution from internal rotation about the C—O bond. [g] Symmetry number is taken into account (–Rln(symmetry number)). [h] Symmetry number. [i] Optical isomer number. –CH_2 group is not planar, and the standard entropies include the entropy of mixing of rotational conformations or optical conformations.

2.4.5 Relative Stability of the Alkyl and Alkoxy Radicals

The C—Cl bond is usually ca. 10 kcal/mol weaker than the C—C or C—H bonds and this should lead to interesting stabilities for the intermediate chloro-radicals in the atmosphere. Reaction scheme 1 shows the ΔH^{o}_{rxn} and E_a for the two non-chlorinated alkyl radicals undergoing β-scission to eliminate a methyl or an OH radical; the isopropoxy radical dissociation to CH_3CHO and methyl has a lower ΔH^{o}_{rxn} value with the transition state lying 13.22 kcal/mol above $(CH_3)_2CHO^{\bullet}$ calculated at the CBSQ//B3 level.

Reaction Scheme 1

	ΔH^{o}_{rxn} (kcal/mol)	E_a(kcal/mol)
$C^{\bullet}H_2CH(OH)CH_3 \rightarrow CH_2=CHCH_3 + OH^{\bullet}$	28.62	28.62
$C^{\bullet}H_2CH(OH)CH_3 \rightarrow syn\text{-}CH_2=CHOH + CH_3^{\bullet}$	19.18	29.02 (CBSQ)
$(CH_3)_2CHO^{\bullet} \rightarrow CH_3CHO + CH_3^{\bullet}$	6.97	13.22 (CBSQ)

Reaction scheme 2 shows the ΔH^{o}_{rxn} and E_a for Cl elimination from one secondary chlorocarbon radical where ΔH^{o}_{rxn} is 18 kcal/mol, but the chloro-isopropoxy radical has a similar bond strength for C—Cl and C—CH$_3$.

Reaction Scheme 2

	ΔH^{o}_{rxn} (kcal/mol)	E_a (kcal/mol)
$C^{\bullet}H_2CCl(OH)CH_3 \rightarrow CH_2=C(OH)CH_3 + Cl^{\bullet}$	18.01	18.01
$(CH_3)_2CClO^{\bullet} \rightarrow CH_3COCH_3 + Cl^{\bullet}$	2.57	2.57
$(CH_3)_2CClO^{\bullet} \rightarrow CH_3C(O)Cl + CH_3^{\bullet}$	2.67	10.75 (CBSQ)

The alkyl-alkoxy and chloroalkoxy radical systems are both unstable with short atmospheric lifetimes. We note that there is no barrier (above the ΔH^{o}_{rxn}) for the Cl elimination reaction of $C^{\bullet}H_2CCl(OH)CH_3$ and its half-life at 298 K can be qualitatively

estimated to be ~1.1 s; which is sufficient time for the radical to undergo association with O_2 under atmospheric and low temperature combustion conditions. Wu and Carr[74,75] reported the lifetime for $CH_2ClO^\bullet$ is less than 1 ms. Hou et al.[63] reported that the three-center elimination of HCl is the most favorable channel for $CH_3CHClO^\bullet$ decomposition, and estimated the lifetime of $CH_3CHClO^\bullet$ under the typical tropospheric condition to be 3.3 μs. The stability of these chloroalkoxy radicals is low, but these intermediate radicals are formed by $OH^\bullet$ radical addition to chloro-olefins in the atmosphere and by $OH^\bullet$, $O^\bullet$, and $HO_2^\bullet$ addition to unsaturated chlorocarbons in combustion environments. The thermochemical properties of these radicals are important in describing the reaction paths and the products of the first and second dissociation reactions.

2.4.6 Group Additivity Values and HBI Group Values

The $C/C_2/Cl/O$ group value in Table 2.12 was derived from the thermodynamic property data of $(CH_3)_2CClOH$. The group values for $\Delta H_f^{\circ}{}_{298}$ and $C_p(T)$ of $C/C_2/Cl/O$ were calculated on the basis of the reaction:

$$(CH_3CCl(OH)CH_3) = (C/C_2/Cl/O) + 2(C/C/H_3) + (O/C/H)$$
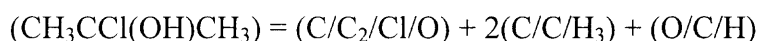
and $S^{\circ}{}_{298}$ of $C/C_2/Cl/O$ was calculated by considering symmetry correction:

$$(CH_3CCl(OH)CH_3) = (C/C_2/Cl/O) + 2(C/C/H_3) + (O/C/H) - Rln(\sigma)$$

where R = 1.987 cal/mol K, σ stands for symmetry number. The thermochemical properties for the $C/C/H_3$ and $O/C/H$ groups were taken from the literature.[65] $\Delta H_f^{\circ}{}_{298}$ in the HBI implementation group is the bond enthalpy of R—H cleavage reaction at the indicated site. $\Delta S^{\circ}{}_{298}$ and $\Delta C_p(T)$ in HBI groups are the differences in respective properties of the molecule and the radical; such that when HBI increment groups for

ΔS°_{298} and $\Delta C_p(T)$ are added to the parent, the result is the corresponding value for the radical.

Table 2.12 Central Group and HBI Group Values

Central group	$\Delta H_f^{\circ}{}_{298}$[b]	S°_{298}[c]	C_p300[c]	C_p400	C_p500	C_p600	C_p800	C_p1000	C_p1500
			Monocarbon-chloro-oxy-hydrocarbon central group						
C/Cl/H$_2$/O	−20.17	36.55	8.88	11.18	13.02	14.35	16.09	17.27	19.19
C/Cl$_2$/H/O	−27.98	41.93	12.61	15.71	17.73	18.80	19.62	19.94	20.60
C/Cl$_3$/O	−28.06	50.54	16.34	18.45	19.65	20.28	20.82	21.06	21.46
			Dicarbon-chloro-oxy-hydrocarbon central group						
C/C/Cl/H/O	-20.53	16.54	8.63	10.81	12.34	13.29	14.35	14.93	15.86
C/C/Cl$_2$/O	-27.62	19.47	12.51	15.41	17.29	18.21	18.56	18.25	17.66
			Tricarbon-chloro-oxy-hydrocarbon central group						
C/C$_2$/Cl/O	-21.53	-15.82	8.59	10.73	11.98	12.56	12.89	12.81	12.66

HBI group[a]	Bond energy[b]	S°_{298}[c]	C_p300[c]	C_p400	C_p500	C_p600	C_p800	C_p1000	C_p1500
			Alkoxy group						
CH$_3$O$^{\bullet}$	104.28	-2.80	-0.88	-0.83	-1.02	-1.28	-1.79	-2.26	-3.16
CCO$^{\bullet}$	103.65	-0.90	-0.52	-0.85	-1.24	-1.59	-2.11	-2.52	-3.32
C$_2$CO$^{\bullet}$	105.44	-1.90	-1.05	-1.36	-1.71	-2.00	-2.40	-2.69	-3.32
			Chloroalkoxy HBI group						
CClO$^{\bullet}$	105.04	-0.94	-1.00	-1.41	-1.85	-2.20	-2.69	-3.02	-3.63
CCClO$^{\bullet}$	105.94	-1.59	-0.99	-1.68	-2.14	-2.46	-2.86	-3.12	-3.66
CCCl$_2$O$^{\bullet}$	105.97	2.16	-0.79	-2.20	-3.35	-4.05	-4.48	-4.45	-4.37
C$_2$CClO$^{\bullet}$	106.11	2.75	-0.44	-1.26	-1.93	-2.45	-3.11	-3.54	-4.32
			Di, trichloromethoxy HBI group						
CCl$_2$O$^{\bullet}$	110.33	1.17	-1.33	-2.50	-3.28	-3.63	-3.71	-3.65	-3.81
CCl$_3$O$^{\bullet}$	109.01	0.80	-0.84	-1.30	-1.67	-1.95	-2.40	-2.77	-3.50
			Hydroxy-alkyl HBI group						
C$^{\bullet}$H$_2$OH	96.21	-2.15	0.44	0.34	-0.10	-0.67	-1.77	-2.68	-4.10
CC$^{\bullet}$OH	94.88	2.14	-0.50	-0.93	-1.41	-1.87	-2.67	-3.31	-4.38
			Hydroxy-α-chloroalkyl HBI group						
C$^{\bullet}$ClOH	95.71	0.10	0.70	0.72	0.19	-0.58	-2.04	-3.08	-4.47
C$^{\bullet}$Cl$_2$OH	97.44	2.26	-0.25	-1.97	-3.22	-3.90	-4.44	-4.64	-5.03
CC$^{\bullet}$ClOH	94.84	-1.96	0.12	-0.14	-0.54	-1.09	-2.26	-3.19	-4.52
			Hydroxy-β-(chloro)ethyl HBI group						
C$^{\bullet}$COH	102.52	0.09	0.75	0.06	-0.72	-1.41	-2.48	-3.26	-4.42
C$^{\bullet}$CClOH	103.22	0.93	1.17	0.65	0.00	-0.67	-1.86	-2.79	-4.20
C$^{\bullet}$CCl$_2$OH	104.03	2.73	0.88	0.16	-0.78	-1.64	-2.89	-3.68	-4.69
			Hydroxy-β-(chloro)propyl HBI group						
C$^{\bullet}$C(OH)C	102.26	4.74	0.83	0.10	-0.70	-1.40	-2.45	-3.16	-4.09
C$^{\bullet}$CCl(OH)C	102.81	4.54	1.11	0.59	-0.03	-0.65	-1.74	-2.62	-4.01

[a] H atoms are assumed to fill in carbon. [a] Units in kcal/mol. [b] Units in cal/mol-K.

Entropy values are intrinsic, i.e., the correction for spin degeneracy of the electronic state and gain and loss of an optical isomer are included when appropriate, but symmetry for either parent or radical is not included in HBI groups. Table 2.12 lists chloro-oxy-alkyl central group data from mono, di, and tri-carbon chloro-alcohols by this work and previous work.[46,59] The HBI group values for $C_2CO^\bullet$, $C_2CClO^\bullet$, $C^\bullet C(OH)C$, and $C^\bullet CCl(OH)C$ derived from this chapter are also listed in Table 2.12 for comparison with other HBI groups from C_1-C_2 chloro-alcohols.[46,59] It can be seen from Table 2.12 that the enthalpy and heat capacity for HBI groups with similar chemical environments are similar; this suggests that these HBI groups can be used to predict accurate thermochemical properties of other radicals with similar chemical environments. The entropies are however slightly different even in the same series.

For example, in the alkoxy series, the HBI values for the entropy of $CH_3O^\bullet$, $CCO^\bullet$, $C_2CO^\bullet$ are –2.80, –0.90, –1.90 cal/mol.K respectively, while bond energies and heat capacities remain similar. This is a result of the nature of intrinsic entropy in the different molecules. A complete set of recommended HBI values with average entropy for use in general group additivity applications is listed in Table 2.13.

Table 2.13 Recommended Hydrogen Bond Increment Group Values

HBI group[a]	Bond energy[b]	S^o_{298}[c]	C_p300[c]	C_p400	C_p500	C_p600	C_p800	C_p1000	C_p1500
CCO$^\bullet$	104.55	-1.40	-0.79	-1.11	-1.48	-1.80	-2.26	-2.61	-3.32
CCClO$^\bullet$	106.03	0.58	-0.72	-1.47	-2.04	-2.46	-2.99	-3.33	-3.99
CCCl$_2$O$^\bullet$	106.00	1.37	-0.75	-1.84	-2.69	-3.25	-3.73	-3.89	-4.18
CC$^\bullet$OH	100.44	1.76	-0.63	-1.38	-2.05	-2.56	-3.20	-3.60	-4.28
CC$^\bullet$ClOH	97.64	-0.10	-0.25	-0.76	-1.30	-1.83	-2.73	-3.40	-4.40
C$^\bullet$COH	102.39	2.42	0.79	0.08	-0.71	-1.41	-2.47	-3.21	-4.26
C$^\bullet$CClOH	103.02	2.74	1.14	0.62	-0.02	-0.66	-1.80	-2.71	-4.11
C$^\bullet$CCl$_2$OH	103.52	2.73	1.01	0.39	-0.40	-1.15	-2.35	-3.19	-4.40

[a] H atoms are assumed to fill valence. [a] Units in kcal/mol. [b] Units in cal/mol-K.

2.5 Chlorinated Ethyl Hydroperoxides and Radicals

2.5.1 Geometries

The fully optimized geometric parameters along with vibrational frequencies and moments of inertia calculated at the B3LYP/6-31G(d,p) level for the three chlorinated ethyl hydroperoxides are presented in Appendix (Table A.5). The calculation at the B3LYP/6-31G(d,p) level gives O—O bond length 1.45 Å in all three chlorinated ethyl hydroperoxides, which is in good agreement with the experimental data (1.452 Å for H_2O_2) of Khachkuruzov and Przhevalskii[76] using IR spectroscopy.

Effects of chlorine β-substitution on molecular geometries can be seen from Table A.5. The C—C bond lengths for β-chloroethyl hydroperoxides are increased with the increased chlorine substitution, but the C—O bond lengths decrease with the increased chlorine substitution. This is because the Cl atom withdraws the electrons through its inductive effect; the lone pairs from the peroxy oxygen are oriented towards the -CH$_2$- group, making the C—O bond length shorter than the normal C—O bond.

Table 2.14 Effects of Chlorine β-Substitution on Bond Length

Species	C—C (Å)	C—O (Å)	O—H (Å)
CH_3CH_2OOH	1.5227	1.4266	0.9707
CH_2ClCH_2OOH	1.5218	1.4213	0.9735
$CHCl_2CH_2OOH$	1.5317	1.4113	0.9728
CCl_3CH_2OOH	1.5458	1.4071	0.9727

As illustrated in Table A.5, the lowest energy conformation for the three chlorinated ethyl hydroperoxides has the –OOH group gauche to the maximum number of chlorine atoms, despite the apparent steric penalty incurred. This is because the gauche orientation of the peroxy group allows for intramolecular interaction between the peroxy H atom and a Cl atom on the chloroethyl group. The inter-atomic distances

between the peroxy H atom and a Cl atom in the chloroethyl group for CH_2ClCH_2OOH, $CHCl_2CH_2OOH$, and CCl_3CH_2OOH are 2.642, 2.742, and 2.751 Å, respectively. These distances provide an indication to the degree of intramolecular hydrogen bonding present in these species.

Table 2.15 Bond Energies

reaction series	bond energy	reaction series	bond energy[a]
OO—H			OO—H
$CH_3CH_2OOH \rightarrow CH_3CH_2OO\bullet + H\bullet$	85.00	$CH_3OOH \rightarrow CH_3OO\bullet + H\bullet$	86.05
$CH_2ClCH_2OOH \rightarrow CH_2ClCH_2OO\bullet + H\bullet$	86.38	$CH_2ClOOH \rightarrow CH_2ClOO\bullet + H\bullet$	92.28
$CHCl_2CH_2OOH \rightarrow CHCl_2CH_2OO\bullet + H\bullet$	87.12	$CHCl_2OOH \rightarrow CHCl_2OO\bullet + H\bullet$	92.22
$CCl_3CH_2OOH \rightarrow CCl_3CH_2OO\bullet + H\bullet$	87.45	$CCl_3OOH \rightarrow CCl_3OO\bullet + H\bullet$	92.21
C—H$_\beta$			C—H
$CH_3CH_2OOH \rightarrow C\bullet H_2CH_2OOH + H\bullet$	102.76	$CH_3CH_2OH \rightarrow C\bullet H_2CH_2OH + H^\bullet$	102.52
$CH_2ClCH_2OOH \rightarrow C\bullet HClCH_2OOH + H\bullet$	99.74	$CH_3CHClOH \rightarrow C\bullet H_2CHClOH + H^\bullet$	103.22
$CHCl_2CH_2OOH \rightarrow C\bullet Cl_2CH_2OOH + H\bullet$	95.56	$CHCl_2OH \rightarrow C\bullet Cl_2OH + H^\bullet$	95.44
C—Cl			C—Cl
$CH_2ClCH_2OOH \rightarrow C\bullet H_2CH_2OOH + Cl\bullet$	85.42	$CH_2ClOH \rightarrow C\bullet H_2OH + Cl^\bullet$	83.02
$CH_2ClCH_2OOH \rightarrow C\bullet HClCH_2OOH + Cl\bullet$	80.08	$CHCl_2OH \rightarrow C\bullet HClOH + Cl^\bullet$	80.34
$CHCl_2CH_2OOH \rightarrow C\bullet Cl_2CH_2OOH + Cl\bullet$	73.74	$CCl_3OH \rightarrow C\bullet Cl_2OH + Cl^\bullet$	72.34
C—O			C—O
$CH_3CH_2OOH \rightarrow CH_3CH_2\bullet^c + HO_2\bullet$	72.30	$CH_3OOH \rightarrow CH_3\bullet + HO_2\bullet$	70.12
$CH_2ClCH_2OOH \rightarrow CH_2ClCH_2\bullet^c + HO_2\bullet$	73.10	$CH_2ClOOH \rightarrow CH_2Cl\bullet + HO_2\bullet$	72.94
$CHCl_2CH_2OOH \rightarrow CHCl_2CH_2\bullet^c + HO_2\bullet$	74.25	$CHCl_2OOH \rightarrow CHCl_2\bullet + HO_2\bullet$	71.71
$CCl_3CH_2OOH \rightarrow CCl_3CH_2\bullet^d + HO_2\bullet$	68.81	$CCl_3OOH \rightarrow CCl_3\bullet + HO_2\bullet$	67.61
O—O			O—O
$CH_3CH_2OOH \rightarrow CH_3CH_2O\bullet + OH\bullet$	44.69	$CH_3OOH \rightarrow CH_3O\bullet + OH\bullet$	45.33
$CH_2ClCH_2OOH \rightarrow CH_2ClCH_2O\bullet^d + OH\bullet$	43.52	$CH_2ClOOH \rightarrow CH_2ClO\bullet + OH\bullet$	46.37
$CHCl_2CH_2OOH \rightarrow CHCl_2CH_2O\bullet^d + OH\bullet$	42.91	$CHCl_2OOH \rightarrow CHCl_2O\bullet + OH\bullet$	48.58

[a]Bond energy calculated in the previous studies[46,59,77] are used for comparison. Units in kcal/mol. [c]Enthalpy values from Seetula.[78] [d] From THERM group additivity estimation

Hydrogen bonding can occur when the distance between a hydrogen atom and an electronegative donor is significantly less the sum of the van der Waals radii. The van der Waals radii are 1.2 Å and 1.8 Å for H and Cl atoms, respectively.[47] Due to the intramolecular hydrogen bonding between the peroxy H atom and a Cl atom, the O—H bond lengths for the three β-chloroethyl hydroperoxides increase 0.03 Å relative to

normal O—H bond in CH_3CH_2OOH. This hydrogen bonding results in an increase in the O—H bond strength by ca. 2 kcal/mol (as shown in Table 2.15). Additional chlorine substitutions on the ethyl hydroperoxides slightly decrease the O—H bond lengths 0.007 ~ 0.008 Å, and increase the O—H bond strength by 1.2 kcal/mol. These O—H bond length decreases coincide with the increased inter-atomic H···Cl distances, which are due to the increased repulsion between the electronegative O and Cl atoms.

2.5.2 Rotational Barriers

Potential energy as function of torsion angle is determined by scanning the dihedral angles from 0° to 360° at 15° increments and allowing the remaining molecular structural parameters to be optimized at the B3LYP/6-31G(d,p) level. The barrier of a given rotation is then calculated as the difference between the highest points on the potential energy surface and the corresponding most stable conformer. The geometries at the points of minima and maxima are fully optimized. The calculated rotational barriers about the C—C, C—O, and O—O bonds of the 3 chlorinated ethylhydroperoxides are shown in Figures 2.9, 2.10, and 2.11, respectively.

The calculated rotational barriers about the C—C bond of the three target species are shown in Figure 2.9. All three curves show three minima and three maxima with barriers between 4.77 and 5.74 kcal/mol; the curve for CCl_3—CH_2OOH shows 3-fold symmetry. These curves represent typical C—C bond rotational potentials, in which the eclipsed structures are corresponding to the maxima and the staggered structures are corresponding to the minima on the potential curves.
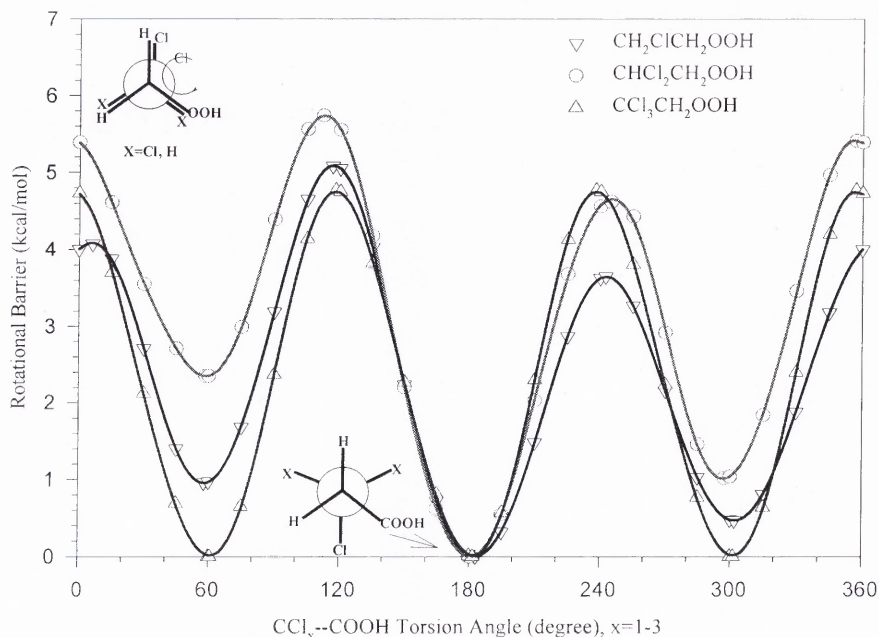
Figure 2.9 Potential barriers for internal rotation about the C—C bond of CH₂ClCH₂OOH, CHCl₂CH₂OOH, and CCl₃CH₂OOH.

Figure 2.10 shows the potential curves for rotational barriers about the C—O bond for three chloroethyl hydroperoxides. The conformers with dihedral $\angle$C-C--O-O $\approx$ 90° are most stable because of two electrostatic interactions. The first is the O···H interaction between the peroxy O atom and the H atom in the -CH₂- group, and the inter-atomic distance between them is 2.37 Å, which is significantly less than the sum of the van der Waals radii for O and H atoms (2.70 Å). The second is the H···Cl interaction between the peroxy H atom and the Cl atom in the chloroethyl group, and the inter-atomic distance is 2.63 Å that is less than the sum of the van der Waals radii of H and Cl (3.0 Å).[47] The conformers with dihedral $\angle$C-C--O-O $\approx$ 180° or 270° do not have the second H···Cl interactions, so they have 0.63 ~ 2.47 kcal/mol higher energy than the lowest energy conformers. The highest rotational barriers about the C—O bond are 7.2 ~ 9.7 kcal/mol, corresponding to the OH—CClₓ (x = 1~3) eclipsed structures.
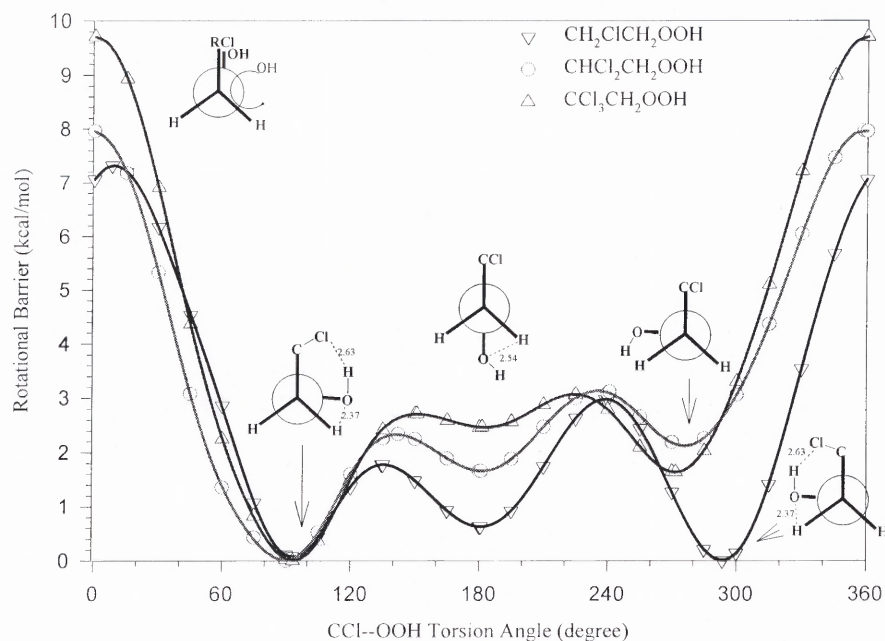
Figure 2.10 Potential barriers for internal rotation about the C—O bond of CH_2ClCH_2OOH, $CHCl_2CH_2OOH$, and CCl_3CH_2OOH
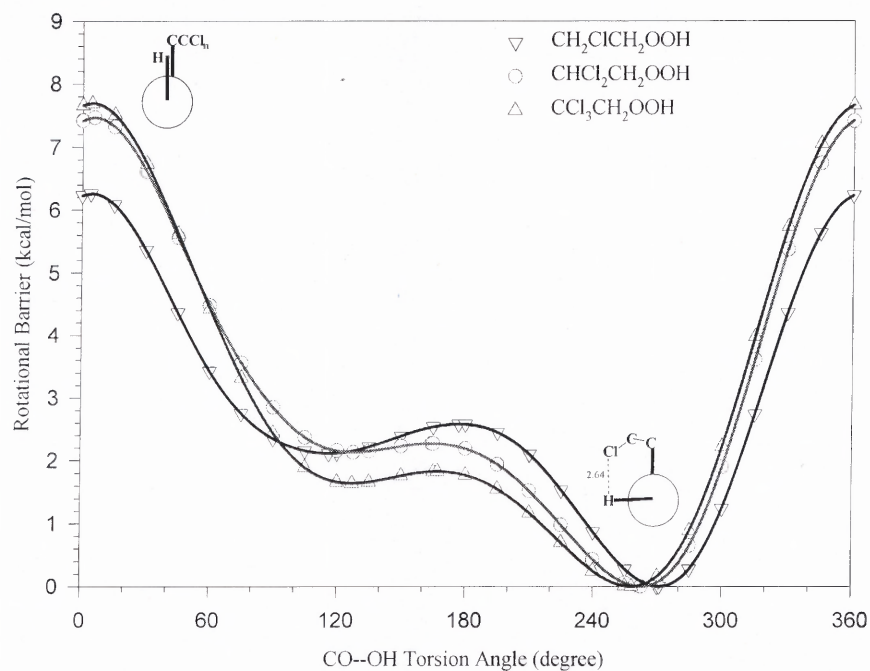
Figure 2.11 Potential barriers for internal rotation about the O—O bond of CH_2ClCH_2OOH, $CHCl_2CH_2OOH$, and CCl_3CH_2OOH.

Figure 2.11 shows calculated rotational barriers about the O—O bond of the three chlorinated ethyl hydroperoxides. The HO—OCCCl$_x$ (x = 1~3) eclipsed structures for the three chlorinated ethyl hydroperoxides correspond to the highest rotational barriers, because the four non-bonding electron pairs on peroxy oxygen atoms eclipse to each other. While the conformers with the four non-bonding electron pairs on the peroxy oxygen atoms staggered to each other and with the nearest interatomic distances between the peroxy H atom and the Cl atom correspond to the most stable conformers.

2.5.3 Enthalpy of Formation

The $\Delta H_f^o{}_{298}$ values are calculated using total energies and working isodesmic reactions. The reaction enthalpies and $\Delta H_f^o{}_{298}$ values for three stable species obtained from three isodesmic reactions are tabulated in Table 2.16, and the $\Delta H_f^o{}_{298}$ values of corresponding radicals are tabulated in Table A.4. The results for $\Delta H_f^o{}_{298}$ values in Table 4 show good consistency for the 3 chloroethyl hydroperoxides over 3 isodesmic reactions and the four calculation methods. The DFT calculations show good agreement with the high level ab initio calculations, indicating the errors inherent in computations for different types of molecule are canceled to a significant extent and lead to reliable results.

The calculated $\Delta H_f^o{}_{298}$ values in Table 2.16 and Table A.5 are the enthalpy values for pure enantiomer of the lowest energy. The recommended $\Delta H_f^o{}_{298}$ values for CH$_2$ClCH$_2$OOH, CHCl$_2$CH$_2$OOH, and CCl$_3$CH$_2$OOH are −45.47 ± 1.20, −48.92 ± 1.50 and −50.21 ± 1.36 kcal/mol, respectively. Here the statistical distribution of rotational conformers are considered and calculated by $\Delta H_f^o{}_{mix} = n_i\,\Delta H_f^o{}_i$, where n_i and $\Delta H_f^o{}_i$ are the Boltzmann equilibrium mole fraction and the enthalpy of formation of the ith conformer.

Manion[79] in an extensive review, compared ab initio calculated values and experimental

results on the relative $\Delta H_f^{\circ}{}_{298}$'s of the isomeric chlorinated C_2 compounds with two to

four chlorine atoms. He reports the theory and experiment are in good agreement with a

largest deviation of 0.79 kcal/mol. Based on this comparison, our calculated $\Delta H_f^{\circ}{}_{298}$

values for the three chlorinated ethyl hydroperoxides should have similar accuracy.

Table 2.16 Reaction Enthalpies at 298K and Calculated $\Delta H_f^{\circ}{}_{298}{}^{a}$

Reaction Series	B3LYP /6-31G(d,p)		B3LYP /6-311+G(3df,2p)		QCISD(T) /6-31G(d,p)		CBSQ//B3LYP /6-31G(d,p)	
	$\Delta H^{\circ}{}_{rxn}$	$\Delta H_f^{\circ}{}_{298}$	$\Delta H^{\circ}{}_{rxn}$	$\Delta H_f^{\circ}{}_{298}$	$\Delta H^{\circ}{}_{rxn}$	$\Delta H_f^{\circ}{}_{298}$	$\Delta H^{\circ}{}_{rxn}$	$\Delta H_f^{\circ}{}_{298}$
1.$CH_2ClCH_2OOH + CH_4 \longrightarrow CH_3OOH + C_2H_5Cl$	4.34	-45.09	3.35	-44.10	4.79	-45.54	5.10	-45.85
2. $CH_2ClCH_2OOH + C_2H_6 \longrightarrow C_2H_5OOH + C_2H_5Cl$	-0.84	-45.46	-1.22	-45.08	-0.86	-45.44	-0.52	-45.78
3. $CH_2ClCH_2OOH + C_3H_8 \longrightarrow C_3H_7OOH + C_2H_5Cl$	-0.32	-46.27	-1.14	-45.45	-0.20	-46.39	-0.90	-45.69
Average value and deviation[b]:								-45.77±1.20
1.$CHCl_2CH_2OOH + CH_4 \longrightarrow C_2H_5OOH + CH_2Cl_2$	1.71	-46.35	1.15	-45.79	3.44	-48.08	4.74	-49.38
2. $CHCl_2CH_2OOH + C_2H_6 \longrightarrow C_3H_7OOH + CH_2Cl_2$	0.61	-47.97	-0.50	-46.86	1.89	-49.25	1.59	-48.95
3. $CHCl_2CH_2OOH + CH_3OH \longrightarrow C_2H_5OOH + CHCl_2OH$	-11.96	-45.54	-10.75	-46.75	-9.61	-47.89	-8.17	-49.33
Average value and deviation[b]:								-49.22±1.50
1.$CCl_3CH_2OOH + CH_4 \longrightarrow CH_3OOH + CH_3CCl_3$	1.51	-49.43	0.19	-48.11	2.62	-50.54	2.53	-50.45
2. $CCl_3CH_2OOH + C_2H_6 \longrightarrow C_2H_5OOH + CH_3CCl_3$	-3.67	-49.80	-4.38	-49.80	-3.03	-50.44	-3.08	-50.39
3. $CCl_3CH_2OOH + C_3H_8 \longrightarrow C_3H_7OOH + CH_3CCl_3$	-3.15	-50.61	-4.30	-49.46	-2.37	-51.39	-3.47	-50.29
Average value and deviation[b]:								-50.38±1.36

[a] Reaction enthalpies include thermal correction and zero-point energy. Units in kcal/mol.
[b] Average value and the deviation for pure enantiomer of the lowest energy at the CBSQ//B
level.

2.5.4 Entropy and Heat Capacity

The $S^{\circ}{}_{298}$ and $C_p(T)$'s ($300 \leq T/K \leq 1500$) for three chlorinated ethylhydroperoxides using

the geometries and harmonic frequencies determined at the B3LYP/6-31G(d,p) level are

summarized in Table 2.17. The torsion frequencies, corresponding to the C—C, C—O,

and O—O bond rotations, are omitted in calculation of $S^{\circ}{}_{298}$ and $C_p(T)$'s; but we replace

their contributions with values from analysis of the internal rotations. TVR, represent the

sum of the contributions from translation, vibration and external rotation to $S^{\circ}{}_{298}$ and

$C_p(T)$'s obtained by statistical mechanics. I.R., represent the contributions from hindered internal rotations about the C—C, C—O and O—O bonds to S^o_{298} and $C_p(T)$'s.

Table 2.17 Ideal Gas-phase Thermodynamic Properties

species		$\Delta H^o_{f\,298}{}^b$	$S^o_{298}{}^c$	C_p300^c	C_p400	C_p500	C_p600	C_p800	C_p1000	C_p1500
CH$_2$ClCH$_2$OOH	TVR ^{d}		71.87	16.34	20.76	24.68	27.93	32.84	36.38	41.83
(1)^h	I.R.^{e}		6.47	2.62	2.29	1.97	1.68	1.21	0.89	0.46
(2)^i	I.R.^{f}		6.30	2.43	2.11	1.84	1.62	1.28	1.04	0.65
	I.R.^{g}		2.06	3.01	3.07	2.82	2.54	2.11	1.82	1.45
	Total	−45.47±1.20	89.24	24.41	28.23	31.32	33.77	37.44	40.13	24.41
CHCl$_2$CH$_2$OOH	TVR ^{d}		77.82	19.73	24.22	27.99	31.01	35.42	38.49	43.11
(1)^h	I.R.^{e}		5.62	3.04	2.92	2.65	2.31	1.69	1.23	0.62
(2)^i	I.R.^{f}		5.27	3.77	3.36	2.77	2.27	1.61	1.22	0.71
	I.R.^{g}		2.11	2.74	2.76	2.59	2.40	2.11	1.90	1.57
	Total	−48.92±1.50	92.33	29.28	33.26	35.99	38.00	40.83	42.84	46.01
CCl$_3$CH$_2$OOH	TVR ^{d}		81.69	24.02	28.38	31.82	34.47	38.22	40.74	44.46
(3)^h	I.R.^{e}		6.80	1.75	1.69	1.61	1.49	1.20	0.94	0.53
(2)^i	I.R.^{f}		4.96	3.87	3.58	2.97	2.43	1.71	1.30	0.79
	I.R.^{g}		2.43	2.66	2.46	2.24	2.09	1.90	1.77	1.54
	Total	−50.21±1.36	96.86	32.30	36.10	38.64	40.48	43.03	44.75	47.32

^{a} Thermodynamic properties are referred to a standard state of an ideal gas of at 1 atm. ^{b} Units in kcal/mol. ^{c} Units in cal/mol/K. ^{d} The sum of contributions from translations, vibrations, and external rotations. ^{e} Contribution from internal rotation about the C—C bond. ^{f} Contribution from internal rotation about the C—O bond. ^{g} Contribution from internal rotation about the O—O bond. ^{h} Symmetry number. ^{i} Optical isomer number.

2.5.5 Group Additivity Correction Terms

Group additivity[64] is a straightforward and reasonably accurate calculation method to estimate thermodynamic properties of hydrocarbons and oxygenated hydrocarbons; but conventional group additivity does not work well for chlorocarbons or other halocarbons, as group additivity does not incorporate effects of next nearest neighbors.[80] In this chapter, three sets of peroxy oxygen -- chlorine interaction terms are defined to be used with Benson type group additivity scheme for calculation of the thermodynamic properties of multichloro peroxy-hydrocarbons.

In the three chlorinated ethyl hydroperoxides, the nearest inter-atomic distances between the Cl atom and the O atom are 3.10 ~ 3.23 Å, so there are significant interactions between the electronegative Cl and the O atoms. The interaction values between chlorine(s) on the ethyl and the peroxy oxygen (OO/Cl, OO/Cl$_2$, and OO/Cl$_3$) are calculated from differences between the sum of defined chlorinated ethyl hydroperoxides group values and the determined thermodynamic properties of the parent compounds. The calculated interaction values are listed in Table 2.18.

Table 2.18 Thermodynamic Properties of Peroxy-Chlorine(s) Interaction Group

interaction group	$\Delta H_{f\,298}^{o}$[a]	S_{298}^{o}[b]	C_p300[b]	C_p400	C_p500	C_p600	C_p800	C_p1000
INT/OO/Cl	2.72	3.20	1.15	0.88	0.46	-0.31	-0.85	-1.55
INT/OO/Cl$_2$	3.51	-0.45	2.77	2.47	1.68	0.61	-0.40	-1.17
INT/OO/Cl$_3$	5.02	0.48	1.95	1.43	0.61	-0.39	-1.17	-1.67

[a] Units in kcal/mol. [b] Units in cal/mol/K.

The interaction values in Table 2.18 indicate a several kcal/mol increase in enthalpy due to destabilizing interaction of chlorine(s) on the ethyl group with the peroxy group. The group additivity corrections for the $\Delta H_{f\,298}^{o}$ are 2.72, 3.51, and 5.02 kcal/mol for the interaction group OO/Cl, OO/Cl$_2$, and OO/Cl$_3$, respectively. Interaction terms for entropies at 298 K and heat capacities listed in Table 2.18 are relatively small.

2.6 Summary

Structures and thermochemical properties on chlorinated alcohols, chlorinated hydroperoxides and corresponding alkoxy, hydroxy alkyl radicals, peroxy and hydroperoxy alkyl radicals are determined by *ab initio* and density functional calculations. Molecular structures and vibration frequencies are determined at the

B3LYP/6-31G(d,p) density functional level, with single point calculations for the energy at the B3LYP/6-311+G(3df,2p), QCISD(T)/6-31G(d,p) and CBSQ//B3LYP/6-31G(d,p) levels. The S^o_{298} and $C_p(T)$'s ($300 \leq T/K \leq 1500$) from vibrational, translational, and external rotational contributions are calculated using the rigid-rotor-harmonic-oscillator approximation based on the vibration frequencies and structures obtained from the density functional study. Potential barriers for the internal rotations are calculated at the B3LYP/6-31G(d,p) level, and hindered rotational contributions to S^o_{298} and $C_p(T)$'s are calculated by using direct integration over energy levels of the internal rotational potentials. The values of $\Delta H^o_{f\,298}$ are determined using isodesmic reactions with group balance if possible. Groups for use in Benson type additivity estimations are determined for the carbon bonded to oxygen and chlorine(s). Hydrogen bond increment groups for the chloroalkoxy, hydroxy chloroalkyl radicals and interaction terms for peroxy group with chlorine(s) on a β carbon are developed for group additivity approach.

CHAPTER 3

KINETIC ANALYSIS ON OH ASSOCIATION WITH CHLOROMETHYL RADICAL AND DISSOCIATION OF CHLOROMETHANOL

3.1 Background

Oxygenated chloro-hydrocarbons play an important role in both industrial and environmental chemistry. The chemical activation reactions of $CH_2Cl + OH$ is considered to be a part of reaction mechanism for the oxidation of chloro-hydrocarbon in combustion and photochemical processes.

Wallington et al.[81] studied the stability and infrared spectra of mono-, di-, and trichloromethanol prepared by UV irradiation of $CH_3OH/Cl_2/N_2$ gas mixtures. They observed that the chlorinated methanols decayed with the first-order kinetics to HCl and the corresponding carbonyl compounds, and that the decomposition was heterogeneous since the decay rates increased with increased contact of the chloromethanols with the reactor walls. They reported the upper limit for chlorinated methanols decomposition of 1.05×10^{-2} s.

Wang et al.[82] studied the unimolecular decomposition of vibrationally exited chloromethanol generated by excited $O^*(^1D)$ inserted in C—H bond of CH_3Cl at the G3(MP2) level, but they did not calculate any reaction rate constant.

Peyerimhoff et al.[83] investigated photo-fragmentation of chloromethanol along C—Cl and C—O coordinates using multi-reference single- and double- excitation configuration interaction (MRD-CI) method. They reported that the reactions of $CH_2ClOH \rightarrow Cl + CH_2OH$ and $CH_2ClOH \rightarrow OH + CH_2Cl$ are energetically not preferred

in the ground state, but the reverse reaction (association) is likely and no barrier is found for these formation processes.

The association reactions: CH_2Cl + OH and Cl + CH_2OH form a chemically activated $[CH_2ClOH]^*$ adduct, which we show dissociates to HCl + CH_2O before it is stabilized. These reactions may serve as a termination reaction in combustion systems and may be a source for conversion of Cl to HCl in the stratosphere. ab initio, density functional, and variational transition state theory (VTST) calculations combined with QRRK theory are preformed in this study to predict the rate constants for association of OH with CH_2Cl and both the activated and stabilized CH_2ClOH dissociation kinetics to product channels.

3.2 Calculation Method

The geometries of the reactants, intermediates, transition states, and products for CH_2Cl + OH reaction system are pre-optimized using PM3 in MOPAC program,[84] followed by optimization and vibrational frequency calculation at the B3LYP/6-31G(d,p) level. The single point energies are calculated at the QCISD(T)/6-31G(d,p) and CBS-Q[6,40] levels using Gaussian98 program.[32] Vibrational frequencies are scaled by 0.9806 as recommended by Scott et al.[42] Transition state geometries are identified by the existence of only one imaginary frequency in the normal mode coordinate analysis, evaluation of the TS geometry, and the reaction's coordinate vibration information.

The bimolecular association reaction of CH_2Cl + OH does not have a well-defined transition state because of the absence of reaction barrier. To reliably predict this association rate, the flexible variational transition state approach originally developed by

Marcus et al.[85-87] has been employed by means of VariFlex code[88] that is aimed at calculating rates at high level of sophistication for barrier-less reactions. The component rates are evaluated at E, J-resolved level. The energy transfer rate coefficients were computed on the basis of the exponential down model with the <ΔE> down value of 230 cm^{-1}. To achieve convergence in the integration over the energy range, an energy grain size of 100 cm^{-1} is used; this grain size provides numerically converged results for all temperature studies with energy spanning range from 15000 cm^{-1} below to 44900 cm^{-1} above the threshold. The total angular momentum J covered the range from 5 to 245 in steps of 10 for the E, J-resolved calculation. For loose, barrierless transition state, the Varshni potential:[89]

$$V = D_e \{1 - \frac{R_0}{R} \exp[-\beta(R^2 - R_0^2)]\}^2 - D_e$$

is employed to represent the potential energy along the individual reaction coordinate. In the above equation, D_e is dissociation energy excluding zero-point vibrational energy, where R is the reaction coordinate, i.e., the distance between the two bonding atoms, and R_0 is the equilibrium value of R.

For the dissociation reactions with saddle point transition states, high-pressure limit rate constants (k_∞) are determined using structural parameters and vibration frequencies from density functional and ab initio calculations and then are fitted by three parameters A_∞, n, and E_a over temperature range from 298 to 2000 K: $k_\infty = A (T)^n \exp(-E_a/RT)$. Entropy differences between reactants and TS are used to determine Arrhenius pre-exponential factor via canonical transition state theory[12] for unimolecular reactions: A = (kT/h)exp($\Delta S^{\neq}/R$). Where h is Plank's constant, k is the Boltzmann constant.

Activation energy is determined as the difference in internal energy between reactant and TS at the CBS-Q level plus the endothermicity of reaction. Branching ratios of the energized adduct to stabilization and product channels are calculated using multi-frequency Quantum Rice-Rampsperger-Kassel theory for $k(E)$ combined with master equation analysis for pressure fall-off.[26]

3.3 Results and Discussion

3.3.1 Potential Energy Surfaces of CH$_2$Cl+OH

The CH$_2$Cl radical association with OH forms the chemically activated CH$_2$ClOH* adduct. The reaction channels of the CH$_2$ClOH* adduct include dissociation back to reactants, elimination via 4-member ring or 3-menber ring transition states, isomerization, and bond fission to dissociation products.

Table 3.1 Harmonic Vibrational Frequencies and Moments of Inertia

species	frequencies (cm^{-1})						moments of inertia (amu-Bohr^2)
TS1	-524.04	282.33	516.68	883.62	1015.12	1158.67	57.03707
	1396.54	1427.71	1597.04	2709.99	3139.30	3290.90	404.4184
							453.4267
TS2	-501.93	75.92	326.20	920.47	1119.15	1136.82	33.22946
	1306.87	1410.23	1522.51	1935.67	3099.30	3658.19	692.7382
							725.9672
TS3	-1104.71	211.61	413.40	460.81	743.73	840.98	54.7674
	990.65	1226.15	1527.66	2075.71	3095.38	3774.97	389.6259
							432.5914
TS4	-2247.70	354.29	599.71	624.21	899.22	1020.93	42.48458
	1291.13	1297.74	1515.47	2025.40	2241.22	3031.34	339.4081
							361.9635
TS5	-1337.01	414.89	551.99	597.93	669.24	770.89	51.8591
	1192.81	1287.71	1324.61	1606.10	2443.38	3671.37	309.1319
							344.1386
TS6	-1563.20	233.95	345.71	422.68	721.47	1022.25	41.61938
	1170.11	1250.63	1527.55	2414.67	3076.49	3204.31	418.7994
							446.9365

The optimized geometries of six transition states at the B3LYP/6-31G(d,p) level are shown in Table A.7, and corresponding vibrational frequencies and moments of inertia are listed in Table 3.1.

The potential energy diagram for CH_2Cl + OH reaction system calculated at the CBS-Q level is shown in Figure 3.1.
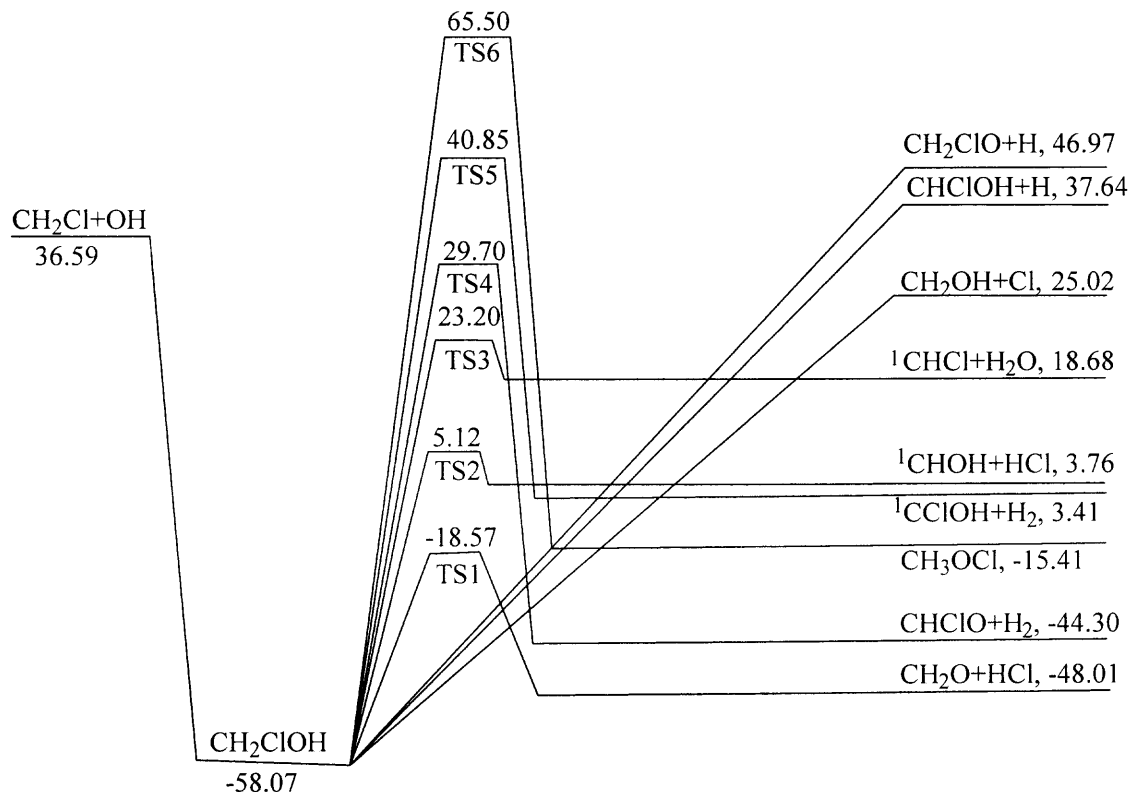
Figure 3.1 Potential energy for CH_2Cl+OH.

Enthalpies for transition states in Figure 3.1 are calculated by two methods. The first method is straightforward using the $\Delta H_{f,298}$ value of stable adduct plus the difference of total energies between adduct and transition state. The second method takes an average of: (i) the calculated energy difference between transition state and adduct; and (ii) the difference between transition state and products plus enthalpy of reaction (ΔH^{o}_{rxn}). The

reaction enthalpies for six transition states in CH_2Cl + OH system determined by these two methods at three different levels are listed in Table 3.2. It can be seen that the reaction enthalpies calculated from forward reaction (Method 1) show good agreement with the average values (Method 2) for all the six reactions at the CBS-Q level. Enthalpies of formation for transition states calculated by first method at the CBS-Q level are used to calculate rate constants.

Table 3.2 Reaction Enthalpies for Dissociation of Chloromethanol[a]

	B3LYP /6-31G(d,p)	QCISD(T) /6-31G(d,p)	CBS-Q //B3LYP/6-31G(d,p)	B3LYP /6-31G(d,p)	QCISD(T) /6-31G(d,p)	CBS-Q //B3LYP/6-31G(d,p)
	$E_{a, forward}$[b]	$E_{a, forward}$[b]	$E_{a, forward}$[b]	$E_{a, average}$[c]	$E_{a, average}$[c]	$E_{a, average}$[c]
TS1	33.59	41.49	39.50	33.71	42.98	39.48
TS2	54.84	63.11	60.02	53.45	63.18	59.55
TS3	74.15	75.90	81.27	69.56	68.01	80.82
TS4	86.12	92.19	87.77	87.15	93.79	88.27
TS5	84.18	87.18	98.92	84.80	88.54	99.43
TS6	97.69	102.38	123.57	101.36	106.43	123.15

[a] Units in kcal mol^{-1}. [b] The reaction enthalpies are calculated from forward reaction, ZPVE and thermal correction are included. [c] The reaction enthalpies are calculated from the average enthalpy values of the forward, reverse, and ΔH^0_{rxn}. $E_{a,average}$ = ½ ($E_{a, forward}$ + $E_{a, reverse}$ + ΔH^0_{rxn}).

3.3.2 Reactions in CH_2Cl + OH System

3.3.2.1 Elimination. The CH_2ClOH^* adduct can undergo molecular elimination of HCl via two different transition states TS1 and TS2. TS1 is the hydroxyl H and the Cl eliminated from CH_2ClOH^* to form HCl + CH_2O with barrier of 39.50 kcal mol^{-1}. The TS2 has the H and Cl atoms eliminate from chloromethyl group in CH_2ClOH^* to form a siglet di-radical ^1CHOH plus HCl with barrier of 63.19 kcal mol^{-1}.

Other elimination channels from the CH_2ClOH^* adduct are: H_2O elimination forming a diradical ^{1}:CHCl with barrier of 81.27 kcal/mol; H_2 elimination forming formyl chloride CHClO with barrier of 87.77 kcal mol^{-1}; H_2 elimination forming a diradical

^{1}CClOH with barrier of 98.92 kcal mol^{-1}. These reaction paths with high barrier and tight transition states, are energetically unimportant in the atmospheric environmental chemistry.

3.3.2.2 Bond Fission.   The C—Cl, C—H, and O—H bond cleavage reactions from the CH$_2$ClOH* adduct will produce three radical sets: C•H$_2$OH + Cl, C•HClOH + H, and CH$_2$ClO• + H, respectively. These bond fission reactions are the reverse process of the barrier-less radical-radical association. The bond dissociation energies are calculated as 81.36, 94.91, 104.58 kcal mol^{-1}, respectively. These bond fission recctions will not occur at low and intermediate temperatures.

3.3.2.3 Isomerization.   CH$_2$ClOH can isomerize to methyl hypochlorite CH$_3$OCl via TS6, which involves the migration of hydroxyl H atom to the C atom accompanied by migration of the Cl atom to the O atom. This is inferring a transition state structure with moving atoms on apposite side of a plane. The activation energy is calculated to be 123.57 kcal/mol. It implies that CH$_3$OCl is kinetically stable; however, the energy of CH$_3$OCl is 42.66 kcal mol^{-1} higher than that of CH$_2$ClOH. The high barrier indicates that this reaction is not important.

3.3.3 Bimolecular Association of CH$_2$Cl+OH

The potential energy for association of CH$_2$Cl to OH was calculated by varying the equilibrium C—O bond length 1.3742 Å to 4.3742 Å with interval of 0.1 Å at the B3LYP/6-31G(d,p) level. A smooth energy potential is obtained as illustrated in Figure 3.2. The DFT calculated total energies at each point are fitted by a Varshni potential energy function[89] with the parameters β = 0.4095 Å and D_e = 99.90 kcal/mol (without ZPE correction). The dissociation energy D_e is predicted at the CBS-QB3 level of theory.

The Lennard-Jones parameters for $CH_2ClOH \cdots N_2$ pair are assumed to be the same as those of the $C_2H_5Cl \cdots N_2$ pair, $\sigma = 3.62$Å, $\varepsilon/k = 97.5$ K.[90]
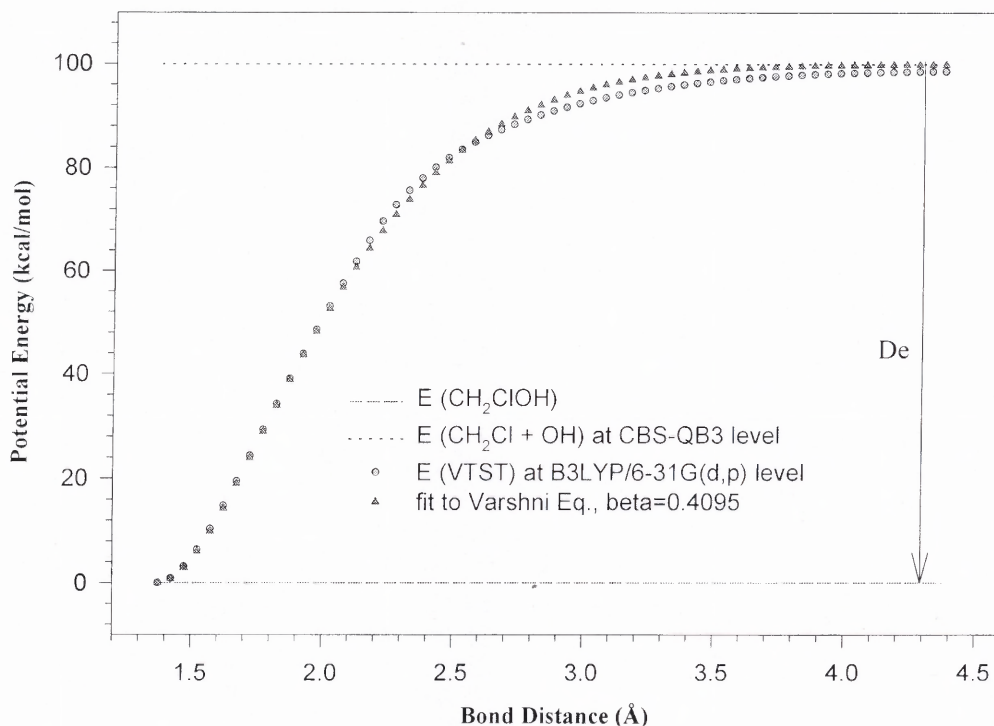
Figure 3.2 Bond dissociation energy for $CH_2ClOH \rightarrow CH_2Cl + OH$.

The calculated bimolecular reaction rate constant vs. temperature for $CH_2Cl + OH$ at the atmospheric condition by VariFlex code is shown in Figure 3. The rate constant can be expressed in units of cm^3 mol^{-1} s^{-1} at the temperature range of $300 \sim 3000$ K by the equation: $k = 8.44 \times 10^{12}$ $T^{0.276}$ $exp(132.23/T)$.

Humpfer et al.[91] measured the association rate constant of $CH_3 + OH$ by mass spectrometry at T = $300 \sim 700$ K and very low pressure range to be: $k = 1.02 \times 10^{14}$ cm^3 mol^{-1} s^{-1}. Baulch et al.[92] in an extensive literature review, reported this rate constant to be: $k = 6.03 \times 10^{13}$ cm^3 mol^{-1} s^{-1}. Fagerstrom et al.[93] measured the rate constant for C_2H_5

+ OH to be: $k = 7.69 \times 10^{13}$ cm^3 mol^{-1} s^{-1} at T = 200 ~ 400 K and P = 0.247 ~ 0.987 atm. Jungkamp et al.[94] measured the association rate constant of CH$_3$O + Cl at 300 K using a discharge flow system with laser-induced fluorescence (LIF) and mass-spectrometric detection as: $k = 6.02 \times 10^{13}$ cm^3 mol^{-1} s^{-1}, and Daele et al.[95] measured it as: $k = 1.17 \times 10^{13}$ cm^3 mol^{-1} s^{-1} using the same techniques. Compared with these experimental data, our theoretically predicted rate constant for CH$_2$Cl + OH has reasonable accuracy.
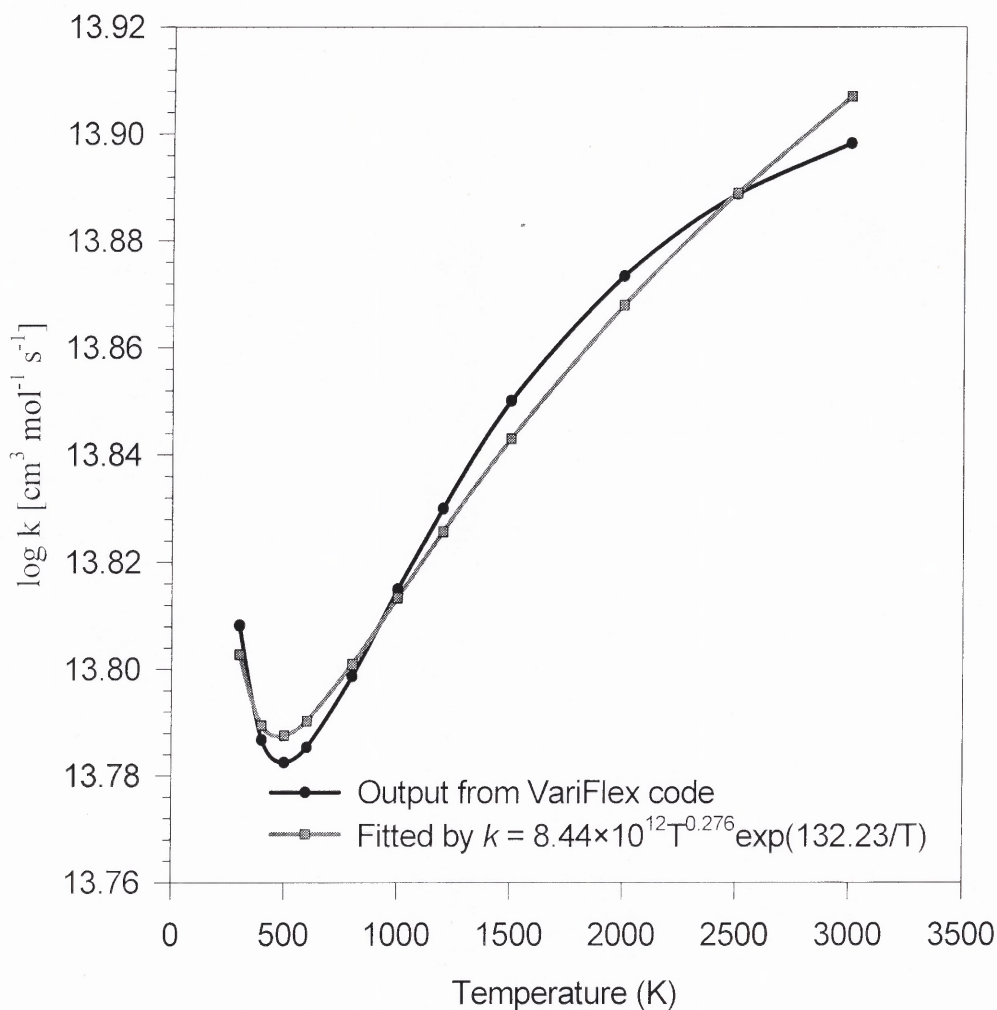
Figure 3.3 Calculated association rate constant of CH$_2$Cl + OH at P = 1 atm.

3.3.4 Decomposition of CH_2ClOH

The high-pressure limit rate constants (k_∞) for the CH_2ClOH dissociation are determined by canonical transition state theory using structural parameters and vibration frequencies of the transition states in this study. The thermochemical data of stable species are taken from our previous study,[46] which is cooperated with internal rotation analysis. The high-pressure limit rate constants used in QRRK analysis are fitted by three parameters A_∞, n, and E_a over temperature range from 298 to 2000 K; these values are listed in Table 3.3, and barriers are shown in Figure 3.1.

Table 3.3 Kinetic Parameters for QRRK Analysis in CH_2Cl + OH System

| reaction	A (s^{-1} or cm^3 mol^{-1} s^{-1})	n	E_a (kcal mol^{-1})
CH_2Cl + OH <=> CH_2ClOH	1.44×10^{13}	0.29216	-0.12186
CH_2ClOH <=> CH_2Cl + OH	7.29×10^{16}	0.0	93.27
CH_2ClOH <=> HCl + CH_2O	2.43×10^{12}	0.23405	39.50
CH_2ClOH <=> HCl + :CHOH	1.11×10^{12}	0.61016	63.11
CH_2ClOH <=> CH_2Cl + OH	2.90×10^{9}	1.37394	80.78
CH_2ClOH <=> H_2 + CH_2ClO	1.64×10^{10}	0.90475	88.26
CH_2ClOH <=> Cl + C•H_2OH	1.33×10^{16} [a]	0.0	81.91
CH_2ClOH <=> H + C•HClOH	4.56×10^{14} [b]	0.0	94.14
	frequency / degeneracy		
CH_2ClOH	512.9 / 3.495	1270.9 / 5.625	3446.6 / 2.380

[a]Estimated from CH_2Cl_2 + M → CH_2Cl + Cl + M, k = 4.00 ×10^{15} cm^3 mol^{-1}s^{-1} from Lim el al.[96], and <MR>. [b]Estimated a trend, y = log k − 0.192 x, here k = 4.10 × 10^{13} cm^3 mol^{-1}s^{-1} from the experimental data[97] for C•H_2OH + H → products, x is the number of Cl atoms on the carbon, and y is the rate constant calculated by the trend for reaction contain Cl atom, and the <MR>.

The calculated temperature dependent rate constants for chemically activated CH_2Cl + OH reaction system at 1 atm from the QRRK combined with Master equation analysis are illustrated in Figure 3.4. The dominant product-channel for CH_2Cl + OH is the dissociation to CH_2O + HCl at all temperatures due to its low barrier. The next dominant product-channel is dissociation to C•H_2OH + Cl at all temperature range since it has relative higher A factor due to its reverse reaction is barrier-less radical-radical

association reaction. Figure 3.5 illustrates the calculated rate constants vs. pressure for the chemically activated reaction $CH_2Cl + OH$ at 1000 K; it shows these rate constants have no pressure dependence over 0.001 ~ 10 atm.
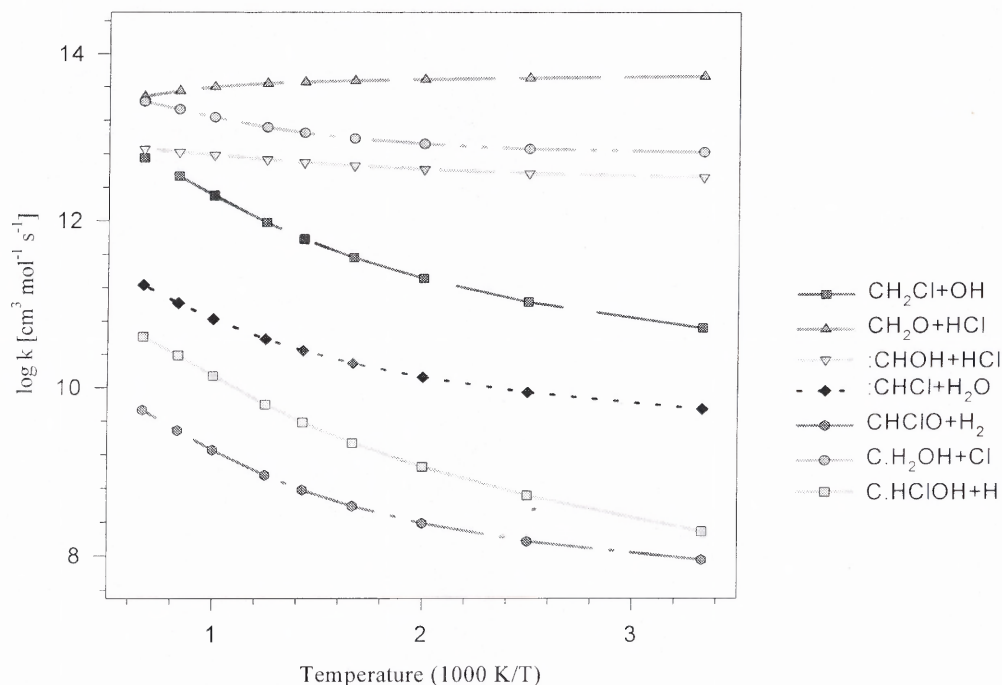
Figure 3.4 Rate constants vs. T for $CH_2Cl + OH$ system at P = 1 atm.

The unimolecular dissociation of stabilized CH_2ClOH to products vs. temperature at 1 atm is shown in Figure 3.6, and its pressure dependent dissociation rate constants at T = 1000 K is shown in Figure 3.7. The dominant product-channel for CH_2ClOH is the dissociation to $CH_2O + HCl$ at all temperatures, and this channel shows a small pressure dependence in the range of 0.001 ~ 10 atm. The calculated rate constant for this dissociation is: $k = 6.62 \times 10^{27} \, T^{-4.83} \exp(21801/T)$ s^{-1} at 1 atm, which is well below than the upper limit inferred from the experiment results of Wallington et al.[81]
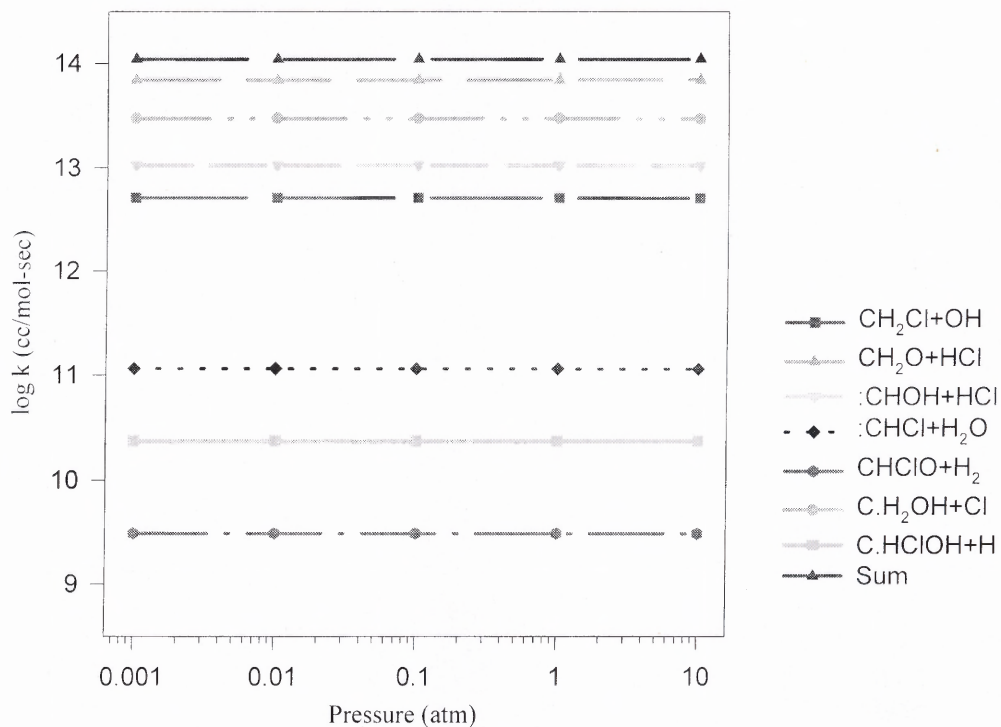
Figure 3.5 Pressure dependent rate constant CH_2Cl+OH at T = 1000 K.
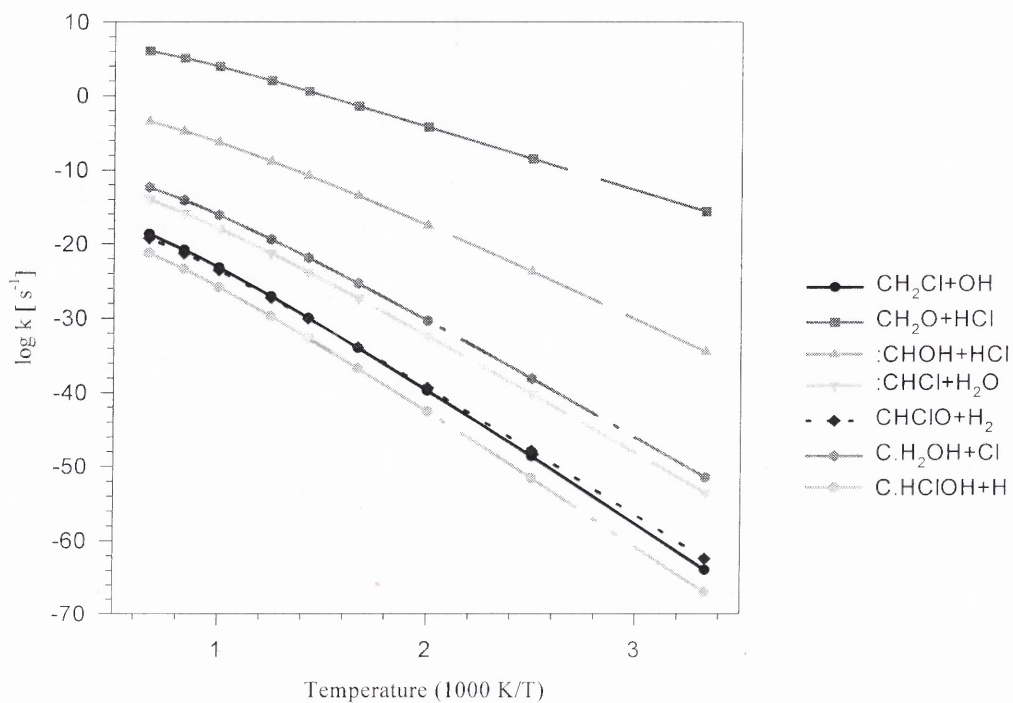
Figure 3.6 Rate constants vs. T for dissociation of CH_2ClOH at P = 1 atm.

Wallington et al. reported that the first-order loss rates of $(3.4 \pm 0.2) \times 10^{-3}$ s^{-1} for CH$_2$ClOH, $(5.5 \pm 0.3) \times 10^{-3}$ for CHCl$_2$OH, and $(9.9 \pm 0.2) \times 10^{-3}$ for CCl$_3$OH in a chamber, and the decays of CH$_2$ClOH and CHCl$_2$OH rate is $(1.6 \pm 0.1) \times 10^{-3}$ s^{-1} and $(9.0 \pm 0.8) \times 10^{-3}$ s^{-1} at another different chamber. They ascribed such differences to heterogeneous decomposition, which is sensitive to the nature and history of the surface of chamber. Their experiments were performed at a total pressure of 700 Torr at 295 ± 2 K, and they concluded that the three chloromethanols have lifetimes of at least 100 seconds (and probably much longer) with respect to homogeneous decomposition in the gas phase, but can decompose rapidly on surface. We suspect they will also decompose rapidly in heterolysis reaction environments.
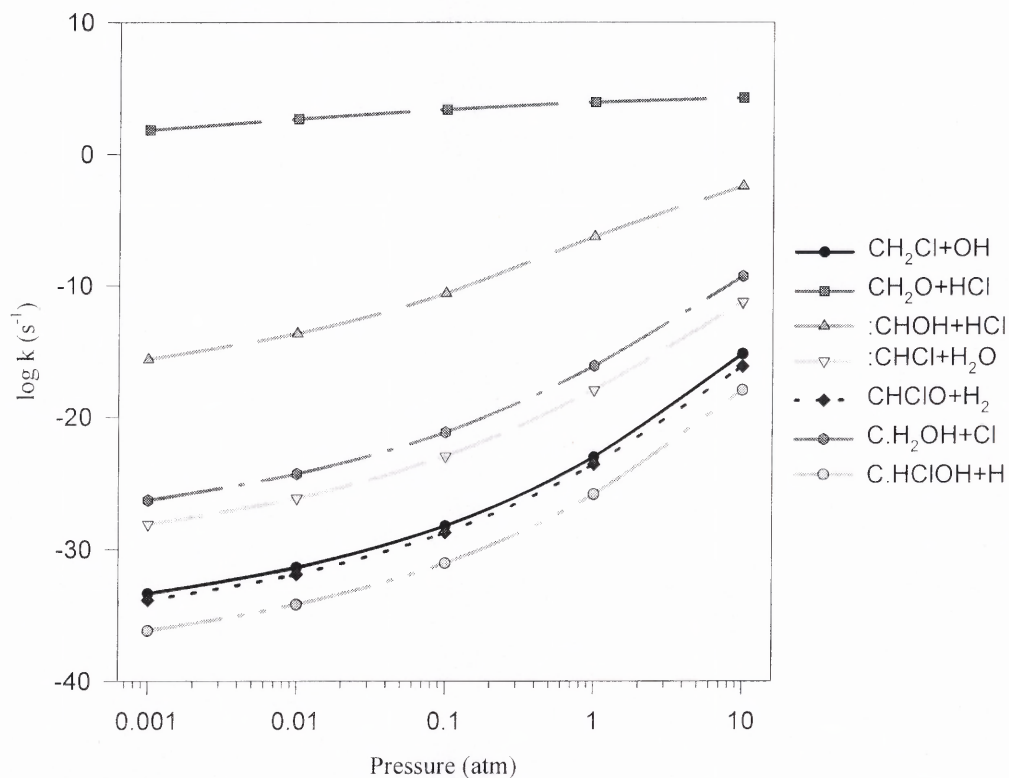
Figure 3.7 Rate constant vs. P for dissociation of CH$_2$ClOH at T = 1000 K.

In this study, the half-life is calculated as 17.6 seconds for the homogeneous decomposition of chloromethanol at 600 K, but its half-life is much longer at room temperature. Our computational results and experimental data suggest that the reported stability and slow homogeneous decay of chloromethanol under atmospheric conditions, where heterogeneous and homogeneous decompositions presented are not inconsistent. However, the decomposition of CH_2ClOH will be rapid in combustion environment or in a thermal heterogeneous / catalysis processes.

This dissociation of activated chloromethanol and other chlorinated methanols, may be a significant mechanism to convert Cl into HCl in stratosphere; particularly for trichloro-methyl radical, which has a little reaction with O_2.

3.4 Summary

Potential energy surfaces for $CH_2Cl + OH$ reaction system are calculated based on DFT B3LYP/6-31G(d,p), ab initio QCISD(T)/6-31G(d,p) and CBS-Q levels of theory. The rate constants for bimolecular association of OH with CH_2Cl radical are calculated to be: $k = 1.48 \times 10^{13}$ T $^{0.292}$ exp(61.46/T) cm^3 mol^{-1} s^{-1} based on variational transition state theory. The high-pressure limit rate constants (k_∞) for reactions with saddle point transition states are determined by canonical transition state theory. Branching ratios of the energized CH_2ClOH adduct to stabilization and product channels are calculated using multi-frequency Quantum Rice-Rampsperger-Kassel (QRRK) theory for $k(E)$ combined with master equation analysis for pressure fall-off. Kinetic parameters for product channels of $CH_2Cl + OH$ system are presented versus temperature and pressure. The activated CH_2ClOH^* adduct dissociation to CH_2O plus HCl is the most important

channel below 1500 K at pressure range of 0.001 ~ 10 atm. The calculated rate constants are useful for predicting reaction paths in applications of combustion and atmospheric modeling regimes, where experimental data are not available.

CHAPTER 4

THERMOCHEMICAL AND KINETIC ANALYSIS ON THE REACTION OF NEOPENTYL RADICAL WITH MOLECULAR OXYGEN

4.1 Overview

Thermochemical properties for reactants, intermediates, products and transition states in the neopentyl radical + O_2 reaction system are analyzed with *ab initio* and density functional calculations to evaluate reaction paths and kinetics for neopentyl oxidation. Enthalpies of formation ($\Delta H_f^o{}_{298}$) are determined using isodesmic reaction analysis at the CBS-Q composite and density functional levels. The entropies ($S^o{}_{298}$) and heat capacities $C_p(T)$'s ($0 \leq T/K \leq 1500$) from vibrational, translational, and external rotational contributions are calculated using statistical mechanics based on the vibrational frequencies and structures obtained from the density functional study. Potential barriers for the internal rotations are calculated at the B3LYP/6-31G(d,p) level, and hindered rotational contributions to $S^o{}_{298}$ and $C_p(T)$'s are calculated by using direct integration over energy levels of the internal rotational potentials. The kinetic analysis on reactions of neopentyl with O_2 is preformed at the CBS-Q calculation level. The reaction forms a chemically activated neopentyl peroxy adduct with energy of 38.13 kcal mol^{-1}. The energized adduct can be stabilized, dissociate back to reactants or isomerize to hydroperoxy-neopentyl radical. The isomer can dissociate to 3,3-dimethyloxetane + OH, to isobutene + CH_2O + OH, to methyl + 2-methyl-2-propenyl-hydroperoxide, isomerize back to neopentyl peroxy radical, or further react with O_2. The $\Delta H_f^o{}_{298}$ values for the neopentyl, neopentyl peroxy and hydroperoxy-neopentyl radicals are calculated as 10.52, –27.61, and –9.43 kcal mol^{-1} at the CBS-Q level. Rate constants to products and

stabilized adducts (isomers) of the chemically activated neopentylperoxy are calculated as functions of pressure and temperature using quantum Rice-Ramsperger-Kassel (QRRK) analysis for $k(E)$ and a master equation analysis for pressure fall-off. An elementary reaction mechanism is constructed to model experimental OH formation profile; it shows that the further reactions of the hydroperoxy-neopentyl radical with O_2 have contributions to the OH profile. Kinetic parameters for intermediate and product formation channels of the neopentyl + O_2 system are presented versus temperature and pressure.

4.2 Background

Abstraction reactions that form alkyl radicals in atmospheric and combustion reaction systems are well characterized, relative to subsequent association reactions of the radical with O_2, which form a chemically activated peroxy radical that can undergo a number of isomerization and dissociation reactions before becoming stabilized. These R• plus O_2 reactions are relatively complex; they involve formation of a peroxy radical, which contains $30 \sim 40$ kcal mol^{-1} of excess internal energy, this can either be lost via collision processes or used for further reaction before stabilization occurs.[98] These reactions are important rate controlling processes in the low and intermediate temperature chemistry of hydrocarbon oxidation, especially the chemistry which occurs prior to ignition in internal combustion engines and in cool flames. The reactions of the alkyl peroxy radical intermediate are, in addition, considered essential to predict negative temperature coefficient (NTC) behavior.[99] Many combustion reaction mechanisms consider the overall reaction of alkyl radicals with O_2 to form conjugate alkenes plus HO_2 to be

dominant processes over the 500 to 900 K temperature ranges, but the details of the pathway(s) are not treated consistently and in some cases the path is not correct. Some authors[100,101] ascribe this reaction to the abstraction of a H atom by O_2, while others[26,102,103] consider it a direct molecular elimination, still others consider it as an isomerization (hydrogen atom transfer) to a hydroperoxy-alkyl isomer that undergoes further reaction (β-scission) to products.

Two features of neopentyl radical facilitate a simpler interpretation of experimental results relative to most alkyl radical oxidation systems: (a) All the C—H bonds in the methyl groups are identical, so only one alkyl radical is involved. (b) The carbon radical site is connected to a quartenary carbon, and the formation of C_5 conjugate alkene + HO_2 is structurally impossible by the above routes. This property of the neopentyl structure eliminates the concerted HO_2 elimination path from the peroxy adducts, only reactions involving stabilization, dissociation by reverse reaction, isomerization and isomer decomposition are dominant here.

There are several experimental and modeling studies on neopentyl radical oxidation.[104-114] Hughes et al[104,105] measured the time dependence of OH radical from photolysis of neopentyl iodide in helium bath with varied concentrations of O_2 at temperatures from 660 to 750 K. An exact analytical solution was postulated incorporating neopentyl decomposition, reversible peroxy formation, and irreversible hydrogen atom transfer isomerization based on the assumption of fast subsequent decomposition via various channels to OH, which given the low species concentration present would be lost primarily by diffusion out of the photolysis zone. OH radical concentration profiles versus time were obtained by laser-induced fluorescence (LIF) and

fitted to a biexponential function, which is combination with the proposed analytical solution allowed rate coefficients for the isomerization process to be extracted and hence, Arrhenius parameters to be calculated as an A factor of 1.58×10^{12} s^{-1} and E_a of 29 kcal mol^{-1}.

The research group of Baldwin and Walker[106] studied the reactions of neopentyl radical in an oxidizing environment using a flow reactor with reaction times ranging up to tens of seconds, with product analysis by gas chromatography. They reported the stable products 3,3-dimethyloxetane, acetone, isobutene, and formaldehyde as a function of oxygen concentration at temperatures from 653 to 793 K. They suggested a mechanism for quantitative interpretation of product yields using steady state and equilibrium relationships, and hence determined Arrhenius parameters for elementary reactions in their mechanism.

Bayes research group[107,108] studied the rate constants of neopentyl radical with O_2 at 266 to 374 K and low pressure of 3 to 3.5 torr. They monitored the pseudo-first-order decay of the neopentyl radicals as a function of partial pressure of O_2 using mass spectrometric detection. Their experimental results show negative temperature dependence for the rate constant of neopentyl radical with O_2. They used an adiabatic channel model calculation to interpret their results with no fall-off analysis and reported the rate constant of this reaction as $k = \{1.3 \times 10^{12} \text{ cm}^3 \text{ mol}^{-1} \text{ s}^{-1}\}(T/300 \text{ K})^{-(2.1 \pm 0.4)}$.

Dagaut et al.[111] studied the oxidation of neopentane in a jet-stirred reactor at pressures of 1, 5, and 10 atm, and temperatures of 800 to 1230 K using probe-sampling of stable species and off-line gas chromatograph analyses. They provided an elementary mechanism to model the concentration profiles of the reactants, stable intermediates, and

products such as CO, CO_2, and hydrocarbons. Their modeling focused on high temperature experiments and their studies were not sensitive to the reactions of peroxy radicals because the β-scission of neopentyl radical to isobutene plus methyl radical dominated at these temperatures.

Curran et al.[114] published a detailed kinetic model on the oxidation of neopentane and compared the experimental results at 500 torr and 753 K by Baker et al,[109,110] and later they modified their mechanism in conjunction with new data from high pressure flow reactor experiments.[113] They estimated thermochemical and kinetic parameters using THERM[115] and other techniques to model stable end-product profiles without transition state or fall-off analysis.

Taatjes et al.[103] recently measured the time-resolved production of OH and HO_2 in pulsed-photolytic Cl-initiated oxidation of neopentane between 573 and 750 K. They observed that their OH measurements are especially sensitive to the direct pathways from R + O_2 to QOOH and to OH + 3,3-dimethyloxetane. They also proposed a kinetic model based on comparison with their previous time-dependent master equation calculation of analogous processes in the reaction of n-propyl with O_2 for modeling OH and HO_2 concentration vs. time profiles at different temperatures.

Thermochemical and kinetic parameters in our theoretical model are based on *ab initio* and density functional calculations, and the reaction mechanism for the neopentyl radical + O_2 system is outlined in the following scheme:
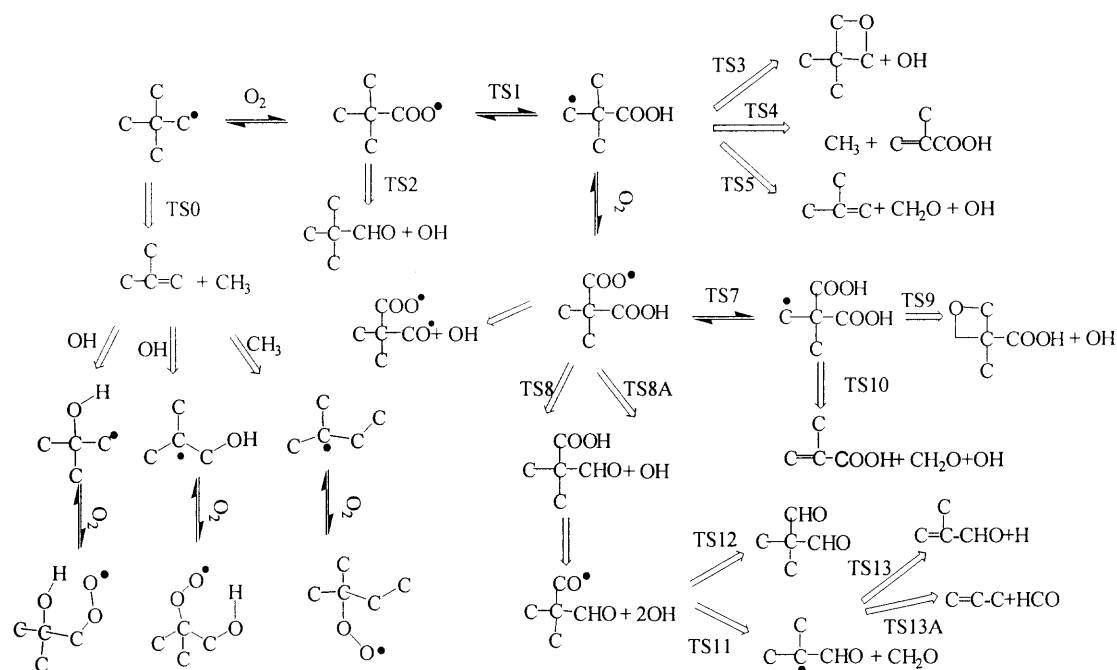
Treatment of the energized complex reactions in our mechanism includes analysis of the decomposition back to reactants, intramolecular transfer of hydrogen atoms to form a hydroperoxy alkyl radical, which can dissociate to products before stabilization. Further isomerizations, dissociations of the stabilized neopentyl peroxy radical and the hydroperoxide alkyl isomer are also included along with a second O_2 addition to the hydroperoxy-neopentyl radical. Several other important reaction paths, as illustrated above, are also included in the elementary reaction mechanism.

Thermochemical properties of reactants, intermediates, products and transition states for the elementary reactions are calculated by *ab initio* and density functional calculations with analysis of internal rotation barriers at the DFT level. High-pressure limit rate constants are calculated by canonical transition state theory or evaluated from literature. Quantum RRK theory[17,116-118] is used for analysis of $k(E)$ and a master equation[26] analysis for fall-off in a kinetic analysis on the chemical activation and

unimolecular dissociation reaction systems. The rate constants are incorporated into a detailed elementary reaction mechanism and are shown to tmodel the experimental OH profile of Hughes et al[104] well. The mechanism also models the experimental HO_2 profile of Taatjes et al well.[103]

4.3 Calculation Method

4.3.1 Computational Details

The geometries of reactants, important intermediates, transition states and products in neopentyl + O_2 reaction system are pre-optimized using PM3 MOPAC[84] calculations, followed by optimizations and frequency calculations at the B3LYP/6-31G(d,p) level using the Gaussian 98 program.[32] The optimized structure parameters are then used to obtain total electronic energies at the B3LYP/6-311++G(3df,2p) and CBS-Q single point levels of calculation. The potential energies for the neopentyl + O_2 system are calculated at the CBS-Q level. For the secondary reaction system – addition of an O_2 to the hydroperoxy neopentyl radical, the potential energies are calculated at the B3LYP/6-311++G(3df,2p) level due to the relatively large molecule size. For iodine-containing species, the effective core-potential basis sets and modified diffuse *sp* functions and d polarization function are employed.[119,120] Rotational barriers for the internal rotational potentials are calculated at the B3LYP/6-31G(d,p) level.

4.3.2 Thermochemical Properties

Contributions from vibrational, translational, external rotational, and electronic to entropies and heat capacities are calculated by statistical mechanics based on the vibrational frequencies and moments of inertia from the DFT optimized structures. The

torsion frequencies are identified by viewing bond motions in the GaussView98 program,[121] and these torsion frequencies are omitted in calculation of S^o_{298} and $C_p(T)$'s, and their contributions are replaced with values from analysis of the internal rotations. Contributions from hindered rotors to S^o_{298} and $C_p(T)$'s are determined by solving the Schrödinger equation with free rotor wave functions, and the partition coefficients are treated by direct integration over energy levels of the intramolecular rotational potential curves which are represented by a truncated Fourier series expansion. The $\Delta H_f^o{}_{298}$ values for reactants, intermediate and products are calculated using total energies from ab initio and DFT calculations and isodesmic reactions with group balance when possible. Transition state (TS) geometries are identified by the existence of only one imaginary frequency in the normal mode coordinate analysis, evaluation of the TS geometry, and the reaction coordinate's vibrational motion. The $\Delta H_f^o{}_{298}$ values of transition state structures are calculated by the $\Delta H_f^o{}_{298}$ of the stable radical adducts from working isodesmic reaction analysis, plus the difference of total energies between the radical adducts and the transition states.

4.3.3 Kinetic Analysis

Unimolecular dissociation and isomerization reactions of the chemically activated and stabilized adducts resulting from addition or combination reactions are analyzed by first constructing potential energy diagrams for the reaction system. DFT and ab initio calculations are used to calculate transition state structures and activation energy for isomerization, β- scission, and dissociation reactions. The enthalpies and entropies are treated with conventional transition state theory to calculate Arrhenius pre-exponential factors and energies of activation that result in high-pressure limit rate constants (k_∞) as

functions of temperature. Nonlinear Arrhenius effects resulting from changes in the thermochemical properties of the respective transition state relative to its adduct with temperature are incorporated using two parameter Arrhenius pre-exponential factor (A, n) in AT^n. High-pressure limit pre-exponential factors for association reactions are obtained from the literature. Equilibrium constants $K_{eq}(T)$ are calculated from thermodynamic properties of reactants and products as a function of temperature. Reverse rate constants are calculated from the principle of microscopic reversibility. Branching ratios of the energized adduct to stabilization and product channels are calculated using multi-frequency Quantum Rice-Rampsperger-Kassel (QRRK) analysis for $k(E)$[66,115] with the steady-state assumption on the energized adduct(s) in combination with a master equation analysis[26,122] for pressure fall-off.

The QRRK calculation evaluates energy dependent rate constants, k(E), of the energized adduct to each channel for the bimolecular chemical activation reaction and includes equilibrium in isomerization reactions. The QRRK analysis described by Chang et al.[17] and Sheng et al.[26] is shown to yield reasonable results and provides a framework by which the effects of temperature and pressure can be evaluated in these complex reaction systems. The QRRK code utilizes a reduced set of three vibration frequencies and their associated degeneracies which accurately reproduce the adduct heat capacity and include one external rotation in calculation of accurate ratios of density of states to partition coefficient, ρ(E)/Q.[18]

Evaluations on the steady state QRRK chemical activation analysis we utilize indicate that it is valid at reaction times on the order of nanoseconds; analysis for longer

times of reaction may require use of the CHEMKIN analysis in order to include reactions of the stabilized adducts depending on temperature, pressure and rate constants.

A 0.5 kcal energy grain used to obtain rate constants as a function of temperature and pressure for chemical activation and dissociation reactions. $(\Delta E)°$down of 570 cal mol^{-1} is used in the master equation analysis with helium as the third body. Lennard-Jones parameters, σ (Angstroms) and ϵ/κ (Kelvins), are obtained from tabulations[90] and from an estimation method based on molar volumes and compressibility.

4.4 Results and Discussion

4.4.1 Geometries

The geometry optimizations for the reactants, transition states, adducts, and products in the neopentyl oxidation system are performed at the B3LYP/6-31G(d,p) level, and the effective core-potential basis sets and modified diffuse sp functions and d polarization function[120] are used for iodine-containing species. The optimized structural parameters for 33 species including transition state structures are listed in Appendix Table B.1. The corresponding unscaled vibrational frequencies and moments of inertia are listed in Table B.2. The notations of several important species in this system are defined as: $C_3CC\bullet$ (neopentyl radical), $C_3CCOO\bullet$ (neopentyl peroxy radical), $C_3\bullet CCOOH$ (hydroperoxy-neopentyl radical), $C_2CYCCOC$ (3,3-dimethyloxetane), $C_2C(OOH)COO\bullet$ (hydroperoxy-neopentylperoxy radical), $C_2\bullet C(COOH)_2$ (dihydroperoxide-neopentyl radical), $C(COOH)CYCCOC$ (3-methyl,3-hydroperoxideoxetane), $C=C(C)COOH$ (isobutenyl hydroperoxide), $C_2C(COOH)CHO$ (2-methyl isopropanal-2-methylhydroperoxide), $C_2C(CHO)CH_2O\bullet$ (2-methyl isopropanal-2-methyoxy radical), and C_3CCI

(neopentyliodide). The transition states of important reactions in this oxidation system are identified as follows:

Alkyl peroxy radical isomerization

$C_3CCOO\bullet \to TS1 \to C_3\bullet CCOOH$

$C_2C(OOH)COO\bullet \to TS7 \to C_2\bullet C(COOH)_2$
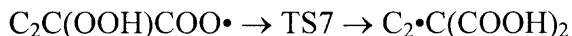
This reaction represents intramolecular, endothermic, transfer of a H atom from a primary methyl carbon atom to the peroxy oxygen radical site via a 6-member ring transition state including the H atom. The cleaving C—H bond stretches to 1.40 Å from 1.09 Å, and the forming O—H bond length is 1.14 Å, which is longer than that of normal O—H bond, 0.978 Å.

Epoxide formation

$C_3\bullet CCOOH \to TS3 \to C_2CYCCOC + OH$

$C_2\bullet C(COOH)_2 \to TS9 \to C(COOH)CYCCOC + OH$
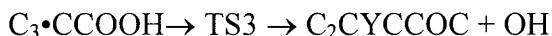
In this reaction type, the carbon radical in the $-CH_2\bullet$ group attacks the peroxy oxygen to form 4-member ring transition state; while the weak RO—OH bond is breaking. The cleaving O—O bond length is 1.68 Å and the forming C—O bond length is 1.99 Å. This reaction is responsible for a major fraction of the OH formation.

β-scission of alkyl radicals

$C_3CC\bullet \to TS0 \to C_2C=C + CH_3$

$C_3\bullet CCOOH \to TS4 \to C_2C=C + CH_2O + OH$

$C_3\bullet CCOOH \to TS5 \to C=C(C)COOH + CH_3$

$C_2\bullet C(COOH)_2 \to TS10 \to C=C(C)COOH + CH_2O + OH$
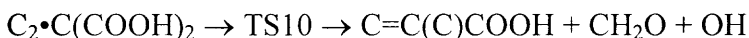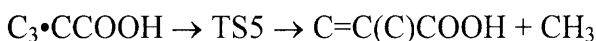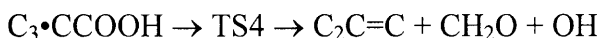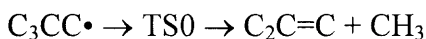
These reactions involve cleavage of an alkyl or oxy-alkyl group moving perpendicular from a near planar isobutenyl structure with simultaneous formation of a π bond (olefin here) on the same carbon. For methyl group dissociation, the C—C bond length stretches from 1.58 Å to 2.31 Å, and the forming C=C bond length is 1.37 Å in the TS0 and TS5 structures.

At temperatures above 1200°C, unimolecular dissociation of the neopentyl radical via TS0, is the primary reaction relative to reaction with O_2.

For the CH_2O + OH elimination from $C_3 \cdot CCOOH$ in TS4, the C—O bond length in the leaving group is decreased slightly from 1.425 to 1.366 Å, and O—O bond length is slightly increased in length from 1.457 to 1.470 Å.

In the structure of TS10, the C—O bond length (1.31 Å) is shorter than that of TS4 and the O—O bond length (1.78 Å) is longer than that of TS4 due to interaction of the hydroperoxy H and O atoms between the two –COOH groups (see Table B.1).

OH elimination from alkyl peroxy group

$C_3CCOO \cdot \rightarrow TS2 \rightarrow C_3CCHO + OH$

$C_2C(OOH)COO \cdot \rightarrow TS8A \rightarrow C_2C(COOH)CHO + OH$
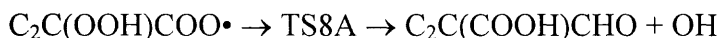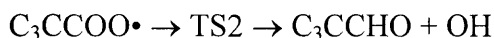
In this reaction group, the peroxy oxygen radical attacks the H atom in the nearest carbon via a 4-member ring transition state. The reaction path passes through a transient intermediate $R\text{-}C \cdot OOH$, where the carbon radical forms a π (carbonyl) bond with the oxygen (gaining ca. 80 kcal mol^{-1}) and cleaves the weak O—OH bond (requiring only ca. 45 kcal mol^{-1}). The C—O (forming), O—O (cleaving), and O—H bond lengths are 1.39, 1.50, and 1.27 A, respectively. The changes in these bond lengths between reactant and

TS suggest that the transition state reacts through the R-C•OOH structure to the intermediate R-CH(=O) + OH.

4.4.2 Thermochemical Properties

4.4.2.1 Enthalpies of Formation.
The enthalpies of formation for reactants, intermediate adducts and products in the neopentyl oxidation system are calculated by isodesmic reactions analysis or taken from available literature.

Table 4.1 Calculated $\Delta H_f{}^o{}_{298}$ Values for Species in $C_3CC\bullet + O_2$ System [a]

Reaction Series	B3LYP /6-31G(d,p)		B3LYP /6-311++G(3df,2p)		CBS-Q//B3LYP /6-31G(d,p)	
	$\Delta H^o{}_{rxn}$	$\Delta H_f{}^o{}_{298}$	$\Delta H^o{}_{rxn}$	$\Delta H_f{}^o{}_{298}$	$\Delta H^o{}_{rxn}$	$\Delta H_f{}^o{}_{298}$
1. $C_3CCOOH + COH \longrightarrow C_3COH + CCOOH$	-10.29	-56.06	-10.10	-56.25	-7.65	-58.70
2. $C_3CCOOH + CCOH \longrightarrow C_3COH + CCCOOH$	-6.12	-57.25	-6.33	-57.04	-4.83	-58.54
3. $C_3CCOOH + CCOH \longrightarrow C_3CCOH + CCOOH$	-1.10	-58.54	-2.18	-57.46	-1.06	-58.58
Average $\Delta H_f{}^o{}_{298}$ at CBS-Q level:					**-58.60**	
1. $C_3CCOO\bullet + CH_3OOH \longrightarrow C_3CCOOH + CH_3OO\bullet$	0.52	-26.08	0.55	-26.10	2.08	-27.63
2. $C_3CCOO\bullet + CCOOH \longrightarrow C_3CCOOH + CCOO\bullet$	0.81	-26.51	0.84	-26.54	1.83	-27.53
3. $C_3CCOO\bullet + C_2COOH \longrightarrow C_3CCOOH + C_2COO\bullet$	0.24	-27.05	0.06	-26.88	0.84	-27.65
Average $\Delta H_f{}^o{}_{298}$ at CBS-Q level:					**-27.61**	
1.$C_3\bullet CCOOH + C_2H_6 \longrightarrow C_3CCOOH + C_2H_5$	-0.51	-9.05	-0.65	-8.91	-0.12	-9.45
2. $C_3\bullet CCOOH + CCOOH \longrightarrow C_3CCOOH + C\bullet COOH$	-3.80	-7.42	-3.62	-7.59	-1.80	-9.41
3. $C_3\bullet CCOOH + CCOH \longrightarrow C_3CCOOH + C\bullet COH$	1.16	-9.34	0.62	-8.81	1.26	-9.44
Average $\Delta H_f{}^o{}_{298}$ at CBS-Q level:					**-9.43**	
1. $C_3CC\bullet + CH_4 \longrightarrow C_3CC + CH_3$	3.73	8.80	3.53	9.00	2.01	10.52
2. $C_3CC\bullet + C_2H_6 \longrightarrow C_3CC + C_2H_5$	-1.03	9.89	-1.17	10.03	-1.65	10.51
Average $\Delta H_f{}^o{}_{298}$ at CBS-Q level:					**-10.52**	
1. $C_3CCHO + CH_4 \longrightarrow C_3CC + CH_2O$	11.76	-59.99	11.22	-59.45	10.30	-58.53
2. $C_3CCHO + C_2H_6 \longrightarrow C_3CC + CH_3CHO$	0.22	-59.86	-0.52	-59.12	-0.69	-58.95
Average $\Delta H_f{}^o{}_{298}$ at CBS-Q level:					**-58.74**	
1. $C=C(C)COOH + CH_4 \longrightarrow C=CCOOH + C_2H_6$	6.21	-19.93	5.79	-19.50	8.65	-22.36
2. $C=C(C)COOH + CH_3OH \longrightarrow C=CCOOH + CCOH$	0.74	-20.16	0.79	-20.21	2.93	-22.34
Average $\Delta H_f{}^o{}_{298}$ at CBS-Q level:					**-22.35**	
1. $CCC\bullet(C)COOH \longrightarrow C_3\bullet CCOOH$	6.36	-15.79	6.07	-15.50	0.98	-10.42
The $\Delta H_f{}^o{}_{298}$ at CBS-Q level:					**-10.42**	

[a] Units in kcal mol^{-1}.

Table 4.1 lists the calculated reaction enthalpies and $\Delta H_f^o{}_{298}$ values for the species in the $C_3CC\bullet + O_2$ system at three calculation levels. The calculated $\Delta H_f^o{}_{298}$ values from

the DFT calculations show good agreement with the higher level ab initio calculations, indicating the errors in the computations for different molecules are canceled to a significant extent, ca. $\pm$ 2 kcal mol^{-1}, by the working reactions. The agreement between the calculation levels and with the literature data suggests reasonable accuracy for the absolute enthalpy values. The average $\Delta H_{f}^{o}{}_{298}$ values from the higher level CBS-Q calculations are selected to construct our kinetic model.

Enthalpies for transition states are calculated by use of two methods. The first method is straightforward using the $\Delta H_{f}^{o}{}_{298}$ values of the stable radical adducts from the working reaction analysis, plus the difference of total energies between the radical adducts and the transition state. The second method takes an average of: (i) the calculated energy difference between the TST structure and the reactant; and (ii) the difference between TST and the products plus enthalpy of reaction (ΔH^{o}_{rxn}). The ΔH^{o}_{rxn} values are calculated by the $\Delta H_{f}^{o}{}_{298}$ values of the reactant and product, which are determined on an absolute basis by the working reaction analysis. Enthalpies of formation for six transition states in the $C_3CC\bullet + O_2$ system determined by these two methods at the three different levels are listed in Table 4.2. It can be seen that the reaction enthalpies calculated from forward reaction (Method 1) show good agreement with the average values (Method 2) for all the six reactions at the CBS-Q level. The reaction enthalpies from DFT calculations only show good agreement with the values from CBS-Q level for the reactions with tight transition states (ring formation). Enthalpies of formation for transition states calculated from the first method at the CBS-Q level are used for the kinetic model. The $\Delta H_{f}^{o}{}_{298}$ of neopentyl radical is calculated as 10.52 kcal mol^{-1} at the CBS-Q level, which gives the C_3CC—H bond dissociation energy of 102.76 kcal mol^{-1}

based on the published $\Delta H_f^{o}{}_{298}$ value for neopentane (-40.14 ± 0.15 kcal mol^{-1}).[123] The above enthalpy value shows good agreement with the value, 10.36 kcal mol^{-1}, reported recently by Sumathi el al. at the CBS-Q calculation level.[124] Holmes el al.[125] measured the heats of formation of alkyl radicals by monoenergetic electron impact, and they reported that their values agree with results from equivalent measurements using ESR spectroscopy. They reported $\Delta H_f^{o}{}_{298}$ of neopentyl radical as 10.1 kcal mol^{-1}.

Table 4.2 The Reaction Enthalpies in the Reactions of Neopentyl + O_2[a]

	B3LYP /6-31G(d,p)	B3LYP /6-311++G(3df,2p)	CBS-Q//B3LYP /6-31G(d,p)	B3LYP /6-31G(d,p)	B3LYP /6-311++G(3df,2p)	CBS-Q//B3LYP /6-31G(d,p)
	$E_{a,\,forward}$[b]	$E_{a,\,forward}$[b]	$E_{a,\,forward}$[b]	$E_{a,\,average}$[c]	$E_{a,\,average}$[c]	$E_{a,\,average}$[c]
TS1	24.00	23.42	23.82	21.65	22.79	23.90
TS2	42.54	42.06	41.61	40.36	43.59	42.21
TS3	14.71	14.14	15.51	14.88	15.74	16.12
TS4	29.97	27.81	25.39	31.82	31.69	25.31
TS5	24.19	22.49	26.52	29.58	32.00	26.36
TS6	54.35	53.23	56.34	57.25	55.98	56.55

[a] Units in kcal mol^{-1}. [b] The reaction enthalpies are calculated from forward reaction. [c] The reaction enthalpies are calculated from the average enthalpy values of the forward, reverse, and ΔH^o_{rxn}. $E_{a,average} = \frac{1}{2}$ ($E_{a,\,forward}$ + $E_{a,\,reverse}$ + ΔH^o_{rxn}).

The $\Delta H_f^{o}{}_{298}$ of neopentyl peroxy is calculated as -27.61 kcal mol^{-1} at the CBS-Q level; Curran et al.[113] estimated it as -26.80 kcal mol^{-1} by group additivity using THERM[115]. The reaction enthalpy of alkyl radicals + O_2 are reported by Knyazev[126] as 32.74, 35.47, 37.14, 36.52 kcal mol^{-1} for CH_3, C_2H_5, i-C_3H_7, t-C_4H_9, respectively; which are obtained from the third-law treatment of the temperature dependencies of the equilibrium constants $K_p(T)$. Clifford et al.[127] reviewed the thermochemistry of alkyl peroxy radicals, and gives the reaction enthalpy of tert-butyl + O_2 as –37 ± 2 kcal mol^{-1}. The well depth for $C_3CC\bullet$ + O_2 is calculated to be 38.13 kcal mol^{-1} in this work

The $\Delta H_f{}^\circ{}_{298}$ values of hydrocarbons, substituted hydrocarbons, and corresponding radicals have been investigated in our previous studies, which show that the CBS-Q enthalpy values based on B3LYP/6-31G(d,p) optimized geometries are in agreement with accepted literature values. The CBS-Q enthalpies are more consistent than those from QCISD(T)/6-31G(d,p) single point calculations when the values for one species are compared through a series of different working reactions. A comparison of $\Delta H_f{}^\circ{}_{298}$ values from CBS-Q calculations with experimental data or accepted literature data on several oxygenated hydrocarbons is listed in Table 4.3.

Table 4.3 Comparison of Calculated $\Delta H_f{}^\circ{}_{298}$ With Experimental Values

Enthalpies of Formation ($\Delta H_f{}^\circ{}_{298}$) in kcal/mol					
Species	CBS-Q	Literature	Species	CBS-Q	Literature
CH_3CH_2OOH	-39.9 ± 1.5	-39.7 ± 0.3[128]	$CH_3CH_2O\bullet$	-3.90 ± 1.27	-3.7 ± 0.8[129]
$CH_3CH_2OO\bullet$	-6.7 ± 2.3	-6.8 ± 2.3[130]	$CH_3CH\bullet OH$	-13.34 ± 0.84	-14.5 ± 3[131]
$C\bullet H_2CH_2OOH$	11.2 ± 2.1	10.96 ± 1.06[128]	$CH_2\bullet CH_2OH$	5.70 ± 0.85	-5.9[132]
$CH_3C\bullet(=O)$	-3.08 ± 0.38	-2.90 ± 0.70[55]	$(CH_3)_2CHOH$	-69.19 ± 0.31	-69.15[50]
$CH_2\bullet OH$	-3.97 ± 1.11	-3.97 ± 0.22[133,134]	$(CH_3)_2CHO\bullet$	-11.85 ± 0.08	-11.0 ± 1.2[68]

4.4.2.2 Internal Rotation Analysis. The calculated internal rotational potentials on the C—C bonds of neopentyl peroxy radical and hydroperoxide neopentyl radical are shown in Figure 4.1, where the normal three-fold rotational barrier for rotation on the CH_3—C bonds is illustrated. The barriers for methyl rotors are near 3.3, while the C_3C—COO• barriers are near 5 kcal mol^{-1}. Figure 4.2 show the rotational potentials on the C—OOH, C—OO• and CO—OH bonds for the above two species, which have relatively high barriers, 4 to 7.5 kcal mol^{-1}. The 6 and 7 kcal mol^{-1} barrier heights are typical of published data on these CO—OH and C—OOH bonds.[77,135]
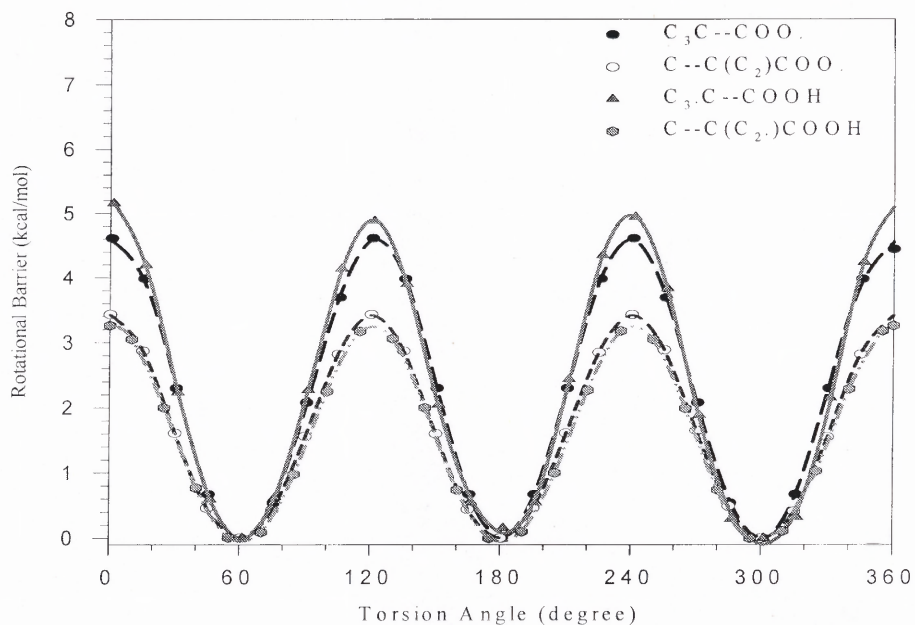
Figure 4.1 Torsional potentials on the C—C bond of neopentyl peroxy radical and hydroperoxy-neopentyl radical.
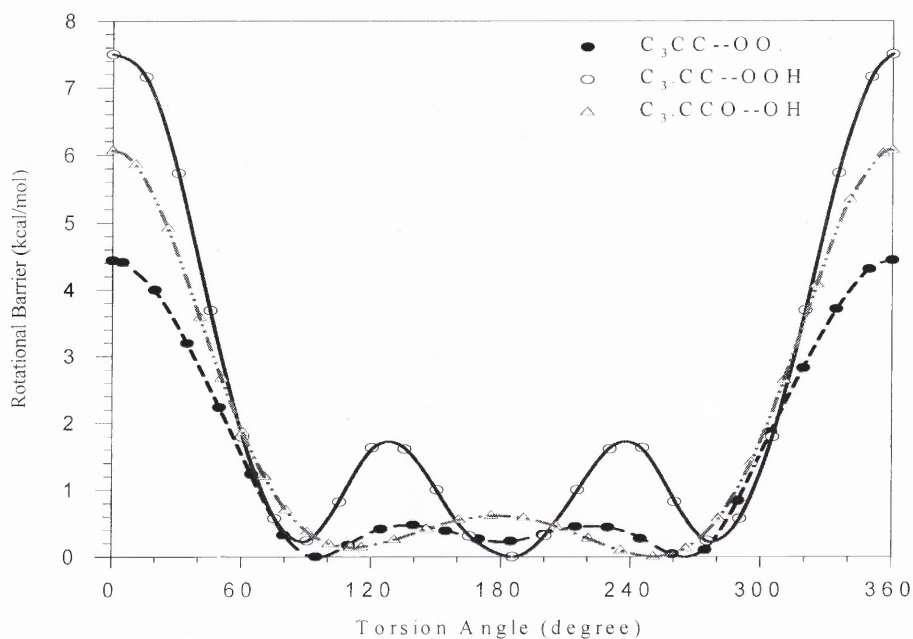

Figure 4.2 Torsional potentials on the C—O and O—O bonds of neopentyl peroxy radical and hydroperoxy-neopentyl radical.
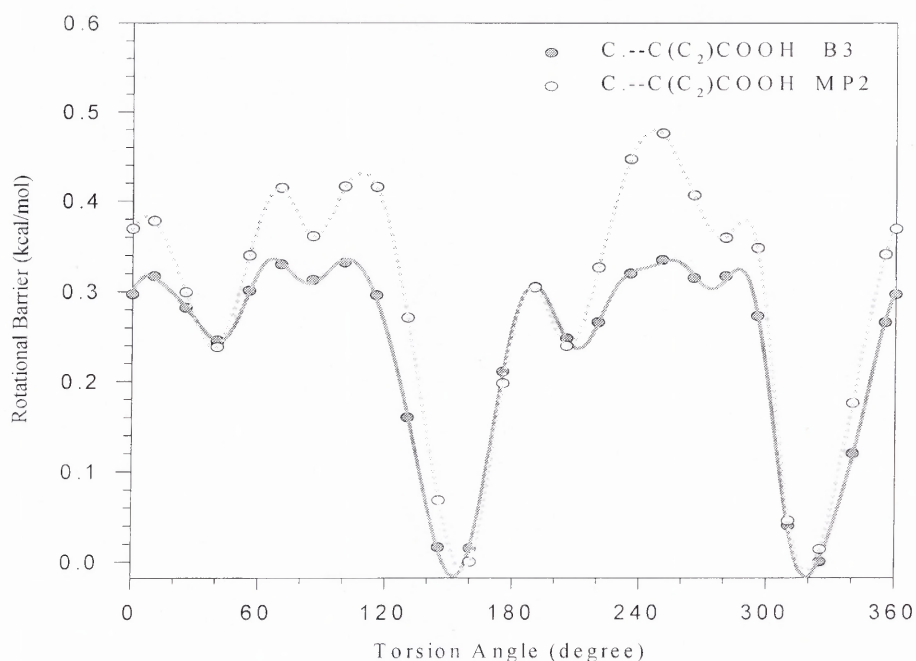
Figure 4.3 Torsional potentials on the C•—C bond of hydroperoxy-neopentyl radical calculated at the B3LYP and MP2 levels.

Table 4.4 Thermodynamic Properties for C₃CCOO• and C₃•CCOOH [a]

species		$\Delta H^o_{f\,298}$[b]	S^o_{298}[c]	C_p300[c]	C_p400	C_p500	C_p600	C_p800	C_p1000	C_p1500
	TVR[d]									
C₃CCOO•			69.17	24.39	32.62	40.25	46.84	57.22	64.9	76.8
(81)[f]	C-O[e]		6.82	1.45	1.47	1.50	1.50	1.46	1.38	1.15
	C(neo)-COO[e]		6.63	2.19	2.28	2.29	2.22	1.95	1.65	1.06
	C-C(neo)[e]		4.30	2.07	2.14	2.07	1.95	1.70	1.52	1.27
	C-C(neo)[e]		4.30	2.07	2.14	2.07	1.95	1.70	1.52	1.27
	C-C(neo)[e]		4.30	2.07	2.14	2.07	1.95	1.70	1.52	1.27
C₃CCOO•		-27.61	95.53	34.25	42.79	50.24	56.40	65.74	72.49	82.81
C₃•CCOOH	TVR[d]		76.48	25.57	33.53	40.75	46.89	56.54	63.71	75.03
(9)[f]	O-O[e]		3.59	1.39	1.41	1.44	1.46	1.47	1.45	1.34
	C-O[e]		6.68	2.05	1.84	1.71	1.63	1.54	1.47	1.23
	C(neo)-COOH[e]		6.37	2.10	2.16	2.19	2.16	1.98	1.75	1.22
	C-C(neo)[e]		4.34	2.08	2.13	2.05	1.93	1.68	1.50	1.26
	C-C(neo)[e]		4.34	2.08	2.13	2.05	1.93	1.68	1.50	1.26
	C-C(neo)[e]		5.15	1.06	1.03	1.02	1.01	1.00	1.00	1.00
C₃•CCOOH		-9.43	106.95	36.33	44.23	51.20	57.00	65.90	72.37	82.33

[a] Thermodynamic properties are referred to a standard state of an ideal gas of at 1 atm. [b] Units in kcal mol⁻¹. [c] Units in cal mol⁻¹ K⁻¹. [d] The sum of contributions from translations, vibrations, and external rotations. [e] Contribution from internal rotations. [f] Symmetry number.

Table 4.5 Ideal Gas Phase Thermodynamic Properties[a]

Species	$\Delta H^{\circ}_{f\,298}$[b]	S°_{298}[c]	C_p300[c]	C_p400	C_p500	C_p600	C_p800	C_p1000	C_p1500
TS0	62.49	91.15	32.08	39.15	45.32	50.54	58.78	65.00	74.95
TS1	40.26	82.48	29.21	36.30	42.35	47.42	55.40	61.51	71.51
TS2	-3.79	86.14	32.97	42.15	50.04	56.54	66.39	·73.48	84.33
TS3	14.00	91.66	34.52	43.00	50.27	56.24	65.31	71.90	82.08
TS4	6.07	99.54	34.99	43.03	50.02	55.83	64.79	71.46	82.01
TS5	15.95	102.74	36.82	44.47	51.01	56.38	64.60	70.67	80.34
TS6	17.09	102.33	37.15	44.86	51.45	56.87	65.18	71.33	81.11
TS7	46.91	102.36	35.07	43.05	50.01	55.78	64.64	71.12	81.21
TS8	-19.99	112.00	44.19	53.85	62.21	69.04	79.20	86.32	96.94
TS8A	-1.61	110.13	40.86	50.43	58.62	65.25	75.05	81.92	92.21
TS9	-9.42	112.78	42.46	51.63	59.44	65.75	75.17	81.89	92.31
TS10	-10.21	114.33	44.45	53.09	60.47	66.50	75.61	82.19	92.49
TS11	-36.38	94.19	32.09	38.67	44.62	49.74	57.81	63.79	72.97
TS12	-11.60	93.56	34.10	41.24	47.40	52.55	60.56	66.43	75.38
TS13	23.56	77.43	22.73	27.89	32.53	36.50	42.79	47.45	54.64
C$_3$CC•	10.52	81.80	29.13	36.45	42.77	48.05	56.31	62.56	72.65
C$_3$CCOOH	-58.60	96.20	35.65	44.34	51.95	58.23	67.80	74.78	85.70
C$_3$CCOO•	-27.61	95.45	34.02	42.39	49.69	55.71	64.84	71.48	81.80
C$_3$•CCOOH	-9.43	105.58	36.33	44.23	51.20	57.00	65.90	72.37	82.33
C$_2$CYCCOC	-35.43	81.19	27.04	34.90	42.01	48.02	57.35	64.21	74.77
C$_2$CYCCOC•	10.92[d]	76.3	23.71	31.05	37.51	42.88	51.13	57.16	66.48
C$_3$CCHO	-58.74	84.46	30.19	37.07	43.21	48.45	56.77	63.02	72.81
CCC•(C)COOH	-10.42	103.92	34.02	41.91	48.99	54.93	64.07	70.74	81.05
C$_2$•C(COOH)$_2$	-25.14	125.49	43.22	51.66	59.00	65.00	73.92	80.24	89.90
C$_2$C(COOH)CHO	-76.83	107.03	37.03	44.58	51.33	57.00	65.71	71.98	81.53
C=C(C)COOH	-22.35	91.94	30.34	35.64	40.27	44.17	50.30	54.94	62.41
C$_2$C(COOH)COO•	-42.39	117.21	41.02	50.08	57.96	64.36	73.83	80.46	90.52
C$_2$C(CH$_2$O•)COO•	-8.25	106.00	36.67	44.97	52.14	57.99	66.73	72.96	82.42
C$_2$C•CHO	-19.16	79.12	22.01	26.89	31.59	35.74	42.41	47.37	55.03
C$_2$C(CHO)$_2$	-75.03	93.95	30.90	37.04	42.58	47.33	54.81	60.30	-75.03
C$_2$C(CHO)CH$_2$O•	-40.63	96.15	32.53	39.60	45.80	50.97	58.94	64.72	73.53
C(COOH)CYCCOC	-52.37	100.43	33.89	42.58	50.34	56.77	66.45	73.28	83.52
C=C(C)C=O	-27.34	74.13	21.19	25.97	30.31	34.05	39.97	44.37	51.17
C$_3$CCl	-15.35	86.23	32.13	40.40	47.51	53.35	62.24	68.73	78.89
C$_3$•CCl	36.07	93.63	32.07	39.81	46.33	51.61	59.52	65.29	74.34
CH$_2$I	55.00[136]	66.30	11.58	12.55	13.30	13.86	14.58	15.00	15.47
IO•	27.70[137]	57.43	7.89	8.24	8.45	8.59	8.73	8.80	8.88

[a] Thermodynamic properties are referred to a standard state of an ideal gas of pure enantiometer at 1 atm. [b] Units in kcal mol^{-1}. [c] Units in cal mol^{-1} K^{-1}. [d] Based on the parent and bond energy calculation.

The torsional potential on the CH$_2$•—C(C$_2$)COOH bond in Figure 4.3 shows a very low, six fold barrier, where only two wells have depth over 0.3 kcal mol^{-1}. This CH$_2$•—C(C$_2$)COOH rotor is nearly a free rotor. Figure 4.3 shows both UB3LYP/6-31G(d,p) and UMP2/6-31G(d,p) calculations, where the barriers are low and similar in

foldness, but the energies are somewhat different. The potential curve from the UB3LYP/6-31G(d,p) level is chosen to calculate the contribution from $CH_2\bullet$—$C(C_2)COOH$ internal rotor to S°_{298} and $C_p(T)$'s for consistency. Table 4.4 illustrates the values from vibrational, translational, external rotational contributions and also each hindered internal rotational contribution to S°_{298} and $C_p(T)$'s for $C_3CCOO\bullet$ and $C_3\bullet CCOOH$. Table 4.5 lists the thermochemical properties of important reactants, transition states, adducts, and products.

4.4.3 Chemical Activation Reaction Analysis

4.4.3.1 $C_3CC\bullet + O_2$.   A potential energy diagram for the $C_3CC\bullet + O_2$ reaction system calculated at the CBS-Q level is shown in Figure 4.4. Neopentyl radical ($\Delta H_f^{\circ}{}_{298}$ = 10.52 kcal mol^{-1}) reacts with O_2 to form a $C_3CCOO\bullet$ radical with a 38.13 kcal mol^{-1} well depth. Reaction channels for the energized adduct $C_3CCOO\bullet^*$ include dissociation back to reactants, stabilization to $C_3CCOO\bullet$, isomerization by hydrogen transfer to the peroxy radical site via TS1 (E_a = 23.82 kcal mol^{-1}) to form a $C_3\bullet CCOOH$ isomer ($\Delta H_f^{\circ}{}_{298}$ = -9.43 kcal mol^{-1}), and dissociation to products (C_3CCHO + OH) via TS2 (E_a = 41.61 kcal mol^{-1}). The barrier for $C_3CCOO\bullet$ isomerization to $C_3\bullet CCOOH$ is calculated as 23.82 kcal mol^{-1}, the chemically activated $C_3CCOO\bullet^*$ adduct has sufficient energy for this isomerization to occur before it is stabilized or reacts back to reactants (reverse). Since the energy of TS3 is ca. 4 kcal mol^{-1} lower than that of the entrance channel, the chemically activated $C_3CCOO\bullet^*$ adduct can isomerize and dissociate to the 3,3-dimethyloxetane + OH directly.

C—C—C• + O₂
(10.52)

[C—C—C—COO•]
C

C—C—COO•
C
(-27.61)

Ea=56.34
(TS6,46.91)

[C⋯C⋯C—COOH]‡
C

Ea=41.61
(TS2, 14.00)

C—C—C⋯O—O ‡
H
(TS2)

C—C—C—O—O ‡
H⋯O
C

TS1, -3.79
Ea=23.82

C⋯O—OH ‡
C—C—C
(TS3, 6.07)
Ea=15.50

[C—C⋯COOH]‡ [C⋯C—COOH]‡
C C
(TS4, 15.95) (TS5,17.09)
Ea=25.38

Ea=26.52
(11.04)

CH₃ +C=CCOOH

CC C•—COOH
C
(-10.42)

(-9.43)

C•
C—C—COOH
C

C
C—C=C + CH₂O + OH
(-21.34)

(-26.54)
C—O
C—C—C + OH
C

C
C—C—CHO + OH
C
(-49.85)

Units: kcal/mol
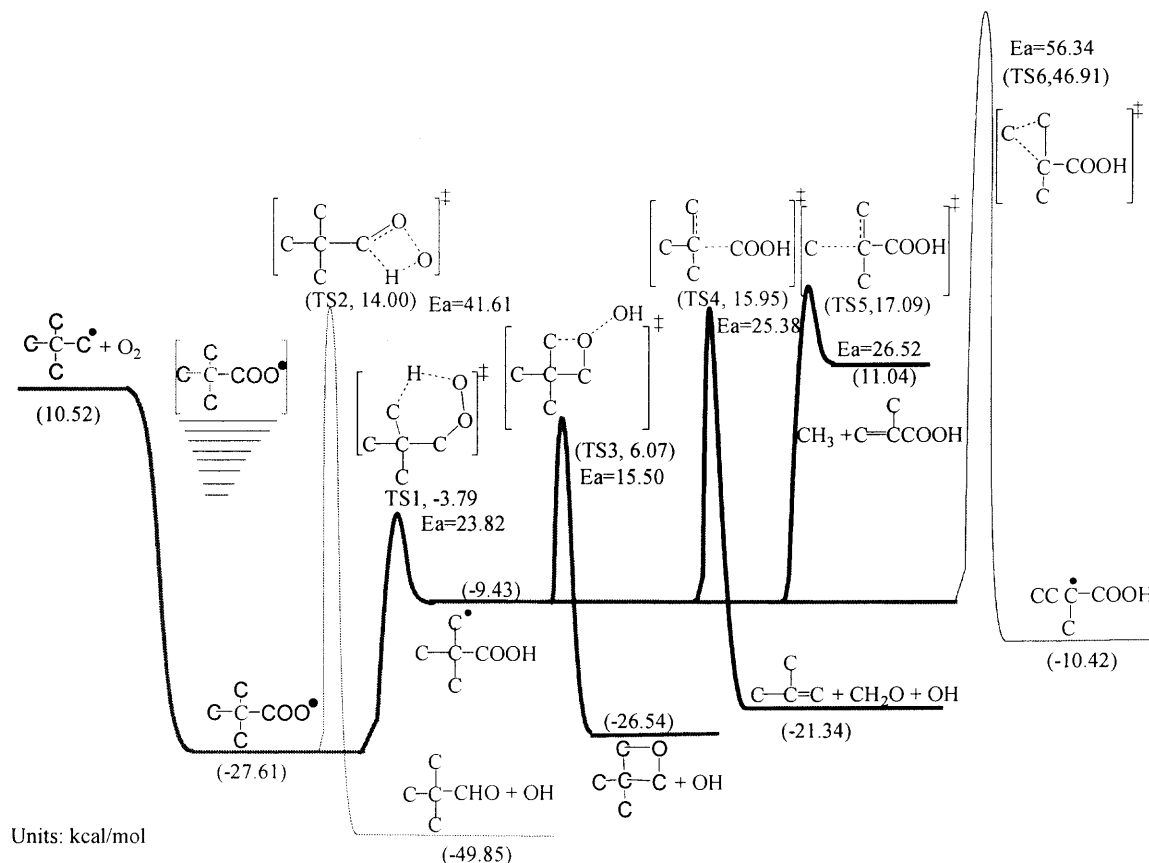
Figure 4.4 Potential energy diagram for C₃CC• + O₂ reaction system.

The energized C₃•CCOOH isomer undergo unimolecular reaction through several forward channels that are important to products or revert back to the peroxy isomer. Forward reactions are dissociation to 3,3-dimethyloxetane + OH via TS3 (E_a= 15.50 kcal mol⁻¹), β-scission to C₂C=C + CH₂O + OH via TS4 (E_a = 25.38 kcal mol⁻¹), and another β-scission (elimination) to C=C(C)COOH + CH₃ via TS5 (E_a = 26.52 kcal mol⁻¹). The C₃•CCOOH isomer can also undergo a very interesting isomerization via TS6 (E_a= 56.34 kcal mol⁻¹) shifting a methyl group onto the -CH₂• radical site forming a tertiary radical; but the high barrier and tight transition state make this channel unimportant. The

dominant channel of this hydroperoxy-neopentyl isomer is reverse reaction back to the peroxy isomer, with a barrier of only 5.64 kcal mol^{-1}.

The 3,3-dimethyloxetane is an important product; it can undergo abstraction reaction to lose a secondary H atom bonded on a carbon in the ring structure, the radical formed will undergo ring opening via C—O bond cleavage to form C_3•CCHO radical with a lower barrier[83], or via C—C bond cleavage to form $C_2C=COC$• radical ($E_a = 33.13$ kcal/mol). The C_3•CCHO radical undergoes β-scission leading to the formation of isobutene + HCO ($E_a = 18.77$ kcal/mol), or methacrolein + CH_3 ($E_a = 27.33$ kcal/mol); the $C_2C=COC$• radical undergoes β-scission to form CH_2O + $C_2C=C$• radical ($E_a = 32.33$ kcal/mol) which will undergo subsequently oxidation reactions.[138]

Table 4.6 Kinetic Parameters for QRRK Analysis in C_3CC• + O_2 System

reaction	A (s^{-1} or cm^3 mol^{-1} s^{-1})	n	E_a(kcal mol^{-1})
C_3CC• + O_2 → C_3CCOO•	1.99×10^{17} [a]	-2.1	0.0
C_3CCOO• → C_3CC• + O_2	6.17×10^{13} [b]	0.0	36.28
C_3CCOO• → C_3•CCOOH	1.24×10^6	1.68963	23.14
C_3CCOO• → C_3CCHO+OH	6.54×10^8	1.23510	41.48
C_3•CCOOH → C_3CCOO•	2.07×10^5	1.12721	5.17
C_3•CCOOH → $C_2CYCCOC$ + OH	2.49×10^{10}	0.50717	15.14
C_3•CCOOH → $C_2C=C$ + CH_2O +OH	2.84×10^{11}	0.44359	25.91
C_3•CCOOH → C=C(C)CQOH + CH$_3$	8.63×10^7	1.55502	26.10
C_3•CCOOH → CCC•(C)COOH	3.63×10^9	0.97602	56.17

	frequency / degeneracy		
C_3CCOO•	455.3 / 17.809	1418.9 / 18.919	3681.3 / 8.773
C_3•CCOOH	403.1/ 17.879	1388.0 / 18.733	3466.4 / 8.388

Lennard-Jones parameter	σ (Å)	ε/k (K)
	5.86	632

[a] From reference 7. [b] From the principle of microscopic reversibility at 700 K.

The high-pressure limit rate constants for this C_3CC• + O_2 system are calculated from canonical transition state theory and fitted by three parameters A_∞, n, and E_a over the temperature range from 298 to 2000 K, $k_\infty = AT^n exp(-E_a/RT)$, by the THERMKIN[72]

program. These are important kinetic parameters and are used as input for QRRK and Master equation analysis. The values of these parameters are listed in Table 4.6, and the thermodynamic analysis for reactions of neopentyl oxidation by THERMKIN are illustrated in Table B.3.
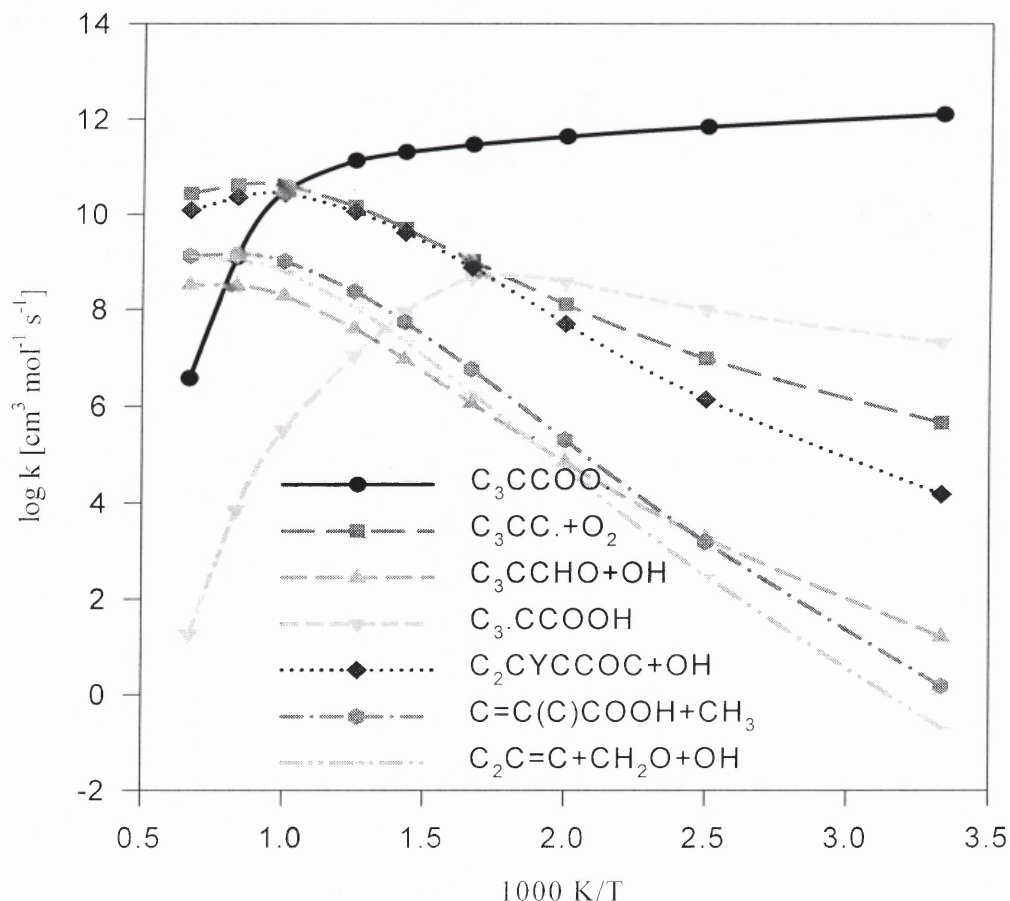
Figures 4.5 Calculated temperature dependent rate constants for chemical activated $C_3CC\bullet + O_2$ system at P = 1 atm.

The calculated temperature dependent rate constants for chemically activated $C_3CC\bullet + O_2$ reaction system from 300 to 1500 K at 1 atm are illustrated in Figure 4.5. The dominant product-channel for $C_3CC\bullet + O_2$ is stabilization to $C_3CCOO\bullet$ below 1000 K. The forward and reverse isomerization and reverse reaction (dissociation) occur

rapidly; the isomerization and the epoxide formation steps have relatively tight transition states with Arrhenius pre-exponential factors of ca. 10^{11} s^{-1} between 300 ~ 1000 K respectively, and the reverse isomerization is fast because of the very low barrier (5.64 kcal mol^{-1}). At the low temperatures of 700 ~ 800 K, the stabilization and isomerization are the dominant channels with 3.1 ~ 10.3 % of total forward reaction forming 3,3-dimethyloxetane + OH. Reverse reaction and dissociation to 3,3-dimethyloxetane + OH are the important reactions of the C$_3$•CCOOH adduct above 1000 K; this results in fall-off by 1000 K.
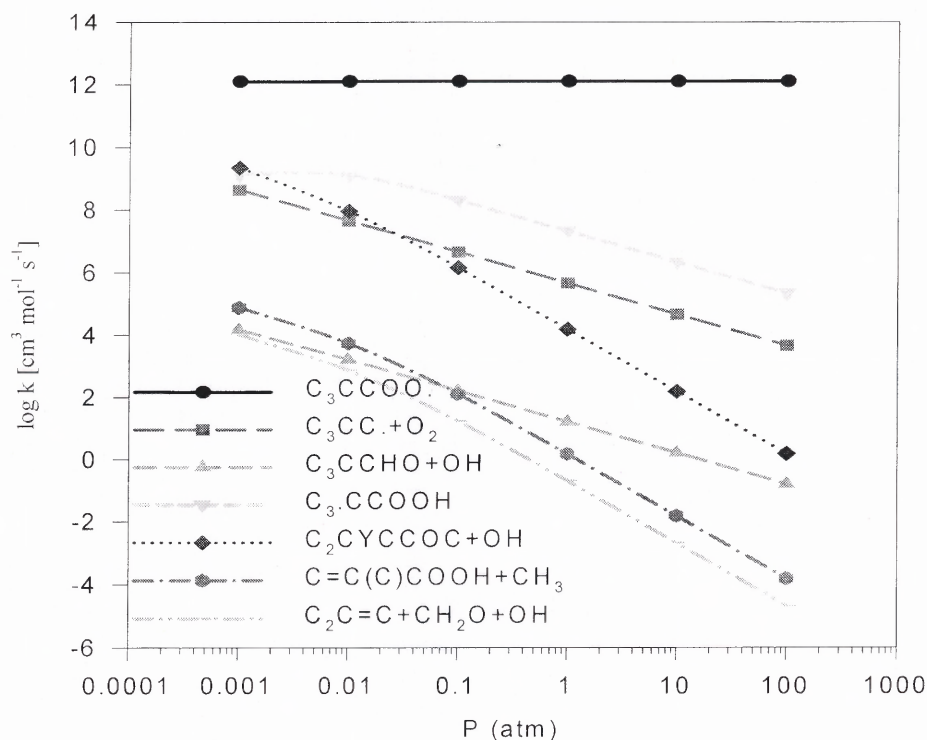
Figures 4.6 Calculated pressure dependent rate constants for chemical activated C$_3$CC• + O$_2$ system at T = 300 K.

Figures 4.6 and 4.7 illustrate the pressure dependence for the rate constants (log k vs P) of the chemically activated reactions, at 300 K and 1000 K. Stabilization to

$C_3CCOO\bullet$ is the dominant channel over all pressures at 300 K; it is also the dominant product channel when pressure is over 1 atm at 1000 K. When pressure is below 1 atm, the dissociation back to $C_3CC\bullet + O_2$ becomes the dominant channel at 1000 K, with the formation of 3,3-dimethyloxetane + OH competitive over the entire temperature range. The rate constants of other product channels decrease as the pressure increases. The next important reactions are formation of isobutene + CH_2O + OH and $C=C(C)COOH + CH_3$, which have similar rates and are lower than the epoxide + OH channel over the entire temperature range.
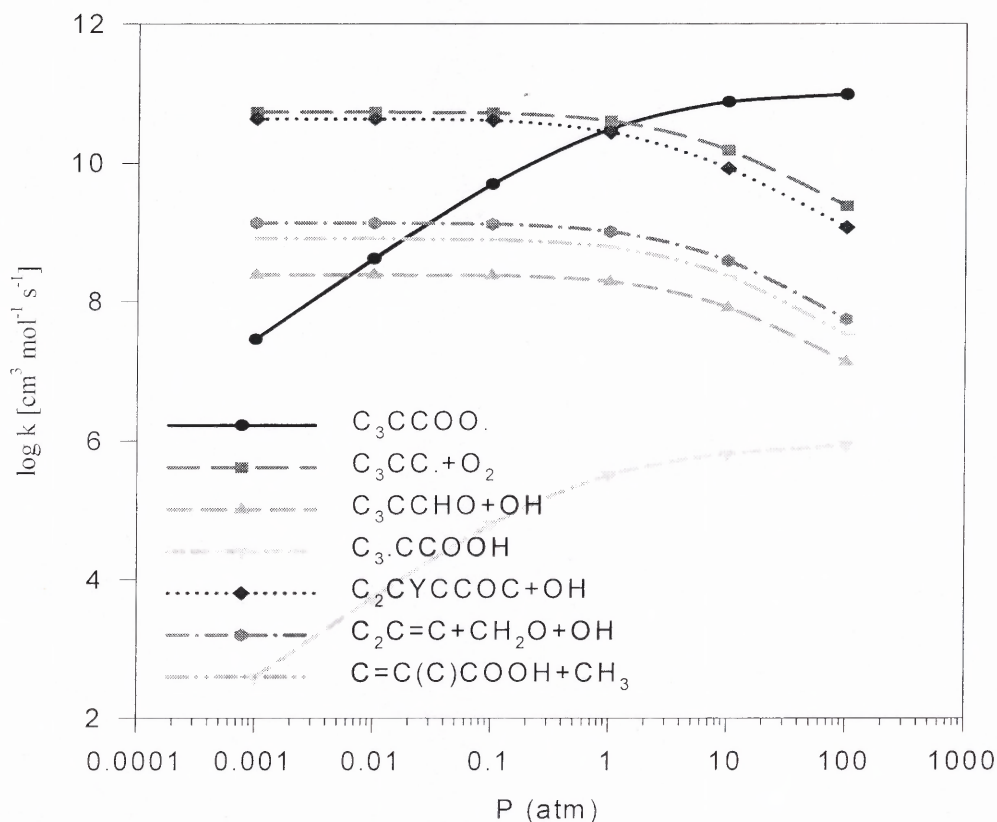
Figures 4.7 Calculated pressure dependent rate constants for chemical activated $C_3CC\bullet$ + O_2 system at T = 1000 K.

4.4.3.2 Dissociation of Adduct. Stabilization of the neopentyl peroxy adduct is an important product in the chemical activation reaction system below 1000 K. There are two important reactions of stabilized $C_3CCOO\bullet$ radical at atmospheric pressure as shown in Figure 4.8. One is isomerization to $C_3\bullet CCOOH$, and this channel is competitive with dissociation back to reactants $C_3CC\bullet + O_2$ above the temperature of 800 K. The isomer $C_3\bullet CCOOH$ has a very low barrier for reverse reaction and thus the neopentyl peroxy radical and the hydroperoxy-neopentyl isomer will exist in a quasi equilibrium, where the lower enthalpy peroxy radical will be the dominant isomer.
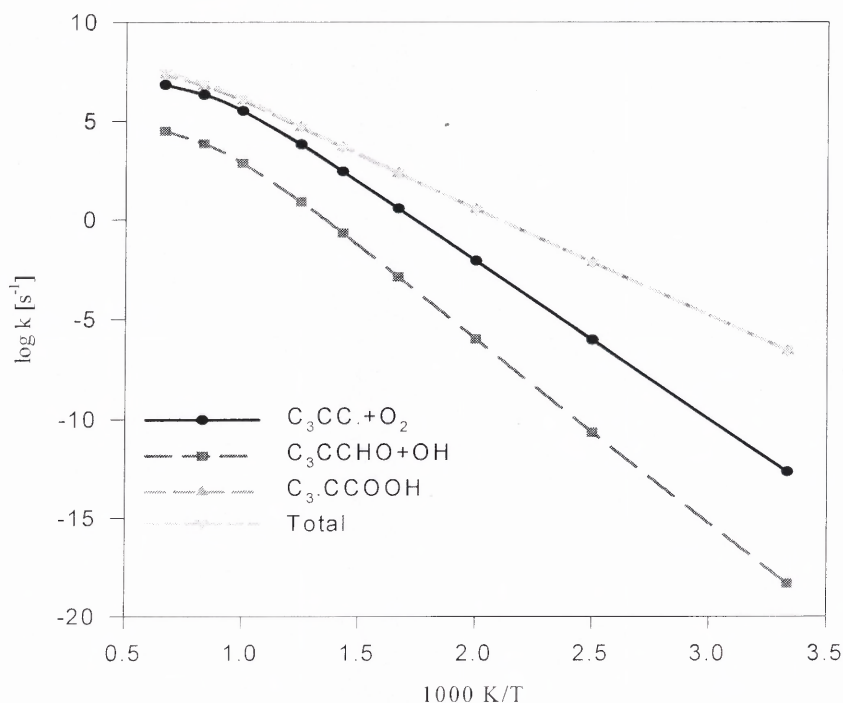
Figure 4.8 Calculated temperature dependent dissociation rate constants for $C_3CCOO\bullet$ at P = 1 atm.

There are four important reactions of stabilized $C_3\bullet CCOOH$ radical at atmospheric pressure as shown in Figure 4.9. The lowest barrier is the isomerization back to $C_3CCOO\bullet$, but the dissociation to 3,3-dimethyloxetane + OH is competitive with the

isomerization over the entire temperature range. The reaction channels for dissociation to $C_2C=C + CH_2O + OH$ and dissociation to $C=C(C)COOH + CH_3$ are similar and several orders of magnitude lower than the epoxide + OH channel over temperature of 300 ~ 1500 K.
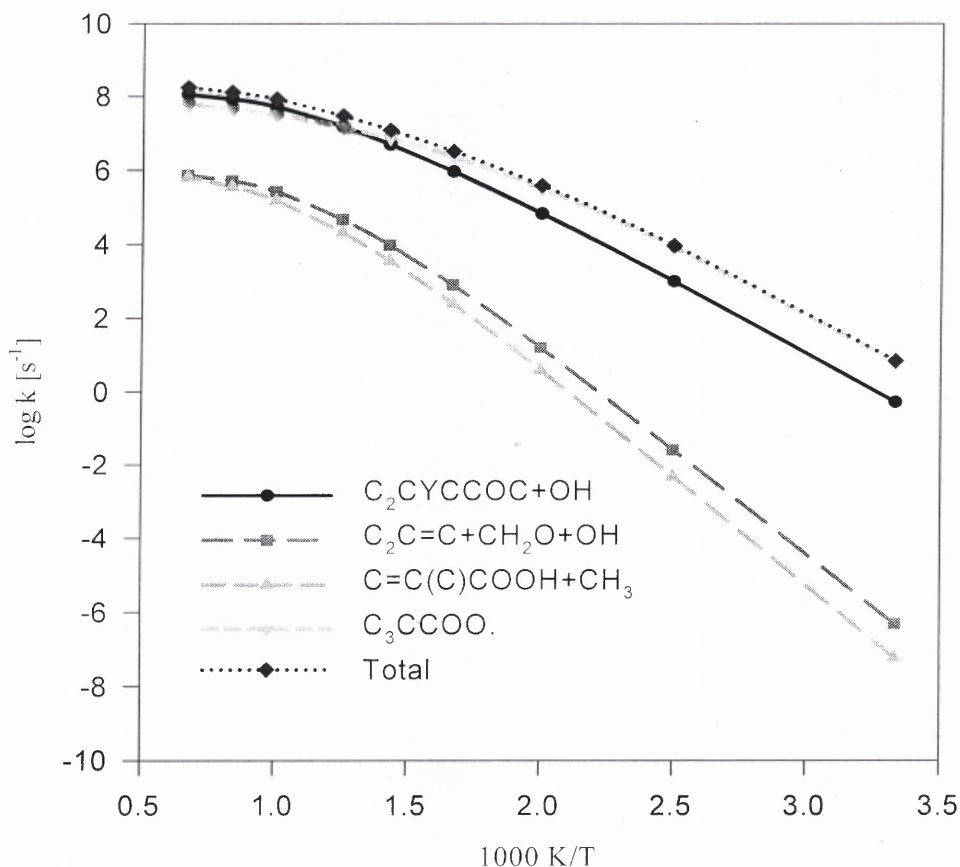
Figure 4.9 Calculated temperature dependent dissociation rate constants for $C_3 \cdot CCOOH$ at P = 1 atm.

The master equation analysis[26] for isomerization or dissociation from stabilized adducts does not include reactions past the adjacent well(s), so it is necessary to account for further reaction of these products in the numerical kinetic integration (Chemkin analysis).

4.4.3.3 C₃•CCOOH + O₂. The potential energy surface for addition of a second O₂ to

hydroperoxy-neopentyl radical (C₃•CCOOH) calculated at the B3LYP/6-311++G(3df,2p)

level is shown in Figure 4.10.
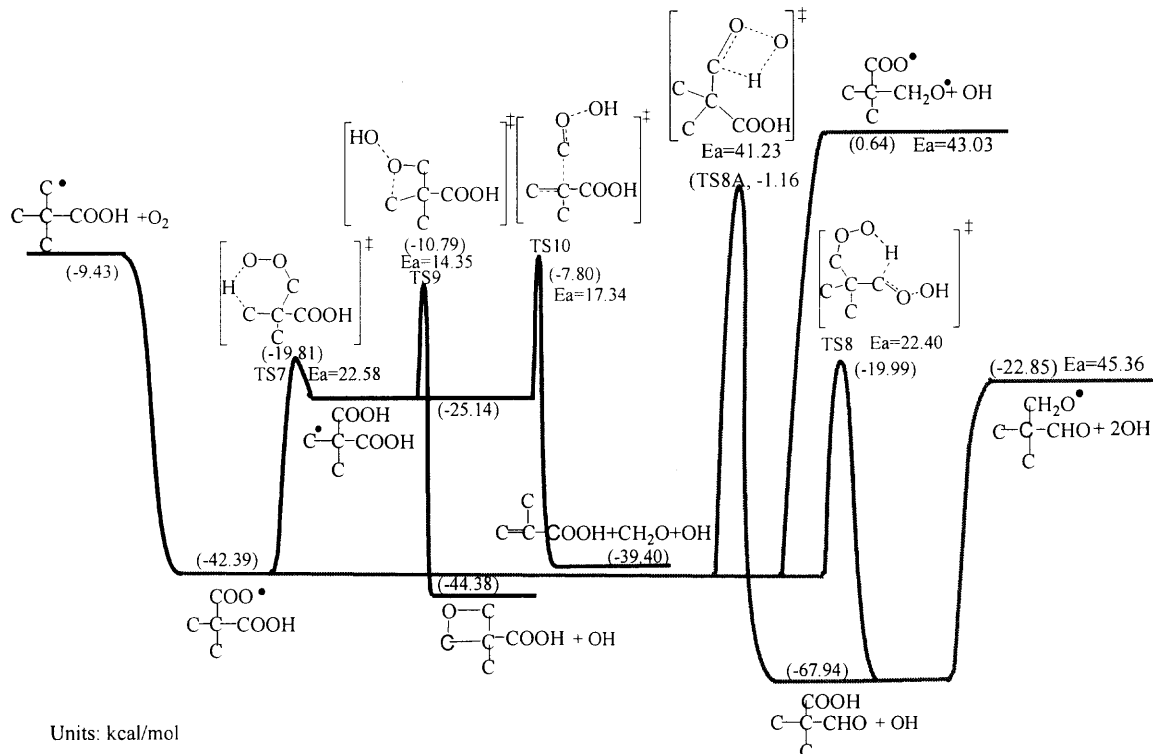
Figure 4.10 Potential energy diagram for C₃•CCOOH + O₂ reaction system.

The C₃•CCOOH reacts with O₂ to form a hydroperoxide-peroxy $C_2C(OOH)COO•$

with a 32.96 kcal mol⁻¹ well depth. Reaction channels for the chemically activated adduct

$C_2C(OOH)COO*$ include dissociation back to reactants, stabilization to

$C_2C(OOH)COO•$, isomerization via hydrogen shift via TS7 (E_a = 22.58 kcal mol⁻¹) to

form a dihydroperoxide isomer $C_2•C(COOH)_2$ ($\Delta H_f°_{298}$ = -25.14 kcal mol⁻¹), and

dissociation to products (C_3CCHO + OH) via two different transition states: TS8 (E_a =

22.40 kcal mol⁻¹) and TS8A (E_a = 41.23 kcal mol⁻¹). The dihydroperoxide isomer

$C_2 \cdot C(COOH)_2$ undergoes dissociation to 3-methyl,3-hydroperoxideoxetane + OH via TS9 (E_a = 14.35 kcal mol^{-1}), β-scission to generate a hydroperoxide olefin C=C(C)COOH and CH_2O + OH via TS10 (E_a = 17.34 kcal mol^{-1}). The stabilized $C_2C(OOH)COO\cdot$ peroxy undergoes homolytic dissociation via cleavage of the weak O—O bond with barrier of 43.03 kcal mol^{-1}. The stable vinyl hydroperoxide produced will also undergo homolytic cleavage of the weak O—O bond in the peroxide moiety to generate OH and vinyl alkoxy (chain branching reaction), serving to accelerate the oxidation process. The vinyl alkoxy radical is an important reaction to form 2-methyl-2-propenal (C=C(C)CHO) which was identified as an important product from neopentyl radical oxidation.[105]

A number of the reaction channels for $C_2C(COOH)COO\cdot$* adduct are similar to those of $C_3CCOO\cdot$* adduct due to the similarity between the two adduct structures. Table 4.7 lists calculated reaction enthalpies for similar reaction channels in Figure 4.4 and Figure 4.10. In Table 4.7, the barriers for the corresponding isomerization channels and dissociation channels in two reaction systems show agreement, especially for the channels with tight transition states (ring formation).

Table 4.7 Comparison and Estimation of Reaction Enthalpies for Similar Channels[a]

	B3LYP /6-31G(d,p)	B3LYP /6-311++G(3df,2p)	CBSQ//B3LYP /6-31G(d,p)		B3LYP /6-31G(d,p)	B3LYP /6-311++G(3df,2p)	corrected[b]
TS1	24.00	23.42	23.82	TS7	22.79	22.58	22.98
TS2	42.54	42.06	41.61	TS8A	41.87	41.26	40.78
TS3	14.71	14.14	15.51	TS9	15.86	14.35	15.72
TS4	29.97	27.81	25.39	TS10	19.28	17.34	14.93
				TS8	22.93	22.40	

[a] Units in kcal/mol. [b] Corrected reaction enthalpies according to the trend calculated from three different levels for the similar reaction channels.

In order to obtain more accurate reaction enthalpies in this second O_2 addition system than those from the DFT calculations, we evaluate the deviation of enthalpies

between the DFT and the CBS-Q levels, and then correct the corresponding DFT level reaction enthalpies to CBS-Q level for these oxygenated species. The barriers calculated from the B3LYP/6-311++G(3df,2p) level in Figure 4.10 are corrected as 22.98, 15.72, 14.93, and 40.78 kcal mol^{-1} for TS7, TS9, TS10, and TS8A, respectively. The correction is 0.4 ~ 1.4 kcal mol^{-1} for the reactions with ring- formation transition states, and is 2.4 kcal mol^{-1} for the dissociation of –CH$_2$OOH group with TS 10.

One new important channel in Figure 4.10, that is not in the C$_3$CC• + O$_2$ system (Figure 4.4), is the exothermic formation of C$_2$C(COOH)CHO + OH via a 6-member ring transition state (TS8) with a 22.40 kcal mol^{-1} barrier. In TS8, the peroxy radical abstracts the weakly bonded H atom in the –CH$_2$OOH group; this H—C(C$_2$)HOOH bond is weak because, as the H atom is leaving, a strong carbonyl bond (gain of ~ 80 kcal mol^{-1}) is forming with the weak O—OH bond (~ 45 kcal mol^{-1}) cleaving.

The chemical activated [C$_2$C(COOH)CHO]* species can undergo dissociation to cleave the weak RO—OH bond to form a 2-methyl isopropanal-2-methyoxy radical (C$_2$C(CHO)CH$_2$O•) plus a second OH (overall reaction C$_3$•CCOOH + O$_2$ → C$_2$C(CHO)CH$_2$O• + 2OH), or it can be stabilized. While the branching ratio to the two products is a function of temperature, it is calculated to be near 1:1 at the conditions modeled in this study. The [C$_2$C(COOH)CHO]* species has ca. 48 kcal mol^{-1} activation energy at the transition state point.

The stabilized C$_2$C(COOH)CHO can undergo bimolecular reaction (abstraction) and the product radicals can dissociate by low energy β-scission. For example, the weakly bonded H atom will be abstracted to form C$_2$C(COOH)C•=O radical, which will dissociate to CO and C$_2$C•COOH, which will further dissociate to isobutene + HO$_2$.

These are important chain branching channels at low temperature and also contribute to OH and HO_2 product formation.

The 2-methyl isopropanal-2-methyoxy radical $C_2C(CHO)CH_2O\bullet$ will undergo β-scission to either $C_2C\bullet(CHO)$ + CH_2O via TS11, or to $C_2C(CHO)_2$ + H via TS12 as outlined in the reaction mechanism scheme. The $C_2C\bullet(CHO)$ radical will undergo the β-scission to C=CC + HCO via TS13A, or C=C(C)CHO + H via TS13, which are important products that were observed in neopentane oxidation.[113]

Table 4.8 Kinetic Parameters for QRRK in $C_3\bullet CCOOH$ + O_2 System

reaction	A (s^{-1} or cm^3 mol^{-1} s^{-1})	n	E_a (kcal mol^{-1})
$C_3\bullet CCOOH$ + O_2 → $C_2C(COOH)COO\bullet$	8.0×10^{11} [a]	0.0	0.0
$C_2C(COOH)COO\bullet$ → $C_3\bullet CCOOH$ + O_2	6.38×10^{14} [a]	0.0	31.74
$C_2C(COOH)COO\bullet$ → $C_2\bullet C(COOH)_2$	1.06×10^8	0.92093	23.00
$C_2C(COOH)COO\bullet$ → $C_2C(COOH)CHO$ + OH	5.36×10^3	2.87418	21.30
$C_2C(COOH)COO\bullet$ → $C_2C(COOH)CHO$ + OH	8.90×10^6	1.59523	40.30
$C_2C(COOH)COO\bullet$ → $C_2C(CH_2O\bullet)COO\bullet$ + OH	1.0×10^{16} [a]	0.0	43.03
$C_2\bullet C(COOH)_2$ → $C_2C(COOH)COO\bullet$	1.01×10^4	1.62435	5.09
$C_2\bullet C(COOH)_2$ → $C(COOH)CYCCOC$ + OH	3.46×10^5	1.68617	15.31
$C_2\bullet C(COOH)_2$ → C=C(C)COOH+CH_2O + OH	1.28×10^5	1.98348	14.48
$C_2C(COOH)CHO$ → $C_2C(CHO)CH_2O\bullet$+ OH	3.20×10^{15}	0.00	45.09
$C_2C(CHO)CH_2O\bullet$→ $C_2C(CHO)_2$ + H	1.97×10^7	1.84217	28.52
$C_2C(CHO)CH_2O\bullet$→ $C_2C\bullet CHO$ + CH_2O	2.32×10^{11}	0.49609	4.56
$C_2C\bullet CHO$ → C=C(C)CHO + H	2.54×10^9	1.20614	42.68
$C_2C\bullet CHO$ → C=CC + HCO	1.33×10^{14} [a]	0.0	39.93

	frequency / degeneracy		
$C_2C(COOH)COO\bullet$	341.0 / 19.431	1445.4 / 25.704	4000.0 / 5.365
$C_2\bullet C(COOH)_2$	386.0 / 21.049	1447.6 / 21.746	3999.0 / 7.205

Lennard-Jones parameter	σ (Å)	ε/k (K)	
	6.40	720.5	

[a] The A factor is by generic reaction or estimated by reverse reaction and microscopic reversibility. [b] Estimated as the sum of reverse E_a and ΔH^o_{rxn}.

The high-pressure limit rate constants for the $C_3\bullet CCOOH$ + O_2 system are fitted by three parameters A_∞, n, and E_a over the temperature range from 298 to 2000 K and these fits along with data are listed vs. temperature in Appendix Table B.3. Important

input kinetic parameters for QRRK and Master equation analysis for this system are listed in Table 4.8.

The calculated temperature dependent rate constants for the chemical activated C_3•CCOOH + O_2 system are illustrated in Figure 4.11 for conditions of 300 to 1500 K at 1 atm. The dominant product for C_3•CCOOH + O_2 is stabilization to $C_2C(OOH)COO$• below 800 K, but reverse reaction becomes the dominant channel above 800 K.
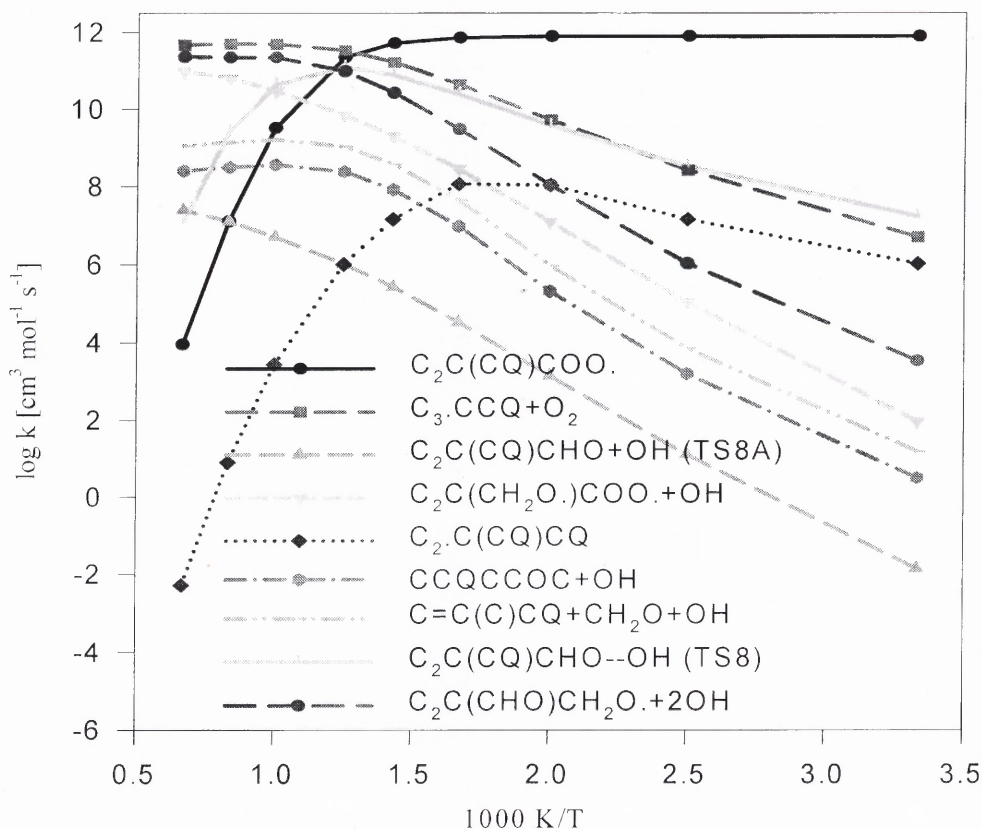

Figure 4.11 Calculated temperature dependent rate constants for chemical activated C_3•CCOOH + O_2 system at P = 1 atm.

The most important new product channel for stabilized $C_2C(OOH)COO$• radical at atmospheric pressure is the formation of $[C_2C(COOH)CHO]^*$ + OH via TS8 as shown in Figure 4.11, this reaction is competitive with the reverse channel to C_3•CCOOH + O_2

below 800 K. The dissociation channel (chain branching) of $[C_2C(COOH)CHO]^*$ to $C_2C(CO\bullet)CHO + 2OH$ becomes slightly dominant above 800 K; it is the important forward channel to products and is an important chain branching step at low and intermediate temperatures. The isomerization to $C_2\bullet C(COOH)_2$ is the next important forward channel below 600 K, and the homolytic cleavage of the weak RO—OH bond in $C_2C(OOH)COO\bullet$ (also a chain branching path) becomes important above 600 K.

A plot of log k vs pressure for the $C_3\bullet CCOOH + O_2$ system at 700 K is shown in Figure 4.12, which illustrates that stabilization to the peroxy radical and reverse reaction channels are dominant at all pressures. The dissociation to $C_2C(COOH)CHO + OH$ and $C_2C(CHO)CH_2O\bullet + 2OH$ are the most important forward channels at all these pressures.
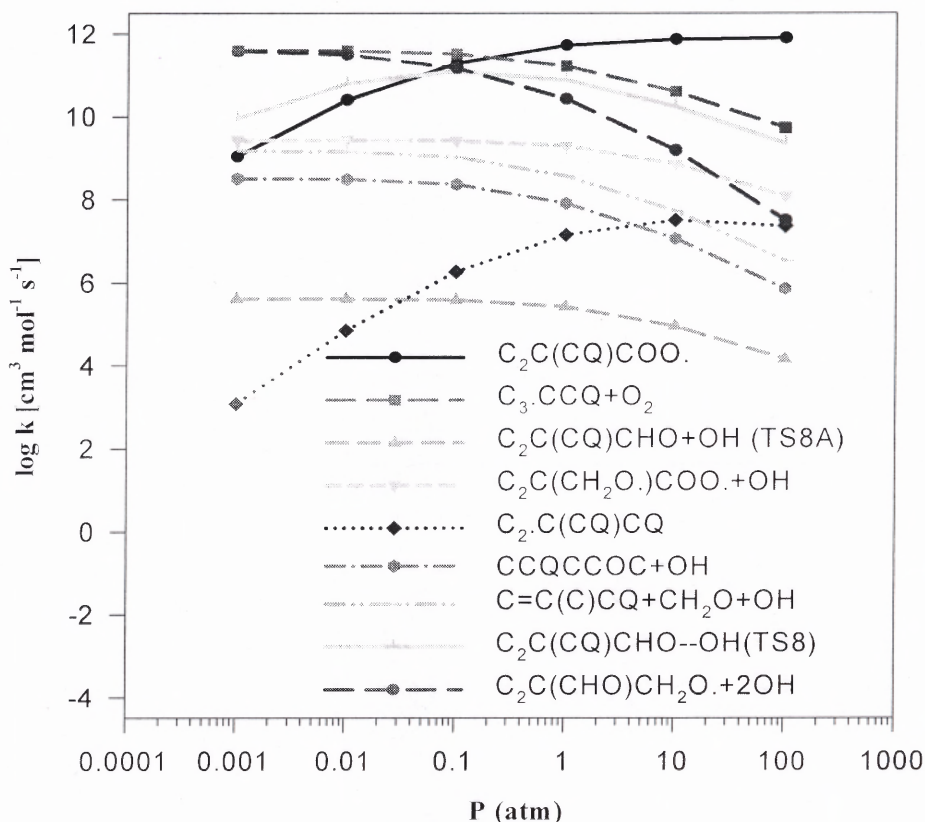
Figure 4.12 Calculated pressure dependent rate constants for chemical activated $C_3\bullet CCOOH + O_2$ system at T = 700 K.

4.4.4 Unimolecular Dissociation of Neopentyl Radical

At higher reaction temperatures, the neopentyl radical will undergo unimolecular dissociation to isobutene + methyl radical in competition with the R• + O_2 association reaction. The rate constant for unimolecular dissociation is calculated as $k = 10^{13.68}$exp(-30.84 kcal mol^{-1}/RT) s^{-1} at the CBS-Q level. It shows good agreement with the experimentally determined rate constant by Slagle et al,[139] $k = 10^{13.9}$exp(-30.9 ± 1.0 kcal mol^{-1}/RT) s^{-1}. The importance of this neopentyl radical unimolecular decomposition is also evaluated.

The OH radical generated by the neopentyl oxidation reactions and the methyl radical from the β-scission reaction above will add to isobutene forming new isobutene adducts: C_3•COH, C_2C•COH and C_2C•CC. These OH and CH_3 addition reactions and the subsequent O_2 addition reactions to these adducts have been calculated and included in our mechanism, but these reactions have little contribution to the OH formation profile. The reaction pathways and high pressure limit rate constants for the oxidation of these isobutene adducts will be discussed in the following chapter on modeling experimental HO_2 formation profiles in the neopentyl oxidation system.

4.4.5 Model and Comparison with Experimental Result

A detailed reaction mechanism (258 reactions of which approximately 170 reactions are pressure dependent, 115 species) for the initial neopentyl oxidation is assembled in Appendix Table B.4, and the CHEMKIN II interpreter and integrator (version 3.1)[140] is used to model the experimental OH formation profile for the reaction time of 0 ~ 3 ms. Abstraction reactions are not considered pressure dependent and therefore do not require fall-off analysis. Abstraction reactions of O, OH, HO_2, and R• radicals are taken from

evaluated literature wherever possible. A procedure from Dean and Bozzelli[141] is used to estimate abstraction rate constants by H, O, OH, and CH₃ radicals when no literature data are available.
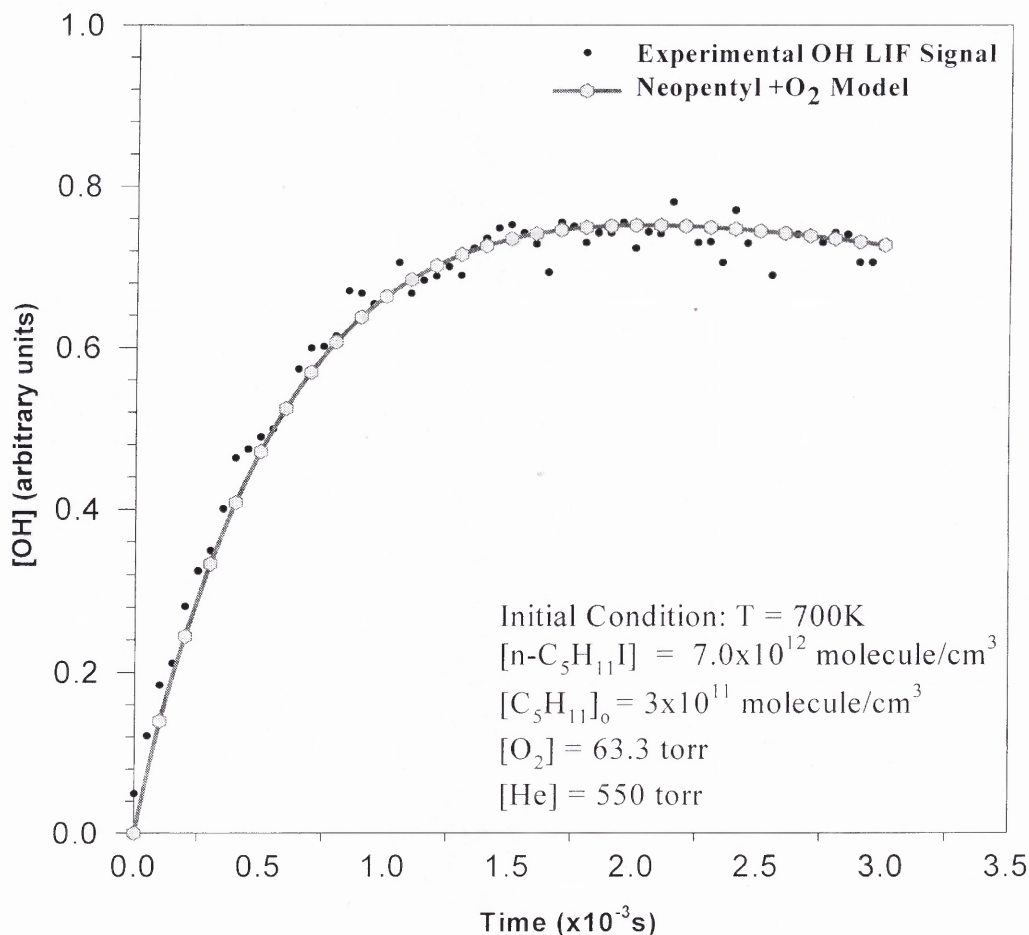
Figure 4.13 Comparison of the present model with the experimental OH LIF measurements of Hughes et al.

The time dependence of OH radical formation profile predicted by our reaction mechanism compared with experimental data published by Hughes et al.[105] is shown in Figure 4.13. The experiment was performed at 700 K, 613.3 torr, with O₂ pressure of 63.3 torr and C₃CC• radical concentration of 3×10^{11} molecule cm⁻³. The solid curve in

Figure 4.13 represents our modeling result for the OH profile, and it shows good agreement with experimental data of Hughes et al. The reactions from the addition of the second O_2, ($C_3 \cdot CCOOH + O_2$) contributes 0.9 to 6.4 % of the total predicated OH formation from the model. Sensitivity analysis on the OH formation at the experimental temperature and pressure is shown in Figure 4.14. The reaction channel for the formation of 3,3-dimethyloxetane + OH is calculated to have the highest sensitivity for the formation of the OH radical, the isomerization to $C_3 \cdot CCOOH$ from $C_3 CCOO \cdot$ radical is the next, the well depth of the chemical activation reaction of $C_3 CC \cdot + OH$ for formation of neopentyl peroxy and 3,3-dimethyloxetane + OH and the unimolecular decomposition of neopentyliodide radical are also important.
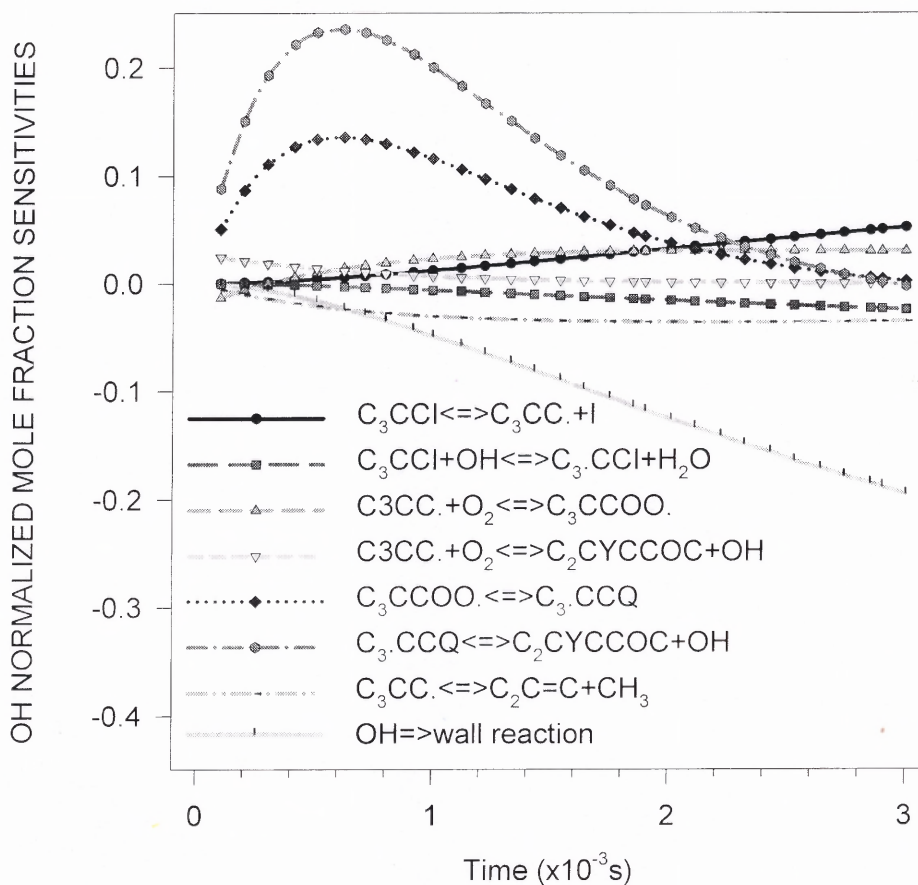
Figure 4.14 Sensitivity analysis on OH formation at T = 700 K and P = 613.3 torr.

The loss of OH radical, is most sensitive to wall reaction, and the unimolecular decomposition of neopentyl radical to isobutene + CH_3 is also important, since it results in the loss of the OH precursor. The entropy of TS3 for the formation of 3,3-dimethyloxetane + OH is calculated as 98.04 cal/mol, and it is increased by 1.5 cal mol^{-1} K^{-1} to fit the OH formation profile with reaction time.

Overall, there are several major reactions responsible for the OH formation: (i) Dissociation of hydroperoxy-neopentyl radical to 3,3-dimethyloxetane + OH; (ii) The addition of a second O_2 to hydroperoxy-neopentyl radical with isomerization and subsequent dissociation reactions; and (iii) Reactions of CH_3 from neopentyl dissociation. Importance of these reaction paths changes with concentrations, pressure and temperature. At a pressure of 613.3 torr and a temperature of 700 K, the formation of 3,3-dimethyloxetane + OH is by far the most important channel to form OH radical.

4.5 Summary

Thermochemical properties of the neopentyl radical + oxygen reaction system and the hydroperoxy neopentyl radical + O_2 reaction system are calculated using ab initio CBS-Q and density functional B3LYP/6-311++G(3df,2p) methods. The barriers for the isomerization of neopentyl peroxy and subsequent epoxide formation reactions are calculated as 23.82 and 15.50 kcal/mol, respectively. Kinetic parameters for intermediate and product formation channels are calculated versus temperature and pressure. A mechanism describing reaction paths and kinetic parameters for the initial steps in the neopentyl oxidation reaction system is developed to model the experimental OH formation profile. Second O_2 addition to the hydroperoxy neopentyl radical has a minor

contribution to the OH profile under the modeled condition, but can be important to chain branching. Several reactions are predicted to be important for OH formation profile. Thermodynamic equilibrium on the reactions of $C_3CCOO\bullet \Leftrightarrow C_3\bullet CCOOH$ and reactions $(C_3\bullet CCOOH \rightarrow$ 3,3-dimethyloxetane $+ OH$, $C_2C{=}C + CH_2O + OH)$, serve to control oxidation rate in this 700 K and 613.3 torr reaction system.

CHAPTER 5

KINETIC ANALYSIS OF 2-HYDROXY-1,1-DIMETHYLETHYL, 2-HYDROXY-2-METHYLPROPYL, AND 1,1-DIMETHYLPROPYL RADICALS OXIDATION

5.1 Overview

The reaction systems of 2-hydroxy-1,1-dimethylethyl, 2-hydroxy-2-methylpropyl, and 1,1-dimethylpropyl radicals plus O_2, which are secondary reactions in neopentyl radical + O_2 oxidation system, are analyzed with *ab initio* and density functional calculations to evaluate reaction paths and kinetics important in neopentyl oxidation. Enthalpies of formation ($\Delta H_f^o{}_{298}$) are determined using isodesmic reaction analysis at the CBS-Q//B3LYP/6-31G(d,p) level. The entropies ($S^o{}_{298}$) and heat capacities $C_p(T)$'s ($0 \leq T/K \leq$ 1500) from vibrational, translational, and external rotational contributions are calculated using statistical mechanics based on the vibrational frequencies and structures obtained from the density functional study. The hindered internal rotor contributions to $S^o{}_{298}$ and $C_p(T)$'s are calculated from the analysis of rotational potentials. $\Delta H_f^o{}_{298}$ values for radicals $C_2C^\bullet COH$, $C_2C(OO^\bullet)COH$, $C_3{}^\bullet COH$, $C_2C(OH)COO^\bullet$, and $C_2C(OO^\bullet)CC$ are calculated as –22.22, –62.71, –24.12, –61.76, and –33.58 kcal mol^{-1} at the CBS-QB3 level. The potential energy surfaces of the three reaction systems are calculated at the CBS-QB3 level. Rate constants are calculated as function of pressure and temperature using quantum Rice-Ramsperger-Kassel (QRRK) analysis for $k(E)$ and master equation for pressure fall-off. Kinetic parameters for intermediate and product formation channels of above reaction systems are presented versus temperature and pressure. An elementary reaction mechanism is constructed to model experimental HO_2 formation profiles at different O_2 concentrations in the neopentane oxidation reactions.

5.2 Background

The reactions of neopentyl radical with molecular oxygen have been investigated for modeling the time dependence of the OH formation profile based on ab initio and density functional computation methods in Chapter 4. Taatjes et al.[103] recently measured the time-resolved production of HO_2 and OH in pulsed-photolytic Cl-initiated oxidation of neopentane between 573 and 750 K. They reported that: (a) significant HO_2 formation is observed above 623 K, where the formation of HO_2 increases with increasing temperature; (b) the HO_2 produced also increases with increasing O_2 at 673 K; (c) their OH measurements are especially sensitive to the direct pathways from R + O_2 to QOOH and to OH + 3,3-dimethyloxetane. They also developed a kinetic model based on the comparison with their previous time-dependent master equation calculation of analogous processes in the reaction of n-propyl with O_2. Taatjes et. al performed B3LYP/6-31G(d,p) calculations for the stationary points on the neopentyl + O_2 system (surface) and adjusted this DFT data by the difference between B3LYP/6-31G(d,p) and QCISD(T)/6-311++G(3df,2pd) energies from their study on the n-propyl + O_2 system. The well depth for neopentyl + O_2 is estimated as 35 kcal mol^{-1}.

The results of Taatjes et. al and from Chapter 4 both show that there is no direct neopentyl + O_2 reaction to form HO_2 that is important. The HO_2 formation is therefore a secondary reaction product. The most significant reaction path producing HO_2 in the mechanism of Taatjes et. al's is identified to be the reaction of OH with neopentylperoxy to form HO_2 and neopentoxy radical. This radical-radical association reaction is expected to be barrier-less and slightly exothermic, and their estimate of the rate constant is taken from the rate of generic reaction $CF_3OO\bullet$ + OH. Their model comparison with

experimental HO_2 concentration vs. time profiles at 673 K for three O_2 concentrations show good agreement; but did not qualitatively reproduce the continued production of HO_2 at longer times. They suggest that inclusion of additional reaction steps for the initial neopentyl + O_2 products might improve the overall agreement.

The important initial, reactive products in the neopentyl radical reaction with O_2 are: neopentyl peroxy radical, OH radical, plus methyl radical and isobutene from CH_3 elimination of neopentyl radical. The addition of CH_3 and OH to the isobutene can form three new radical products, which will undergo further oxidation by reaction with O_2. These radicals are 2-hydroxy-1,1-dimethylethyl radical, 2-hydroxy-2-methylpropyl radical, and 1,1-dimethylpropyl radical.

An elementary mechanism based on *ab initio* and density functional calculations and our earlier mechanism[142] for modeling OH formation is constructed to model HO_2 formation profiles in this study. The mechanism includes OH addition to isobutene at both of the CD/H2 and CD/C2 carbon atoms and CH_3 addition to the CD/H2 carbon along with O_2 association reactions with these isobutene adducts. The model is shown to predict well for the experimental time-dependent formation of HO_2 profile at different O_2 concentrations reported by Taatjes et. al[103], and the important reaction pathways that effect on production of HO_2 radical in the mechanism are illustrated.

5.3 Calculation Method

The geometries of reactants, intermediates, transition states and products in neopentyl + O_2 reaction system are calculated at the B3LYP/6-31G(d,p) level using the Gaussian 98 program.[32] The optimized structure parameters are then used to obtain total electronic

energies at the B3LYP/6-311++G(3df,2p) and CBS-Q//B3LYP/6-31G(d,p) single point levels of calculation. Contributions from vibrational, translational, external rotational, and electronic to entropies and heat capacities are calculated by statistical mechanics based on the vibrational frequencies and moments of inertia from the DFT optimized structures. The torsion frequencies are omitted in calculation of S^{o}_{298} and $C_p(T)$'s, and their contributions are replaced with values from the analysis of internal rotations. The $\Delta H_f^{o}{}_{298}$ values for reactants, intermediate and products are calculated using total energies from *ab initio* CBS-Q and DFT calculations and use of isodesmic reactions with group balance when possible. The $\Delta H_f^{o}{}_{298}$ values of transition state structures are calculated by the $\Delta H_f^{o}{}_{298}$ of stable radical adducts from working isodesmic reaction analysis, plus the difference of total energies between transition states and radical adducts at the CBS-Q level.

Unimolecular dissociation and isomerization reactions of the chemically activated and stabilized adducts resulting from addition or combination reactions are analyzed by first constructing potential energy diagrams for the reaction system. DFT and ab initio calculations are then used to calculate transition state structures and activation energy for isomerization, β- scission, and dissociation reactions. The enthalpies and entropies of the reactants and transition state structures are treated with conventional transition state theory to calculate Arrhenius pre-exponential factors and energies of activation, which result in high pressure limit rate constants (k_∞) as function of temperature.

Branching ratios of the energized adduct to stabilization and product channels are then calculated using multi-frequency Quantum Rice-Rampsperger-Kassel (QRRK) analysis for $k(E)$[66,115] with the steady-state assumption on the energized adduct(s) in

combination with a master equation analysis for fall-off.[26] A 0.5 kcal energy grain used to obtain rate constants as a function of temperature and pressure for chemical activation and dissociation reactions. $(\Delta E)^{\circ}$down of 570 cal mol^{-1} is used in the master equation analysis with helium as the third body. Lennard-Jones parameters, σ (Angstroms) and ε/κ (Kelvins), are obtained from tabulations[90] and from an estimation method based on molar volumes and compressibility.

5.4 Results and Discussion

5.4.1 Geometries

The geometry optimizations for the reactants, transition states, adducts, and products in the isobutene-OH and isobutene-CH$_3$ adducts oxidation systems are performed at the B3LYP/6-31G(d,p) level. The optimized structural parameters for 41 species including transition state structures are listed in Appendix Table C.1. The corresponding un-scaled vibrational frequencies and moments of inertia are listed in Table C.2. The notations of several important reactants and products in these systems are defined as: C$_2$•COH (2-hydroxy-1,1-dimethylethyl), C$_3$•COH (2-hydroxy-2-methylpropyl), C$_2$•CCC (1,1-dimethylpropyl), C$_2$C=COH (2-methyl-1-propen-1-ol), C=C(C)COH (2-methyl-2-propen-1-ol), C=C(C)OH (1-propen-2-ol), C$_2$C=O (acetone), C=C(C)CC (2-methyl-1-butene), C$_2$C=CC (2-methyl-2-butene), and C$_2$CyCOCC (2,2-dimethyl-oxetane). The transition states of important reactions in these oxidation systems are identified as follows:

Peroxy radical isomerization:

C$_2$C(OO•)COH→ TS14 → C$_2$C(OOH)CH$_2$O•

C₂C(OO•)COH→ TS15 → C₂•C(OOH)COH

C₂C(OO•)COH→ TS16 → C₂C(OOH)C•OH

C₂C(OH)COO• → TS22 → C₂C(O•)COOH

C₂C(OH)COO• → TS23 → C₂•C(OH)COOH

C₂C(OO•)CC→ TS28 → C₂C(OOH)CC•

C₂C(OO•)CC→ TS29 → C₂•C(OOH)CC

C₂C(OO•)CC→ TS30 → C₂C(OOH)C•C
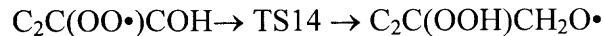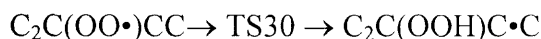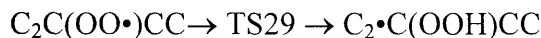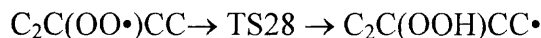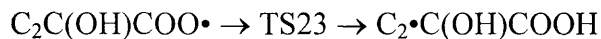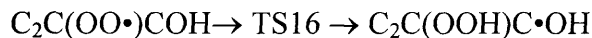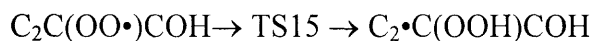
This class of reaction represents intramolecular, endothermic, transfer of an H atom from a OH or CH₃ group to the peroxy oxygen radical site via a 5 or 6-member ring transition state (includes the H atom). The cleaving O—H bond stretches to 1.35 ~ 1.365 Å from 0.96 Å, and the cleaving C—H bond stretches to (1.34,1.37) ~ 1.42 Å from 1.09Å, and the forming OO—H bond length is 1.08 ~ 1.14 (1.20, 1.25) Å, which is longer than the OO—H bond of 0.97 Å.

Epoxide formation:

C₂C(OOH)CC• → TS31 → C₂CyCOCC + OH
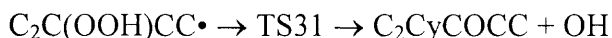
In this reaction, the carbon radical in the –CH₂• group attacks the carbon bonded peroxy oxygen to form 4-member ring transition state, while the weak RO—OH bond is breaking. The cleaving O—O bond length is 1.67 Å and the forming C—O bond length is 1.99 Å.

HO₂ group elimination (β-scission):

C₂C(OOH)C•OH → TS18 → C₂C=COH + HO₂

C₂•C(OOH)COH → TS21 → C=C(C)COH + HO₂

C₂C(OOH)C•C → TS32 → C₂C=CC + HO₂

$C_2 \bullet C(OOH)CC \rightarrow TS35 \rightarrow C=C(C)CC + HO_2$
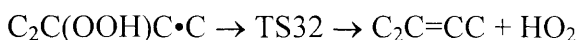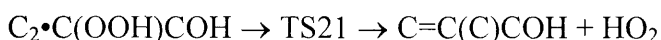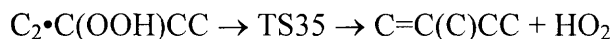
This reaction type represents the elimination (beta scission) of a HO_2 radical from a hydroperoxide alkyl radical with olefin formation in the carbon backbone. The cleaving C—O bond length is 1.94 ~ 1.99 Å, the forming O—OH bond decreases from 1.46 to 1.40 ~ 1.42 Å and the forming C=C bond length is 1.38 ~1.39 Å in the transition states.

Concerted HO$_2$ elimination:

$C_2C(OO\bullet)COH \rightarrow TS19 \rightarrow C2C=COH + HO_2$

$C_2C(OO\bullet)COH \rightarrow TS20 \rightarrow C=C(C)COH + HO_2$

$C_2C(OO\bullet)CC \rightarrow TS33 \rightarrow C=C(C)CC + HO_2$

$C_2C(OO\bullet)CC \rightarrow TS34 \rightarrow C_2C=CC + HO_2$
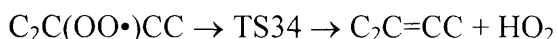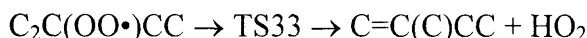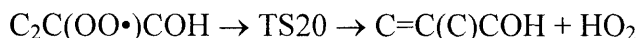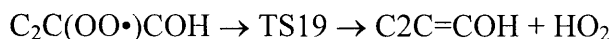
This reaction class represents a concerted elimination of HO_2 radical from its alkyl peroxy parent to form an olefin. The cleaving C—O and C—H bond lengths are 2.28 ~ 2.31 Å and 1.340 ~ 1.36 Å respectively; and the forming C=C and O—O bond lengths are 1.39 ~ 1.51 Å and 1.28 Å.

Alkyl group elimination:

$C_2C(O\bullet)COOH \rightarrow TS24 \rightarrow C_2C=O + CH_2O + OH$

$C_2C(O\bullet)COOH \rightarrow TS25 \rightarrow CC(=O)COOH + CH_3$

$C_2\bullet C(OH)COOH \rightarrow TS26 \rightarrow C=C(C)OH + CH_2O + OH$
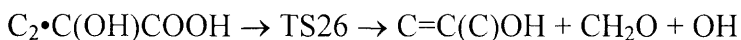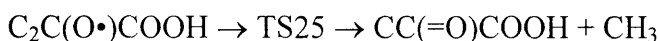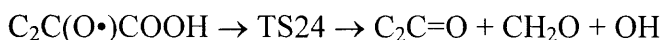
This type of reaction represents an alkyl group or oxy-alkyl group leaving (perpendicular) from a near planar ethylene structure. For methyl dissociation in TS25, the C—C bond length stretches from 1.58 Å to 2.17 Å, and the forming C=O bond length is 1.24 Å in the TS structure.

For the C•H$_2$OOH (immediately dissociates to CH$_2$O + OH) elimination in TS24 and TS26, the cleaving C—C bond length in the leaving group stretches from 2.06 ~ 2.21 Å, and the O—O bond length lengthens slightly from 1.45 ~ 1.47 Å.

5.4.2 Thermochemical Properties

The enthalpies of formation for reactants, intermediate and products are calculated by isodesmic reactions analysis or taken from available literature. The enthalpies of standard species used in isodesmic reaction analysis are listed in Table 5.1, and Appendix Table C.3 lists the calculated reaction enthalpies and $\Delta H_f^o{}_{298}$ values for the species in above oxidation systems at the three calculation levels. The average $\Delta H_f^o{}_{298}$ values from high-level CBS-Q calculations are used for the kinetic model.

Enthalpies of formation for transition states are calculated by using the $\Delta H_f^o{}_{298}$ values of stable radical adducts plus difference of total energies between the radical adducts and the transition states. The enthalpies of 21 transition states in the three isobutene adduct oxidation systems determined at the three different levels are listed in Table 5.2.

Table 5.1 $\Delta H_f^o{}_{298}$ for Standard Species in Isodesmic Reactions

species	$\Delta H_f^o{}_{298}$ (kcal/mol)		species	$\Delta H_f^o{}_{298}$ (kcal/mol)	
CH$_4$	−17.89 ± 0.07	(Cox)[60]	CH$_3$OO•	−2.15 ± 1.22	(Knyazev)[126]
CH$_3$•	34.82 ± 0.2	(Stull)[51]	CCOOH	−39.7 ± 0.3	(Chen)[128]
C$_2$H$_6$	−20.24 ± 0.12	(Cox)[60]	C•H$_2$CH$_2$OOH	10.96 ± 1.06	(Chen)[128]
C$_2$H$_5$•	28.80 ± 0.50	(Marshall)[143]	CH$_3$CH$_2$OO•	−6.8 ± 2.3	(Blanksby)[130]
C$_3$H$_8$	−25.02 ± 0.12	(Pedley)[56]	CCCOOH	−44.7 ± 0.41	(Chen)[128]
CH$_3$OH	−48.07 ± 0.05	(Cox)[60]	C•CCOOH	2.44	(Chen)[144]
C$_2$H$_5$OH	−56.21 ± 0.10	(Pedley)[56]	CCCOO•	−12.13	(Chen)[144]
CH$_3$C•HOH	−13.34 ± 0.84	(Sun)[59]	(CH$_3$)$_2$COO•	−17.2	(Chen)[144]
C$_2$COH	−65.19 ± 2.2	(Sun)[145]	C$_3$•CCOOH	−9.43	(Sun)[142]
C•H$_2$CH(OH)CH$_3$	−14.95 ± 2.8	(Sun)[145]	C$_3$CCOOH	−58.60	(Sun)[142]
C$_3$COH	−74.72 ± 0.21	(Wiberg)[146]	C$_2$CYCCOC	−35.43 ± 0.40	(Ringner)[147]
C$_3$CO•	−23.14	(Chen)[102]			

Table 5.2 Calculated Reaction Enthalpies [a]

	B3LYP	B3LYP	CBSQ//B3LYP		B3LYP	B3LYP	CBSQ//B3LYP
	/6-31G(d,p)	/6-311++G(3df,2p)	/6-31G(d,p)		/6-31G(d,p)	/6-311++G(3df,2p)	/6-31G(d,p)
TS14	23.34	23.94	21.88	TS25	14.49	12.17	12.94
TS15	41.87	41.26	35.46	TS26	21.91	20.37	24.01
TS16	34.65	33.57	28.41	TS28	24.50	23.62	24.28
TS17	7.37	4.78	6.15	TS31	16.00	15.63	17.58
TS18	5.45	5.64	11.65	TS29	36.51	35.94	33.60
TS19	35.24	33.12	31.93	TS30	32.38	31.59	33.08
TS20	34.66	32.29	31.98	TS32	10.94	10.06	11.98
TS21	22.84	18.70	15.67	TS33	25.12	23.80	29.54
TS22	16.76	17.44	22.81	TS34	25.37	24.14	29.82
TS23	28.06	26.30	26.73	TS35	10.06	9.05	13.61
TS24	8.98	6.25	9.31				

[a] Units in kcal mol^{-1}.

Contributions from vibrational, translational, external rotational, and electronic degeneracy to S^o_{298} and $C_p(T)$'s are calculated by statistical mechanics, and the contributions from internal rotations are replaced with values from previous work[142] by evaluation of similar internal rotations. Table C.4 lists the thermochemical properties of reactants, transition states, intermediates, and products in the reaction systems calculated by this work.

5.4.3 Analysis for Chemical Activation Reactions

5.4.3.1 $C_2C \cdot COH + O_2$. The potential energy diagram for the $C_2C \cdot COH + O_2$ reaction system calculated at the CBS-Q level is shown in Figure 5.1. The reaction channels for the energized adduct $[C_2C(OO \cdot)COH]^*$ include dissociation back to reactants, stabilization to $C_2C(OO \cdot)COH$, several isomerizations followed by dissociation to products, and the concerted HO_2 elimination reaction. The $C_2C \cdot COH$ radical ($\Delta H_f^o{}_{298} = -22.22$ kcal mol^{-1}) reacts with O_2 to form a chemically activated peroxy adduct $C_2C(OO \cdot)COH^*$ with a 40.49 kcal mol^{-1} well depth. This well depth allows the energized

peroxy adduct with sufficient energy to react over the barriers of two different concerted HO$_2$ elimination paths and three H atom transfer isomerization reactions, followed by the isomers dissociation before stabilization. The three isomerization reactions for C$_2$C(OO•)COH adduct are: (1) hydrogen transfer from the hydroxyl group to the peroxy radical site via six-member ring TS14 (E_a = 21.88 kcal mol^{-1}) to form a C$_2$C(OOH)CH$_2$O• ($\Delta H_f{}^{\circ}{}_{298}$ = -43.52 kcal mol^{-1}); (2) H atom transfer from a methyl via five-member ring TS15 (E_a = 35.46 kcal mol^{-1}) to form a C$_2$•C(OOH)COH ($\Delta H_f{}^{\circ}{}_{298}$ = -46.68 kcal mol^{-1}); (3) H atom transfer from the alcohol carbon via five-member ring TS16 (E_a = 28.41 kcal mol^{-1}) to form a C$_2$C(OOH)C•OH ($\Delta H_f{}^{\circ}{}_{298}$ = -49.16 kcal mol^{-1}).
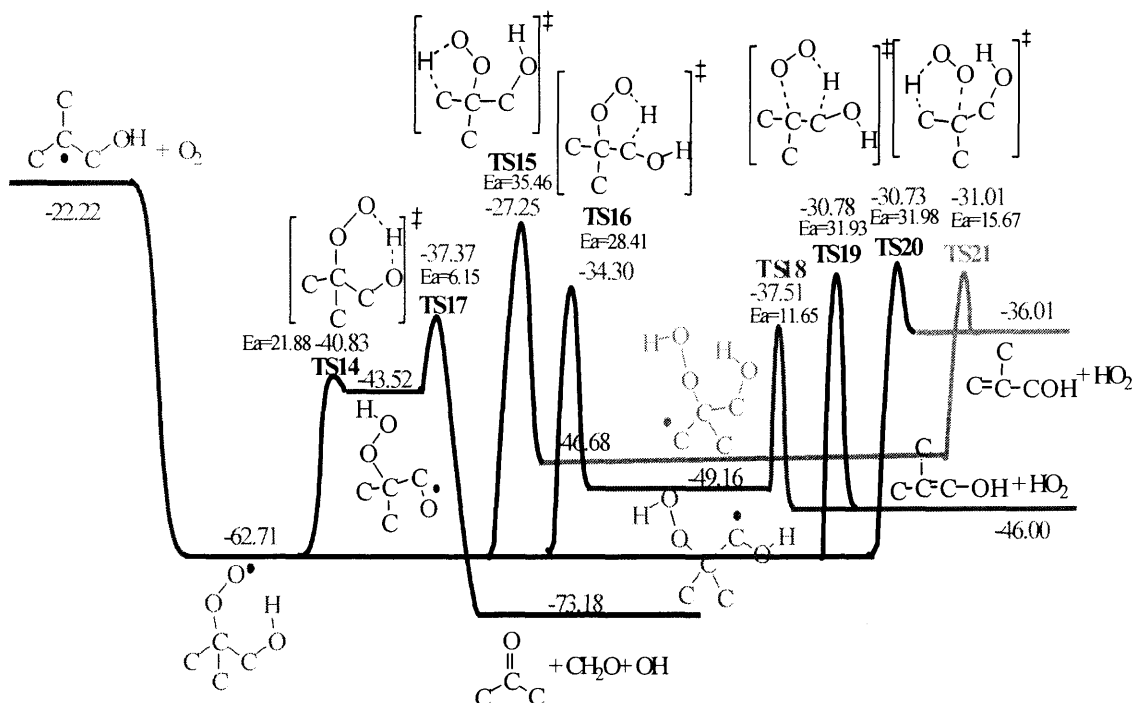
Figure 5.1 Potential energy diagram for C$_2$C•COH + O$_2$ reaction system.

The concerted HO_2 elimination reactions for $C_2C(OO\bullet)COH$ adduct are: (1) via five-member ring TS19 (Ea = -31.93 kcal mol^{-1}) to $C=C(C)COH + HO_2$; (2) via five-member ring TS20 (Ea = -31.98 kcal mol^{-1}) to $C_2C=COH + HO_2$.

The forming alkoxy $C_2C(OOH)CH_2O\bullet$ isomer will undergo β-scission via TS17 (E_a = 6.15 kcal mol^{-1}) and rapidly decompose to acetone, formaldehyde, and OH radical. The resulting hydroperoxide-alkyl radicals will also undergo β-scissions (HO_2 elimination) to form vinyl alcohols plus HO_2. The $C_2C(OOH)C\bullet OH$ isomer dissociates to $C_2C=COH + HO_2$ via TS18 (E_a = 11.65 kcal mol^{-1}), and $C_2\bullet C(OOH)COH$ isomer dissociates to $C_2C=COH + HO_2$ via TS21 (E_a = 15.67 kcal mol^{-1}). The concerted elimination of HO_2 radical from the peroxy $C_2C(OO\bullet)COH$ adduct also results in these same two vinyl alcohols.
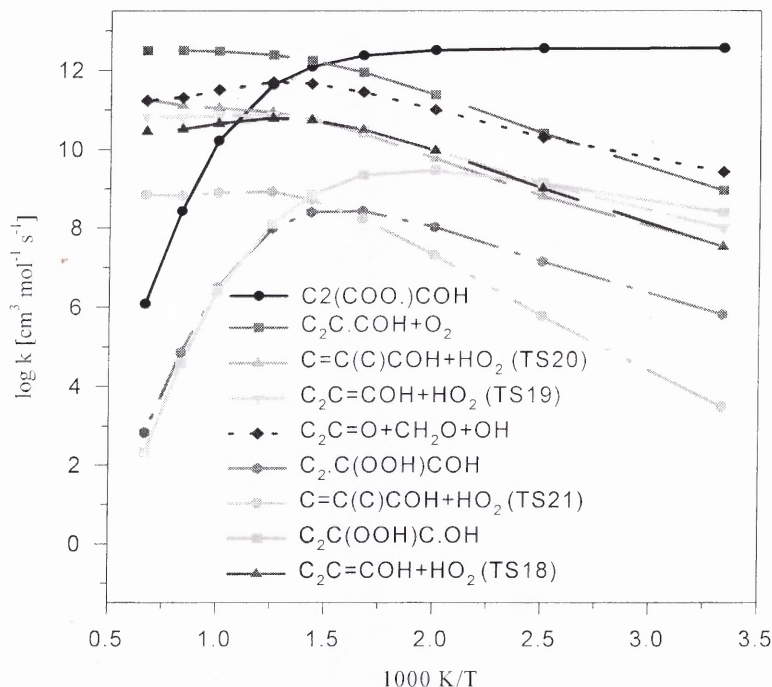
Figure 5.2 Calculated temperature dependent rate constants for chemical activated $C_2C\bullet COH + O_2$ system at P = 0.1 atm,

The high-pressure limit rate constants from canonical transition state theory for $C_2C•COH + O_2$ system are fitted by three parameters A_∞, n, and E_a over temperature range from 298 to 2000 K, $k_\infty = AT^n exp(-E_a/RT)$, by THERMKIN code.[72] The input and output kinetic parameters for QRRK and Master equation analysis are listed in Table C.5.

The calculated pressure dependent rate constants for the chemical activation product channels of $C_2C•COH + O_2$ vs temperature at P = 0.1 atm are presented in Figure 5.2. This figure shows that the dominant product-channel for $C_2C•COH + O_2$ is stabilization to $C_2C(OO•)COH$ below 700 K and dissociation back to $C_2C•COH + O_2$ becomes the dominant channel when temperature is over 700 K. Dissociation to $C_2C=O + CH_2O + OH$ is the more important product channel relative to the channels generating HO_2 and vinyl alcohols.
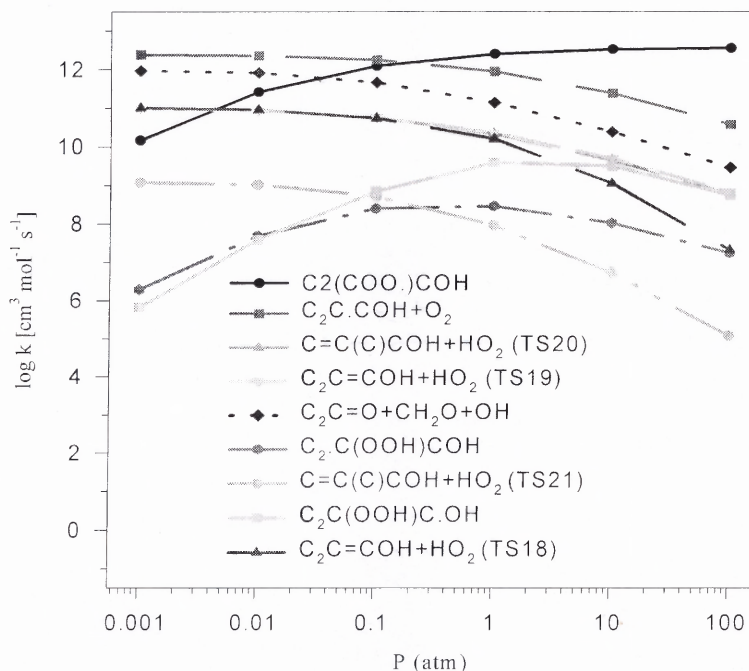
Figure 5.3 Calculated pressure dependent rate constants for chemical activated $C_2C•COH + O_2$ system at T = 700 K.

Figure 5.3 illustrates the pressure dependent rate constants of the chemically activated reactions at 700 K. The stabilization to the $C_2C(OO\bullet)COH$ is a dominant channel when pressure is over 0.1 atm at 700 K, and when pressure is lower than 0.1 atm, the dissociation back to $C_2C\bullet COH + O_2$ becomes the dominant channel.

5.4.3.2 $C_3\bullet COH + O_2$. The potential energy surface for the $C_3\bullet COH + O_2$ reaction system calculated at the CBS-Q level is shown in Figure 5.4. The $C_3\bullet COH$ radical reacts with O_2 to form a peroxy $C_2C(OH)COO\bullet$ adduct with a 37.64 kcal mol^{-1} well depth. Reaction channels for the energized adduct $[C_2C(OH)COO\bullet]^*$ include dissociation back to reactants, stabilization to $C_2C(OH)COO\bullet$, isomerization (hydrogen shift) via two different transition states to produce two hydroperoxide isomers: TS22 (E_a = 22.81 kcal mol^{-1}) to $C_2C(O\bullet)COOH$ ($\Delta H_f^\circ{}_{298}$ = -41.30 kcal mol^{-1}), TS23 (E_a = 26.71 kcal mol^{-1}) to $C_2\bullet C(OH)COOH$ ($\Delta H_f^\circ{}_{298}$ = -44.27 kcal mol^{-1}). The resulting alkoxy isomer $C_2C(O\bullet)COOH$ dissociates to $C_2C=O + CH_2O + OH$ via TS24 (E_a = 9.31 kcal mol^{-1}), also dissociates to $CH_3 + CC(=O)COOH$ via TS25 (E_a = 12.94 kcal mol^{-1}). The forming hydroperoxide alkyl radicals will undergo dissociations to vinyl alcohol or vinyl hydroperoxide. The stable vinyl hydroperoxide product will also undergo homolytic cleavage of the weak O—O bond in the peroxide moiety to generate OH and vinyl alkoxy species.

The high-pressure limit rate constants for $C_3\bullet COH + O_2$ system as shown above are fitted by three parameters A_∞, n, and E_a over temperature range from 298 to 2000 K. The input and output kinetic parameters for QRRK and Master equation analysis for this system are listed in Table C.6.

Unit: kcal/mol
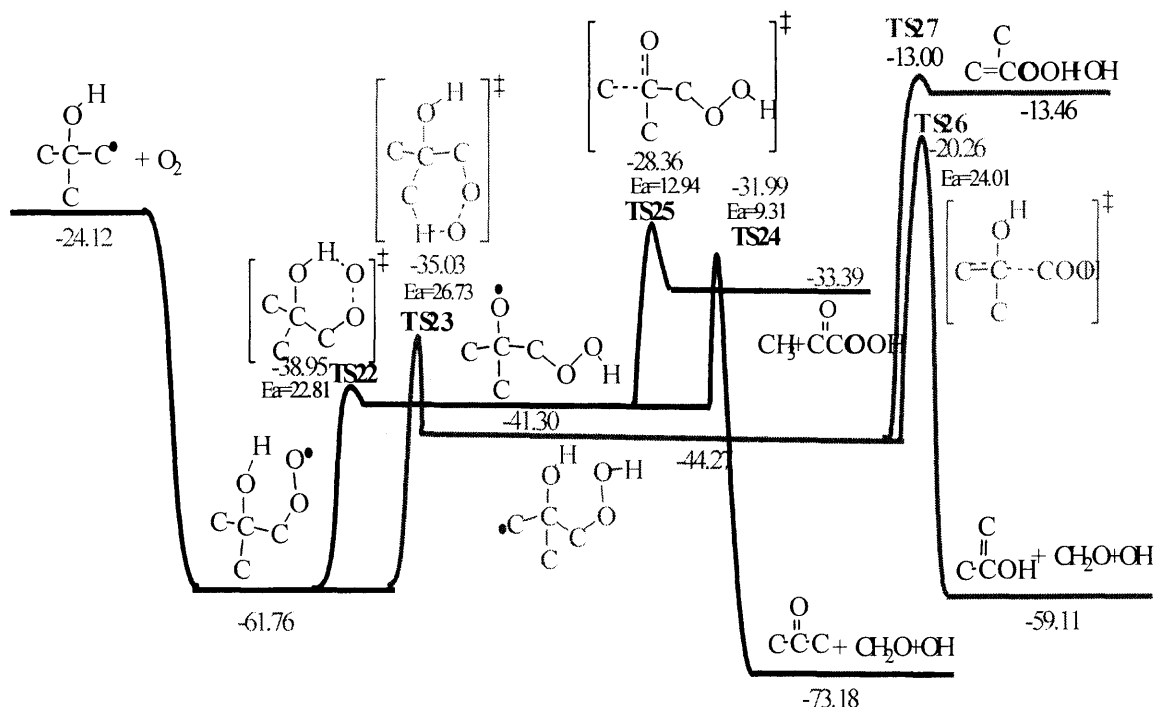
Figure 5.4 Potential energy diagram for $C_3 \cdot COH + O_2$ reaction system.

The chemical activation calculated pressure dependent rate constants for the product channels of $C_3 \cdot COH + O_2$ versus temperature at 0.1 atm are shown in Figure 5.5. It shows that the dominant product is stabilization to $C_2(COH)COO \cdot$ below 700 K, and dissociation back to $C_3 \cdot COH + O_2$ becomes the dominant channel when temperature is over 700 K. The reaction channel involving H-shift and dissociation to $C_2C=O + CH_2O + OH$ is the most important new product channel.

Figure 5.6 illustrates the pressure dependent rate constants of the chemically activated reaction at 700 K. The stabilization to $C_2(COH)COO \cdot$ is a dominant channel when pressure is over 0.1 atm at 700 K, and when pressure is lower than 0.1 atm, the dissociation back to $C_3 \cdot COH + O_2$ becomes the dominant channel.
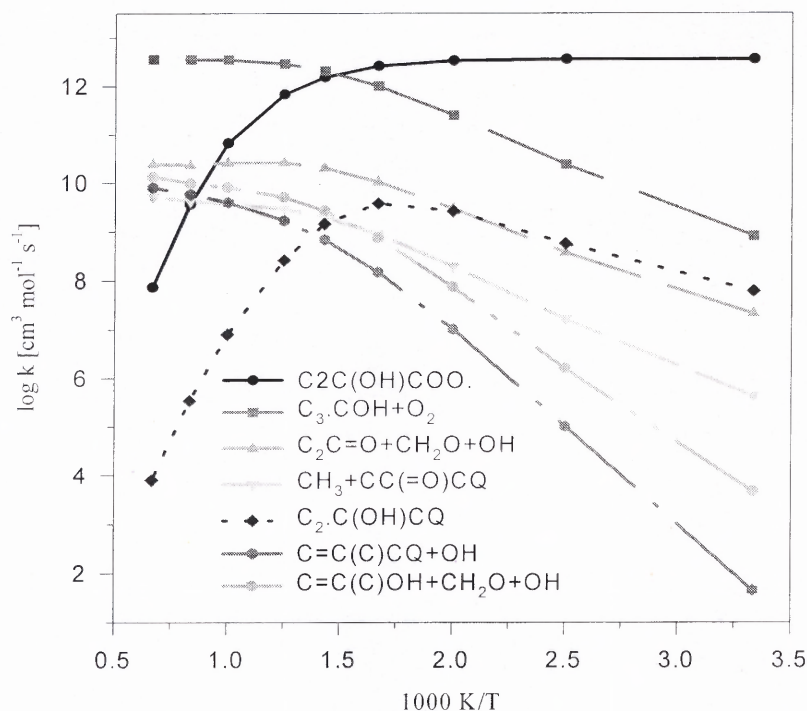
Figure 5.5 Calculated temperature dependent rate constants for chemical activated $C_3 \cdot COH + O_2$ system at P = 0.1 atm.
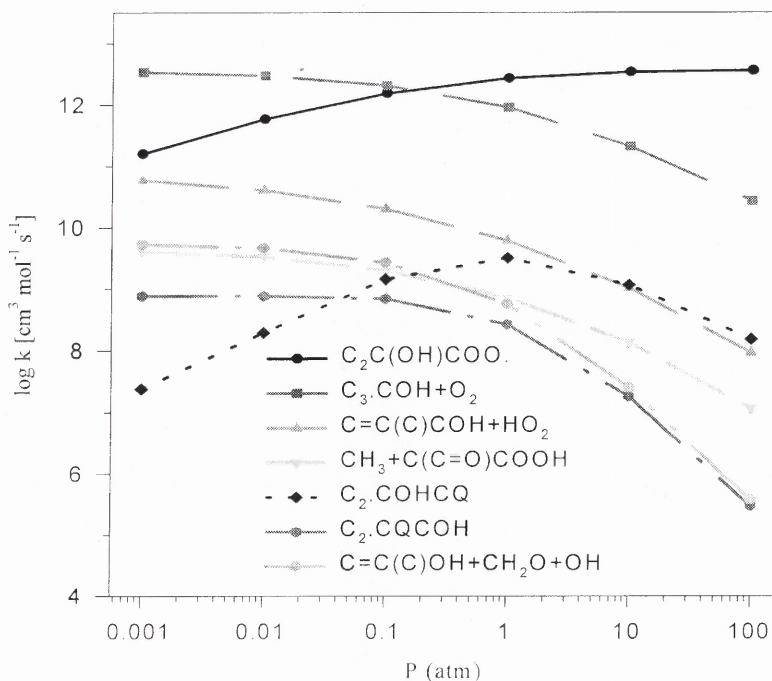

Figure 5.6 Calculated pressure dependent rate constants for chemical activated $C_3 \cdot COH + O_2$ system at T = 700 K.

5.4.3.3 $C_2C•CC + O_2$. The potential energy diagram for the reactions of $C_3•CC + O_2$ calculated at the CBS-Q level is shown in Figure 7. A number of the reaction channels for $[C_2C(OO•)CC]^*$ adduct are similar to those of $[C_2C(OO•)COH]^*$ adduct in Figure 1 due to the similarity between the two adduct structures. The $\Delta H_f°_{298}$ value of $C_2C•CC$ radical is adopted from Tsang et al.[55], 6.7 kcal mol^{-1}, and this results a well depth of 40.28 kcal mol^{-1} for $C_3•CC + O_2$; it shows good agreement with the well depth of $C_2C•COH + O_2$ as shown above. Chen and Bozzelli[102] calculated the well depth of tert-butyl radical + O_2 to be 36.88 kcal mol^{-1} at the CBS-q//MP2(full)/6-31G(d,p) level, and Knyazev et al.[126] reported this well depth as 36.52 kcal mol^{-1} from the third-law of treatment of the temperature dependencies of equilibrium constants.
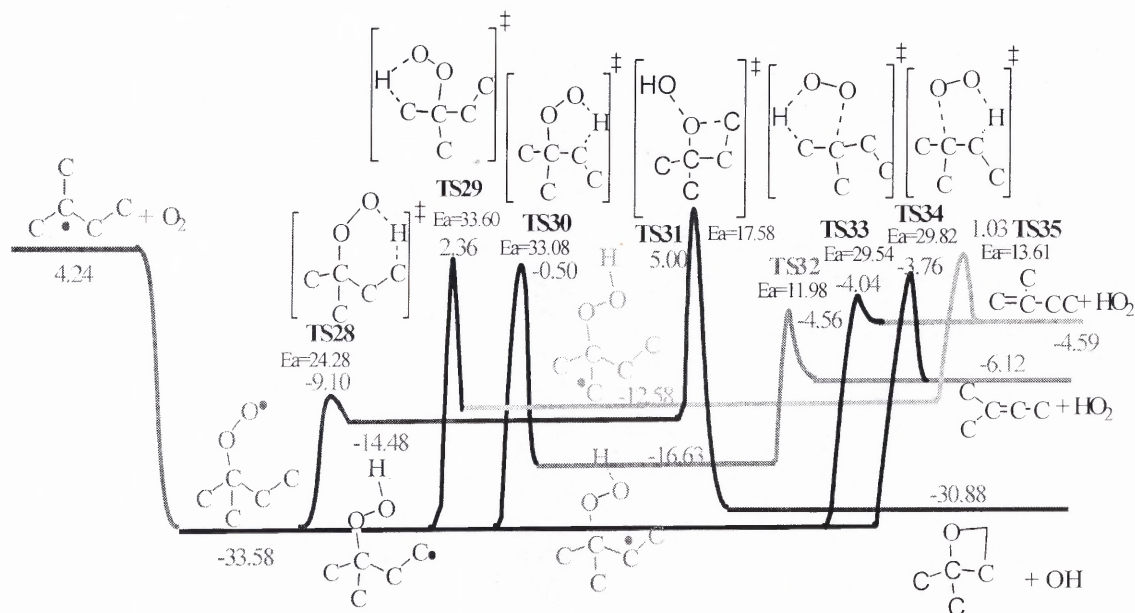
Figure 5.7 Potential energy diagram for $C_2C•CC + O_2$ reaction system.

As those of the other peroxy radicals reaction paths, the energized $[C_2C(OO•)CC]^*$ adduct include dissociation to reactants, stabilization, concerted HO_2

eliminations to products or isomerizations followed by dissociations to products. The important hydrogen transfer isomerization reactions are: (1) six-member ring TS28 (E_a = 24.28 kcal mol^{-1}) to form C$_2$C(OOH)CC• ($\Delta H_f°_{298}$ = -14.48 kcal mol^{-1}); (2) five-member ring TS29 (E_a = 33.31 kcal mol^{-1}) to form C$_2$•C(OOH)CC ($\Delta H_f°_{298}$ = -12.58 kcal mol^{-1}); (3) five-member ring TS30 (E_a = 33.08 kcal mol^{-1}) to form C$_2$C(OOH)C•C ($\Delta H_f°_{298}$ = -16.63 kcal mol^{-1}). The concerted HO$_2$ elimination reactions are: (1) TS33 (Ea = 29.54 kcal mol^{-1}) to C=C(C)CC + HO$_2$; (2) TS34 (Ea = 29.82 kcal mol^{-1}) to C$_2$C=CC + HO$_2$.

The hydroperoxide alky radicals formed by hydrogen transfer reactions will undergo dissociation to form alkene plus HO$_2$ and epoxide plus OH. The C$_2$C(OOH)CC• isomer dissociates to C$_2$CyCOCC + CH$_2$O + OH via TS31 (E_a = 17.58), the C$_2$C(OOH)C•C isomer dissociates to C$_2$C=CC + HO$_2$ via TS32 (E_a = 11.98), and the C$_2$•C(OOH)CC isomer dissociates to C$_2$C=CC + HO$_2$ via TS35 (E_a = 13.61 kcal mol^{-1}).

The high-pressure limit rate constants for this C$_2$C•CC + O$_2$ system, fitted by three parameters A_∞, n, and E_a over temperature range from 298 to 2000 K, along with the input and output kinetic parameters for QRRK and Master equation analysis are listed in Table C.7.

The calculated pressure dependent rate constants for the product channels of C$_2$C•CC + O$_2$ vs. temperature at P = 0.1 atm are illustrated in Figure 5.8. The dominant product-channel is stabilization to C$_2$C(OO•)CC below 500 K and dissociation back to C$_2$C•CC + O$_2$ becomes dominant when temperature is over 500 K. The channels concerted eliminations of HO$_2$ forming conjugate alkene are the most important product channels. Figure 5.9 illustrates the pressure dependence for the rate constants of the chemically activated reactions at 700 K. The dissociation back to C$_2$C•CC + O$_2$ is the

dominant channel at almost all the pressures, and the stabilization to the $C_2C(OO\bullet)CC$ is the next dominant.
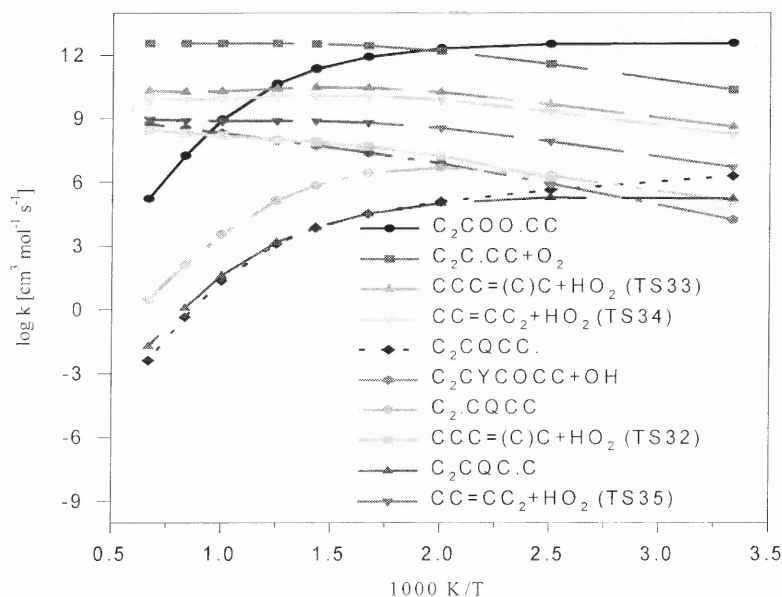
Figure 5.8 Calculated temperature dependent rate constants for chemical activated $C_2C\bullet CC + O_2$ system at P = 0.1 atm.
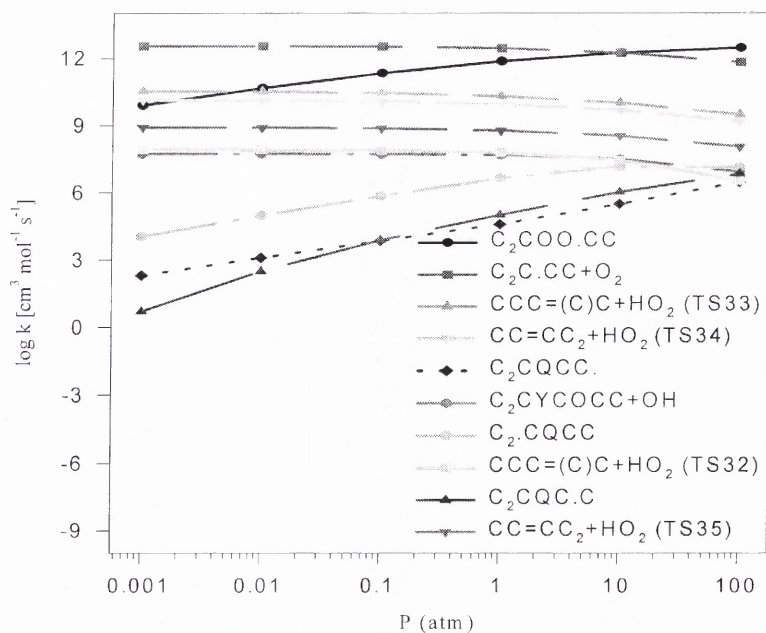
Figure 5.9 Calculated pressure dependent rate constants for chemical activated $C_2C\bullet CC + O_2$ system at T = 700 K.

5.4.4   Comparison of Model and Experiment

A detailed reaction mechanism (314 reactions, 126 species) for this neopentyl oxidation system is assembled in Table C.8, and the CHEMKIN II interpreter and integrator (version 3.1)[140] is used to model the experimental HO_2 formation profile for reaction time range $0 \sim 40$ ms, 673 K, and 59.3 torr. Abstraction reactions of O, OH, HO_2, and R• radicals are taken from evaluated literature. A procedure from Dean and Bozzelli[141] is used to estimate abstraction rate constants by H, O, OH, and CH_3 radicals when no literature data are available.
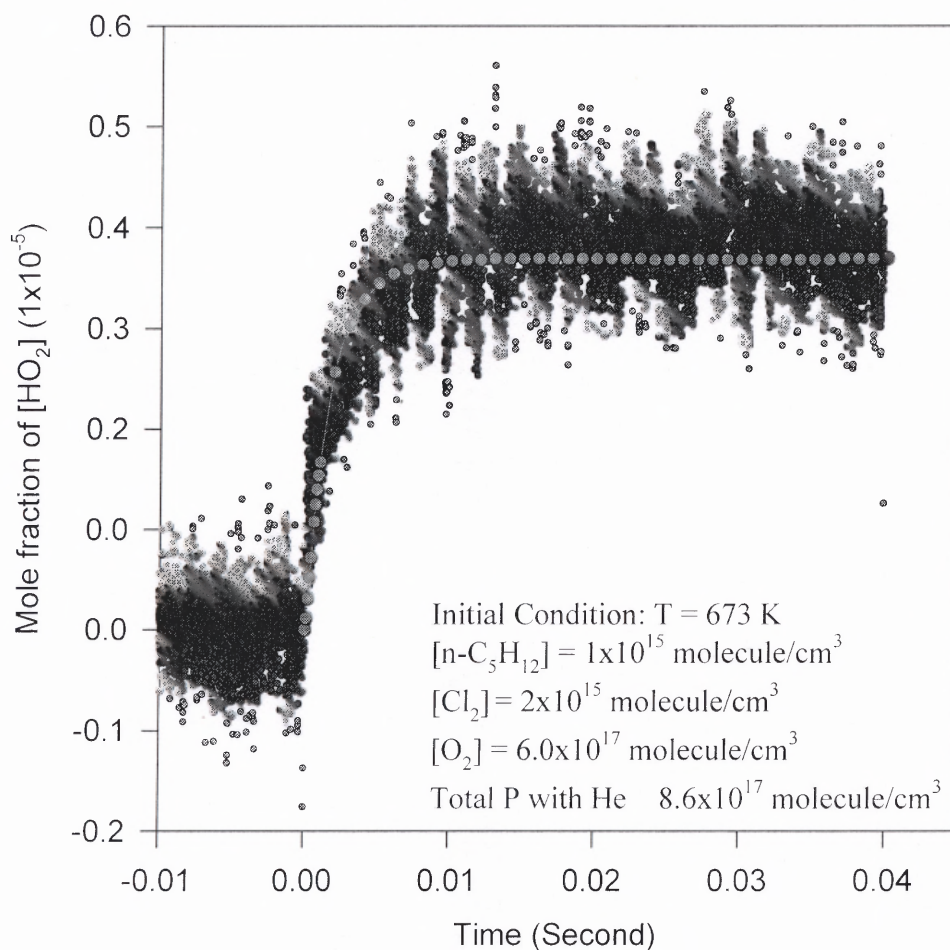
Figure 5.10 Comparison of the present model with the experimental HO_2 measurements of Taatjes et al.[2]

Figure 5.10 illustrates the time dependence of HO_2 radical formation profile predicted by our model compared with the experimental data published by Taajes et al.[103] The experiment was performed at 673 K, and the typical concentration are reported as: $[Cl_2]$ = 2 $\times 10^{15}$ molecule cm^{-3}, $[Cl]_o$ = 2 $\times 10^{15}$ molecule cm^{-3}, $[neo-C_5H_{12}]$ = 1 $\times 10^{15}$ molecule cm^{-3}, $[O_2]$ = 6.7 $\times 10^{16}$ ~ 6.0 $\times 10^{17}$ molecule cm^{-3}, with balance He up to a total density of 8.6 $\times$ 10^{17} molecule cm^{-3}. The green solid dot curve in Figure 5.10 represents our model for the HO_2 formation profile at the higher oxygen concentration, O_2 = 6.0 $\times 10^{17}$ molecule cm^{-3}; it shows good agreement with experimental data of Taajes et al. Figure 5.11 illustrates the predicted time dependence of the HO_2 radical compared with experimental data at the lower oxygen concentration, O_2 = 6.7 $\times 10^{16}$ molecule cm^{-3}; it shows good agreement with experimental data also.
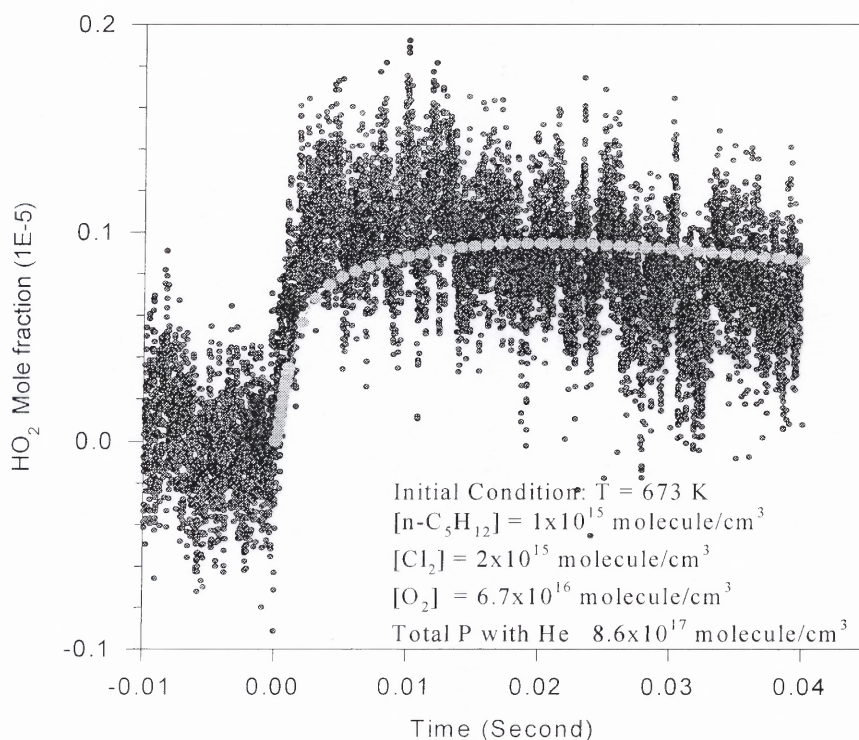
Figure 5.11 Comparison of the present model with the experimental HO_2 measurements of Taatjes et al.[2]

The unique molecular structure of neopentane eliminates the reaction path for formation of C_5 conjugate alkene plus HO_2 in the low temperature oxidation reactions, so the formation of HO_2 must be attributed to its secondary reactions. A sensitivity analysis by using CHEMKIN (version 3.6.1)[148] on the HO_2 at the experimental condition (T = 673 K, P = 59.3 torr, $[O_2]$ = 6.0 $\times 10^{17}$ molecule cm^{-3}) at the reaction time of 5, 10, 20 30 milliseconds is illustrated in Figure 5.12.

Legend:
- 5 ms
- 10 ms
- 20 ms
- 30 ms

5. OH+Cl2<=>HOCl+Cl
11. C3CC.+O2<=>C2CYCCOC+OH
17. C3.CCQ<=>C2CYCCOC+OH
22. C2CYCCOC+OH<=>C2CYCCOC.+H2O
54. C3.CCQ+O2<=>C2CCQCHO+OH
66. C2CCQCHO<=>C2CCO.CHO+OH
70. C2C.CHO<=>C*CC+HCO
74. C2C*C+OH<=>C2C.COH
176. C3CC+OH<=>C3CC.+H2O
197. C3CCOO.+C3CCOO.<=>C3CCO.+C3CCO.+O2
198. C3CCOO.+C3CCOO.<=>C3CCHO+C3CCOH+O2
199. C3CCOO.+HO2<=>C3CCOOH+O2
200. C3CCOO.+OH<=>HO2+C3CCO.
217. C3CCOOH<=>C3CCO.+OH
240. C3CCHO+OH<=>C3CC.*O+H2O
243. C3CCHO+O2<=>C3CC.*O+HO2
266. CH2O+OH=H2O+HCO
296. H+O2+M<=>HO2+M
299. HO2+H<=>OH+OH
301. HO2+OH<=>O2+H2O
302. HO2+HO2<=>O2+H2O2

Percent Sensitivity

Figure 5.12 Sensitivity analysis on HO_2 formation at T = 673 K, P = 59.3 torr, and $[O_2]$ = 6.0 $\times 10^{17}$ molecule cm^{-3}.

Figure 5.12 shows that neopentyl peroxy radical self-reaction which generates neopentoxy radical plus O_2 is the most sensitive for HO_2 formation before 7 milliseconds. This is because that the neopentoxy radical will rapidly decompose to formaldehyde plus t-butyl radical which reacts with O_2 to form HO_2 by HO_2 elimination path, which is impossible in $C_3CC\bullet$ + O_2 reaction system. Another important channel for HO_2 formation

is OH reaction with 3,3-dimethyloxetane that is a main product for neopentyl radical oxidation ($C_2CyCCOC + OH \rightarrow C_2CyCCOC\bullet + H_2O$),[142] since the resulting radical will undergo ring opening to generate HO_2 precursors such as $HC\bullet O$ and CH_2O ($C_2CyCCOC\bullet \rightarrow C_2C=C + HC\bullet O$). The next sensitive channel for HO_2 formation is OH abstraction of H atoms from neopentane radical ($C_3CC + OH \rightarrow C_3CC\bullet + H_2O$). Other reactions pathways responsible for the formation of HO_2 are: $C_2CC(OOH)CHO \rightarrow C_2C(CHO)CH_2O\bullet + OH$, which is responsible for chain branching and results in HO_2 precursors; ($C_2C(CHO)CH_2O\bullet \rightarrow C_2C\bullet CHO + CH_2O$; $C_2C\bullet CHO \rightarrow C=CC + HCO$); $C_3CCOO\bullet + OH \rightarrow HO_2 + C_3CCO\bullet$ as reported by Taatjes et al.; $H + O_2 + M \rightarrow HO_2 + M$; $CH_2O + OH \rightarrow H_2O + HC\bullet O$, and $C_2C=C + OH \rightarrow C_2C\bullet COH$. These reactions are responsible for either direct formation of HO_2, or the intermediates formation producing HO_2. A typical intermediate is $HC\bullet O$, which reacts with O_2 to forming HO_2 plus CO.[149]

The $HO_2 + OH \rightarrow O_2 + H_2O$ reaction is indicated to be the most sensitive channel for the loss of HO_2, and the neopentyl peroxy radical self-reaction which generates 2,2-dimethylpropanal and 2,2-dimethylpropanol plus O_2 is also sensitive. Other reactions paths sensitive for the loss of HO_2 are: $HO_2 + HO_2 \rightarrow O_2 + H_2O_2$, $C_3CCHO + OH \rightarrow C_3CC\bullet=O + H_2O$, $C_3CCHO + O_2 \rightarrow C_3CC\bullet=O + HO_2$, $HO_2 + H \rightarrow OH+OH$.

5.5 Summary

The potential energy surfaces on the reaction systems of 2-hydroxy-1,1-dimethylethyl, 2-hydroxy-2-methylpropyl, and 1,1-dimethylpropyl radicals plus O_2 and thermochemical properties of the species in these reaction systems are calculated based on *ab initio* CBS-Q and density functional theories. A mechanism describing reaction paths and kinetic

parameters for these oxidation reaction systems incorporating the mechanism in Chapter 4 are developed to model the experimental HO_2 formation profiles. The kinetic parameters for intermediate and product formation channels of above systems are calculated versus temperature and pressure. Several reactions are predicted to be important for HO_2 formation profile.

CHAPTER 6

THERMOCHEMICAL AND KINETIC ANALYSIS OF 2-METHYLBENZYL RADICAL OXIDATION REACTIONS

6.1 Background

Aromatic compounds are an important component of anthropogenic emissions from incomplete combustion and other evaporative emissions from solvents and fuels. Photochemical oxidation of aromatic hydrocarbons, such as benzene, toluene, and xylenes, is an important component in the chemistry of the reactive hydrocarbons in the atmosphere.[150]

Several reaction mechanisms have been proposed for interpretation of experimental laboratory and smog chamber photooxidation data.[150-152] Emdee et al.[153] studied the oxidation of o-xylene by flow reactor measurement at about 1150 K, and they proposed reaction pathways for oxidation of o-xylene at high temperature. They reported that ortho-xylene has higher reactivity compared with meta-xylene and para-xylene.

The reactions of the radicals from ortho xylene with O_2 are important at low and intermediate temperature oxidations. A partial reaction mechanism for the 2-methylbenzyl radical + O_2 system is outlined in the scheme 1. In this study, partial elementary reactions, energy well depths, and absolute rate constants for 2-methylbenzyl radical reactions with molecular oxygen are initially determined with computational chemistry at density functional levels. The reaction of 2-methylbenzyl radical (from ortho-xylene) with O_2 is shown to have a more energetically favorable path for peroxy radical isomerization compared with its isomers: 3-methyl and 4-methyl - benzyl radicals. The resonance form of 2-methylbenzyl radical with radical site in benzene ring, can also

react with O_2, but the adduct formed in this reaction has a low barrier to reverse reaction

(18.2 kcal mol^{-1}) and O_2 will mostly add to the methyl group.

Scheme 1
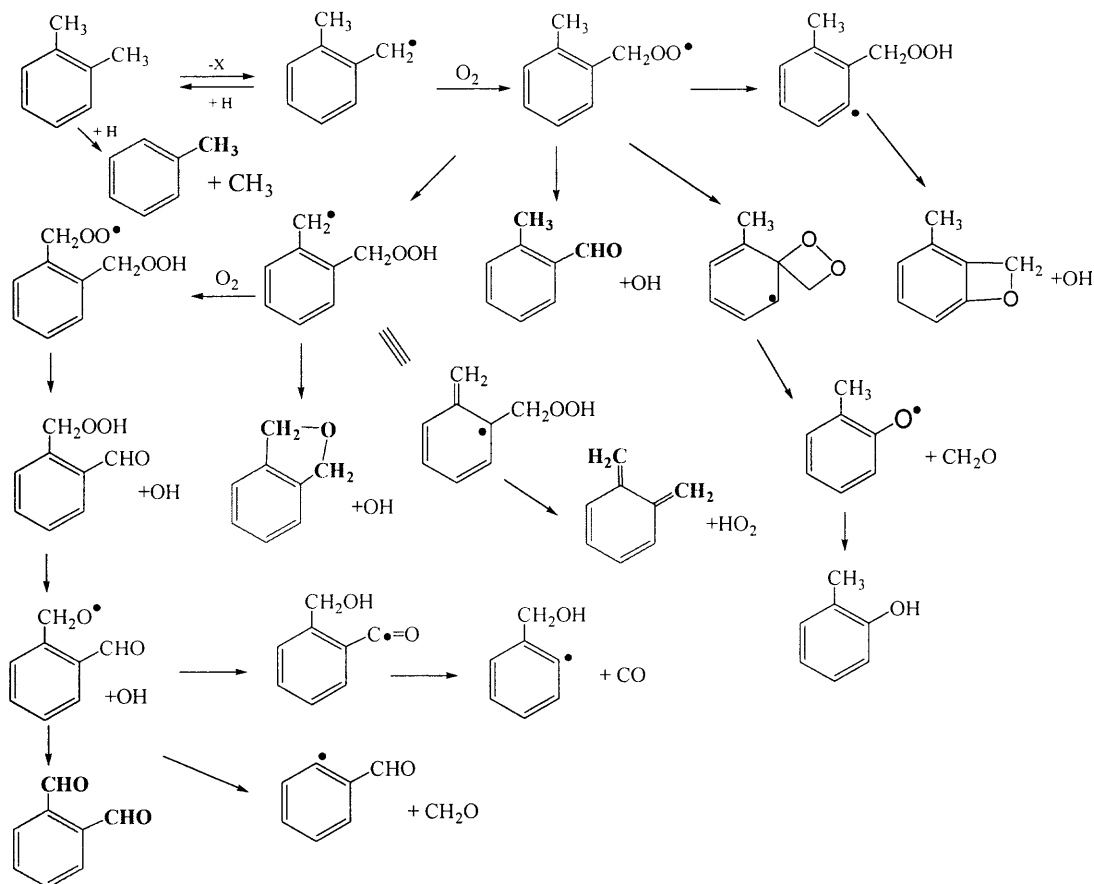
6.2 Results and Discussion

6.2.1 Thermochemical Properties

The geometries of reactants, important intermediates, transition states and products in

ortho-xylene radical + O_2 system are optimized using PM3 MOPAC[84] calculations,

followed by optimizations and frequency calculations at the B3LYP/6-31G(d,p) level

using the Gaussian98 program.[32] The optimized geometry parameters of adduct ortho-

$C_6H_4(CH_3)CH_2OO\bullet$ and six transition states are shown in Appendix Table D.1; the corresponding vibrational frequencies and moments of inertia are listed in Table D.2.

The optimized structure parameters are used to obtain total electronic energies at the B3LYP/6-311++G(3df,2p) level. Vibrational frequencies are scaled by 0.9806 as recommended by Scott et al.[42] for zero-point vibrational energies and thermal energies.

Enthalpies of formation for reactants, intermediates, and products are calculated using isodesmic working reaction analysis. Table D.3 lists the isodesmic reactions, reaction enthalpies and calculated $\Delta H^o_{f\,298}$ values for the important species in 2-methylbenzyl + O_2 system at two DFT calculation levels. In our previous study, the calculated $\Delta H^o_{f\,298}$ values from the DFT calculations were shown good agreement with the higher-level ab initio CBS-Q//B3 results.[142] The $\Delta H_f{}^\circ_{298}$ values for ortho-$C_6H_4(CH_3)CH_2OO\bullet$, ortho-$C_6H_4(CH_2OOH)CH_2\bullet$, and ortho-$C_6H_4(CH_2OOH)CH_2OO\bullet$ are calculated as 19.83, 24.13, and 5.81 kcal mol^{-1} at the B3LYP/6-311++G(3df,2p) level.

Enthalpies for transition states are calculated by using the $\Delta H_f{}^\circ_{298}$ value of stable adduct plus the difference of total energy between adduct and transition state. In this study, the barriers for transition states are also calculated at the KMLYP/6-311+G(d,p) level, since KMLYP method[154] is reported to accurately predict transition state barriers with smaller errors than B3LYP[155], BHandHLYP, and G2.[156] KMLYP/6-311+G(d,p) calculation are preformed for geometry optimization and vibrational frequencies. Transition state barriers are corrected by zero-point energies, while the enthalpy of reaction are adjusted for thermal corrections at 298 K. Zero-point energies and thermal corrections for KMLYP are obtained using un-scaled harmonic frequencies since transition state barriers are slightly affected by scaling factor. The reaction enthalpies for

seven transition states in 2-methylbenzyl + O_2 system determined at the B3LYP/6-31G(d,p), B3LYP/6-311++G(3df,2p), KMLYP/6-311+G(d,p) levels are listed in Table 6.1. The reaction enthalpies show good agreement at the three calculation levels. The data calculated at the B3LYP/6-311++G(3df,2p) are used to calculate rate constants.

Table 6.1 Reaction Enthalpies [a]

species	B3LYP /6-31G(d,p)	B3LYP /6-311++G(3df,2p)	KM BLYP/6-311+G(d,p)
TS1	21.20	21.21	20.77
TS2	34.08	34.91	36.11
TS3	30.97	30.90	29.94
TS4	38.21	38.21	39.40
TS6	15.91	16.07	
TS7	30.21	29.90	27.88
TS8	23.31	21.59	
TSM	60.58	60.05	
TSP	75.18	73.62	

[a] Units in kcal mol^{-1}. The reaction enthalpies are calculated from forward reaction, ZPVE and thermal correction are included.

The entropies and heat capacity contributions from vibrational, translational, and external rotational contributions are calculated using statistical mechanics based on the vibrational frequencies and structures obtained from the density functional study. Potential barriers for the internal rotations are calculated at the B3LYP/6-31G(d,p) level, and hindered rotational contributions to entropies and heat capacities are calculated by using direct integration over energy levels of the internal rotational potentials.

6.2.2 Analysis of Internal Rotors

The calculated internal rotational potentials on the $C_{benzene}$—CH_3 bond in ortho-$C_6H_4(CH_3)CH_2OO\bullet$ is shown in Figure 6.1. It shows the normal 3-fold rotational barrier for methyl rotation on the $C_{benzene}$—CH_3 bond; this radical has the lowest energy when the dihedral $\angle H(13)$-$C(7)$-$C(6)$-$C(5) = 0$, this is due to the intramolecular interaction between

the peroxy O(18) atom and H(15) atom in the methyl group (see structure in Appendix Table D.1), since the intramolecular distance between these two atoms is 2.65 Å which is near to the sum of the van der Waals radii of H and O (2.6 Å).
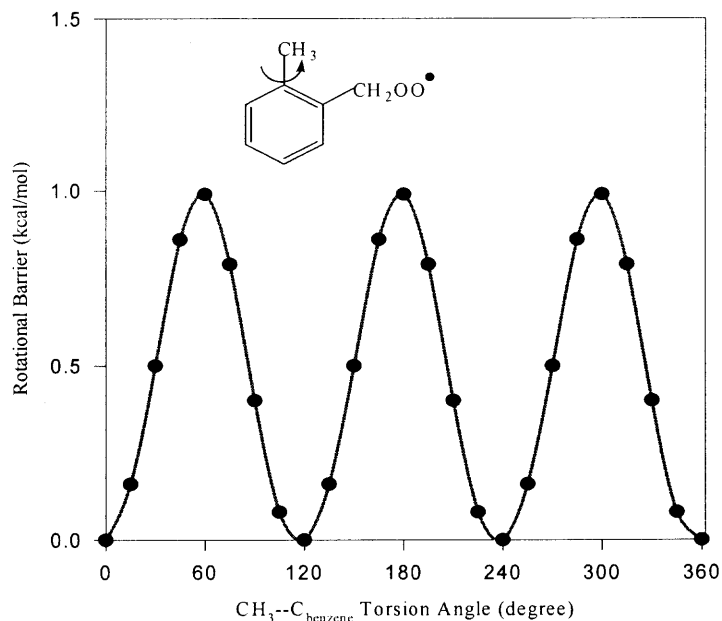
**Figure 6.1** The internal rotational potentials on the $C_{benzene}$—CH_3 bond in ortho-$C_6H_4(CH_3)CH_2OO\bullet$.

The calculated rotational potentials for the $CH_2COO\bullet$ group rotation on the C—$C_{benzene}$ bond in ortho-$C_6H_4(CH_3)CH_2OO\bullet$ is shown in Figure 6.2. This radical has the highest energy when the peroxy central oxygen is near cis to the benzene bond of the ortho link (the dihedral $\angle C(6)$-$C(1)$-$C(8)$-$O(18)$ = –24.8°, and the dihedral $\angle C(1)$-$C(8)$-$O(18)$-$O(19)$ = 174.5°). The high energy is mostly due to steric effect between $CH_2OO\bullet$ group and the methyl group, as the carbon – oxygen bond is pointed toward the methyl group. The second maxima corresponds to the structure with the peroxy central oxygen pointed away from the methyl and again near cis with the benzene ring, the dihedral

$\angle C(7)\text{-}C(6)\text{-}C(1)\text{-}C(8) = 0°$, $\angle C(1)\text{-}C(8)\text{-}O(18)\text{-}O(19) = 180°$. This orientation of the $CH_2OO\bullet$ group reduces the steric effect, and has a slightly reduced energy.
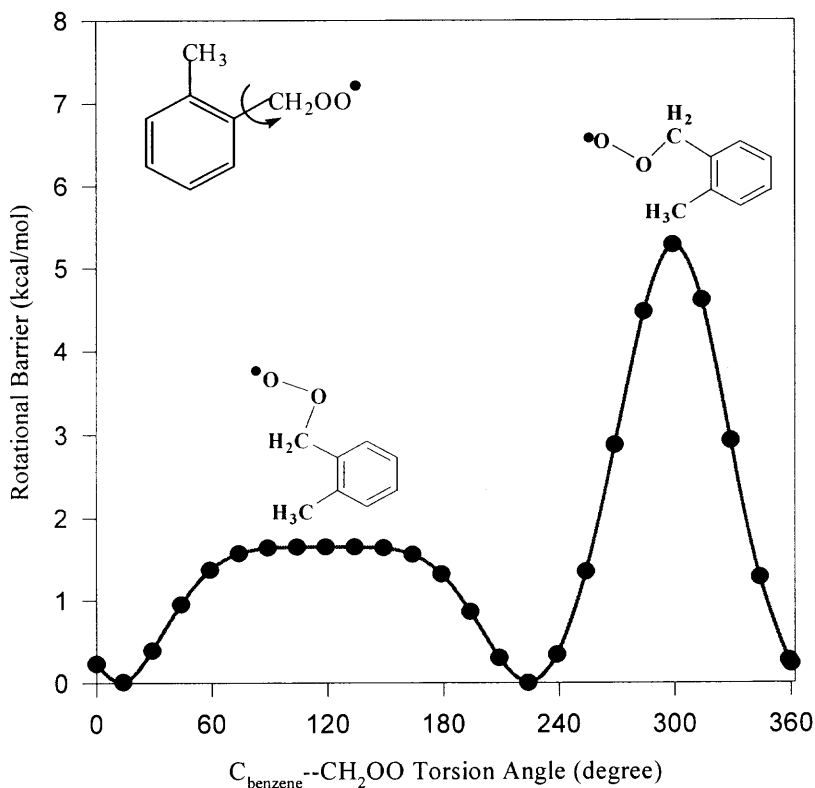
Figure 6.2 The rotational potentials on the C—$C_{benzene}$ bond in ortho-$C_6H_4(CH_3)CH_2OO\bullet$.

Figure 6.3 shows the calculated rotational potentials for OO$\bullet$ group rotation on the R—OO$\bullet$ bond in ortho-$C_6H_4(CH_3)CH_2OO\bullet$ radical. It shows three-fold barrier that is highly non-symmetric with barrier height about 3.62 kcal mol^{-1}.

The calculated rotational potentials for the OH group rotation on the RO—OH bond in ortho-$C_6H_4(CH_2OOH)CH_2\bullet$ radical is illustrated in Figure 6.4; the 5.65 kcal mol^{-1} barrier height is typical of published data on the RO—OH bond rotations.[77,135]
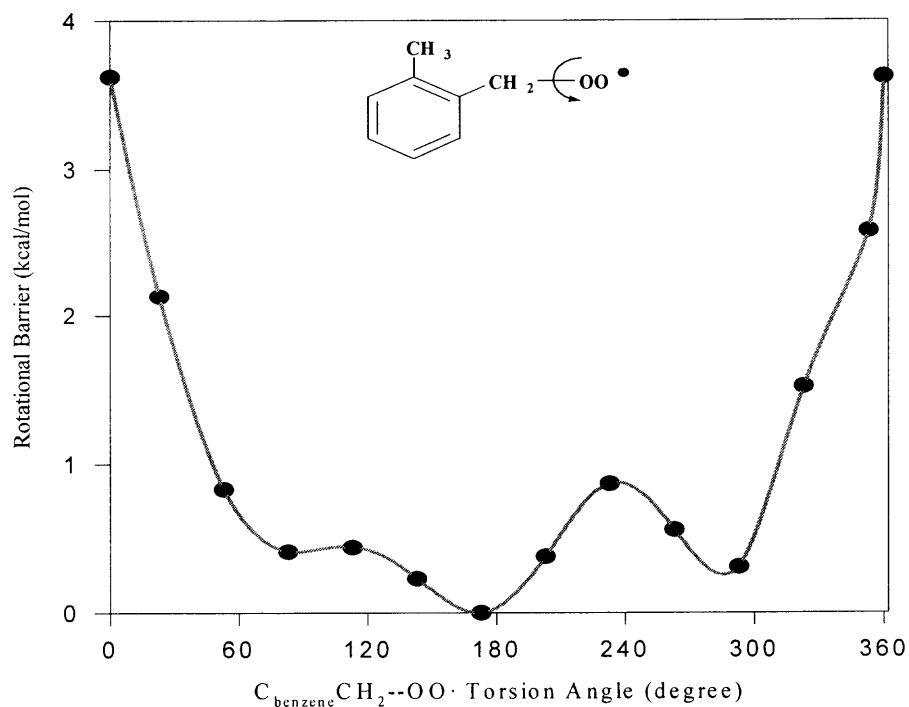
Figure 6.3 The rotational potentials on the R—OO• bond in ortho-C₆H₄(CH₃)CH₂OO•
radical.
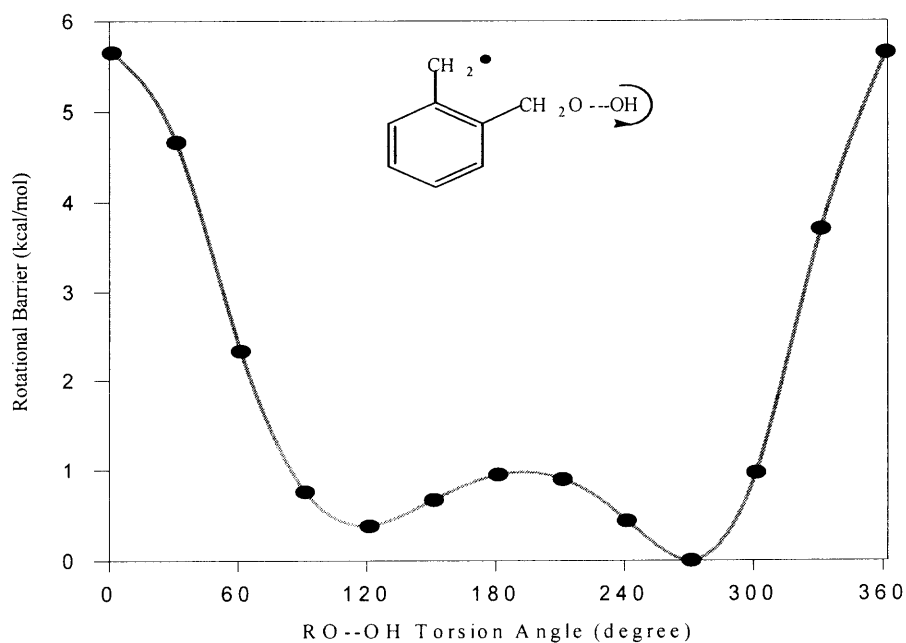
Figure 6.4 The calculated rotational potentials on the RO—OH bond in ortho-
C₆H₄(CH₂OOH)CH₂• radical.

6.2.3 Reactivity of Ortho-, Meta, and Para-Xylenes

To compare the reactivity of ortho-, meta-, para-oxylene radicals, the activation energy

for isomerization of the corresponding xylene peroxy radicals are calculated at the

B3LYP/6-311++G(3df,2p) level. The activation energy for 2-methylbenzyl peroxy

radical isomerization to 2-methylbenzyl methyl-hydroperoxide via a 7-member ring

transition state is 21.21 kcal mol^{-1}, but 3-methylbenzyl peroxy radical needs 60.05 kcal

mol^{-1} activation energy via a 8-member ring transition state, and 4-methylbenzyl methyl-

hydroperoxide needs 73.62 kcal mol^{-1} activation energy via a 9-member ring transition

state, to isomerize to the corresponding methylbenzyl methyl-hydroperoxides. The high

barriers for meta- and pare-xylene radicals are because the meta-, para interactions in

corresponding TS structures bend benzene rings out of a planar position (the dihedral

angle for four carbon in benzene ring those involved in transition state are 25° and 32°),

therefore, results in some loss of aromaticity. The activation energies for the

isomerization of meta-, para-oxylene of peroxy radicals are also listed in Table 6.1. These

data shows ortho-xylene is the most reactive compared with its meta-xylene and para-

xylene isomers, and it shows agreement with the experimental results.[153]
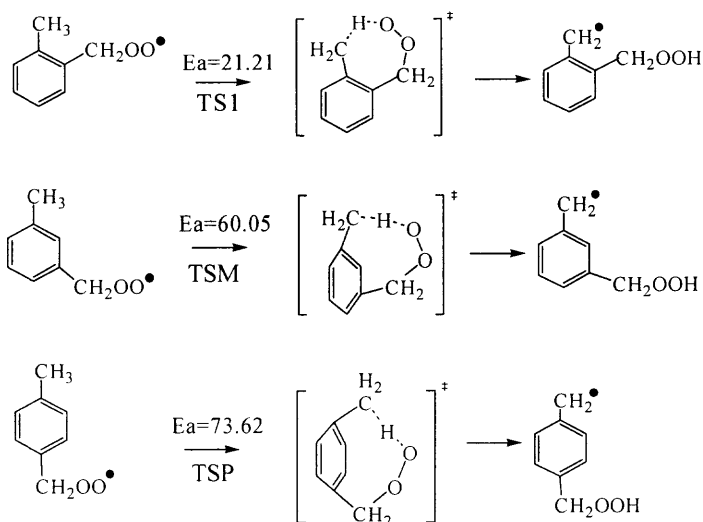
6.2.4 Kinetic Analysis of 2-Methylbenzyl + O₂ System

A potential energy diagram for the 2-methylbenzyl + O_2 reaction system calculated at the B3LYP/6-311++G(3df,2p) level is shown in Figure 6.5. The 2-methylbenzyl radical reacts with O_2 to form a chemically activated ortho-$C_6H_4(CH_3)CH_2OO\bullet^*$ adduct, which can be stabilized, dissociate back to reactants, or isomerize via three different paths. TS1 is a H atom transfer to the peroxy radical forming 2-methylbenzyl methyl-hydroperoxide (ortho-$C_6H_4(CH_2OOH)CH_2\bullet$) with activation energy of 21.21 kcal mol^{-1}. This barrier is much lower than those of 3-methylbenzyl and 4-methylbenzyl radicals since the ortho interaction between the H atom and peroxy oxygen atom in the TS structure keep the benzene ring almost planar. This is a near thermoneutral reaction – abstraction of a benzyl H atom and formation of a hydroperoxide through a 7-member ring transition state. The barrier of 21 kcal mol^{-1} is similar to the well depth of O_2 addition to ortho-xylene radical.
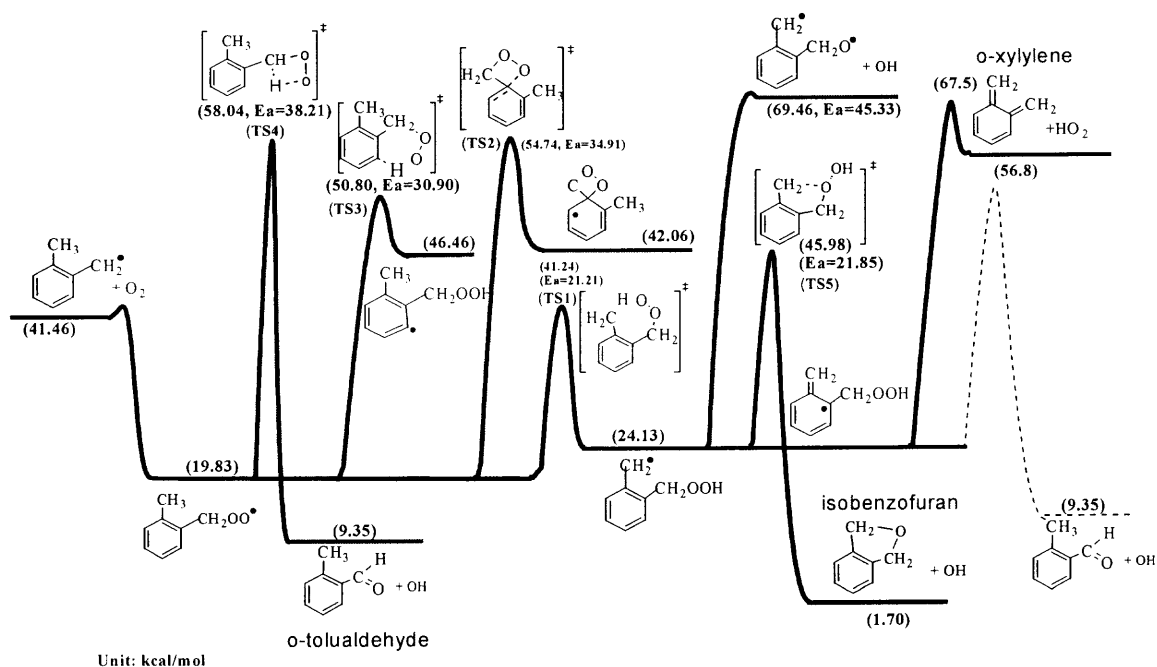
Figure 6.5 Potential energy diagram for the 2-methylbenzyl + O_2 reaction system.

The forming 2-methylbenzyl methyl-hydroperoxide will undergo dissociation via TS5 to produce major product isobenzofuran with barrier of 21.85 kcal/mol. In TS2 the peroxy radical attacks the ipso aromatic carbon (carbon bonded to the —$CH_2OO\bullet$ group, via 4-member ring transition state with a barrier of 34.91 kcal mol^{-1}. This breaks the aromatic resonance and forms a bicylcic molecule with a cyclohexadienyl radical and a peroxide ring. This bicyclic can undergo reverse reaction or cleave a carbon – carbon bond to form ortho phenoxy radical and formaldehyde, CH_2O.
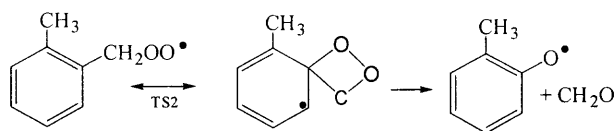
In TS3 the peroxy oxygen abstracts an H atom from an ortho position on the in benzene ring via 6-member ring transition state with a barrier of 30.90 kcal mol^{-1}. The peroxy ROO—H bond formed is only 86.5 kcal mol^{-1} and the phenyl—H bond cleaved is 113 kcal mol^{-1}, thus the barrier is only 2.4 kcal mol^{-1}above the endothermicity. While the barrier of 30.9 kcal mol^{-1} is ca 10 kcal mol^{-1} above the energy of the initial xylene radical + O_2 reactants, the reaction is important. It forms a phenyl radical, which reacts rapidly and is highly exoergic with O_2. The main products from the methyl substituted phenyl + O_2 reaction will be ring opening to CO + HC≡CH + CH_3-C≡C + HC•O.

The reaction described as TS4 has the peroxy radical abstracting a H atom from the ipso (peroxy) carbon via a 4-member ring transition state to form an intermediate alkyl-hydroperoxide radical (RC•OOH) that immediately dissociates via a β scission reaction to form a strong carbonyl and cleave the weak RO—OH bond. The resulting products are ortho-$C_6H_4(CH_3)CH(=O)$ + OH, but the 4-member ring transition state results in a barrier of 38.21 kcal mol^{-1}.

6.2.5 Reaction of Ortho-C₆H₄(CH₂OOH)CH₂• Isomer

Figure 6.6 shows the further oxidation reactions of the isomer, ortho-$C_6H_4(CH_2OOH)CH_2\bullet$, as calculated at the B3LYP/6-311++G(3df,2p) level. This isomer reacts with a second O_2 to form a chemically activated ortho-$C_6H_4(CH_2OOH)CH_2OO\bullet^*$ adduct, which can be stabilized or can isomerize and dissociate to new products.

TS6 has a 7-member ring structure where the $C_6H_4(CH_2OOH)CH_2OO\bullet$ peroxy radical abstracts a H atom from the CH_2OOH carbon, with a barrier of 16.07 kcal mol^{-1}, a RC•OOH moiety is formed, which as in the case of TS4 above, immediately dissociates to ortho-methyl-hydroperoxide benzylaldehyde (ortho-$C_6H_4(CH_2OOH)CHO$) + OH.
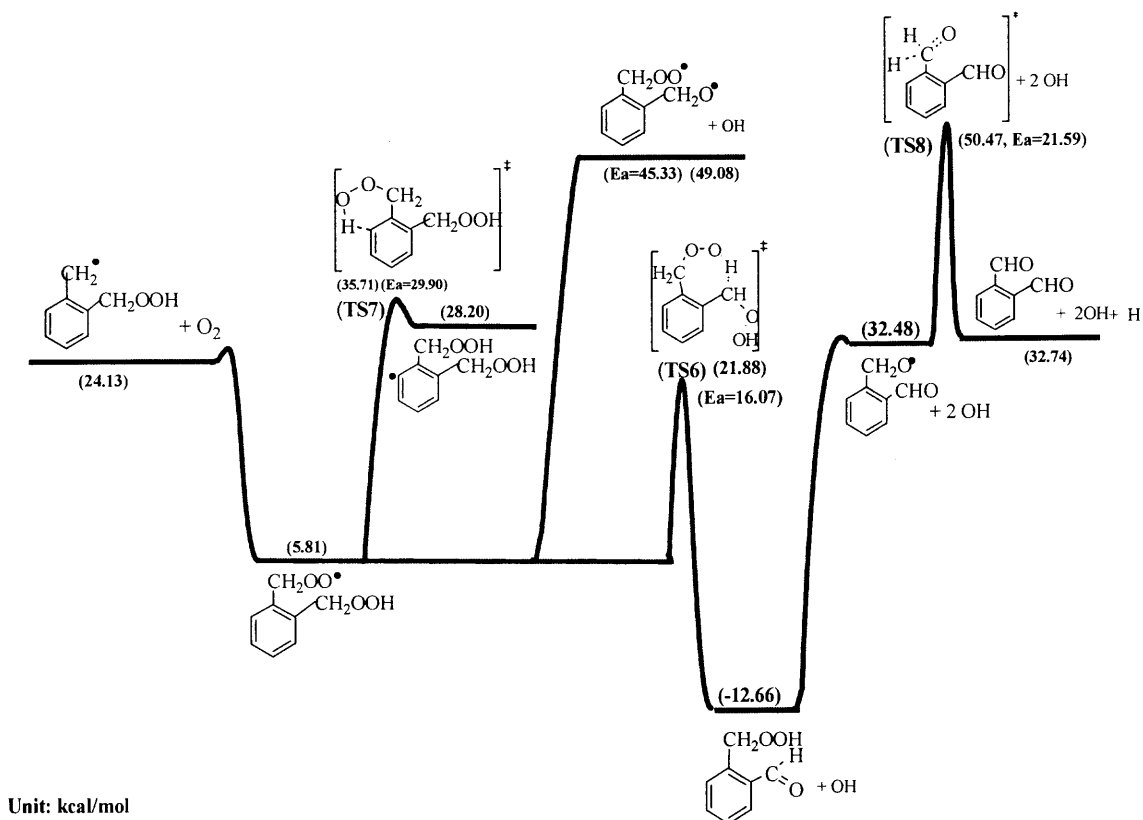
Figure 6.6 Isomer ortho-$C_6H_4(CH_2OOH)CH_2\bullet$ oxidation reaction system.

TS7 has a similar structure as that of TS3, in which the peroxy radical abstracts an H from an ortho position on the benzene ring. The barrier for TS7 is calculated to be 29.90 kcal mol^{-1}. As above the phenyl radical formed will rapidly react with O_2 and under go ring opening and dissociation to lower molecular weight products.

The stabilized ortho-$C_6H_4(CH_2OOH)CH_2OO\bullet$ adduct and stable ortho-$C_6H_4(CH_2OOH)CHO$ undergo homolytic cleavage of the weak O—O bonds with the barrier of ca. 44 kcal mol^{-1}. The ortho-$C_6H_4(CHO)CH_2O\bullet$ radical will then undergo unimolecular dissociation via TS8 to ortho-$C_6H_4(CHO)_2$ + H with barrier of 21.59 kcal mol^{-1}.

6.2.5 Kinetic Parameters

The high-pressure limit rate constants (k_∞) for the chemically activated 2-methylbenzyl + O_2 system are determined by canonical transition state theory using structural parameters and vibration frequencies. The high-pressure limit rate constants used in QRRK analysis are fitted by three parameters A_∞, n, and E_a over temperature range from 298 to 2000 K; Lennard-Jones parameters, σ (Angstroms) and ε/κ (Kelvins), are estimated from tabulations,[90] and these input data for QRRK analysis are listed in Table 6.2.

The calculated temperature dependent rate constants for 2-methylbenzyl + O_2 reaction system at 1 atm from the QRRK combined with Master equation analysis are illustrated in Figure 6.7. The dominant product-channel is stabilization to ortho-$C_6H_4(CH_3)CH_2OO\bullet$ below 800 K, and reverse reaction becomes dominant when temperature is above 800 K.

Table 6.2 Kinetic Parameters for QRRK in 2-Methylbenzyl Radical + O$_2$ System

reaction	A (s^{-1} or cm^3 mol^{-1} s^{-1})	n	E_a (kcal mol^{-1})
$C_6H_4(CH_3)CH_2\bullet + O_2 \rightarrow C_6H_4(CH_3)CH_2OO\bullet$	$1.09 \times 10^{10\,a}$	0.56725	2.29
$C_6H_4(CH_3)CH_2OO\bullet \rightarrow C_6H_4(CH_3)CH_2\bullet + O_2$	$2.28 \times 10^{12\,b}$	0.0	20.38
$C_6H_4(CH_3)CH_2OO\bullet \rightarrow C_6H_4(CH_3OOH)CH_2\bullet$	5.54×10^4	1.75768	20.71
$C_6H_4(CH_3)CH_2OO\bullet \rightarrow C_6H_3(CH_3)cyCCOO$	2.97×10^8	0.80402	35.03
$C_6H_4(CH_3)CH_2OO\bullet \rightarrow C_6H_3(CH_3)CH_2OOH$	6.91×10^6	1.29173	30.64
$C_6H_4(CH_3)CH_2OO\bullet \rightarrow C_6H_4(CH_3)CHO+OH$	1.91×10^7	1.37657	37.90
	frequency / degeneracy		
$C_6H_4(CH_3)CH_2OO\bullet$	396.7 / 16.936	1312.3 / 24.033	3255.4 / 8.531
Lennard-Jones parameter	σ (Å)	ε/k (K)	
	6.28	604	
$C_6H_4(CH_2OOH)CH_2\bullet + O_2 \rightarrow C_6H_4(CQ)CH_2OO\bullet$	$1.09 \times 10^{10\,a}$	0.56725	2.29
$C_6H_4(CQ)CH_2OO\bullet \rightarrow C_6H_4(CH_2OOH)CH_2\bullet + O_2$	$2.28 \times 10^{12\,b}$	0.0	16.88
$C_6H_4(CQ)CH_2OO\bullet \rightarrow C_6H_4(CQ)CHO + OH$	5.04×10^3	1.73546	15.29
$C_6H_4(CQ)CH_2OO\bullet \rightarrow C_6H_3(CH_2OOH)CH_2OOH$	3.70×10^4	1.49904	29.37
$C_6H_4(CQ)CH_2OO\bullet \rightarrow C_6H_4(COO\bullet)CH_2O\bullet + OH$	3.50×10^{15}	0.0	44.0
	frequency / degeneracy		
$C_6H_4(CQ)CH_2OO\bullet$	360.9 / 21.323	1301.6 / 25.926	3496.3 / 7.251
Lennard-Jones parameter	σ (Å)	ε/k (K)	
	6.60	685	

[a] Estimated from $C_2\bullet C=C+O_2$ by Chen et al.[128] [b] From the principle of microscopic reversibility at 700 K
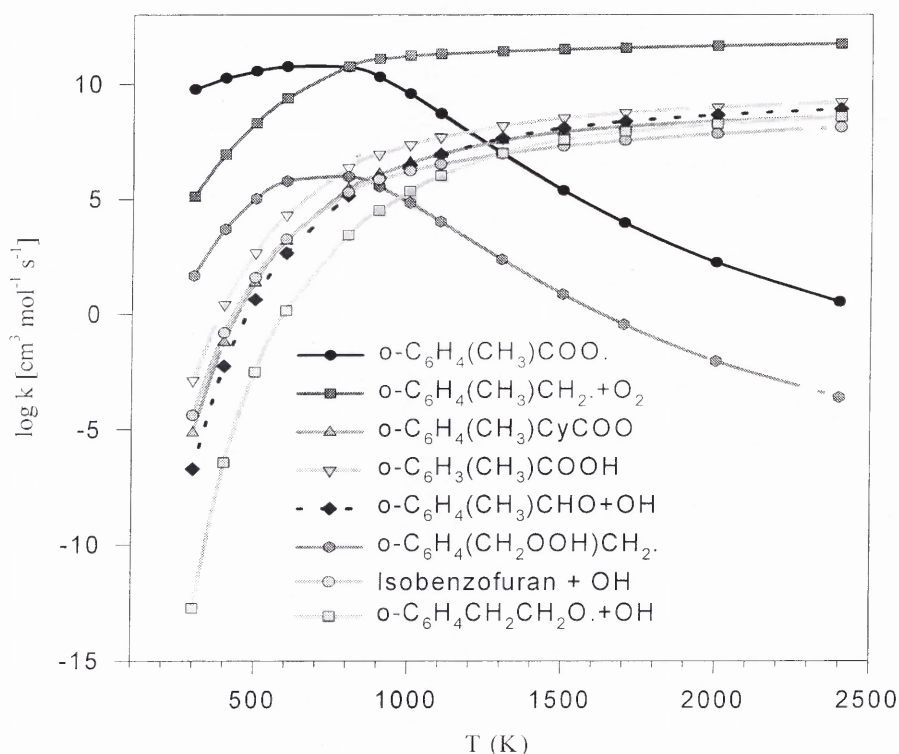
Figure 6.7 Rate constants for chemical activation reaction: o-C$_6$H$_4$(CH$_3$)CH$_2\bullet$+O$_2$ at P = 1 atm.
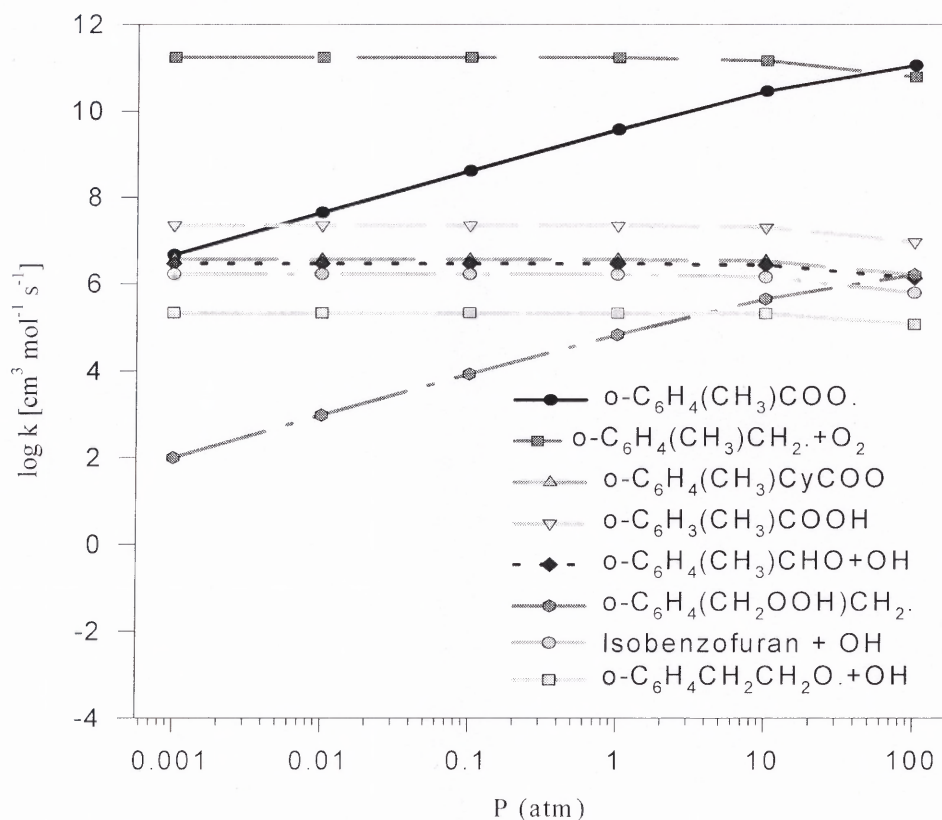
Figure 6.8 Rate constants for chemical activation reaction: o-$C_6H_4(CH_3)CH_2\bullet + O_2$ at T = 1000 K.

Figure 6.8 shows the calculated rate constants vs. pressure for the chemically activated reaction 2-methylbenzyl + O_2 at 1000 K; it shows the rate constants for stabilization and isomerization channel are increased with increased pressure, but other reaction channels have no pressure dependence over 0.001 ~ 10 atm.

The calculated temperature dependent dissociation rate constants for stabilized ortho-$C_6H_4(CH_3)CH_2OO\bullet$ radical reaction system at 1 atm are illustrated in Figure 6.9. The dominant channel is reverse back to ortho-$C_6H_4(CH_3)CH_2\bullet + O_2$ at all temperatures, and the next dominant channel is the preoxy radical isomerization to ortho-$C_6H_4(CH_2OOH)CH_2\bullet$ radical.
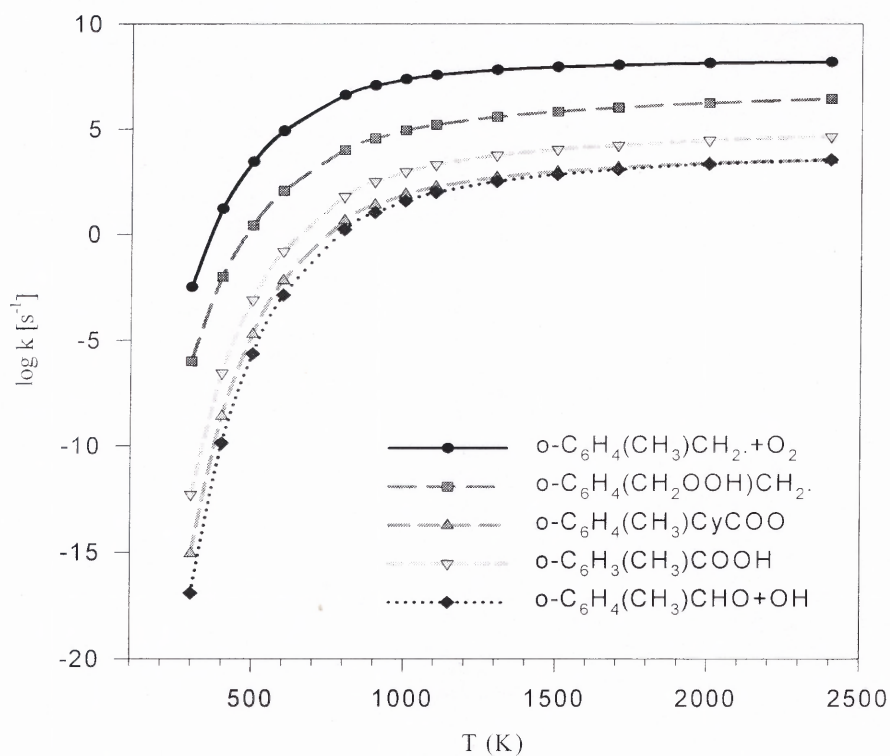
Figure 6.9 Rate constants for dissociation reaction: o-C$_6$H$_4$(CH$_3$)CH$_2$OO• at P = 1 atm.
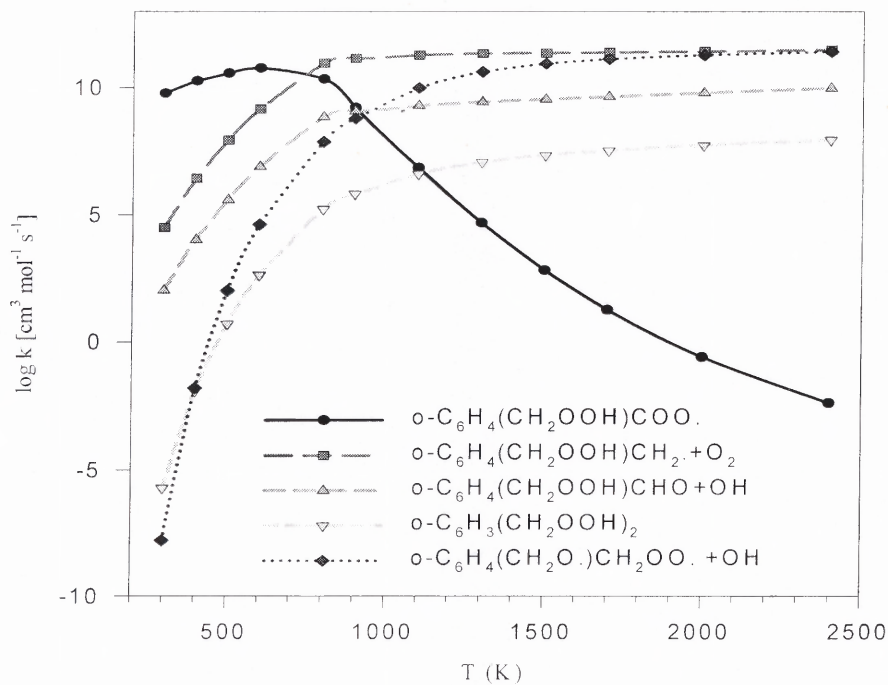
Figure 6.10 Rate constants for chemical activation reaction: o-C$_6$H$_4$(CH$_2$OOH)CH$_2$•+O$_2$ at P = 1 atm.

The calculated temperature dependent rate constants for $C_6H_4(CH_2OOH)CH_2\bullet$ + O_2 reaction system at 1 atm are showed in Figure 6.10. The dominant product-channel is stabilization to ortho-$C_6H_4(CH_2OOH)CH_2OO\bullet$ below 700 K and reverse reaction dominates at the temperatures above 700 K.

6.3 Summary
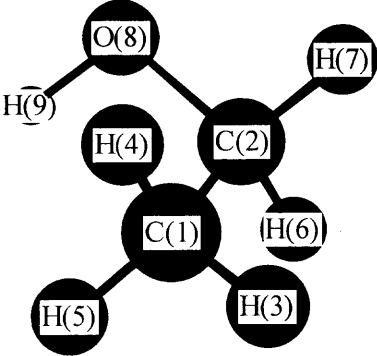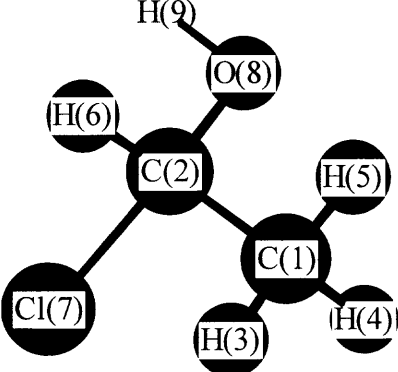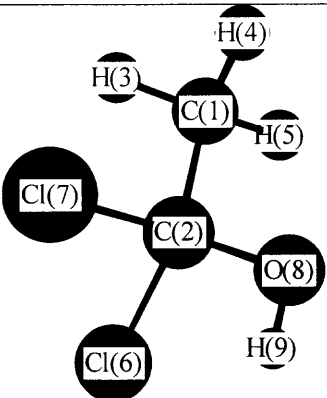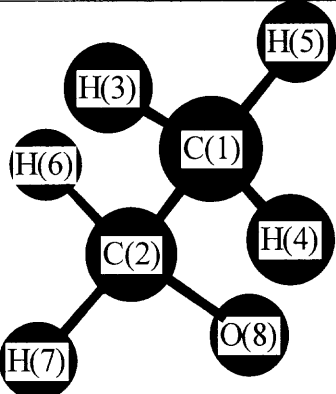
Thermochemical properties for reactants, intermediates, products and transition states important in 2-methylbenzyl radical + O_2 reaction system are calculated at the density functional levels. Potential barriers for the internal rotations are calculated at the B3LYP/6-31G(d,p) level. Potential energy surfaces are calculated at the DFT B3LYP/6-31G(d,p) and B3LYP/6-311++G(3df,2p) levels, and compared with the reaction enthalpies calculated at the KMLYP/6-311+G(d,p) level. Important initial product and intermediate channels in low temperature o-xylene oxidation system are stabilization, reverse dissociation, isomerization of the peroxy radical to the hydroperoxide isomer which dissociates to isobenzofuran plus OH. The intermediate stable products are predicted to be o-tolualdehyde, phthaladehyde, isobenzofuran, and o-xylylene.

APPENDIX A

TABLES IN THE THERMOCHEMICAL AND KINETIC ANALYSIS OF CHLORINATED ALCOHOLS, HYDROPEROXIDES AND RADICALS

This appendix lists the geometrical parameters, reaction enthalpies, and calculated enthalpies of formation for chlorinated alcohols, alkyl hydroperoxides, and corresponding radicals, as discussed in Chapter 2 and Chapter 3.

Table A.1 Geometrical Parameters for Ethanols [a]

Molecule	Bond Length		Bond Angle		Dihedral Angle	
				CH_3CH_2OH		
	r21	1.5258	a312	111.02	d4123	120.49
	r31	1.0956	a412	110.48	d5123	240.39
	r41	1.0940	a512	111.06	d6213	58.16
	r51	1.0969	a621	110.09	d7213	300.48
	r62	1.1020	a721	110.15	d8213	182.98
	r72	1.0948	a821	112.85	d9821	297.98
	r82	1.4235	a982	107.46		
	r98	0.9663				
				$CH_3CHClOH$		
	r21	1.5114	a312	110.81	d4123	120.94
	r31	1.0910	a412	109.89	d5123	239.95
	r41	1.0921	a512	108.73	d6213	55.00
	r51	1.0947	a621	112.60	d7213	302.35
	r62	1.0944	a721	109.37	d8213	181.29
	r72	1.8757	a821	109.15	d9821	183.86
	r82	1.3794	a982	108.99		
	r98	0.9672				
				CH_3CCl_2OH		
	r21	1.5138	a312	110.74	d4123	120.57
	r31	1.0891	a412	108.61	d5123	239.44
	r41	1.0923	a512	108.64	d6213	58.59
	r51	1.0924	a621	109.90	d7213	301.65
	r62	1.8459	a721	109.87	d8213	180.13
	r72	1.8466	a821	109.63	d9821	180.17
	r82	1.3583	a982	109.57		
	r98	0.9693				
				$CH_3CH_2O^\bullet$		
	r21	1.5276	a312	110.98	d4123	120.18
	r31	1.0953	a412	110.41	d5123	-120.29
	r41	1.0939	a512	110.43	d6213	57.44
	r51	1.0938	a621	111.36	d7213	-56.89
	r62	1.1101	a721	111.60	d8213	179.59
	r72	1.1094	a821	115.59		
	r82	1.3706				

[a] Distance in Angstrom, Angles in Degree.

Table A.1 (Continued)

Molecule	Bond Length		Bond Angle		Dihedral Angle	
			CH₃CHClO•			

$CH_3CHClO^\bullet$
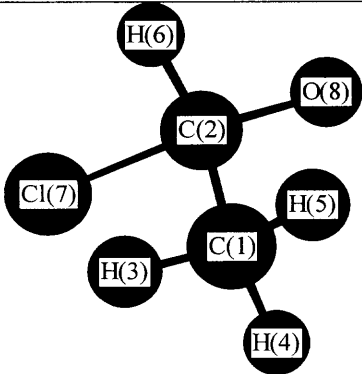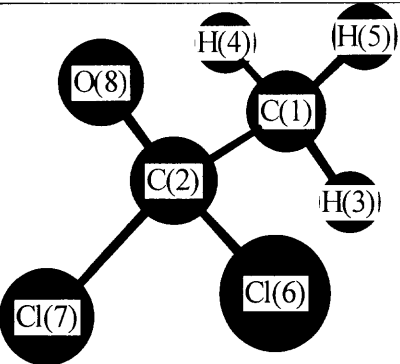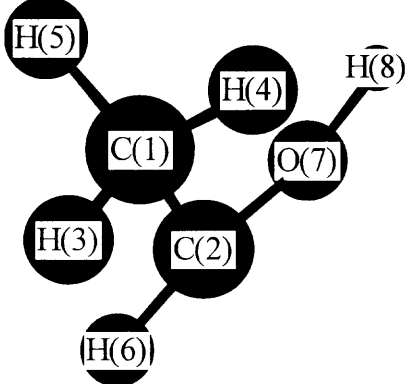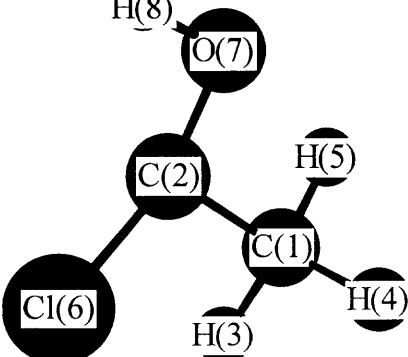
	Bond Length		Bond Angle		Dihedral Angle	
r21	1.5452	a312	109.16	d4123	119.77
r31	1.0903	a412	109.36	d5123	239.56
r41	1.0908	a512	108.77	d6213	57.47
r51	1.0925	a621	109.98	d7213	305.72
r62	1.1051	a721	108.68	d8213	178.69
r72	1.8798	a821	111.54		
r82	1.3155				

$CH_3CCl_2O^\bullet$

	Bond Length		Bond Angle		Dihedral Angle	
r21	1.5209	a312	110.46	d4123	119.53
r31	1.0903	a412	108.35	d5123	238.62
r41	1.0930	a512	108.82	d6213	63.47
r51	1.0915	a621	110.41	d7213	304.35
r62	1.8788	a721	109.68	d8213	173.51
r72	1.8413	a821	116.24		
r82	1.3138				

$CH_3C^\bullet HOH$

	Bond Length		Bond Angle		Dihedral Angle	
r21	1.4911	a312	110.43	d4123	119.19
r31	1.0939	a412	111.59	d5123	239.60
r41	1.1000	a512	113.04	d6213	40.51
r51	1.1046	a621	120.83	d7213	185.20
r62	1.0858	a721	119.34	d8721	29.17
r72	1.3758	a872	108.59		
r87	0.9672				

$CH_3C^\bullet ClOH$

	Bond Length		Bond Angle		Dihedral Angle	
r21	1.4921	a312	110.55	d4123	239.06
r31	1.0914	a412	111.78	d5123	119.81
r41	1.0998	a512	108.81	d6213	51.95
r51	1.0941	a621	115.80	d7213	187.99
r62	1.7999	a721	114.12	d8721	178.24
r72	1.3552	a872	109.30		
r87	0.9685				

Table A.1 (Continued)

Molecule	Bond Length	Bond Angle	Dihedral Angle

C$^{\bullet}$H$_2$CH$_2$OH
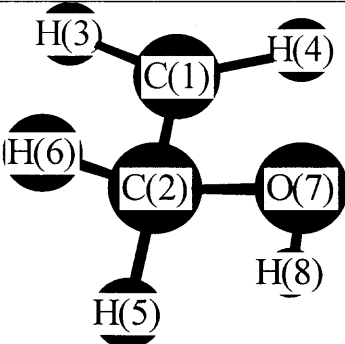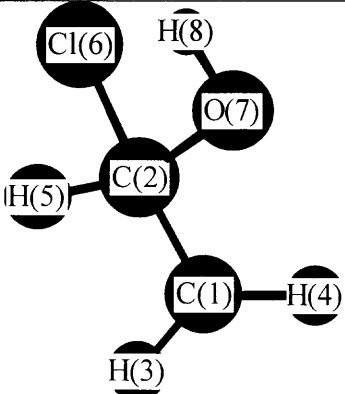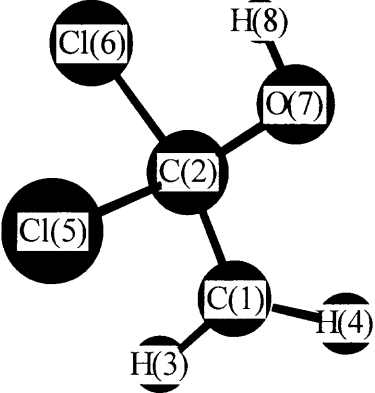
r21	1.4828	a312	120.33	d4123	189.92
r31	1.0838	a412	119.45	d5213	74.94
r41	1.0836	a521	110.03	d6213	319.03
r52	1.1107	a621	109.93	d7213	196.32
r62	1.1056	a721	109.13	d8721	188.37
r72	1.4235	a872	107.80		
r87	0.9654				

C$^{\bullet}$H$_2$CHClOH

r21	1.4462	a312	119.81	d4123	168.16
r31	1.0820	a412	119.04	d5123	32.40
r41	1.0832	a521	115.29	d6213	285.47
r52	1.0915	a621	106.25	d7213	166.87
r62	1.9980	a721	112.28	d8721	178.06
r72	1.3662	a872	109.02		
r87	0.9674				

C$^{\bullet}$H$_2$CCl$_2$OH

r21	1.4615	a312	119.86	d4123	179.99
r31	1.0800	a412	118.38	d5213	57.63
r41	1.0823	a521	109.81	d6213	302.38
r52	1.8688	a621	109.78	d7213	180.02
r62	1.8692	a721	111.04	d8721	180.11
r72	1.3559	a872	109.49		
r87	0.9689				
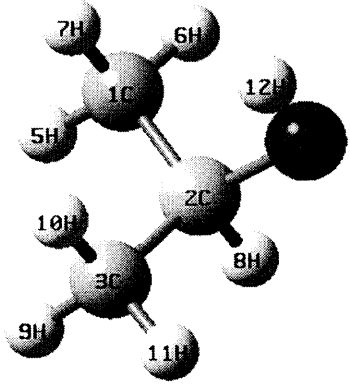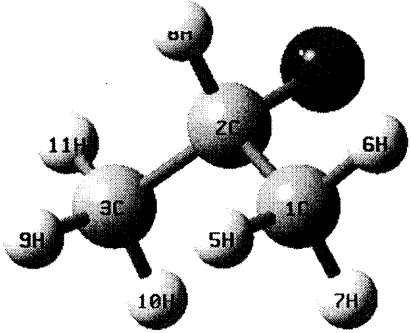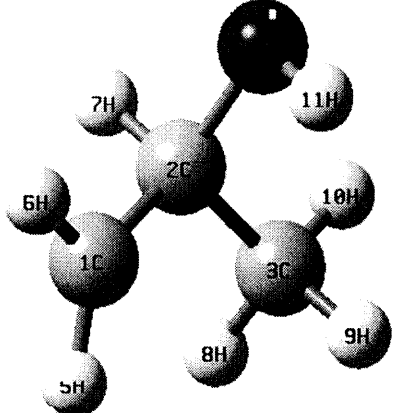
Table A.2 Reaction Enthalpies at 298 K and Calculated $\Delta H_f{}^{\circ}{}_{298}$ Values

Reaction Series	B3LYP /6-31G(d,p)		B3LYP /6-311+G(3df,2p)		QCISD(T) /6-31G(d,p)		CBSQ//B3LYP /6-31G(d,p)		G3MP2 //MP2(full)/6-31G(d)	
	$\Delta H^{\circ}{}_{rxn}$	$\Delta H_f{}^{\circ}{}_{298}$	$\Delta H^{\circ}{}_{rxn}$	$\Delta H_f{}^{\circ}{}_{298}$	$\Delta H^{\circ}{}_{rxn}$	$\Delta H_f{}^{\circ}{}_{298}$	$\Delta H^{\circ}{}_{rxn}$	$\Delta H_f{}^{\circ}{}_{298}$	$\Delta H^{\circ}{}_{rxn}$	$\Delta H_f{}^{\circ}{}_{298}$
1. **CH₃CHClOH**+CH₄ —→ C₂H₅OH + CH₃Cl	10.85	-68.68	10.22	-66.34	10.96	-68.79	11.22	-69.05	11.40	-69.23
2. **CH₃CHClOH**+C₂H₆ —→ n-C₃H₇OH + CH₃Cl	9.28	-69.61	8.72	-69.05	8.83	-69.16	8.44	-68.77	8.66	-68.99
3. **CH₃CHClOH**+ CH₃OH—→ C₂H₅OH+ CH₂ClOH	1.65	-67.76	1.93	-68.04	2.62	-68.73	2.96	-69.07	2.98	-69.09
4. **CH₃CHClOH**+CH₄ —→ CH₃OH+ C₂H₅Cl	12.33	-69.36	11.08	-68.11	12.10	-69.13	11.94	**-68.97**	12.16	**-69.19**
5. **CH₃CHClOH**+C₂H₆ —→ C₂H₅OH + C₂H₅Cl	6.86	-69.58	6.09	-68.81	6.54	-69.26	6.21	**-68.93**	6.42	**-69.14**
6. **CH₃CHClOH**+ C₃H₈—→ n-C₃H₇OH+C₂H₅Cl	6.90	-69.69	6.32	-69.11	6.62	-69.41	6.21	**-69.00**	6.49	**-69.28**
7. **CH₃CHClOH**+C₂H₆ —→CH₃OH+CH₃CHClCH₃	8.20	-71.04	6.77	-69.61	6.58	-69.42	5.13	**-67.97**	5.73	**-68.57**
Average value and deviation[b]:								**-68.72±0.50**		**-69.05±0.32**
1. **CH₃CCl₂OH** + CH₄ —→ CH₃CH₂OH+ CH₂Cl₂	15.53	-76.59	13.88	-74.94	16.96	-78.02	17.28	-78.34	16.63	-77.69
2. **CH₃CCl₂OH** + C₂H₆ —→ n-C₃H₇OH + CH₂Cl₂	13.96	-77.52	12.38	-75.94	14.83	-78.39	14.51	-78.07	13.88	-77.44
3. **CH₃CCl₂OH** + CH₃OH—→ C₂H₅OH+ CHCl₂OH	1.86	-75.78	1.98	-75.90	3.90	-77.82	4.38	-78.30	3.99	-77.91
4. **CH₃CCl₂OH** + CH₄ —→ CH₃OH+ CH₃CHCl₂	15.14	-76.42	12.91	-74.19	15.38	-76.66	14.53	**-75.81**	14.51	**-75.79**
5. **CH₃CCl₂OH** + C₂H₆ —→ C₂H₅OH + CH₃CHCl₂	9.67	-76.64	7.93	-74.90	9.81	-76.78	8.81	**-75.78**	8.77	**-75.74**
6. **CH₃CCl₂OH** + C₃H₈—→ n-C₃H₇OH+ CH₃CHCl₂	9.71	-76.75	8.16	-75.20	9.89	-76.93	8.80	**-75.84**	8.84	**-75.88**
7. **CH₃CCl₂OH** + C₂H₆ —→ CH₃OH+CH₃CCl₂CH₃	10.40	-80.47	8.18	-78.25	8.23	-78.30	5.49	**-75.56**	5.63	**-75.70**
Average value and deviation[b]:								**-75.75±0.13**		**-75.78±0.08**

[a] Reaction enthalpies include thermal correction and zero-point energy. Units in kcal/mol.

[b] The deviation are between the isodesmic reactions (see text).

Table A.3 Geometrical Parameters for Papanols

Molecule	Bond Length[a]		Bond Angle[b]		Dihedral Angle[c]		Frequencies[d] Moments of Inertia[e]		

(CH₃)₂CHOH

	Bond Length		Bond Angle		Dihedral Angle		Frequencies		
r21	1.5300	a321	112.63	d4213	234.60	236	1090	1512
r32	1.5300	a421	111.11	d5123	299.70	274	1151	1522
r42	1.4296	a512	111.42	d6123	179.02	309	1194	3029
r51	1.0952	a612	110.34	d7123	59.34	357	1319	3033
r61	1.0935	a712	110.66	d8213	120.63	427	1368	3053
r71	1.0978	a821	108.76	d9321	60.29	472	1412	3096
r82	1.0969	a932	111.42	d10321	300.65	819	1422	3107
r93	1.0952	a1032	110.66	d11321	180.97	924	1430	3128
r103	1.0978	a1132	110.34	d12421	63.13	941	1498	3130
r113	1.0935	a1242	107.19			975	1499	3790
r124	0.9675							

12.91 226.57 381.05

(CH₃)₂CHO•

	Bond Length		Bond Angle		Dihedral Angle		Frequencies		
r21	1.5381	a321	113.77	d4213	230.45	203	1051	1509
r32	1.5381	a421	112.55	d5123	302.02	244	1089	1518
r42	1.3749	a512	111.15	d6123	181.06	355	1169	2851
r51	1.0944	a612	110.23	d7123	61.70	392	1204	3046
r61	1.0927	a712	109.94	d8213	119.13	450	1263	3052
r71	1.0948	a821	107.62	d9321	57.98	809	1394	3120
r82	1.1151	a932	111.15	d10321	298.30	895	1419	3126
r93	1.0944	a1032	109.94	d11321	178.94	916	1494	3139
r103	1.0948	a1132	110.23			988	1499	3141
r113	1.0928							

196.32 225.23 373.91

C•H₂CH(OH)CH₃

	Bond Length		Bond Angle		Dihedral Angle		Frequencies		
r21	1.4923	a321	112.96	d4213	234.09	136	962	1507
r32	1.5329	a421	111.08	d5123	339.65	251	1031	1509
r42	1.4355	a512	121.71	d6123	167.34	339	1145	2978
r51	1.0850	a612	119.25	d7213	120.60	363	1168	3039
r61	1.0851	a721	109.51	d8321	60.20	423	1258	3108
r72	1.1026	a832	111.07	d9321	300.40	443	1346	3136
r83	1.0953	a932	110.69	d10321	180.59	566	1408	3158
r93	1.0963	a1032	110.08	d11421	54.72	838	1415	3267
r103	1.0928	a1142	106.55			910	1465	3786
r114	0.9678							

200.67 216.75 369.84

[a] Bond length in Å; [b] bond angle in degree. [c] Dihedral angle in degree. [d] Frequencies in cm⁻¹. [e] Moments of inertia in amu.Bohr².

Table A.3 (Continued)

Molecule	Bond Length[a]		Bond Angle[b]		Dihedral Angle[c]		Frequencies[d] Moments of Inertia[e]		

(CH₃)₂CClOH

	Bond Length		Bond Angle		Dihedral Angle		Frequencies		
r21	1.5188	a321	114.24	d4213	242.73	244	946	1493
r32	1.5243	a421	107.22	d5213	125.94	278	1014	1509
r42	1.8995	a521	107.59	d6521	182.02	293	1025	1514
r52	1.3843	a652	108.68	d7123	297.86	305	1131	3052
r65	0.9678	a712	108.68	d8123	178.93	362	1161	3064
r71	1.0950	a812	109.98	d9123	57.89	400	1276	3125
r81	1.0911	a912	110.86	d10321	62.23	448	1384	3143
r91	1.0909	a1032	108.64	d11321	302.12	475	1424	3154
r103	1.0953	a1132	111.27	d12321	181.69	553	1436	3171
r113	1.0915	a1232	110.83			829	1491	3798
r123	1.0940							
						376.92	593.87 617.63	

(CH₃)₂CClO•

	Bond Length		Bond Angle		Dihedral Angle		Frequencies		
r21	1.5489	a321	112.66	d5213	122.56	226	911	1489
r32	1.5481	a421	106.32	d6321	180.64	262	959	1490
r42	1.9094	a521	109.59	d7123	299.37	270	1001	1512
r52	1.3178	a632	109.89	d8123	179.36	298	1069	3069
r63	1.0904	a712	108.73	d9123	59.54	335	1129	3072
r71	1.0930	a812	109.92	d10321	60.64	366	1201	3159
r81	1.0904	a912	108.83	d11321	300.47	387	1381	3162
r91	1.0909	a1032	108.73			549	1417	3176
r103	1.0930	a1132	108.89			815	1477	3178
r113	1.0909		243.91					
						358.27	582.35 624.68	

C•H₂CCl(OH)CH₃

	Bond Length		Bond Angle		Dihedral Angle		Frequencies		
r21	0.9680	a312	108.83	d4312	65.07	168	673	1474
r31	1.3674	a431	106.26	d5312	175.58	257	823	1500
r43	2.0598	a531	111.24	d6531	168.51	266	962	1513
r53	1.4455	a653	119.88	d7531	336.79	277	1025	3053
r65	1.0819	a753	119.10	d8312	312.39	350	1062	3129
r75	1.0826	a831	114.88	d9831	55.75	398	1177	3165
r83	1.5182	a983	110.78	d10831	176.09	425	1316	3191
r98	1.0930	a1083	111.07	d11831	296.16	474	1406	3308
r108	1.0905	a1183	108.46			478	1430	3801
r118	1.0958							
						366.93	606.51 628.91	

Table A.4 Reaction Enthalpies at 298K and Calculated $\Delta H_f^{\circ}{}_{298}$ Values[a]
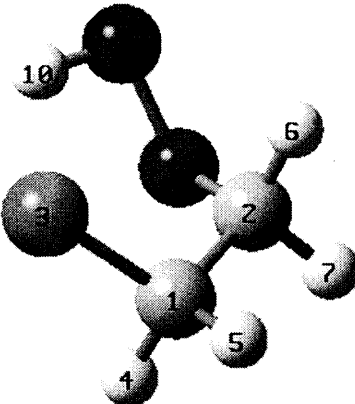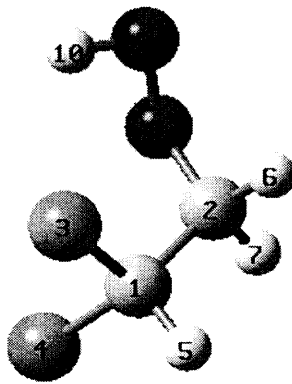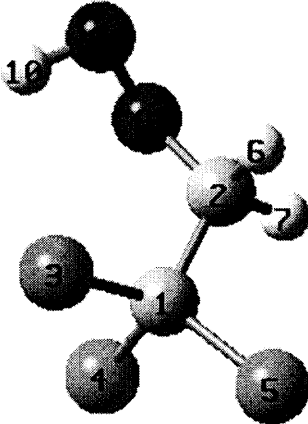
Reaction Series	B3LYP /6-31G(d,p)		B3LYP /6-311+G(3df,2p)		CBSQ//B3LYP /6-31G(d,p)	
	$\Delta H^{\circ}{}_{rxn}$	$\Delta H_f^{\circ}{}_{298}$	$\Delta H^{\circ}{}_{rxn}$	$\Delta H_f^{\circ}{}_{298}$	$\Delta H^{\circ}{}_{rxn}$	$\Delta H_f^{\circ}{}_{298}$
1.1 $(CH_3)_2CHOH + CH_4 \longrightarrow CH_3OH + C_3H_8$	9.26	-64.47	8.33	-63.54	10.12	-65.33
1.2 $(CH_3)_2CHOH + CH_4 \longrightarrow C_2H_5OH + C_2H_6$	5.40	-63.87	5.07	-63.54	7.16	-65.63
1.3 $(CH_3)_2CHOH + C_2H_6 \longrightarrow C_2H_5OH + C_3H_8$	3.79	-64.69	3.35	-64.25	4.40	-65.30
1.4 $(CH_3)_2CHOH + C_2H_6 \longrightarrow CH_3OH + i\text{-}C_4H_{10}$	6.86	-66.77	5.63	-65.54	5.06	-64.97
1.5 $(CH_3)_2CHOH + CH_3Cl \longrightarrow CH_3OH + CH_3CHClCH_3$	2.76	-66.27	1.62	-65.13	1.08	-64.59
1.6 $(CH_3)_2CHOH + CH_3Cl \longrightarrow CH_2ClOH + C_3H_8$	0.06	-63.58	0.04	-63.56	1.86	-65.38
1.7 $(CH_3)_2CHOH + CH_3Cl \longrightarrow CH_3CHClOH + C_2H_6$	-5.44	-63.86	-5.15	-64.15	-4.05	-65.25
1.8 $(CH_3)_2CHOH + C_2H_5Cl \longrightarrow CH_3CHClOH + C_3H_8$	-3.07	-63.79	-2.75	-64.11	-1.82	-65.04
Average value and deviation[b]:					**-65.19±0.31**	
2.1 $(CH_3)_2CHO^{\bullet} + CH_4 \longrightarrow C_3H_8 + CH_3O^{\bullet}$	8.28	-11.31	7.65	-10.68	8.86	-11.89
2.2 $(CH_3)_2CHO^{\bullet} + C_2H_6 \longrightarrow C_3H_8 + C_2H_5O^{\bullet}$	2.61	-11.29	2.26	-10.94	3.20	-11.88
2.3 $(CH_3)_2CHO^{\bullet} + CH_3OH \longrightarrow (CH_3)_2CHOH + CH_3O^{\bullet}$	-0.99	-12.02	-0.68	-12.33	-1.26	-11.75
2.4 $(CH_3)_2CHO^{\bullet} + C_2H_5OH \longrightarrow (CH_3)_2CHOH + C_2H_5O^{\bullet}$	-1.18	-11.79	-1.09	-11.88	-1.20	-11.77
2.5 $(CH_3)_2CHO^{\bullet} + CH_3OH \longrightarrow CH_3CH_2CH_2OH + CH_3O^{\bullet}$	2.85	-11.64	2.90	-11.69	3.13	-11.92
2.6 $(CH_3)_2CHO^{\bullet} + C_2H_5OH \longrightarrow CH_3CH_2CH_2OH + C_2H_5O^{\bullet}$	2.66	-11.41	2.49	-11.24	3.19	-11.94
2.7 $(CH_3)_2CHO^{\bullet} + CH_2ClOH \longrightarrow (CH_3)_2CHOH + CH_2ClO^{\bullet}$	-0.69	-11.56	-1.07	-11.18	-0.50	-11.75
2.8 $(CH_3)_2CHO^{\bullet} + CH_3CHClOH \longrightarrow (CH_3)_2CHOH + CH_3CHClO^{\bullet}$	0.20	-11.55	0.06	-11.41	0.58	-11.93
Average value and deviation[b]:					**-11.85±0.08**	
3.1 $C^{\bullet}H_2CH(OH)CH_3 + CH_4 \longrightarrow (CH_3)_2CHOH + CH_3^{\bullet}$	4.04	-16.52	3.83	-16.31	2.55	-15.03
3.2 $C^{\bullet}H_2CH(OH)CH_3 + C_2H_6 \longrightarrow (CH_3)_2CHOH + C_2H_5^{\bullet}$	-0.72	-15.43	-0.87	-15.28	-1.11	-15.04
3.3 $C^{\bullet}H_2CH(OH)CH_3 + CH_3OH \longrightarrow (CH_3)_2CHOH + C^{\bullet}H_2OH$	-6.54	-14.54	-5.83	-15.25	-6.01	-15.07
3.4 $C^{\bullet}H_2CH(OH)CH_3 + C_2H_5OH \longrightarrow (CH_3)_2CHOH + CH_3C^{\bullet}HOH$	-8.55	-13.86	-7.86	-14.55	-7.33	-15.08
3.5 $C^{\bullet}H_2CH(OH)CH_3 + C_2H_5OH \longrightarrow (CH_3)_2CHOH + C^{\bullet}H_2CH_2OH$	0.95	-15.72	0.37	-15.14	0.27	-15.04
3.6 $C^{\bullet}H_2CH(OH)CH_3 + CH_2ClOH \longrightarrow (CH_3)_2CHOH + C^{\bullet}HClOH$	-7.32	-14.26	-6.41	-15.17	-6.59	-14.99
3.7 $C^{\bullet}H_2CH(OH)CH_3 + CH_3CHClOH \longrightarrow (CH_3)_2CHOH+ C^{\bullet}H_2CHClOH$	-1.13	-14.07	-0.63	-13.44	0.87	-14.94
3.8 $C^{\bullet}H_2CH(OH)CH_3 + CH_3CHClOH \longrightarrow (CH_3)_2CHOH+ CH_3C^{\bullet}ClOH$	-8.78	-13.67	-8.08	-14.37	-7.43	-15.02
Average value and deviation[b]:					**-15.03±0.05**	

[a] Reaction enthalpies include thermal correction and zero-point energy. Units in kcal/mol.
[b] Average value is calculated at the CBSQ//B3 level, and the deviation is between the working reactions.

Table A.4 (Continued)

Reaction Series	B3LYP /6-31G(d,p)		B3LYP /6-311+G(3df,2p)		CBSQ//B3LYP /6-31G(d,p)	
	ΔH°_{rxn}	$\Delta H_f{}^\circ_{298}$	ΔH°_{rxn}	$\Delta H_f{}^\circ_{298}$	ΔH°_{rxn}	$\Delta H_f{}^\circ_{298}$
4.1 $(CH_3)_2CClOH + CH_4 \longrightarrow (CH_3)_2CHOH + CH_3Cl$	11.21	-78.08	10.36	-77.23	13.03	-79.90
4.2 $(CH_3)_2CClOH + CH_4 \longrightarrow CH_2ClOH + C_3H_8$	11.27	-76.47	10.40	-75.60	14.88	-80.08
4.3 $(CH_3)_2CClOH + CH_4 \longrightarrow CH_3CHClOH + C_2H_6$	5.76	-76.74	5.21	-76.19	8.97	-79.95
4.4 $(CH_3)_2CClOH + C_2H_6 \longrightarrow (CH_3)_2CHOH + CH_3CH_2Cl$	7.22	-78.96	6.24	-77.98	8.02	-79.76
4.5 $(CH_3)_2CClOH + C_2H_6 \longrightarrow CH_3CHClOH + C_3H_8$	4.15	-77.56	3.49	-76.90	6.20	-79.61
4.6 $(CH_3)_2CClOH + CH_3OH \longrightarrow (CH_3)_2CHOH + CH_2ClOH$	2.00	-77.18	2.07	-77.25	4.76	-79.94
4.7 $(CH_3)_2CClOH + CH_3OH \longrightarrow CH_3CHClOH + C_2H_5OH$	0.29	-76.96	0.23	-76.90	3.25	-79.92
4.8 $(CH_3)_2CClOH + CH_2ClOH \longrightarrow 2\ CH_3CHClOH$	-1.35	-77.84	-1.70	-77.49	0.29	-79.48
Average value and deviation[b]:					**-79.83±0.20**	
5.1 $(CH_3)_2CClO^\bullet + CH_4 \longrightarrow CH_3CHClO^\bullet + C_2H_6$	5.54	-22.68	5.11	-22.25	8.96	-26.10
5.2 $(CH_3)_2CClO^\bullet + CH_4 \longrightarrow CH_2ClO^\bullet + C_3H_8$	10.16	-22.42	9.16	-21.42	13.78	-26.04
5.3 $(CH_3)_2CClO^\bullet + C_2H_6 \longrightarrow CH_3CHClO^\bullet + C_3H_8$	3.92	-23.49	3.39	-22.96	6.19	-25.76
5.4 $(CH_3)_2CClO^\bullet + C_3H_8 \longrightarrow CH_3CHClO^\bullet + iso\text{-}C_4H_{10}$	3.14	-24.98	2.42	-24.26	3.90	-25.74
5.5 $(CH_3)_2CClO^\bullet + CH_3OH \longrightarrow CH_3O^\bullet + (CH_3)_2CClOH$	-1.41	-26.24	-0.84	-26.81	-1.85	-25.80
5.6 $(CH_3)_2CClO^\bullet + C_2H_5OH \longrightarrow C_2H_5O^\bullet + (CH_3)_2CClOH$	-1.61	-26.00	-1.25	-26.36	-1.79	-25.81
5.7 $(CH_3)_2CClO^\bullet + CH_2ClOH \longrightarrow CH_2ClO^\bullet + (CH_3)_2CClOH$	-1.11	-25.78	-1.23	-25.65	-1.10	-25.79
5.8 $(CH_3)_2CClO^\bullet + CH_3CHClOH \longrightarrow CH_3CHClO^\bullet + (CH_3)_2CClOH$	-0.23	-25.76	-0.10	-25.89	-0.02	-25.97
Average value and deviation[b]:					**-25.88±0.14**	
6.1 $C^\bullet H_2CCl(OH)CH_3 + CH_4 \longrightarrow (CH_3)_2CClOH + CH_3^\bullet$	5.47	-32.59	4.74	-31.86	1.99	-29.10
6.2 $C^\bullet H_2CCl(OH)CH_3 + C_2H_6 \longrightarrow (CH_3)_2CClOH + C_2H_5^\bullet$	0.71	-31.50	0.04	-30.83	-1.67	-29.11
6.3 $C^\bullet H_2CCl(OH)CH_3 + CH_3Cl \longrightarrow (CH_3)_2CClOH + CH_2Cl^\bullet$	-0.57	-31.96	-1.39	-31.13	-3.40	-29.13
6.4 $C^\bullet H_2CCl(OH)CH_3 + CH_3OH \longrightarrow (CH_3)_2CClOH + C^\bullet H_2OH$	-5.11	-30.61	-4.92	-30.80	-6.58	-29.14
6.5 $C^\bullet H_2CCl(OH)CH_3 + C_2H_5OH \longrightarrow (CH_3)_2CClOH + CH_3C^\bullet HOH$	-7.12	-29.93	-6.95	-30.10	-7.90	-29.15
6.6 $C^\bullet H_2CCl(OH)CH_3 + C_2H_5OH \longrightarrow (CH_3)_2CClOH + C^\bullet H_2CH_2OH$	2.38	-31.79	1.28	-30.68	-0.30	-29.11
6.7 $C^\bullet H_2CCl(OH)CH_3 + CH_2ClOH \longrightarrow (CH_3)_2CClOH + C^\bullet HClOH$	-5.89	-30.32	-5.50	-30.72	-7.16	-29.06
6.8 $C^\bullet H_2CCl(OH)CH_3 + CH_3CHClOH \longrightarrow (CH_3)_2CClOH + CH_3C^\bullet ClOH$	-7.35	-29.73	-7.17	-29.92	-8.00	-29.09
Average value and deviation[b]:					**-29.11±0.03**	

Table A.5 Geometry Parameters for Ethyl Hydroperoxides

Molecule	Bond Length[a]		Bond Angle[b]		Dihedral Angle[c]		Frequencies[d] Moments of Inertia[e]		

CH₂ClCH₂OOH

	Bond Length[a]		Bond Angle[b]		Dihedral Angle[c]		Frequencies[d]		
r21	1.5218	a312	113.14	d4123	118.85	104	902	1405
r31	1.8220	a412	110.76	d5123	240.70	143	963	1461
r41	1.0907	a512	110.71	d6213	57.82	261	1067	1480
r51	1.0919	a621	112.01	d7213	177.20	342	1072	3036
r62	1.0937	a721	107.27	d8213	292.70	422	1222	3097
r72	1.0989	a821	113.52	d9821	92.75	508	1282	3114
r82	1.4213	a982	108.29	d10982	271.05	648	1341	3166
r98	1.4513	a1098	101.17			845	1389	3720
r109	0.9735							
						277.36	690.73	904.71

CHCl₂CH₂OOH

r21	1.5317	a312	112.52	d4123	124.53	54	674	1307
r31	1.8100	a412	111.10	d5123	242.41	147	730	1384
r41	1.7989	a512	109.99	d6213	58.42	197	877	1402
r51	1.0897	a621	109.31	d7213	176.87	273	952	1455
r62	1.0948	a721	107.15	d8213	293.52	288	1043	3055
r72	1.0963	a821	115.21	d9821	89.98	319	1094	3116
r82	1.4112	a982	108.28	d10982	262.57	469	1252	3143
r98	1.4524	a1098	100.93			579	1281	3738
r109	0.9727							
						680.85	994.20	1427.15

CCl₃CH₂OOH

r21	1.5458	a312	111.38	d4123	121.03	66	398	1097
r31	1.8053	a412	110.10	d5123	240.54	150	509	1305
r41	1.7951	a512	107.39	d6213	60.68	171	565	1378
r51	1.8035	a621	109.06	d7213	179.55	222	695	1397
r62	1.0927	a721	106.92	d8213	296.25	256	791	1455
r72	1.0945	a821	113.89	d9821	93.22	293	889	3077
r82	1.4071	a982	108.56	d10982	258.09	300	1028	3145
r98	1.4522	a1098	100.79			329	1059	3740
r109	0.9726							
						1029.96	1670.23	1794.54

[a] Bond length in Å; [b] bond angle in degree. [c] Dihedral angle in degree. [d] Frequencies in cm⁻¹. [e] Moments of inertia in amu.Bohr².

Table A.6 Reaction Enthalpies[a] at 298K and Calculated $\Delta H_f^{\circ}{}_{298}$ of Radicals

Reaction Series	B3LYP /6-31G(d,p)		B3LYP /6-311+G(3df,2p)		QCISD(T) /6-31G(d,p)		CBSQ//B3LYP /6-31G(d,p)	
	$\Delta H^{\circ}{}_{rxn}$	$\Delta H_f^{\circ}{}_{298}$	$\Delta H^{\circ}{}_{rxn}$	$\Delta H_f^{\circ}{}_{298}$	$\Delta H^{\circ}{}_{rxn}$	$\Delta H_f^{\circ}{}_{298}$	$\Delta H^{\circ}{}_{rxn}$	$\Delta H_f^{\circ}{}_{298}$
$CH_2ClCH_2OO\bullet + CH_4 \rightarrow CH_3CH_2OO\bullet + CH_3Cl$	1.22	-9.73	0.80	-9.31	2.63	-11.14	2.74	-11.25
$CH_2ClCH_2OO\bullet + C_2H_6 \rightarrow CH_3CH_2OO\bullet + CH_3CH_2Cl$	-2.77	-10.63	-2.77	-10.63	-1.79	-11.61	-2.27	-11.13
Average value and deviation[b]:								**-11.19±1.20**
$CHCl_2CH_2OO\bullet + CH_4 \rightarrow CH_3OO\bullet + CH_3CHCl_2$	0.75	-11.80	0.11	-11.16	2.19	-13.24	2.61	-13.66
$CHCl_2CH_2OO\bullet + C_2H_6 \rightarrow CH_3CH_2OO\bullet + CH_3CHCl_2$	-4.65	-13.00	-5.29	-12.36	-3.29	-14.36	-3.50	-14.15
Average value and deviation[b]:								**-13.90±1.88**
$CCl_3CH_2OO\bullet + CH_4 \rightarrow CH_3OO\bullet + CH_3CCl_3$	-1.98	-11.99	-2.54	-11.43	-0.32	-13.65	0.65	-14.62
$CCl_3CH_2OO\bullet + C_2H_6 \rightarrow CH_3CH_2OO\bullet + CH_3CCl_3$	-7.38	-13.19	-7.94	-12.63	-5.80	-14.77	-5.46	-15.11
Average value and deviation[b]:								**-14.86±1.62**
$C\bullet HClCH_2OOH + CH_4 \rightarrow CH_3OOH + CH_3Cl$	2.32	2.92	1.88	3.36	3.05	2.19	3.10	2.14
$C\bullet HClCH_2OOH + C_2H_6 \rightarrow CH_3CH_2OOH + CH_3CH_2Cl$	-2.87	2.56	-2.69	2.38	-2.60	2.29	-2.51	2.20
Average value and deviation[b]:								**2.17±1.60**
$C\bullet Cl_2CH_2OOH + CH_4 \rightarrow CH_3OOH + CH_3CHCl_2$	2.49	-3.97	1.77	-3.25	3.50	-4.98	4.01	-5.49
$C\bullet Cl_2CH_2OOH + C_2H_6 \rightarrow CH_3CH_2OOH + CH_3CHCl_2$	-2.70	-4.33	-2.80	-4.23	-2.15	-4.88	-1.61	-5.42
Average value and deviation[b]:								**-5.46±1.67**

[a] Reaction enthalpies include thermal correction and zero-point energy. Units in kcal/mol. [b] Average value and deviation for pure enantiomer of the lowest energy at the CBSQ//B3 level. The $\Delta H_f^{\circ}{}_{298}$ values for $CH_{3-x}Cl_xC\bullet HOOH$ (x =1~3) are not presented because the species dissociate to the corresponding aldehyde + OH exothermically with little or no barrier to dissociation ($CH_{3-x}Cl_xC\bullet HOOH \rightarrow CH_{3-x}Cl_xCHO + OH$). These secondary bond energies are estimated about 90 kcal/mol, but we expect abstraction bond energies to be similar to those from abstraction or from resonantly stabilized radical sites.

Table A.7 TS Geometrical Parameters of Chlorinated Methanol Dissociation

Molecule	definition	value	Molecule	definition	value
TS1	r21	1.2727	TS2	r21	1.2837
	r31	1.0902		r31	1.0969
	r41	1.0829		r41	1.1650
	r54	2.4030		r54	1.7922
	r62	1.0328		r62	0.9763
	a312	116.24		a312	117.13
	a412	121.92		a412	118.25
	a541	90.76		a541	179.93
	a621	102.64		a621	114.35
	d4123	187.90		d4123	179.66
	d5412	300.78		d5412	286.23
	d6213	203.27		d6213	0.00
TS3	r21	1.9829	TS4	r21	1.2874
	r31	1.7308		r31	1.8557
	r41	1.0959		r41	1.0992
	r52	1.1372		r51	1.3937
	r62	0.9717		r65	0.9878
	a312	106.13		a312	119.56
	a412	98.26		a412	122.89
	a521	39.86		a512	108.35
	a621	102.01		a651	62.68
	d4123	249.33		d4123	136.93
	d5213	241.46		d5123	248.86
	d6213	143.70		d6512	354.26
TS5	r21	1.9829	TS6	r21	1.0908
	r31	1.7308		r31	1.0924
	r41	1.0959		r41	3.0468
	r52	1.1372		r51	1.3464
	r62	0.9717		r65	1.1332
	a312	106.13		a312	118.99
	a412	98.26		a412	105.09
	a521	39.86		a512	118.43
	a621	102.01		a651	67.77
	d4123	249.33		d4123	242.75
	d5213	241.46		d5123	202.31
	d6213	143.70		d6512	239.57
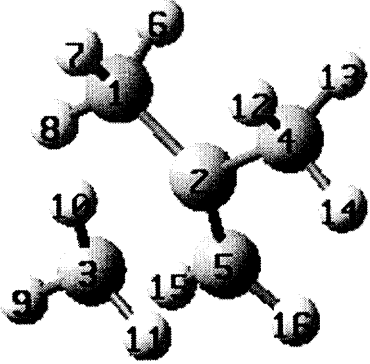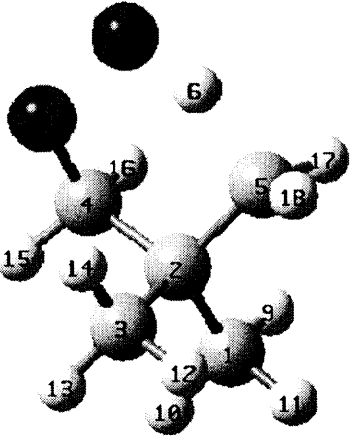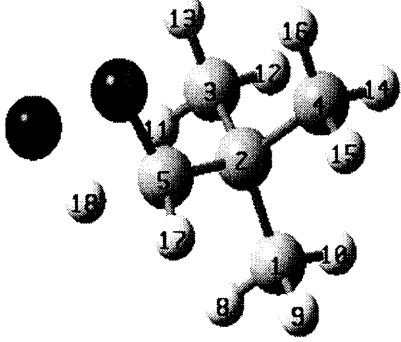
[a] Distance in angstrom, and angles in degree.

APPENDIX B
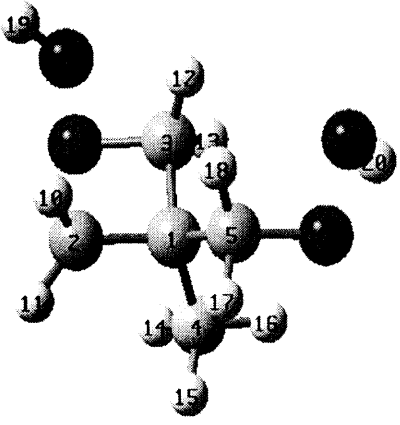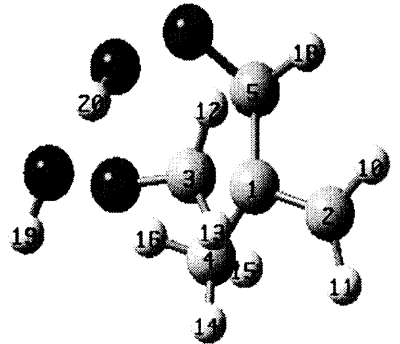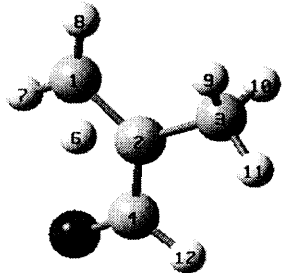
TABLES IN THE THERMOCHEMICAL AND KINETIC ANALYSIS OF REACTION OF NEOPENTYL RADICAL WITH MOLECULAR OXYGEN
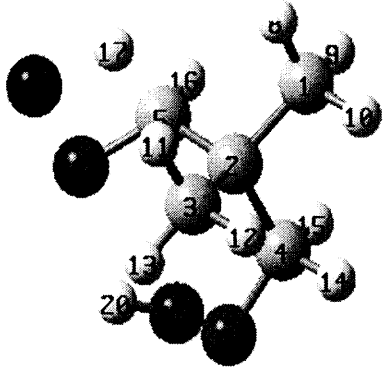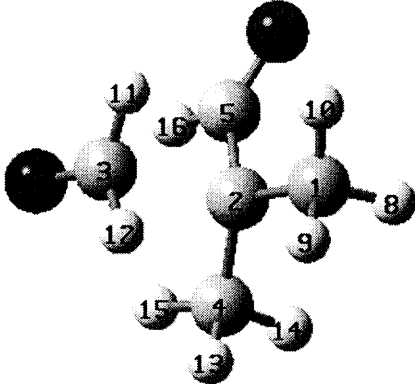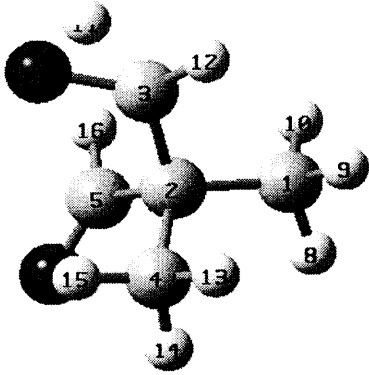
This appendix lists the geometrical parameters, harmonic vibrational frequencies,

thermodynamic analysis and detailed reaction mechanism for reactions of neopentyl

radical oxidation, as discussed in Chapter 4.
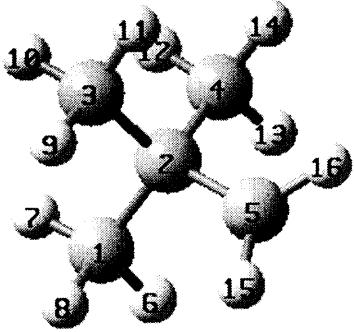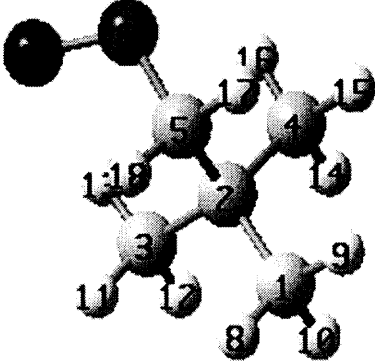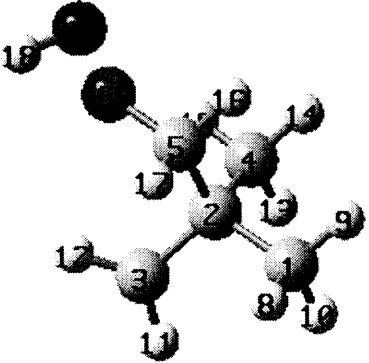
Table B.1 Geometrical Parameters for Species in Neopentyl Oxidation System
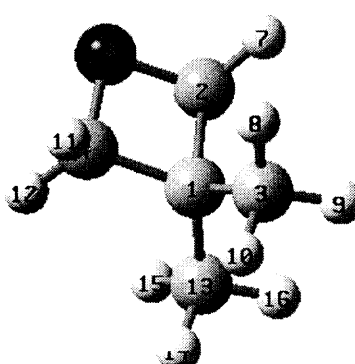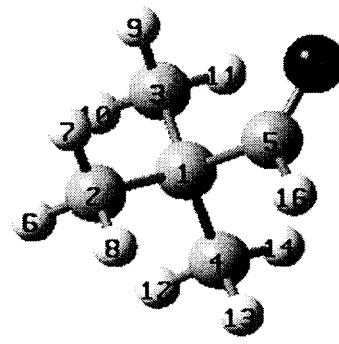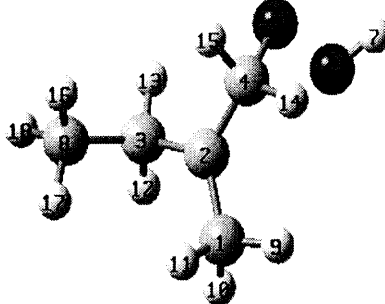
Species	Bond Length Å		Bond Angle degree		Dihedral Angle degree	
TS0	r21	1.5179	a321	96.48	d4213	259.66
	r32	2.3111	a421	115.25	d5213	105.66
	r42	1.5179	a521	119.67	d6123	166.03
	r52	1.3696	a612	109.77	d7123	47.04
	r61	1.0983	a712	112.10	d8123	285.34
	r71	1.0935	a812	111.57	d9321	61.72
	r81	1.0934	a932	101.96	d10321	301.78
	r93	1.0846	a1032	100.70	d11321	181.85
	r103	1.0857	a1132	101.96	d12421	53.28
	r113	1.0846	a1242	112.10	d13421	294.29
	r124	1.0935	a1342	109.77	d14421	174.98
	r134	1.0983	a1442	111.57	d15521	343.42
	r144	1.0934	a1552	121.40	d16521	169.43
	r155	1.0859	a1652	121.40		
	r165	1.0859				
TS1	r21	1.5456	a321	110.55	d4213	240.86
	r32	1.5393	a421	107.76	d5213	122.75
	r42	1.5617	a521	110.79	d6521	143.68
	r52	1.5174	a652	99.41	d7652	330.69
	r65	1.4168	a765	152.23	d8421	184.12
	r76	1.1457	a842	110.06	d9123	179.86
	r84	1.4196	a912	111.44	d10123	59.46
	r91	1.0950	a1012	110.77	d11123	299.94
	r101	1.0962	a1112	110.62	d12321	62.57
	r111	1.0941	a1232	110.70	d13321	302.84
	r123	1.0948	a1332	111.00	d14321	182.86
	r133	1.0955	a1432	110.76	d15421	68.03
	r143	1.0931	a1542	110.76	d16421	305.86
	r154	1.0954	a1642	110.91	d17521	37.12
	r164	1.0971	a1752	116.45	d18521	257.37
	r175	1.0912	a1852	117.29		
	r185	1.0899				
TS2	r21	1.5388	a321	110.68	d4213	238.56
	r32	1.5390	a421	110.02	d5213	121.42
	r42	1.5489	a521	108.55	d6521	186.14
	r52	1.5197	a652	117.01	d7652	115.68
	r65	1.3927	a765	89.20	d8123	301.67
	r76	1.5051	a812	111.29	d9123	180.95
	r81	1.0952	a912	111.55	d10123	61.35
	r91	1.0959	a1012	110.33	d11321	56.58
	r101	1.0945	a1132	111.20	d12321	296.73
	r113	1.0946	a1232	110.20	d13321	176.57
	r123	1.0946	a1332	110.75	d14421	61.91
	r133	1.0925	a1442	109.94	d15421	302.26
	r144	1.0955	a1542	111.48	d16421	181.55
	r154	1.0953	a1642	110.82	d17521	46.52
	r164	1.0938	a1752	117.60	d18765	358.67
	r175	1.0974	a1876	82.87		
	r187	1.2707				
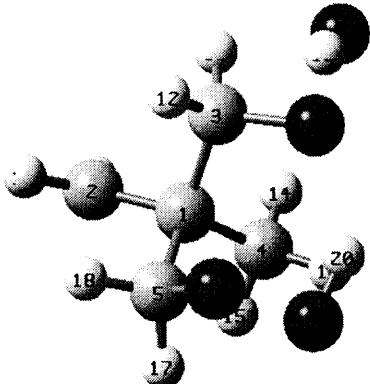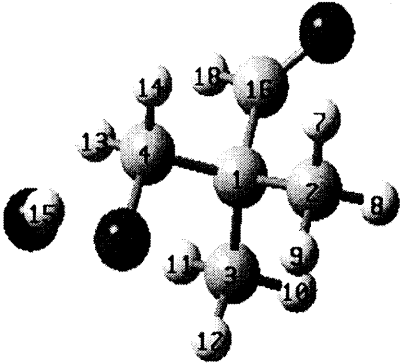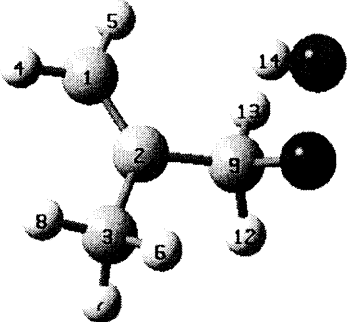
TS3	r21	1.5357	a321	113.46	d4213	234.07
	r32	1.5420	a421	111.28	d5213	108.54
	r42	1.5357	a521	113.29	d6321	139.95
	r52	1.5166	a632	98.17	d7123	184.00
	r63	1.4392	a712	110.94	d8123	64.37
	r71	1.0953	a812	110.68	d9123	304.39
	r81	1.0959	a912	111.34	d10321	23.39
	r91	1.0950	a1032	112.92	d11321	257.44
	r103	1.0988	a1132	115.03	d12421	297.86
	r113	1.0949	a1242	110.99	d13421	177.69
	r124	1.0955	a1342	110.42	d14421	57.84
	r134	1.0942	a1442	110.79	d15521	123.77
	r144	1.0950	a1552	121.17	d16521	323.85
	r155	1.0847	a1652	119.37	d17632	167.40
	r165	1.0859	a1763	101.80	d181763	129.87
	r176	1.6862	a18176	94.58		
	r1817	0.9708				

TS4	r21	1.5179	a321	120.57	d4213	253.29
	r32	1.3667	a421	97.67	d5213	154.19
	r42	2.3149	a521	113.36	d6521	174.08
	r52	1.5225	a652	115.55	d7652	81.96
	r65	1.4224	a765	107.71	d8123	274.01
	r76	1.4605	a812	110.30	d9123	154.32
	r81	1.0983	a912	112.33	d10123	33.15
	r91	1.0942	a1012	111.01	d11321	342.43
	r101	1.0929	a1132	120.60	d12321	168.62
	r113	1.0859	a1232	121.40	d13421	71.06
	r123	1.0830	a1342	102.41	d14421	310.51
	r134	1.0843	a1442	102.12	d15421	190.74
	r144	1.0863	a1542	98.77	d16521	56.51
	r154	1.0838	a1652	110.55	d17521	297.81
	r165	1.0962	a1752	109.76	d18765	120.13
	r175	1.0995	a1876	99.21		
	r187	0.9710				

TS5	r21	2.2725	a321	111.40	d4321	68.27
	r32	1.3662	a432	107.30	d5123	152.02
	r43	1.4741	a512	96.72	d6123	35.53
	r51	1.5201	a612	95.72	d7123	-86.35
	r61	1.5176	a712	102.54	d8215	38.89
	r71	1.3744	a821	99.52	d9215	-83.14
	r82	1.0877	a921	103.85	d10432	150.19
	r92	1.0898	a1043	98.11	d11512	72.00
	r104	0.9713	a1151	111.65	d12512	-49.90
	r115	1.0943	a1251	112.32	d13512	-168.81
	r125	1.0945	a1351	109.97	d14612	47.22
	r135	1.0979	a1461	112.08	d15612	-73.72
	r146	1.0943	a1561	111.20	d16612	166.42
	r156	1.0922	a1661	109.88	d17712	85.50
	r166	1.0980	a1771	121.29	d18712	-87.36
	r177	1.0847	a1871	121.26		
	r187	1.0864				

TS6

r21	1.5073	a321	114.18	d4321	300.16
r32	1.4377	a432	107.30	d5123	242.67
r43	1.4552	a512	114.11	d6123	105.98
r51	1.8266	a612	117.06	d7123	319.33
r61	1.5076	a712	116.48	d8213	235.54
r71	1.4809	a821	110.65	d9213	114.12
r82	1.0969	a921	112.39	d10432	94.94
r92	1.1009	a1043	100.01	d11512	112.40
r104	0.9740	a1151	137.73	d12512	348.20
r115	1.1087	a1251	98.69	d13512	235.20
r125	1.0946	a1351	97.67	d14612	48.93
r135	1.0954	a1461	111.71	d15612	289.29
r146	1.0957	a1561	110.48	d16612	169.70
r156	1.0994	a1661	111.45	d17712	155.28
r166	1.0963	a1771	120.03	d18712	352.09
r177	1.0840	a1871	120.10		
r187	1.0837				

TS7

r21	1.5472	a312	107.77	d4123	237.48
r31	1.5549	a412	109.80	d5123	118.27
r41	1.5228	a512	107.60	d6512	164.33
r51	1.5645	a651	111.32	d7651	290.11
r65	1.4262	a765	107.08	d8312	153.04
r76	1.4222	a831	116.16	d9831	66.86
r83	1.4153	a983	108.08	d10213	55.58
r98	1.4544	a1021	110.74	d11213	295.65
r102	1.0945	a1121	111.15	d12213	175.26
r112	1.0958	a1221	110.96	d13312	38.24
r122	1.0941	a1331	109.22	d14312	279.59
r133	1.0976	a1431	110.04	d15412	117.49
r143	1.0982	a1541	117.06	d16412	337.20
r154	1.0879	a1641	116.25	d17765	55.38
r164	1.0909	a1776	99.27	d18512	43.61
r177	1.1540	a1851	110.35	d19512	281.12
r185	1.0952	a1951	111.04	d20983	260.31
r195	1.0937	a2098	98.64		
r209	0.9780				

TS8

r21	1.5460	a312	108.90	d4123	235.61
r31	1.5414	a412	109.85	d5123	116.17
r41	1.5373	a512	108.38	d6512	186.85
r51	1.5539	a651	110.20	d7651	71.98
r65	1.4225	a765	106.75	d8312	268.69
r76	1.4172	a831	121.28	d9831	284.84
r83	1.3787	a983	108.68	d10213	63.12
r98	1.4725	a1021	110.46	d11213	302.91
r102	1.0943	a1121	111.68	d12213	182.61
r112	1.0951	a1221	110.65	d13765	306.06
r122	1.0959	a1376	99.93	d14312	35.33
r137	1.1912	a1431	113.49	d15412	62.08
r143	1.0951	a1541	110.96	d16412	303.56
r154	1.0939	a1641	109.46	d17412	183.32
r164	1.0956	a1741	111.45	d18512	70.44
r174	1.0902	a1851	110.50	d19512	308.51
r185	1.0952	a1951	111.35	d20983	137.04
r195	1.0973	a2098	99.21		
r209	0.9718				

TS9					
	r21	1.5158	a312	95.93	d4123	244.17
	r31	1.5420	a412	111.08	d5123	119.60
	r41	1.5342	a512	111.22	d6512	176.88
	r51	1.5397	a651	114.83	d7651	72.01
	r65	1.4214	a765	106.68	d8312	336.74
	r76	1.4609	a831	97.50	d9831	193.47
	r83	1.4420	a983	101.96	d10213	279.13
	r98	1.6859	a1021	119.45	d11213	119.93
	r102	1.0862	a1121	120.87	d12312	93.30
	r112	1.0845	a1231	113.09	d13312	219.71
	r123	1.0956	a1331	115.20	d14412	57.35
	r133	1.0939	a1441	110.09	d15412	297.31
	r144	1.0935	a1541	111.01	d16412	177.58
	r154	1.0956	a1641	110.81	d17512	61.81
	r164	1.0932	a1751	109.85	d18512	302.00
	r175	1.0973	a1851	110.91	d19983	234.81
	r185	1.0978	a1998	94.77	d20765	235.23
	r199	0.9710	a2076	99.86		
	r207	0.9709				

TS9

TS10					
r21	1.4102	a312	99.68	d4123	247.43
r31	1.9213	a412	115.48	d5123	110.30
r41	1.5278	a512	114.43	d6512	225.90
r51	1.5488	a651	117.89	d7651	291.13
r65	1.4132	a765	108.68	d8312	203.18
r76	1.4537	a831	102.59	d9831	181.60
r83	1.3137	a983	107.52	d10213	278.54
r98	1.7859	a1021	121.48	d11213	90.15
r102	1.0865	a1121	121.04	d12312	82.45
r112	1.0861	a1231	99.13	d13312	324.55
r123	1.0931	a1331	104.62	d14412	48.42
r133	1.0959	a1441	111.25	d15412	289.32
r144	1.0935	a1541	108.97	d16412	170.10
r154	1.0958	a1641	111.20	d17512	100.66
r164	1.0884	a1751	107.93	d18512	342.69
r175	1.0984	a1851	109.67	d19983	239.83
r185	1.0961	a1998	91.81	d20765	97.03
r199	0.9730	a2076	98.44		
r207	0.9826				

TS10

TS13					
r21	1.4772	a321	119.94	d4213	195.76
r32	1.5100	a421	118.20	d5421	353.33
r42	1.4657	a542	124.10	d6213	101.81
r54	1.2281	a621	60.81	d7123	166.69
r62	1.2353	a712	118.38	d8123	349.92
r71	1.0817	a812	120.10	d9321	45.08
r81	1.0817	a932	111.76	d10321	285.71
r93	1.0946	a1032	110.55	d11321	165.73
r103	1.0969	a1132	111.12	d12421	175.28
r113	1.0940	a1242	114.43		
r124	1.1105				

TS13
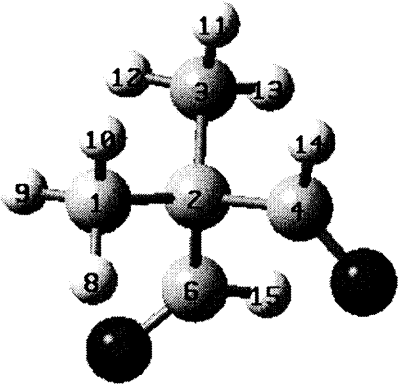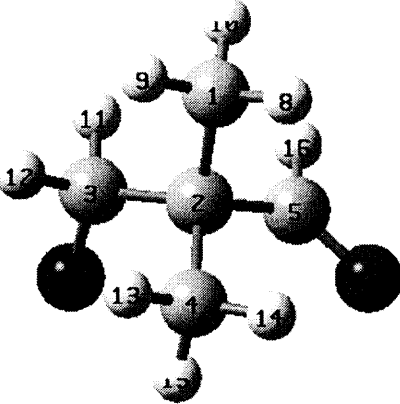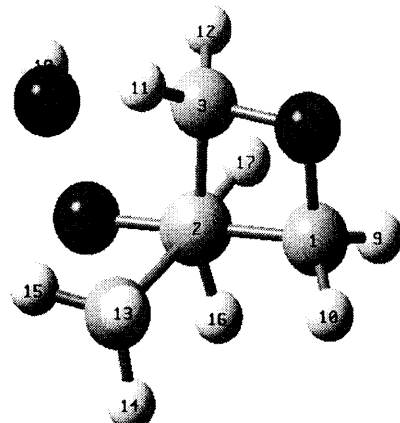
TS8A

r21	1.5419	a321	111.08	d4213	240.37
r32	1.5374	a421	107.01	d5213	121.93
r42	1.5599	a521	107.89	d6521	194.18
r52	1.5188	a652	118.31	d7652	110.91
r65	1.3954	a765	89.73	d8123	302.23
r76	1.5022	a812	110.88	d9123	181.70
r81	1.0942	a912	111.77	d10123	61.67
r91	1.0959	a1012	110.56	d11321	62.34
r101	1.0945	a1132	110.99	d12321	302.36
r113	1.0935	a1232	110.13	d13321	182.50
r123	1.0947	a1332	110.77	d14421	60.06
r133	1.0910	a1442	108.02	d15421	301.08
r144	1.0976	a1542	111.10	d16521	52.74
r154	1.0966	a1652	117.82	d17765	0.84
r165	1.0957	a1776	82.42	d18421	175.41
r177	1.2733	a1842	115.42	d191842	81.87
r184	1.4165	a19184	107.50	d201918	253.94
r1918	1.4541	a201918	100.61	4	
r2019	0.9745				

TS11

r21	1.5059	a321	104.45	d4213	246.22
r32	2.0070	a421	117.39	d5213	104.37
r42	1.5088	a521	115.54	d6521	353.69
r52	1.4930	a652	123.37	d7321	181.25
r65	1.2162	a732	105.87	d8123	178.70
r73	1.2606	a812	109.34	d9123	60.09
r81	1.0981	a912	111.51	d10123	296.77
r91	1.0936	a1012	111.38	d11321	56.96
r101	1.0918	a1132	96.64	d12321	302.81
r113	1.1058	a1232	91.63	d13421	52.11
r123	1.1079	a1342	111.17	d14421	293.53
r134	1.0941	a1442	109.83	d15421	173.10
r144	1.0983	a1542	111.41	d16521	174.89
r154	1.0922	a1652	114.87		
r165	1.1083				

TS12

r21	1.5463	a321	109.53	d4213	238.56
r32	1.5130	a421	111.56	d5213	117.78
r42	1.5403	a521	107.15	d6521	106.85
r52	1.5320	a652	124.98	d7321	166.57
r65	1.2077	a732	118.46	d8123	176.46
r73	1.3914	a812	110.58	d9123	57.05
r81	1.0935	a912	110.17	d10123	297.19
r91	1.0949	a1012	111.68	d11732	248.19
r101	1.0953	a1173	58.25	d12321	315.54
r117	1.2054	a1232	117.55	d13421	55.79
r123	1.0971	a1342	110.61	d14421	295.31
r134	1.0942	a1442	110.13	d15421	176.19
r144	1.0927	a1542	110.34	d16521	289.51
r154	1.0928	a1652	114.04		
r165	1.1155				

C₃CC•

r21	1.5430	a321	108.96	d4213	240.74
r32	1.5531	a421	109.73	d5213	119.75
r42	1.5428	a521	109.89	d6123	178.76
r52	1.5021	a612	111.02	d7123	58.55
r61	1.0948	a712	110.94	d8123	298.72
r71	1.0958	a812	111.02	d9321	60.10
r81	1.0957	a932	111.06	d10321	300.15
r93	1.0948	a1032	110.65	d11321	180.19
r103	1.0972	a1132	111.04	d12421	60.57
r113	1.0948	a1242	110.95	d13421	300.38
r124	1.0957	a1342	111.02	d14421	180.41
r134	1.0948	a1442	111.01	d15521	323.85
r144	1.0957	a1552	120.62	d16521	155.91
r155	1.0861	a1652	120.68		
r165	1.0860				

C₃CCOO•

r21	1.5416	a321	109.78	d4213	238.76
r32	1.5392	a421	109.85	d5213	119.75
r42	1.5402	a521	106.75	d6521	176.81
r52	1.5391	a652	112.29	d7652	94.53
r65	1.4584	a765	111.90	d8123	300.69
r76	1.3249	a812	111.55	d9123	179.74
r81	1.0957	a912	111.57	d10123	60.19
r91	1.0958	a1012	110.18	d11321	58.64
r101	1.0947	a1132	111.36	d12321	298.92
r113	1.0950	a1232	110.09	d13321	179.02
r123	1.0953	a1332	111.53	d14421	61.66
r133	1.0931	a1442	110.44	d15421	302.02
r144	1.0949	a1542	111.28	d16421	181.58
r154	1.0960	a1642	111.18	d17521	60.79
r164	1.0936	a1752	110.82	d18521	297.20
r175	1.0952	a1852	112.13		
r185	1.0926				

C₃•CCOOH

r21	1.5435	a321	110.08	d4213	239.04
r32	1.5021	a421	109.25	d5213	120.22
r42	1.5529	a521	107.58	d6521	179.49
r52	1.5428	a652	108.01	d7652	182.72
r65	1.4253	a765	106.74	d8123	299.93
r76	1.4541	a812	111.37	d9123	178.95
r81	1.0948	a912	111.22	d10123	59.51
r91	1.0954	a1012	110.18	d11321	320.31
r101	1.0949	a1132	119.92	d12321	153.26
r113	1.0857	a1232	120.62	d13421	61.18
r123	1.0840	a1342	110.38	d14421	301.63
r134	1.0944	a1442	110.51	d15421	181.62
r144	1.0969	a1542	111.03	d16521	59.73
r154	1.0918	a1652	110.43	d17521	299.66
r165	1.0979	a1752	110.34	d18765	250.68
r175	1.0994	a1876	100.10		
r187	0.9716				

C₂CYCCOC					
r21	1.4949	a321	120.2497	d4213	172.16
r32	1.5008	a421	120.6432	d5421	132.90
r42	1.4937	a542	114.0835	d6542	294.23
r54	1.4375	a654	106.8393	d7654	242.96
r65	1.4606	a765	99.2584	d8321	75.78
r76	0.9711	a832	113.7766	d9123	164.31
r83	1.5460	a912	111.7634	d10123	43.56
r91	1.0950	a1012	111.2371	d11123	284.69
r101	1.0981	a1112	112.7498	d12321	314.29
r111	1.1036	a1232	109.4687	d13321	198.06
r123	1.0990	a1332	109.0740	d14421	7.85
r133	1.0957	a1442	111.5704	d15421	246.47
r144	1.0982	a1542	112.1332	d16832	59.98
r154	1.1037	a1683	111.2240	d17832	299.78
r168	1.0953	a1783	111.4030	d18832	179.78
r178	1.0949	a1883	110.8063		
r188	1.0951				

C₃CCHO					
r21	1.5450	a312	111.14	d4123	236.83
r31	1.5325	a412	109.46	d5123	120.81
r41	1.5450	a512	107.22	d6213	63.55
r51	1.5249	a621	110.02	d7213	303.85
r62	1.0950	a721	111.31	d8213	183.01
r72	1.0947	a821	111.56	d9312	59.21
r82	1.0958	a931	111.01	d10312	298.90
r93	1.0934	a1031	110.45	d11312	178.60
r103	1.0949	a1131	111.00	d12412	59.59
r113	1.0934	a1241	110.02	d13412	300.14
r124	1.0950	a1341	111.56	d14412	179.30
r134	1.0958	a1441	111.31	d15512	238.76
r144	1.0947	a1551	125.64	d16512	58.75
r155	1.2106	a1651	113.83		
r165	1.1167				

CCC•(C)COOH					
r21	1.4949	a321	120.24	d4213	172.16
r32	1.5008	a421	120.64	d5421	132.90
r42	1.4937	a542	114.08	d6542	294.23
r54	1.4375	a654	106.83	d7654	242.96
r65	1.4606	a765	99.25	d8321	75.78
r76	0.9711	a832	113.77	d9123	164.31
r83	1.5460	a912	111.76	d10123	43.56
r91	1.0950	a1012	111.23	d11123	284.69
r101	1.0981	a1112	112.74	d12321	314.29
r111	1.1036	a1232	109.46	d13321	198.06
r123	1.0990	a1332	109.07	d14421	7.85
r133	1.0957	a1442	111.57	d15421	246.47
r144	1.0982	a1542	112.13	d16832	59.98
r154	1.1037	a1683	111.22	d17832	299.78
r168	1.0953	a1783	111.40	d18832	179.78
r178	1.0949	a1883	110.80		
r188	1.0951				

C2•C(COOH)₂

r21	1.5028	a312	106.94	d4123	240.02
r31	1.5542	a412	109.30	d5123	118.27
r41	1.5444	a512	107.57	d6512	210.58
r51	1.5629	a651	116.49	d7651	289.46
r65	1.4197	a765	108.72	d8312	192.79
r76	1.4539	a831	109.20	d9831	183.69
r83	1.4356	a983	107.47	d10213	288.47
r98	1.4491	a1021	120.83	d11213	100.05
r102	1.0861	a1121	120.70	d12312	72.50
r112	1.0848	a1231	110.19	d13312	312.02
r123	1.0972	a1331	110.41	d14412	61.96
r133	1.0954	a1441	110.66	d15412	302.86
r144	1.0955	a1541	109.61	d16412	183.14
r154	1.0945	a1641	111.83	d17512	84.20
r164	1.0893	a1751	109.87	d18512	325.30
r175	1.0968	a1851	109.44	d19983	95.10
r185	1.0970	a1998	100.72	d20765	94.89
r199	0.9736	a2076	98.78		
r207	0.9779				

C₂C(COOH)CHO

r21	1.5332	a312	111.65	d4123	123.43
r31	1.5475	a412	111.43	d5412	295.59
r41	1.5449	a541	107.36	d6541	185.22
r54	1.4233	a654	106.55	d7213	177.79
r65	1.4539	a721	110.91	d8213	58.79
r72	1.0936	a821	110.55	d9213	298.32
r82	1.0929	a921	110.44	d10312	303.79
r92	1.0925	a1031	110.56	d11312	183.46
r103	1.0942	a1131	111.39	d12312	63.92
r113	1.0957	a1231	110.16	d13412	176.06
r123	1.0916	a1341	110.85	d14412	55.75
r134	1.0983	a1441	110.55	d15654	249.11
r144	1.0997	a1565	100.09	d16123	241.11
r156	0.9717	a1612	110.59	d171612	0.87
r161	1.5285	a17161	125.14	d181612	179.79
r1716	1.2096	a18161	114.19		
r1816	1.1154				

C=C(C)COOH

r21	1.3369	a321	122.37	d4213	178.33
r32	1.5075	a421	119.80	d5421	108.14
r42	1.5132	a542	114.93	d6542	80.05
r54	1.4326	a654	107.19	d7123	0 .43
r65	1.4619	a712	121.74	d8123	180.55
r71	1.0866	a812	121.73	d9321	1.19
r81	1.0865	a932	111.38	d10321	239.77
r93	1.0932	a1032	111.33	d11321	122.04
r103	1.0943	a1132	110.86	d12421	352.70
r113	1.0970	a1242	110.29	d13421	232.20
r124	1.0951	a1342	111.55	d14654	230.96
r134	1.0980	a1465	99.35		
r146	0.9705				

C₂C(OOH)COO•						
	r21	1.5438	a312	106.88	d4123	240.33
	r31	1.5476	a412	110.22	d5123	120.74
	r41	1.5392	a512	106.16	d6512	169.97
	r51	1.5360	a651	110.92	d7651	207.75
	r65	1.4675	a765	111.90	d8312	182.04
	r76	1.3228	a831	115.96	d9831	273.54
	r83	1.4214	a983	107.83	d10213	56.58
	r98	1.4543	a1021	110.43	d11213	296.62
	r102	1.0947	a1121	111.85	d12213	175.88
	r112	1.0958	a1221	111.00	d13312	56.76
	r122	1.0945	a1331	111.05	d14312	297.99
	r133	1.0967	a1431	108.33	d15412	55.21
	r143	1.0975	a1541	110.21	d16412	295.62
	r154	1.0949	a1641	111.15	d17412	174.93
	r164	1.0951	a1741	111.06	d18512	52.59
	r174	1.0919	a1851	111.52	d19512	289.25
	r185	1.0922	a1951	112.02	d20983	102.40
	r195	1.0947	a2098	100.304		
	r209	0.9743				

C₂C(CH₂O•)CCOO•						
	r21	1.5401	a321	110.90	d4213	238.94
	r32	1.5365	a421	107.13	d5421	178.79
	r42	1.5351	a542	110.45	d6542	140.06
	r54	1.4586	a654	111.84	d7213	120.82
	r65	1.3235	a721	108.33	d8721	189.33
	r72	1.5535	a872	116.51	d9123	302.95
	r87	1.3644	a912	110.49	d10123	182.81
	r91	1.0949	a1012	111.78	d11123	62.28
	r101	1.0961	a1112	111.15	d12321	57.74
	r111	1.0947	a1232	110.49	d13321	298.27
	r123	1.0954	a1332	110.90	d14321	177.50
	r133	1.0952	a1432	110.76	d15421	60.80
	r143	1.0914	a1542	110.71	d16421	297.97
	r154	1.0966	a1642	112.60	d17721	59.84
	r164	1.0928	a1772	111.17	d18721	305.62
	r177	1.1077	a1872	107.98		
	r187	1.1129				

C₂C•CHO						
	r21	1.4926	a321	119.88	d4213	180.03
	r32	1.4918	a421	120.39	d5421	179.95
	r42	1.4349	a542	124.17	d6123	301.31
	r54	1.2391	a612	111.07	d7123	180.17
	r61	1.0989	a712	112.03	d8123	59.06
	r71	1.0940	a812	111.07	d9321	58.80
	r81	1.0990	a932	110.93	d10321	300.99
	r93	1.0986	a1032	110.92	d11321	179.91
	r103	1.0987	a1132	110.31	d12421	359.97
	r113	1.0910	a1242	115.56		
	r124	1.1096				

C₂C(CHO)₂					

r21	1.5378	a321	111.14	d4213	118.64
r32	1.5486	a421	108.84	d5421	117.00
r42	1.5270	a542	125.11	d6213	238.88
r54	1.2101	a621	111.48	d7621	6.78
r62	1.5280	a762	124.13	d8123	178.72
r76	1.2094	a812	111.11	d9123	59.66
r81	1.0927	a912	109.89	d10123	299.79
r91	1.0926	a1012	110.78	d11321	64.11
r101	1.0947	a1132	110.46	d12321	304.83
r113	1.0951	a1232	110.24	d13321	184.30
r123	1.0939	a1332	111.68	d14421	297.38
r133	1.0950	a1442	113.79	d15621	185.04
r144	1.1151	a1562	114.57		
r156	1.1101				

C₂C(CHO)CH₂O•					

r21	1.5448	a321	108.72	d4213	237.87
r32	1.5464	a421	111.77	d5213	116.44
r42	1.5317	a521	107.16	d6521	111.23
r52	1.5269	a652	125.24	d7321	176.43
r65	1.2087	a732	115.65	d8123	177.08
r73	1.3673	a812	110.81	d9123	57.64
r81	1.0936	a912	110.27	d10123	297.67
r91	1.0955	a1012	111.90	d11321	56.30
r101	1.0963	a1132	110.77	d12321	302.22
r113	1.1121	a1232	110.64	d13421	56.39
r123	1.1084	a1342	110.63	d14421	295.79
r134	1.0952	a1442	110.73	d15421	176.50
r144	1.0922	a1542	110.27	d16521	293.07
r154	1.0931	a1652	114.12		
r165	1.1167				

C(COOH)CYCCOC					

r21	1.5515	a321	83.61	d4123	5.96
r32	1.5512	a412	92.25	d5213	245.93
r41	1.4418	a521	114.43	d6213	116.06
r52	1.5274	a621	113.34	d7621	180.08
r62	1.5284	a762	114.73	d8762	64.85
r76	1.4239	a876	107.15	d9123	250.43
r87	1.4587	a912	115.05	d10123	122.28
r91	1.1007	a1012	115.72	d11321	238.10
r101	1.0975	a1132	115.82	d12321	109.54
r113	1.0964	a1232	114.85	d13521	48.12
r123	1.0960	a1352	110.54	d14521	288.28
r135	1.0943	a1452	111.03	d15521	168.50
r145	1.0963	a1552	110.73	d16621	65.45
r155	1.0930	a1662	109.93	d17621	305.71
r166	1.0985	a1762	110.91	d18876	112.18
r176	1.0996	a1887	99.89		
r188	0.9713				
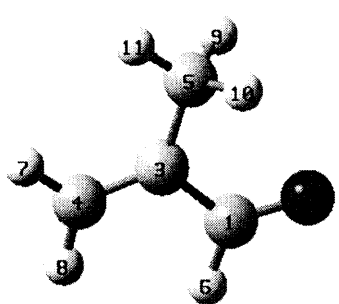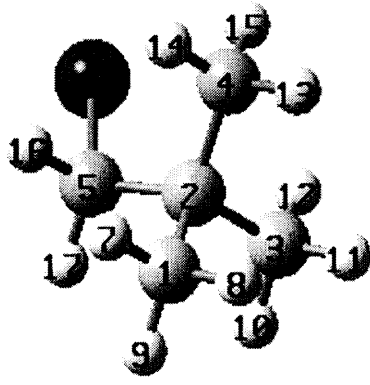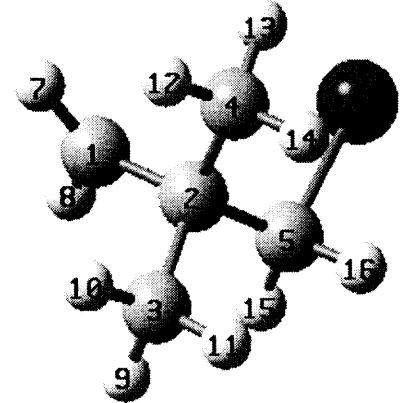
C=C(C)C=O	r21	1.2159	a312	123.98	d4312	179.98
	r31	1.4830	a431	117.73	d5312	0.00
	r43	1.3410	a531	117.07	d6123	179.97
	r53	1.5025	a612	121.14	d7431	179.99
	r61	1.1127	a743	122.26	d8431	0.00
	r74	1.0856	a843	120.97	d9531	58.69
	r84	1.0873	a953	110.46	d10531	301.40
	r95	1.0949	a1053	110.46	d11531	180.04
	r105	1.0949	a1153	111.55		
	r115	1.0923				
C₃CCl	r21	1.5493	a321	109.13	d4213	239.34
	r32	1.5380	a421	109.13	d5213	119.67
	r42	1.5380	a521	105.04	d6521	179.99
	r52	1.5357	a652	116.62	d7123	179.85
	r65	2.2149	a712	111.52	d8123	60.33
	r71	1.0965	a812	110.02	d9123	300.81
	r81	1.0961	a912	111.52	d10321	59.91
	r91	1.0965	a1032	111.28	d11321	300.26
	r103	1.0968	a1132	110.33	d12321	180.37
	r113	1.0961	a1232	111.34	d13421	59.73
	r123	1.0946	a1342	110.33	d14421	300.08
	r134	1.0961	a1442	111.28	d15421	179.62
	r144	1.0968	a1542	111.34	d16521	61.57
	r154	1.0946	a1652	111.84	d17521	298.41
	r165	1.0905	a1752	111.84		
	r175	1.0905				
C₃•CCl	r21	1.4997	a321	109.17	d4213	240.26
	r32	1.5614	a421	110.91	d5213	115.49
	r42	1.5310	a521	111.09	d6521	59.51
	r52	1.5377	a652	115.07	d7123	92.93
	r65	2.2111	a712	120.66	d8123	283.02
	r71	1.0851	a812	120.65	d9321	58.41
	r81	1.0860	a932	111.39	d10321	298.80
	r93	1.0955	a1032	109.94	d11321	179.31
	r103	1.0951	a1132	111.10	d12421	59.38
	r113	1.0976	a1242	110.21	d13421	299.47
	r124	1.0959	a1342	111.27	d14421	178.85
	r134	1.0938	a1442	111.02	d15521	302.03
	r144	1.0965	a1552	111.76	d16521	178.52
	r155	1.0902	a1652	112.16		
	r165	1.0905				

Table B.2 Harmonic Vibrational Frequencies (cm^{-1}) for Species in Neopentyl Oxidation System

species	Frequencies (Based on B3LYP/6-31g(d,p) level)												moments of inertia (amu-Bohr^2)
TS0	-485.11	109.39	173.30	213.56	238.50	241.63	372.01	391.89	422.67	522.03	548.94	618.97	405.41437
	790.30	814.37	883.98	957.75	977.08	1032.67	1069.87	1084.50	1292.63	1412.44	1421.86	1436.61	473.88436
	1439.96	1441.34	1493.65	1503.47	1507.11	1516.82	1584.74	3028.19	3032.51	3096.71	3098.59	3104.49	493.60732
	3130.11	3131.69	3151.30	3238.99	3259.89	3267.22							
TS1	-1563.34	111.25	230.78	248.18	275.55	306.21	324.00	391.09	430.54	455.26	485.42	547.60	456.05610
	646.99	761.84	886.89	914.94	943.33	947.19	971.96	1003.59	1030.97	1050.94	1073.62	1136.63	932.84675
	1210.05	1233.48	1251.31	1316.99	1364.74	1409.17	1428.12	1468.35	1481.05	1500.93	1507.06	1516.80	974.62749
	1523.98	1587.85	3034.62	3038.85	3045.85	3100.45	3104.70	3107.93	3113.45	3121.07	3134.33	3191.56	
TS2	-1817.17	79.73	114.33	213.42	233.82	259.55	279.25	304.19	342.54	385.83	410.37	532.89	459.49822
	650.11	767.32	810.05	887.92	931.92	940.89	950.78	971.58	1044.12	1056.86	1096.11	1141.45	1016.60904
	1227.51	1244.42	1285.79	1364.73	1406.32	1415.00	1444.81	1491.92	1501.54	1502.73	1516.25	1518.20	1062.51318
	1534.79	1960.47	3037.63	3040.59	3050.80	3062.27	3107.15	3111.24	3116.13	3120.64	3127.25	3142.12	
TS3	-777.50	72.42	137.26	154.53	212.94	245.90	285.63	314.09	327.81	398.35	413.75	427.44	395.25070
	543.50	570.59	781.29	826.49	913.17	930.38	959.69	971.06	1002.89	1013.59	1061.76	1100.58	1168.44288
	1187.72	1232.61	1248.88	1292.16	1350.40	1411.16	1427.48	1482.10	1501.50	1502.59	1515.46	1524.90	1190.10550
	1535.88	3018.99	3035.95	3042.21	3089.61	3107.06	3112.57	3114.11	3124.12	3153.81	3260.50	3788.59	
TS4	-485.40	59.24	130.89	138.40	181.94	196.74	207.24	225.53	271.69	353.03	377.09	436.66	513.80545
	519.29	545.51	574.19	621.92	809.44	830.90	869.74	885.72	948.70	996.88	1022.22	1062.12	1092.63266
	1076.28	1258.73	1296.11	1371.59	1400.45	1418.75	1435.46	1438.35	1445.89	1468.16	1501.91	1509.02	1189.71393
	1585.52	3015.30	3029.77	3078.18	3094.81	3103.85	3131.89	3162.93	3257.13	3266.58	3277.01	3756.28	
TS5	-472.74	35.20	93.45	144.98	157.03	191.94	204.85	225.44	260.02	371.19	383.06	418.08	485.44325
	452.48	566.35	599.73	779.42	796.02	812.00	941.52	957.47	975.99	1028.98	1066.77	1080.49	1135.07083
	1105.60	1207.09	1291.86	1392.94	1406.40	1418.21	1434.80	1452.32	1493.35	1500.73	1506.34	1514.48	1195.91466
	1569.99	3028.78	3033.05	3089.20	3091.13	3095.79	3119.32	3141.09	3153.01	3222.49	3245.10	3769.81	
TS6	-1255.04	55.30	93.68	130.94	190.39	251.39	265.35	323.18	357.34	376.24	397.07	497.80	459.09757
	596.42	628.35	688.87	802.97	871.59	946.08	954.44	960.50	975.78	1004.47	1045.25	1103.16	990.40575
	1244.11	1297.35	1325.08	1344.18	1373.17	1390.92	1420.03	1432.24	1464.45	1477.60	1500.55	1506.44	1100.35951
	1525.62	2841.82	2999.05	3006.97	3016.55	3065.99	3071.29	3099.60	3111.18	3161.48	3269.88	3698.43	
TS7	-1551.14	95.37	130.16	183.23	224.66	253.16	275.01	324.25	332.24	377.62	421.64	454.85	
	475.21	517.81	568.05	589.11	652.96	786.32	874.72	902.24	914.99	934.85	975.76	986.32	1044.60978
	1019.34	1032.64	1041.85	1086.02	1117.89	1160.56	1203.34	1240.88	1305.58	1326.28	1363.79	1400.05	1059.79955
	1420.51	1423.62	1463.86	1472.47	1488.86	1509.58	1513.28	1585.64	3024.97	3040.61	3058.57	3078.45	1562.24197

	3108.61	3113.72	3122.45	3130.66	3210.84	3644.90							
TS8	-1748.50	48.38	117.80	147.43	193.39	237.83	254.05	269.54	292.72	307.38	354.74	392.38	1004.94017
	424.29	484.95	499.46	569.22	652.96	759.50	821.56	881.40	912.91	944.64	959.06	991.62	1228.75072
	1015.70	1044.07	1073.38	1129.31	1185.73	1206.00	1225.37	1241.57	1313.77	1344.73	1373.21	1406.01	1663.99975
	1409.52	1435.59	1481.45	1499.82	1507.67	1517.52	1523.74	1588.51	3034.37	3039.28	3050.93	3094.13	
	3104.78	3109.46	3114.51	3121.02	3163.98	3763.87							
TS8A	-1809.25	72.40	88.29	126.19	178.66	202.14	226.93	237.18	251.67	286.88	353.41	376.77	1013.97087
	448.62	468.08	505.03	568.06	670.62	777.89	818.96	874.91	880.19	920.23	932.99	958.35	1210.00782
	1019.57	1034.47	1078.42	1093.08	1131.83	1194.58	1217.85	1247.68	1330.05	1353.19	1388.65	1398.21	1763.49835
	1415.49	1440.25	1467.90	1499.86	1502.66	1515.61	1523.61	1965.30	3033.33	3042.87	3058.30	3084.54	
TS9	-789.74	63.17	80.62	114.11	147.06	167.16	177.18	219.36	255.92	261.54	307.53	336.13	741.51363
	398.94	405.47	429.16	506.10	556.07	646.09	786.16	825.03	874.68	918.24	947.70	970.43	1833.89706
	983.74	1007.06	1025.41	1048.65	1090.89	1185.22	1211.08	1219.55	1265.28	1323.67	1343.16	1377.77	2152.48895
	1391.18	1420.99	1470.71	1480.30	1509.49	1515.93	1532.04	3029.49	3047.38	3050.76	3085.67	3107.02	
	3119.65	3137.36	3151.91	3259.39	3767.88	3787.02							
TS10	-811.72	59.77	107.71	153.55	165.73	195.97	203.80	231.17	236.12	267.74	297.08	316.87	1007.25816
	348.68	374.01	421.46	454.20	497.48	588.02	670.16	794.36	818.74	882.12	897.71	921.95	1421.41271
	939.94	978.28	1028.05	1056.96	1079.89	1159.11	1243.85	1262.20	1299.96	1317.79	1368.10	1395.36	1882.73360
	1424.75	1467.92	1485.43	1494.98	1508.92	1525.75	1540.38	3027.42	3035.55	3052.97	3090.25	3119.38	
TS11	-458.08	88.68	121.41	187.43	193.87	208.47	246.84	273.70	324.72	362.20	394.14	590.42	604.02445
	701.56	792.00	944.48	958.55	1001.96	1010.38	1015.29	1161.01	1237.65	1247.88	1296.94	1403.34	825.86966
	1416.44	1419.42	1428.59	1483.54	1484.13	1502.63	1507.91	1587.04	1771.40	2903.01	2955.75	2973.18	1006.13421
	3031.11	3037.82	3102.38	3105.21	3146.95	3151.86							
TS12	-2011.60	77.82	101.94	186.85	216.25	237.35	280.85	306.46	338.43	352.84	529.63	602.86	601.40317
	664.88	769.87	898.96	925.01	935.05	958.34	1012.47	1043.27	1158.91	1185.70	1230.04	1262.04	778.59064
	1360.15	1403.75	1414.60	1433.22	1494.58	1498.64	1513.72	1521.57	1839.64	2405.48	2869.82	3043.63	967.95605
	3055.81	3060.83	3113.95	3129.98	3134.19	3145.64							
TS13	-1664.57	174.00	214.21	267.36	352.07	432.48	496.38	594.33	687.99	835.91	927.05	967.60	207.48677
	1005.98	1056.81	1204.43	1269.70	1347.26	1415.77	1430.76	1443.37	1499.34	1514.39	1717.65	2247.23	457.88187
	2918.51	3035.37	3096.48	3122.04	3189.35	3315.69							643.63383
C3CC•	115.27	224.69	275.72	282.03	306.80	331.20	385.44	415.90	416.67	532.97	739.42	910.54	389.84934
	918.13	953.85	954.35	963.71	1036.18	1081.16	1207.65	1272.56	1286.08	1406.12	1410.20	1432.22	396.61134
	1476.84	1493.52	1498.59	1500.41	1517.07	1517.52	1532.50	3027.13	3031.88	3038.09	3097.82	3102.16	405.66953
	3106.62	3109.30	3114.16	3115.49	3143.88	3248.11							

Species													
$C_3CCOO\bullet$	70.91	107.25	222.21	232.58	270.51	274.06	307.78	337.78	391.14	409.08	477.41	560.35	447.25729
	742.15	889.42	920.54	939.39	948.84	965.86	970.39	1051.66	1088.86	1171.57	1239.04	1254.13	1034.49632
	1283.93	1324.86	1372.41	1414.61	1417.37	1446.68	1478.93	1495.13	1498.94	1502.93	1521.34	1521.86	1065.83164
	1533.04	3036.04	3040.27	3046.81	3063.96	3105.19	3108.59	3111.11	3116.43	3126.94	3132.07	3136.01	
$C_3\bullet CCOOH$	88.36	128.89	148.56	179.49	206.90	229.31	265.36	317.43	328.40	335.60	411.46	431.65	409.19180
	505.53	552.07	773.85	910.10	927.75	941.59	955.41	961.82	1010.72	1068.21	1080.34	1181.47	1191.78130
	1233.37	1263.49	1301.41	1366.93	1394.01	1406.78	1426.11	1470.20	1498.23	1499.33	1514.74	1522.24	1209.33621
	1534.09	3007.75	3035.17	3039.97	3058.13	3106.04	3112.26	3115.26	3144.49	3155.94	3266.07	3747.58	
$C_2CYCCOC$	45.31	224.94	264.57	313.76	342.36	390.66	407.16	639.18	850.61	887.82	929.68	944.97	349.91537
	965.68	977.10	1026.82	1043.39	1067.36	1161.64	1164.42	1227.82	1270.45	1300.44	1313.63	1390.52	575.31855
	1418.92	1437.76	1500.66	1502.78	1516.36	1517.89	1533.06	1553.87	3003.99	3014.83	3031.35	3037.83	638.70958
	3056.01	3057.50	3099.03	3104.38	3110.32	3112.34							
C_3CCHO	77.80	199.84	248.17	248.64	277.82	319.43	347.26	386.62	402.81	595.83	766.48	888.16	408.28679
	935.11	954.78	962.40	970.49	1061.72	1074.43	1235.43	1243.16	1300.02	1408.20	1416.50	1420.05	655.80077
	1448.68	1493.66	1497.99	1500.12	1515.13	1520.09	1531.72	1829.24	2859.75	3036.04	3039.51	3052.91	664.77166
	3107.30	3110.81	3116.46	3117.31	3125.16	3133.75							
$CCC\bullet (C)COOH$	20.08	51.39	65.31	106.68	176.52	194.00	213.36	266.59	364.07	401.58	447.21	567.10	476.77613
	747.63	793.68	859.27	930.75	962.08	988.02	996.90	1014.23	1056.49	1071.44	1240.60	1257.19	1155.73397
	1298.00	1325.96	1360.11	1364.41	1399.78	1417.12	1423.00	1471.06	1483.03	1499.34	1504.36	1513.84	1365.88475
	1520.66	2967.29	2974.09	3020.35	3039.83	3041.14	3046.64	3080.09	3102.13	3110.77	3115.98	3756.92	
$C_2\bullet C(COOH)_2$	54.09	107.49	119.08	173.44	187.42	204.25	220.89	265.42	294.61	299.87	334.17	357.23	1019.99831
	402.92	424.43	480.40	544.47	583.41	627.07	786.50	880.35	901.22	937.63	947.32	966.39	1273.76709
	976.65	1018.50	1029.55	1077.17	1180.62	1211.53	1229.07	1284.76	1332.55	1374.48	1383.98	1399.95	1752.82245
	1426.05	1430.03	1465.64	1481.49	1505.64	1513.06	1522.83	3034.59	3037.28	3053.76	3089.41	3092.25	
$C_2C(COOH)CHO$	59.83	84.02	107.48	170.66	206.55	220.98	230.69	274.22	316.16	335.07	369.86	405.40	498.06713
	454.73	662.04	777.73	891.49	934.35	943.29	954.70	972.56	1017.42	1062.09	1086.80	1203.85	1611.37533
	1224.83	1261.44	1305.61	1370.09	1398.56	1412.09	1419.68	1443.77	1495.76	1504.50	1512.69	1521.65	1678.11276
	1537.16	1831.02	2873.19	3005.49	3047.37	3054.37	3061.59	3116.31	3133.98	3143.63	3149.04	3748.15	
$C=C(C)COOH$	52.12	130.61	181.82	206.56	275.93	389.75	418.68	442.63	591.22	734.33	833.75	881.79	333.65046
	943.65	979.31	983.31	1012.80	1068.92	1093.90	1267.71	1317.20	1372.42	1384.03	1421.84	1457.08	723.82040
	1478.77	1492.47	1512.23	1733.86	3031.55	3038.67	3087.70	3099.02	3131.32	3149.94	3234.30	3722.08	842.90740
$C_2C(OOH)COO\bullet$	29.12	84.77	117.05	183.69	207.68	218.90	245.33	255.48	288.26	335.46	377.02	416.54	1061.18759
	454.35	462.15	515.30	576.59	780.14	872.41	898.46	930.55	944.67	953.17	959.89	1035.30	1234.76043
	1056.60	1075.76	1182.63	1188.06	1234.41	1257.07	1308.79	1343.66	1373.27	1398.70	1412.47	1416.27	1832.62622

1439.46	1468.77	1492.13	1502.13	1506.59	1519.11	1525.97	3032.92	3041.94	3049.29	3069.01	3087.54	
3112.16	3114.38	3120.41	3138.42	3146.51	3708.30							

C$_2$C(CH$_2$O•)CCOO•												
68.03	102.13	124.10	202.42	225.38	240.36	265.66	319.09	342.77	371.09	438.63	477.12	620.33544
532.41	602.75	746.84	899.98	917.67	949.32	965.70	971.27	1036.29	1081.84	1100.07	1165.36	1293.46452
1228.34	1244.04	1280.54	1320.77	1345.20	1371.91	1389.60	1416.71	1440.15	1485.04	1499.17	1506.19	1446.83928
1521.08	1523.76	2893.71	2918.11	3038.10	3047.83	3062.31	3103.82	3118.61	3133.21	3141.69	3151.21	

C$_2$C•CHO												
123.82	138.92	228.50	288.73	359.91	380.31	605.32	821.00	928.98	963.16	963.53	1024.84	216.60274
1056.56	1277.58	1355.24	1402.92	1423.15	1433.19	1477.89	1478.99	1498.48	1514.42	1592.08	2930.79	453.41331
3010.79	3018.44	3055.20	3060.80	3115.64	3154.07							647.80465

C$_2$C(CHO)$_2$												
61.33	70.80	192.44	222.74	239.50	287.69	315.42	334.52	364.26	547.88	622.60	770.80	589.02019
899.11	926.23	954.49	967.10	1022.33	1057.32	1184.65	1237.11	1271.71	1406.46	1415.71	1422.98	756.16413
1442.51	1496.46	1498.37	1514.71	1521.77	1819.26	1837.06	2877.94	2934.17	3043.72	3057.16	3116.64	940.39473
3127.13	3132.67	3145.80										

C$_2$C(CHO)CH$_2$O•												
76.92	104.75	206.00	216.34	236.75	281.03	298.81	343.60	361.52	513.78	550.02	606.77	600.32814
774.16	898.89	922.96	961.85	994.79	1028.67	1082.40	1102.63	1196.32	1243.49	1299.85	1349.56	775.52722
1376.95	1410.50	1420.07	1443.46	1498.66	1499.82	1515.32	1522.86	1836.34	2859.11	2890.36	2931.27	958.29590
3038.02	3053.40	3105.21	3126.03	3127.79	3146.22							

C(COOH)CYCCOC												
56.14	71.69	123.55	192.49	238.66	251.40	295.06	372.70	395.07	397.42	516.97	709.66	517.24367
850.99	868.60	908.50	936.77	952.94	966.25	1016.47	1032.04	1043.28	1049.89	1160.17	1163.73	1269.61211
1192.63	1233.28	1291.38	1312.57	1334.11	1357.43	1390.07	1403.41	1430.54	1476.48	1506.91	1514.85	1382.67316
1528.56	1552.57	2995.72	3011.41	3037.53	3043.31	3055.89	3068.72	3085.80	3110.79	3136.81	3754.82	

C=C(C)C=O												
127.68	184.14	263.28	400.97	438.41	627.73	705.91	833.87	969.67	978.55	1020.89	1042.07	209.78553
1079.29	1335.12	1406.16	1426.97	1465.72	1486.90	1503.67	1713.39	1797.82	2902.13	3052.75	3111.83	411.02314
3142.29	3153.49	3241.47										609.76017

C$_3$CCI												
100.45	156.57	217.31	247.29	275.00	280.30	332.89	380.22	411.47	448.72	601.53	742.63	417.27297
830.11	908.03	948.92	952.22	978.97	1046.82	1050.22	1141.54	1206.03	1268.26	1285.67	1311.29	2115.98775
1428.31	1433.35	1457.73	1495.06	1510.24	1516.90	1517.49	1536.07	1537.10	1548.84	3041.14	3045.15	2121.31214
3051.51	3107.94	3109.50	3111.69	3115.00	3118.38	3127.05	3131.19	3182.82				

C$_3$•CCI												
96.44	112.37	148.08	235.78	250.99	279.18	312.43	372.95	394.28	426.39	519.50	604.64	402.28476
753.78	833.13	900.02	938.06	963.47	995.39	1036.08	1101.07	1159.33	1244.16	1280.32	1315.56	2059.70441
1418.51	1438.62	1477.40	1498.18	1514.07	1517.89	1530.17	1538.84	3038.95	3050.50	3108.02	3114.21	2076.20218
3116.48	3125.33	3136.31	3165.55	3183.61	3267.30							

Table B.3 Thermodynamic Analysis for Reactions of Neopentyl Oxidation

```
THERMODYNAMIC ANALYSIS for REACTION
Rx            C3CC.      = TS0
Hf {Kcal/mol}   10.520      40.260
S {cal/mol K}   81.800      82.480

dHr {kcal/mol}   (298K) =       29.74    dHr avg (298., 1500. K) =       29.56
dU (dE) {kcal/mol} (")  =       29.74    dUr avg (298., 1500. K) =       29.56
dSr {cal/mol K}  ( "  ) =        .68     dSr avg (298., 1500. K) =        .41
dGr {kcal/mol}   ( "  ) =       29.54    dGr avg (298., 1500. K) =       29.19
         Kc      ( "  ) =    2.222E-22   Kc avg (298., 1500. K ) =    7.993E-08
Fit Af/Ar    : A = 2.806E+00 n =  -.10 alpha = 3.374E-04 avg error   2.64 %
Fit Af/Ar w/ddU: A = 8.228E+00 n =  -.28 alpha = 3.875E-04 avg error   4.92 %

     T (K)   dH(Kcal/mol)  dU(Kcal/mol) dS(cal/mol K)      Kc        dG(Kcal/mol)
     300.00    2.974E+01    2.974E+01    6.800E-01     3.029E-22      2.954E+01
     400.00    2.973E+01    2.973E+01    6.491E-01     7.898E-17      2.947E+01
     500.00    2.970E+01    2.970E+01    5.768E-01     1.396E-13      2.941E+01
     600.00    2.964E+01    2.964E+01    4.810E-01     2.026E-11      2.935E+01
     800.00    2.949E+01    2.949E+01    2.580E-01     1.001E-08      2.928E+01
    1000.00    2.928E+01    2.928E+01    2.919E-02     4.041E-07      2.925E+01
    1200.00    2.905E+01    2.905E+01   -1.805E-01     4.669E-06      2.927E+01
    1500.00    2.871E+01    2.871E+01   -4.330E-01     5.269E-05      2.936E+01
    2000.00    2.828E+01    2.828E+01   -6.839E-01     5.754E-04      2.965E+01

The model fitted is for uni-molecular reaction.

The 3 parameters for the model equation of A(T) = Aprime * T^n * exp(-Ea/RT)
     Aprime = 5.1673E+11        n =    .59344     Ea =    3.0075E+04

Temp(K)         AF(T)           T_K^n         k_calc(T)          k_fit
300.00         8.802E+12       2.951E+01       1.893E-09        1.870E-09
400.00         1.155E+13       3.501E+01       6.582E-04        6.665E-04
500.00         1.393E+13       3.997E+01       1.454E+00        1.473E+00
600.00         1.593E+13       4.453E+01       2.533E+02        2.548E+02
800.00         1.898E+13       5.282E+01       1.668E+05        1.657E+05
1000.00        2.114E+13       6.030E+01       8.421E+06        8.320E+06
1200.00        2.283E+13       6.719E+01       1.168E+08        1.155E+08
1500.00        2.514E+13       7.671E+01       1.647E+09        1.644E+09
2000.00        2.954E+13       9.099E+01       2.398E+10        2.429E+10


        THERMODYNAMIC ANALYSIS for REACTION
Rx           C3CCOO.     = TS1
Hf {Kcal/mol}  -27.610      -3.790
S {cal/mol K}   95.450      86.140

dHr {kcal/mol}   (298K) =       23.82    dHr avg (298., 1500. K) =       24.03
dU (dE) {kcal/mol} (")  =       23.82    dUr avg (298., 1500. K) =       24.03
dSr {cal/mol K}  ( "  ) =       -9.31    dSr avg (298., 1500. K) =       -9.08
dGr {kcal/mol}   ( "  ) =       26.60    dGr avg (298., 1500. K) =       32.19
         Kc      ( "  ) =    3.185E-20   Kc avg (298., 1500. K ) =    1.495E-08
Fit Af/Ar    : A = 4.984E-02 n =  -.37 alpha =-1.203E-03 avg error   5.35 %
Fit Af/Ar w/ddU: A = 4.794E-02 n =  -.41 alpha =-1.793E-03 avg error  11.12 %

     T (K)   dH(Kcal/mol)  dU(Kcal/mol) dS(cal/mol K)      Kc        dG(Kcal/mol)
     300.00    2.382E+01    2.382E+01   -9.317E+00     4.082E-20      2.661E+01
     400.00    2.375E+01    2.375E+01   -9.514E+00     8.758E-16      2.756E+01
     500.00    2.376E+01    2.376E+01   -9.508E+00     3.449E-13      2.851E+01
     600.00    2.382E+01    2.382E+01   -9.399E+00     1.863E-11      2.946E+01
     800.00    2.406E+01    2.406E+01   -9.046E+00     2.806E-09      3.130E+01
    1000.00    2.443E+01    2.443E+01   -8.639E+00     5.915E-08      3.307E+01
    1200.00    2.487E+01    2.487E+01   -8.238E+00     4.669E-07      3.476E+01
    1500.00    2.561E+01    2.561E+01   -7.689E+00     3.869E-06      3.714E+01
    2000.00    2.690E+01    2.690E+01   -6.950E+00     3.481E-05      4.080E+01

The model fitted is for uni-molecular reaction.
```

The 3 parameters for the model equation of A(T) = Aprime * T^n * exp(-Ea/RT)
    Aprime = 1.2393E+06   n =   1.68963   Ea =   2.3136E+04

Temp(K)	AF(T)	T_K^n	k_calc(T)	k_fit
300.00	5.749E+10	1.533E+04	2.551E-07	2.646E-07
400.00	6.942E+10	2.492E+04	7.299E-03	7.043E-03
500.00	8.702E+10	3.633E+04	3.593E+00	3.466E+00
600.00	1.103E+11	4.944E+04	2.329E+02	2.287E+02
800.00	1.757E+11	8.038E+04	4.678E+04	4.757E+04
1000.00	2.695E+11	1.172E+05	1.232E+06	1.274E+06
1200.00	3.958E+11	1.595E+05	1.168E+07	1.207E+07
1500.00	6.522E+11	2.325E+05	1.209E+08	1.226E+08
2000.00	1.261E+12	3.780E+05	1.451E+09	1.388E+09

           THERMODYNAMIC ANALYSIS for REACTION
Rx   C3CCOO.   = TS2
Hf {Kcal/mol} -27.610   14.000
S {cal/mol K}   95.450   91.660

dHr {kcal/mol}   (298K) =   41.61   dHr avg (298., 1500. K) =   41.77
dU (dE) {kcal/mol} (") =   41.61   dUr avg (298., 1500. K) =   41.77
dSr {cal/mol K} (") =   -3.79   dSr avg (298., 1500. K) =   -3.50
dGr {kcal/mol} (") =   42.74   dGr avg (298., 1500. K) =   44.91
         Kc   (") =   4.657E-32   Kc avg (298., 1500. K) =   1.207E-11
Fit Af/Ar   : A = 2.316E-02 n =   .33 alpha = 1.158E-04 avg error   .36 %
Fit Af/Ar w/ddU: A = 5.530E-03 n =   .59 alpha = 3.211E-04 avg error   .80 %

T (K)	dH(Kcal/mol)	dU(Kcal/mol)	dS(cal/mol K)	Kc	dG(Kcal/mol)
300.00	4.161E+01	4.161E+01	-3.787E+00	7.182E-32	4.275E+01
400.00	4.166E+01	4.166E+01	-3.641E+00	2.750E-24	4.312E+01
500.00	4.172E+01	4.172E+01	-3.515E+00	9.889E-20	4.348E+01
600.00	4.178E+01	4.178E+01	-3.410E+00	1.088E-16	4.382E+01
800.00	4.188E+01	4.188E+01	-3.256E+00	7.008E-13	4.449E+01
1000.00	4.197E+01	4.197E+01	-3.157E+00	1.369E-10	4.513E+01
1200.00	4.204E+01	4.204E+01	-3.092E+00	4.642E-09	4.575E+01
1500.00	4.213E+01	4.213E+01	-3.025E+00	1.584E-07	4.667E+01
2000.00	4.229E+01	4.229E+01	-2.935E+00	5.457E-06	4.816E+01

The model fitted is for uni-molecular reaction.

The 3 parameters for the model equation of A(T) = Aprime * T^n * exp(-Ea/RT)
    Aprime = 6.5426E+08   n =   1.23510   Ea =   4.1485E+04

Temp(K)	AF(T)	T_K^n	k_calc(T)	k_fit
300.00	9.294E+11	1.147E+03	4.490E-19	4.475E-19
400.00	1.334E+12	1.636E+03	2.292E-11	2.297E-11
500.00	1.776E+12	2.155E+03	1.030E-06	1.034E-06
600.00	2.247E+12	2.700E+03	1.360E-03	1.364E-03
800.00	3.238E+12	3.851E+03	1.168E+01	1.167E+01
1000.00	4.255E+12	5.073E+03	2.853E+03	2.843E+03
1200.00	5.275E+12	6.355E+03	1.161E+05	1.155E+05
1500.00	6.819E+12	8.371E+03	4.950E+06	4.939E+06
2000.00	9.512E+12	1.194E+04	2.274E+08	2.287E+08

           THERMODYNAMIC ANALYSIS for REACTION
Rx   C3.CCQ   = TS1
Hf {Kcal/mol} -9.430   -3.790
S {cal/mol K} 105.580   86.140

dHr {kcal/mol}   (298K) =   5.64   dHr avg (298., 1500. K) =   5.42
dU (dE) {kcal/mol} (") =   5.64   dUr avg (298., 1500. K) =   5.42
dSr {cal/mol K} (") =   -19.44   dSr avg (298., 1500. K) =   -20.05
dGr {kcal/mol} (") =   11.44   dGr avg (298., 1500. K) =   23.45
         Kc   (") =   4.135E-09   Kc avg (298., 1500. K) =   1.987E-06
Fit Af/Ar   : A = 1.037E-01 n = -1.43 alpha =-1.772E-03 avg error   7.30 %
Fit Af/Ar w/ddU: A = 5.817E+00 n = -2.24 alpha =-3.064E-03 avg error 17.57 %

T (K)	dH(Kcal/mol)	dU(Kcal/mol)	dS(cal/mol K)	Kc	dG(Kcal/mol)
300.00	5.634E+00	5.634E+00	-1.946E+01	4.385E-09	1.147E+01

```
400.00    5.360E+00    5.360E+00    -2.026E+01    4.402E-08    1.346E+01
500.00    5.196E+00    5.196E+00    -2.063E+01    1.661E-07    1.551E+01
600.00    5.117E+00    5.117E+00    -2.077E+01    3.942E-07    1.758E+01
800.00    5.135E+00    5.135E+00    -2.075E+01    1.151E-06    2.174E+01
1000.00   5.309E+00    5.309E+00    -2.056E+01    2.215E-06    2.587E+01
1200.00   5.582E+00    5.582E+00    -2.031E+01    3.493E-06    2.996E+01
1500.00   6.126E+00    6.126E+00    -1.991E+01    5.693E-06    3.599E+01
2000.00   7.246E+00    7.246E+00    -1.927E+01    9.916E-06    4.579E+01
```

The model fitted is for uni-molecular reaction.

The 3 parameters for the model equation of A(T) = Aprime * T^n * exp(-Ea/RT)
        Aprime = 2.7043E+05   n =   1.12721   Ea =   5.1660E+03

```
Temp(K)        AF(T)            T_K^n          k_calc(T)        k_fit
300.00        3.487E+08        6.198E+02        2.741E+04        2.888E+04
400.00        3.116E+08        8.571E+02        3.669E+05        3.486E+05
500.00        3.233E+08        1.102E+03        1.730E+06        1.645E+06
600.00        3.602E+08        1.354E+03        4.928E+06        4.805E+06
800.00        4.852E+08        1.872E+03        1.918E+07        1.963E+07
1000.00       6.678E+08        2.408E+03        4.616E+07        4.837E+07
1200.00       9.078E+08        2.957E+03        8.735E+07        9.162E+07
1500.00       1.390E+09        3.803E+03        1.779E+08        1.817E+08
2000.00       2.559E+09        5.259E+03        4.132E+08        3.876E+08
```

```
        THERMODYNAMIC ANALYSIS for REACTION
Rx            C3.CCQ      = TS3
Hf {Kcal/mol}   -9.430        6.070
S {cal/mol K}  105.580       99.540
```

```
dHr {kcal/mol}    (298K) =        15.50    dHr avg (298., 1500. K) =        15.15
dU (dE) {kcal/mol} (")   =        15.50    dUr avg (298., 1500. K) =        15.15
dSr {cal/mol K}   ( " )  =        -6.04    dSr avg (298., 1500. K) =        -6.70
dGr {kcal/mol}    ( " )  =        17.30    dGr avg (298., 1500. K) =        21.17
        Kc        ( " )  =     2.075E-13    Kc avg (298., 1500. K ) =     7.128E-06
Fit Af/Ar     : A = 5.334E+00 n =  -.85 alpha =-4.339E-04 avg error    .90 %
Fit Af/Ar w/ddU: A = 1.975E+02 n = -1.52 alpha =-1.031E-03 avg error    .72 %
```

```
    T (K)   dH(Kcal/mol)  dU(Kcal/mol) dS(cal/mol K)      Kc       dG(Kcal/mol)
    300.00    1.550E+01    1.550E+01    -6.048E+00    2.439E-13    1.731E+01
    400.00    1.537E+01    1.537E+01    -6.425E+00    1.581E-10    1.794E+01
    500.00    1.524E+01    1.524E+01    -6.698E+00    7.449E-09    1.859E+01
    600.00    1.513E+01    1.513E+01    -6.913E+00    9.521E-08    1.927E+01
    800.00    1.490E+01    1.490E+01    -7.233E+00    2.223E-06    2.069E+01
    1000.00   1.470E+01    1.470E+01    -7.459E+00    1.433E-05    2.216E+01
    1200.00   1.453E+01    1.453E+01    -7.613E+00    4.884E-05    2.367E+01
    1500.00   1.438E+01    1.438E+01    -7.730E+00    1.641E-04    2.597E+01
    2000.00   1.438E+01    1.438E+01    -7.734E+00    5.472E-04    2.985E+01
```

The model fitted is for uni-molecular reaction.

The 3 parameters for the model equation of A(T) = Aprime * T^n * exp(-Ea/RT)
        Aprime = 2.4929E+10   n =   .50717   Ea =   1.5738E+04

```
Temp(K)        AF(T)            T_K^n          k_calc(T)        k_fit
300.00        2.978E+11        1.804E+01        1.524E+00        1.538E+00
400.00        3.286E+11        2.088E+01        1.318E+03        1.309E+03
500.00        3.579E+11        2.338E+01        7.760E+04        7.690E+04
600.00        3.856E+11        2.564E+01        1.190E+06        1.182E+06
800.00        4.375E+11        2.967E+01        3.706E+07        3.709E+07
1000.00       4.881E+11        3.323E+01        2.985E+08        3.009E+08
1200.00       5.422E+11        3.645E+01        1.221E+09        1.236E+09
1500.00       6.388E+11        4.082E+01        5.130E+09        5.180E+09
2000.00       8.501E+11        4.723E+01        2.280E+10        2.244E+10
```

```
        THERMODYNAMIC ANALYSIS for REACTION
Rx            C3.CCQ      = TS4
Hf {Kcal/mol}   -9.430       15.950
S {cal/mol K}  105.580      102.740
```

```
dHr {kcal/mol}    (298K)  =        25.38    dHr avg (298., 1500. K) =        25.20
dU (dE) {kcal/mol} (")    =        25.38    dUr avg (298., 1500. K) =        25.20
dSr {cal/mol K}   ( " )   =        -2.84    dSr avg (298., 1500. K) =        -3.06
dGr {kcal/mol}    ( " )   =        26.23    dGr avg (298., 1500. K) =        27.95
        Kc        ( " )   =     5.939E-20   Kc avg (298., 1500. K ) =     1.601E-07
Fit Af/Ar     : A = 8.032E-02 n =   .25 alpha = 9.172E-04 avg error   3.62 %
Fit Af/Ar w/ddU: A = 9.145E-02 n =   .26 alpha = 1.359E-03 avg error   7.40 %

     T (K)   dH(Kcal/mol)  dU(Kcal/mol) dS(cal/mol K)      Kc        dG(Kcal/mol)
     300.00    2.538E+01    2.538E+01   -2.836E+00    7.734E-20    2.623E+01
     400.00    2.542E+01    2.542E+01   -2.724E+00    3.275E-15    2.651E+01
     500.00    2.541E+01    2.541E+01   -2.747E+00    1.963E-12    2.678E+01
     600.00    2.536E+01    2.536E+01   -2.842E+00    1.388E-10    2.706E+01
     800.00    2.515E+01    2.515E+01   -3.126E+00    2.781E-08    2.766E+01
    1000.00    2.487E+01    2.487E+01   -3.447E+00    6.482E-07    2.831E+01
    1200.00    2.452E+01    2.452E+01   -3.760E+00    5.149E-06    2.903E+01
    1500.00    2.395E+01    2.395E+01   -4.188E+00    3.940E-05    3.023E+01
    2000.00    2.289E+01    2.289E+01   -4.797E+00    2.822E-04    3.248E+01
```

The model fitted is for uni-molecular reaction.

The 3 parameters for the model equation of $A(T) = Aprime * T^n * exp(-Ea/RT)$
     Aprime = 2.8350E+11   n =   .44359   Ea =   2.5913E+04

```
Temp(K)         AF(T)              T_K^n          k_calc(T)          k_fit
300.00        1.500E+12          1.256E+01        4.835E-07        4.704E-07
400.00        2.116E+12          1.426E+01        2.730E-02        2.803E-02
500.00        2.614E+12          1.575E+01        2.045E+01        2.101E+01
600.00        2.991E+12          1.708E+01        1.736E+03        1.760E+03
800.00        3.456E+12          1.940E+01        4.635E+05        4.579E+05
1000.00       3.676E+12          2.142E+01        1.351E+07        1.317E+07
1200.00       3.768E+12          2.322E+01        1.287E+08        1.255E+08
1500.00       3.798E+12          2.564E+01        1.231E+09        1.218E+09
2000.00       3.727E+12          2.913E+01        1.176E+10        1.216E+10
```

```
        THERMODYNAMIC ANALYSIS for REACTION
Rx          C3.CCQ      = TS5
Hf {Kcal/mol}  -9.430      17.090
S {cal/mol K} 105.580     102.330

dHr {kcal/mol}    (298K)  =        26.52    dHr avg (298., 1500. K) =        26.76
dU (dE) {kcal/mol} (")    =        26.52    dUr avg (298., 1500. K) =        26.76
dSr {cal/mol K}   ( " )   =        -3.25    dSr avg (298., 1500. K) =        -2.84
dGr {kcal/mol}    ( " )   =        27.49    dGr avg (298., 1500. K) =        29.31
        Kc        ( " )   =     7.053E-21   Kc avg (298., 1500. K ) =     7.477E-08
Fit Af/Ar     : A = 9.504E-02 n =   .10 alpha =-5.347E-04 avg error   1.96 %
Fit Af/Ar w/ddU: A = 3.554E-02 n =   .26 alpha =-7.003E-04 avg error   3.78 %

     T (K)   dH(Kcal/mol)  dU(Kcal/mol) dS(cal/mol K)      Kc        dG(Kcal/mol)
     300.00    2.652E+01    2.652E+01   -3.244E+00    9.295E-21    2.749E+01
     400.00    2.659E+01    2.659E+01   -3.036E+00    6.388E-16    2.781E+01
     500.00    2.664E+01    2.664E+01   -2.927E+00    5.178E-13    2.811E+01
     600.00    2.669E+01    2.669E+01   -2.831E+00    4.538E-11    2.839E+01
     800.00    2.687E+01    2.687E+01   -2.586E+00    1.242E-08    2.894E+01
    1000.00    2.715E+01    2.715E+01   -2.276E+00    3.707E-07    2.942E+01
    1200.00    2.749E+01    2.749E+01   -1.961E+00    3.662E-06    2.985E+01
    1500.00    2.800E+01    2.800E+01   -1.582E+00    3.750E-05    3.037E+01
    2000.00    2.881E+01    2.881E+01   -1.115E+00    4.050E-04    3.104E+01
```

The model fitted is for uni-molecular reaction.

The 3 parameters for the model equation of $A(T) = Aprime * T^n * exp(-Ea/RT)$
     Aprime = 8.6330E+07   n =   1.55502   Ea =   2.6101E+04

```
Temp(K)         AF(T)              T_K^n          k_calc(T)          k_fit
300.00        1.221E+12          7.112E+03        5.810E-08        5.914E-08
400.00        1.808E+12          1.112E+04        5.324E-03        5.251E-03
500.00        2.388E+12          1.574E+04        5.394E+00        5.289E+00
600.00        3.008E+12          2.090E+04        5.674E+02        5.599E+02
```

800.00	4.535E+12	3.269E+04	2.071E+05	2.087E+05
1000.00	6.628E+12	4.624E+04	7.724E+06	7.877E+06
1200.00	9.318E+12	6.140E+04	9.157E+07	9.339E+07
1500.00	1.410E+13	8.687E+04	1.172E+09	1.180E+09
2000.00	2.377E+13	1.359E+05	1.688E+10	1.648E+10

```
        THERMODYNAMIC ANALYSIS for REACTION
Rx         C3.CCQ    = TS6
Hf {Kcal/mol}  -9.430     46.910
S {cal/mol K} 105.580    102.360
```

dHr {kcal/mol} (298K) =	56.34	dHr avg (298., 1500. K) =	56.16
dU (dE) {kcal/mol} (") =	56.34	dUr avg (298., 1500. K) =	56.16
dSr {cal/mol K} (") =	-3.22	dSr avg (298., 1500. K) =	-3.63
dGr {kcal/mol} (") =	57.30	dGr avg (298., 1500. K) =	59.43
Kc (") =	9.873E-43	Kc avg (298., 1500. K) =	3.573E-15

```
Fit Af/Ar      : A = 2.098E+01 n =  -.88 alpha =-9.850E-04 avg error   2.95 %
Fit Af/Ar w/ddU: A = 3.575E+02 n = -1.42 alpha =-1.766E-03 avg error   7.46 %
```

T (K)	dH(Kcal/mol)	dU(Kcal/mol)	dS(cal/mol K)	Kc	dG(Kcal/mol)
300.00	5.634E+01	5.634E+01	-3.227E+00	1.775E-42	5.731E+01
400.00	5.622E+01	5.622E+01	-3.574E+00	3.167E-32	5.765E+01
500.00	5.611E+01	5.611E+01	-3.821E+00	4.350E-26	5.802E+01
600.00	5.602E+01	5.602E+01	-3.976E+00	5.286E-22	5.841E+01
800.00	5.596E+01	5.596E+01	-4.072E+00	6.628E-17	5.922E+01
1000.00	5.603E+01	5.603E+01	-3.993E+00	7.593E-14	6.003E+01
1200.00	5.619E+01	5.619E+01	-3.848E+00	8.397E-12	6.081E+01
1500.00	5.647E+01	5.647E+01	-3.639E+00	9.459E-10	6.193E+01
2000.00	5.701E+01	5.701E+01	-3.334E+00	1.100E-07	6.367E+01

The model fitted is for uni-molecular reaction.

The 3 parameters for the model equation of $A(T) = Aprime * T^n * exp(-Ea/RT)$
      Aprime = 3.6326E+09   n =   .97602   Ea =   5.6165E+04

Temp(K)	AF(T)	T_K^n	k_calc(T)	k_fit
300.00	1.232E+12	2.617E+02	1.109E-29	1.143E-29
400.00	1.379E+12	3.465E+02	2.639E-19	2.571E-19
500.00	1.523E+12	4.308E+02	4.532E-13	4.391E-13
600.00	1.690E+12	5.147E+02	6.608E-09	6.484E-09
800.00	2.148E+12	6.815E+02	1.105E-03	1.119E-03
1000.00	2.793E+12	8.474E+02	1.582E+00	1.631E+00
1200.00	3.606E+12	1.012E+03	2.100E+02	2.166E+02
1500.00	5.006E+12	1.259E+03	2.956E+04	2.994E+04
2000.00	7.782E+12	1.667E+03	4.585E+06	4.407E+06

```
        THERMODYNAMIC ANALYSIS for REACTION
Rx         C2CCQCQ.   = TS7
Hf {Kcal/mol} -42.390    -19.410
S {cal/mol K} 117.210    105.760
```

dHr {kcal/mol} (298K) =	22.98	dHr avg (298., 1500. K) =	22.96
dU (dE) {kcal/mol} (") =	22.98	dUr avg (298., 1500. K) =	22.96
dSr {cal/mol K} (") =	-11.45	dSr avg (298., 1500. K) =	-11.53
dGr {kcal/mol} (") =	26.39	dGr avg (298., 1500. K) =	33.33
Kc (") =	4.479E-20	Kc avg (298., 1500. K) =	7.913E-09

```
Fit Af/Ar      : A = 3.430E-03 n =  -.02 alpha = 8.825E-05 avg error   3.14 %
Fit Af/Ar w/ddU: A = 3.169E-03 n =  -.01 alpha = 1.386E-04 avg error   6.41 %
```

T (K)	dH(Kcal/mol)	dU(Kcal/mol)	dS(cal/mol K)	Kc	dG(Kcal/mol)
300.00	2.298E+01	2.298E+01	-1.146E+01	5.690E-20	2.642E+01
400.00	2.290E+01	2.290E+01	-1.169E+01	8.556E-16	2.758E+01
500.00	2.290E+01	2.290E+01	-1.168E+01	2.720E-13	2.874E+01
600.00	2.293E+01	2.293E+01	-1.163E+01	1.271E-11	2.991E+01
800.00	2.296E+01	2.296E+01	-1.158E+01	1.565E-09	3.223E+01
1000.00	2.289E+01	2.289E+01	-1.166E+01	2.806E-08	3.455E+01
1200.00	2.276E+01	2.276E+01	-1.178E+01	1.905E-07	3.690E+01
1500.00	2.261E+01	2.261E+01	-1.190E+01	1.276E-06	4.045E+01
2000.00	2.260E+01	2.260E+01	-1.190E+01	8.483E-06	4.641E+01

The model fitted is for uni-molecular reaction.

The 3 parameters for the model equation of A(T) = Aprime * T^n * exp(-Ea/RT)
        Aprime = 1.0647E+08   n = .92093   Ea = 2.3004E+04

Temp(K)	AF(T)	T_K^n	k_calc(T)	k_fit
300.00	1.957E+10	1.911E+02	3.557E-07	3.535E-07
400.00	2.327E+10	2.491E+02	7.131E-03	7.136E-03
500.00	2.910E+10	3.059E+02	2.834E+00	2.862E+00
600.00	3.590E+10	3.618E+02	1.589E+02	1.606E+02
800.00	4.906E+10	4.716E+02	2.609E+04	2.605E+04
1000.00	5.901E+10	5.791E+02	5.847E+05	5.781E+05
1200.00	6.649E+10	6.850E+02	4.763E+06	4.709E+06
1500.00	7.851E+10	8.413E+02	3.988E+07	3.983E+07
2000.00	1.044E+11	1.096E+03	3.535E+08	3.575E+08

        THERMODYNAMIC ANALYSIS for REACTION
Rx   C2CCQCQ.   = TS8A
Hf {Kcal/mol} -42.390   -1.610
S {cal/mol K} 117.210   110.130

dHr {kcal/mol} (298K) =	40.78	dHr avg (298., 1500. K) =	41.05		
dU (dE) {kcal/mol} (") =	40.78	dUr avg (298., 1500. K) =	41.05		
dSr {cal/mol K} (") =	-7.08	dSr avg (298., 1500. K) =	-6.66		
dGr {kcal/mol} (") =	42.89	dGr avg (298., 1500. K) =	47.04		
Kc (") =	3.610E-32	Kc avg (298., 1500. K) =	3.663E-12		

Fit Af/Ar   : A = 1.029E-02 n = .14 alpha =-5.032E-04 avg error   2.97 %
Fit Af/Ar w/ddU: A = 2.294E-03 n = .39 alpha =-5.969E-04 avg error   5.30 %

T (K)	dH(Kcal/mol)	dU(Kcal/mol)	dS(cal/mol K)	Kc	dG(Kcal/mol)
300.00	4.078E+01	4.078E+01	-7.082E+00	5.519E-32	4.290E+01
400.00	4.079E+01	4.079E+01	-7.069E+00	1.475E-24	4.361E+01
500.00	4.085E+01	4.085E+01	-6.931E+00	4.255E-20	4.431E+01
600.00	4.095E+01	4.095E+01	-6.753E+00	4.056E-17	4.500E+01
800.00	4.119E+01	4.119E+01	-6.404E+00	2.222E-13	4.631E+01
1000.00	4.146E+01	4.146E+01	-6.105E+00	4.020E-11	4.756E+01
1200.00	4.174E+01	4.174E+01	-5.847E+00	1.316E-09	4.876E+01
1500.00	4.222E+01	4.222E+01	-5.493E+00	4.443E-08	5.046E+01
2000.00	4.305E+01	4.305E+01	-5.014E+00	1.582E-06	5.308E+01

The model fitted is for uni-molecular reaction.

The 3 parameters for the model equation of A(T) = Aprime * T^n * exp(-Ea/RT)
        Aprime = 8.9043E+06   n = 1.59523   Ea = 4.0295E+04

Temp(K)	AF(T)	T_K^n	k_calc(T)	k_fit
300.00	1.770E+11	8.945E+03	3.450E-19	3.501E-19
400.00	2.376E+11	1.415E+04	1.230E-11	1.210E-11
500.00	3.184E+11	2.021E+04	4.433E-07	4.374E-07
600.00	4.177E+11	2.703E+04	5.071E-04	5.046E-04
800.00	6.642E+11	4.277E+04	3.704E+00	3.731E+00
1000.00	9.647E+11	6.105E+04	8.376E+02	8.476E+02
1200.00	1.318E+12	8.166E+04	3.290E+04	3.329E+04
1500.00	1.969E+12	1.166E+05	1.389E+06	1.396E+06
2000.00	3.342E+12	1.845E+05	6.593E+07	6.486E+07

        THERMODYNAMIC ANALYSIS for REACTION
Rx   C2CCQCQ.   = TS8
Hf {Kcal/mol} -42.390   -19.990
S {cal/mol K} 117.210   112.000

dHr {kcal/mol} (298K) =	22.40	dHr avg (298., 1500. K) =	23.56		
dU (dE) {kcal/mol} (") =	22.40	dUr avg (298., 1500. K) =	23.56		
dSr {cal/mol K} (") =	-5.21	dSr avg (298., 1500. K) =	-3.11		
dGr {kcal/mol} (") =	23.95	dGr avg (298., 1500. K) =	26.35		
Kc (") =	2.756E-18	Kc avg (298., 1500. K) =	3.930E-07		

Fit Af/Ar   : A = 7.850E-07 n = 2.01 alpha = 1.713E-04 avg error   2.54 %
Fit Af/Ar w/ddU: A = 8.505E-11 n = 3.68 alpha = 1.189E-03 avg error   5.83 %

T (K)	dH(Kcal/mol)	dU(Kcal/mol)	dS(cal/mol K)	Kc	dG(Kcal/mol)
300.00	2.241E+01	2.241E+01	-5.192E+00	3.480E-18	2.396E+01
400.00	2.275E+01	2.275E+01	-4.218E+00	4.459E-14	2.443E+01
500.00	2.314E+01	2.314E+01	-3.330E+00	1.428E-11	2.481E+01
600.00	2.356E+01	2.356E+01	-2.570E+00	7.167E-10	2.510E+01
800.00	2.436E+01	2.436E+01	-1.423E+00	1.083E-07	2.550E+01
1000.00	2.506E+01	2.506E+01	-6.402E-01	2.418E-06	2.570E+01
1200.00	2.570E+01	2.570E+01	-5.210E-02	2.029E-05	2.576E+01
1500.00	2.673E+01	2.673E+01	7.085E-01	1.822E-04	2.566E+01
2000.00	2.858E+01	2.858E+01	1.774E+00	1.838E-03	2.503E+01

The model fitted is for uni-molecular reaction.

The 3 parameters for the model equation of $A(T) = Aprime * T^n * exp(-Ea/RT)$
   Aprime = 5.3565E+03   n =   2.87418   Ea =   2.1295E+04

Temp(K)	AF(T)	T_K^n	k_calc(T)	k_fit
300.00	4.583E+11	1.317E+07	2.175E-05	2.158E-05
400.00	9.975E+11	3.012E+07	3.716E-01	3.730E-01
500.00	1.950E+12	5.719E+07	1.488E+02	1.505E+02
600.00	3.430E+12	9.658E+07	8.960E+03	9.047E+03
800.00	8.146E+12	2.208E+08	1.805E+06	1.799E+06
1000.00	1.510E+13	4.193E+08	5.039E+07	4.978E+07
1200.00	2.436E+13	7.081E+08	5.074E+08	5.016E+08
1500.00	4.464E+13	1.345E+09	5.694E+09	5.684E+09
2000.00	1.017E+14	3.074E+09	7.658E+10	7.753E+10

    THERMODYNAMIC ANALYSIS for REACTION
Rx   C2.CQCQ   = TS7
Hf {Kcal/mol} -25.140   -19.410
S {cal/mol K} 125.490   105.760

dHr {kcal/mol}	(298K) =	5.73	dHr avg (298., 1500. K) =		5.93
dU (dE) {kcal/mol}	(") =	5.73	dUr avg (298., 1500. K) =		5.93
dSr {cal/mol K}	(") =	-19.73	dSr avg (298., 1500. K) =		-19.53
dGr {kcal/mol}	(") =	11.61	dGr avg (298., 1500. K) =		23.49
Kc	(") =	3.070E-09	Kc avg (298., 1500. K) =		1.948E-06

Fit Af/Ar   : A = 1.939E-04 n = -.32 alpha =-1.047E-03 avg error   6.10 %
Fit Af/Ar w/ddU: A = 1.419E-04 n = -.31 alpha =-1.530E-03 avg error 12.52 %

T (K)	dH(Kcal/mol)	dU(Kcal/mol)	dS(cal/mol K)	Kc	dG(Kcal/mol)
300.00	5.727E+00	5.727E+00	-1.974E+01	3.258E-09	1.165E+01
400.00	5.627E+00	5.627E+00	-2.004E+01	3.516E-08	1.364E+01
500.00	5.632E+00	5.632E+00	-2.003E+01	1.447E-07	1.565E+01
600.00	5.706E+00	5.706E+00	-1.990E+01	3.741E-07	1.764E+01
800.00	5.968E+00	5.968E+00	-1.952E+01	1.266E-06	2.159E+01
1000.00	6.295E+00	6.295E+00	-1.916E+01	2.734E-06	2.545E+01
1200.00	6.652E+00	6.652E+00	-1.883E+01	4.700E-06	2.925E+01
1500.00	7.255E+00	7.255E+00	-1.839E+01	8.401E-06	3.483E+01
2000.00	8.397E+00	8.397E+00	-1.773E+01	1.611E-05	4.386E+01

The model fitted is for uni-molecular reaction.

The 3 parameters for the model equation of $A(T) = Aprime * T^n * exp(-Ea/RT)$
   Aprime = 1.0139E+04   n =   1.62435   Ea =   5.0883E+03

Temp(K)	AF(T)	T_K^n	k_calc(T)	k_fit
300.00	3.029E+08	1.056E+04	2.037E+04	2.102E+04
400.00	3.482E+08	1.685E+04	2.930E+05	2.833E+05
500.00	4.366E+08	2.421E+04	1.507E+06	1.465E+06
600.00	5.603E+08	3.256E+04	4.677E+06	4.625E+06
800.00	9.016E+08	5.196E+04	2.111E+07	2.145E+07
1000.00	1.354E+09	7.465E+04	5.697E+07	5.846E+07
1200.00	1.913E+09	1.004E+05	1.175E+08	1.205E+08
1500.00	2.995E+09	1.442E+05	2.626E+08	2.652E+08
2000.00	5.554E+09	2.302E+05	6.713E+08	6.485E+08

    THERMODYNAMIC ANALYSIS for REACTION

```
Rx          C2.CQCQ     = TS9
Hf {Kcal/mol}  -25.140      -9.420
S {cal/mol K}  125.490    112.780


dHr {kcal/mol}  (298K) =       15.72   dHr avg (298., 1500. K) =      16.14
dU (dE) {kcal/mol} (") =        15.72   dUr avg (298., 1500. K) =      16.14
dSr {cal/mol K}  ( " ) =       -12.71   dSr avg (298., 1500. K) =     -11.95
dGr  {kcal/mol}  ( " ) =        19.51   dGr avg (298., 1500. K) =      26.88
       Kc       ( " ) =   4.989E-15    Kc avg (298., 1500. K ) =   2.913E-07
Fit Af/Ar     : A = 2.995E-05 n =   .70 alpha = 2.399E-05 avg error   1.42 %
Fit Af/Ar w/ddU: A = 1.187E-06 n =  1.29 alpha = 3.631E-04 avg error   2.86 %


     T (K)  dH(Kcal/mol)  dU(Kcal/mol) dS(cal/mol K)      Kc       dG(Kcal/mol)
     300.00     1.572E+01     1.572E+01  -1.270E+01   5.876E-15    1.953E+01
     400.00     1.584E+01     1.584E+01  -1.238E+01   4.379E-12    2.079E+01
     500.00     1.598E+01     1.598E+01  -1.205E+01   2.395E-10    2.201E+01
     600.00     1.614E+01     1.614E+01  -1.176E+01   3.541E-09    2.320E+01
     800.00     1.644E+01     1.644E+01  -1.134E+01   1.075E-07    2.551E+01
    1000.00     1.668E+01     1.668E+01  -1.106E+01   8.631E-07    2.774E+01
    1200.00     1.691E+01     1.691E+01  -1.086E+01   3.529E-06    2.994E+01
    1500.00     1.729E+01     1.729E+01  -1.058E+01   1.478E-05    3.315E+01
    2000.00     1.805E+01     1.805E+01  -1.014E+01   6.479E-05    3.833E+01
```

The model fitted is for uni-molecular reaction.

The 3 parameters for the model equation of $A(T) = Aprime * T^n * \exp(-Ea/RT)$
      Aprime = 3.4675E+05   n =   1.68617   Ea =   1.5309E+04

```
Temp(K)         AF(T)           T_K^n           k_calc(T)         k_fit
300.00      1.045E+10        1.503E+04         3.673E-02       3.662E-02
400.00      1.643E+10        2.441E+04         3.649E+01       3.653E+01
500.00      2.421E+10        3.556E+04         2.495E+03       2.506E+03
600.00      3.355E+10        4.835E+04         4.427E+04       4.445E+04
800.00      5.545E+10        7.854E+04         1.792E+06       1.789E+06
1000.00      7.968E+10        1.144E+05         1.798E+07       1.789E+07
1200.00      1.059E+11        1.556E+05         8.823E+07       8.785E+07
1500.00      1.526E+11        2.267E+05         4.619E+08       4.622E+08
2000.00      2.532E+11        3.682E+05         2.700E+09       2.711E+09
```


        THERMODYNAMIC ANALYSIS for REACTION
```
Rx          C2.CQCQ     = TS10
Hf {Kcal/mol}  -25.140     -10.210
S {cal/mol K}  125.490    114.330


dHr {kcal/mol}  (298K) =       14.93   dHr avg (298., 1500. K) =      15.62
dU (dE) {kcal/mol} (") =        14.93   dUr avg (298., 1500. K) =      15.62
dSr {cal/mol K}  ( " ) =       -11.16   dSr avg (298., 1500. K) =      -9.82
dGr  {kcal/mol}  ( " ) =        18.26   dGr avg (298., 1500. K) =      24.45
       Kc       ( " ) =   4.129E-14    Kc avg (298., 1500. K ) =   1.136E-06
Fit Af/Ar     : A = 1.073E-06 n =  1.46 alpha = 5.317E-04 avg error   3.45 %
Fit Af/Ar w/ddU: A = 3.319E-09 n =  2.54 alpha = 1.378E-03 avg error  10.27 %


     T (K)  dH(Kcal/mol)  dU(Kcal/mol) dS(cal/mol K)      Kc       dG(Kcal/mol)
     300.00     1.494E+01     1.494E+01  -1.114E+01   4.824E-14    1.828E+01
     400.00     1.522E+01     1.522E+01  -1.033E+01   2.673E-11    1.935E+01
     500.00     1.549E+01     1.549E+01  -9.729E+00   1.270E-09    2.035E+01
     600.00     1.573E+01     1.573E+01  -9.278E+00   1.741E-08    2.130E+01
     800.00     1.614E+01     1.614E+01  -8.683E+00   4.913E-07    2.309E+01
    1000.00     1.646E+01     1.646E+01  -8.329E+00   3.818E-06    2.479E+01
    1200.00     1.673E+01     1.673E+01  -8.082E+00   1.535E-05    2.643E+01
    1500.00     1.717E+01     1.717E+01  -7.758E+00   6.350E-05    2.881E+01
    2000.00     1.804E+01     1.804E+01  -7.256E+00   2.768E-04    3.256E+01
```

The model fitted is for uni-molecular reaction.

The 3 parameters for the model equation of $A(T) = Aprime * T^n * \exp(-Ea/RT)$
      Aprime = 1.2770E+05   n =   1.98347   Ea =   1.4479E+04

```
Temp(K)         AF(T)           T_K^n           k_calc(T)         k_fit
300.00      2.294E+10        8.190E+04         3.015E-01       2.957E-01
```

```
  400.00      4.602E+10      1.449E+05      2.228E+02      2.269E+02
  500.00      7.788E+10      2.256E+05      1.323E+04      1.350E+04
  600.00      1.173E+11      3.239E+05      2.176E+05      2.199E+05
  800.00      2.109E+11      5.731E+05      8.189E+06      8.103E+06
 1000.00      3.150E+11      8.921E+05      7.955E+07      7.799E+07
 1200.00      4.281E+11      1.281E+06      3.838E+08      3.771E+08
 1500.00      6.300E+11      1.994E+06      1.985E+09      1.978E+09
 2000.00      1.081E+12      3.528E+06      1.153E+10      1.179E+10
```

```
       THERMODYNAMIC ANALYSIS for REACTION
Rx          C2CCO.CHO  = TS11
Hf {Kcal/mol}  -40.630     -36.380
S {cal/mol K}   96.150      94.190
```

```
dHr {kcal/mol}   (298K) =        4.25    dHr avg (298., 1500. K) =        3.93
dU (dE) {kcal/mol} (")  =        4.25    dUr avg (298., 1500. K) =        3.93
dSr {cal/mol K} ( " )   =       -1.96    dSr avg (298., 1500. K) =       -2.53
dGr {kcal/mol}  ( " )   =        4.83    dGr avg (298., 1500. K) =        6.20
         Kc     ( " )   =    2.858E-04   Kc avg (298., 1500. K ) =    3.116E-02
Fit Af/Ar      : A = 1.448E+01 n =  -.64 alpha =-1.940E-04 avg error    2.17 %
Fit Af/Ar w/ddU: A = 3.171E+02 n = -1.21 alpha =-6.164E-04 avg error    2.91 %
```

```
      T (K)   dH(Kcal/mol)  dU(Kcal/mol) dS(cal/mol K)      Kc       dG(Kcal/mol)
      300.00    4.249E+00     4.249E+00    -1.963E+00    2.987E-04    4.838E+00
      400.00    4.179E+00     4.179E+00    -2.162E+00    1.754E-03    5.044E+00
      500.00    4.075E+00     4.075E+00    -2.392E+00    4.962E-03    5.271E+00
      600.00    3.955E+00     3.955E+00    -2.611E+00    9.739E-03    5.522E+00
      800.00    3.712E+00     3.712E+00    -2.962E+00    2.181E-02    6.081E+00
     1000.00    3.502E+00     3.502E+00    -3.197E+00    3.435E-02    6.699E+00
     1200.00    3.336E+00     3.336E+00    -3.349E+00    4.576E-02    7.354E+00
     1500.00    3.143E+00     3.143E+00    -3.493E+00    6.006E-02    8.382E+00
     2000.00    2.919E+00     2.919E+00    -3.623E+00    7.746E-02    1.017E+01
```

The model fitted is for uni-molecular reaction.

The 3 parameters for the model equation of $A(T) = Aprime * T^n * exp(-Ea/RT)$
      Aprime = 2.3174E+11   n =   .49609   Ea =   4.5585E+03

```
Temp(K)         AF(T)            T_K^n          k_calc(T)          k_fit
300.00        2.328E+12        1.694E+01        1.867E+09        1.874E+09
400.00        2.807E+12        1.954E+01        1.462E+10        1.462E+10
500.00        3.125E+12        2.182E+01        5.170E+10        5.143E+10
600.00        3.360E+12        2.389E+01        1.218E+11        1.210E+11
800.00        3.754E+12        2.755E+01        3.635E+11        3.629E+11
1000.00       4.169E+12        3.078E+01        7.157E+11        7.193E+11
1200.00       4.635E+12        3.369E+01        1.144E+12        1.154E+12
1500.00       5.389E+12        3.764E+01        1.877E+12        1.890E+12
2000.00       6.728E+12        4.341E+01        3.228E+12        3.195E+12
```

```
       THERMODYNAMIC ANALYSIS for REACTION
Rx          C2CCO.CHO  = TS12
Hf {Kcal/mol}  -40.630     -11.600
S {cal/mol K}   96.150      93.560
```

```
dHr {kcal/mol}   (298K) =       29.03    dHr avg (298., 1500. K) =       29.52
dU (dE) {kcal/mol} (")  =       29.03    dUr avg (298., 1500. K) =       29.52
dSr {cal/mol K} ( " )   =       -2.59    dSr avg (298., 1500. K) =       -1.70
dGr {kcal/mol}  ( " )   =       29.80    dGr avg (298., 1500. K) =       31.04
         Kc     ( " )   =    1.421E-22   Kc avg (298., 1500. K ) =    2.837E-08
Fit Af/Ar      : A = 3.553E-03 n =   .76 alpha =-1.023E-04 avg error     .25 %
Fit Af/Ar w/ddU: A = 1.054E-04 n =  1.40 alpha = 2.056E-04 avg error    1.75 %
```

```
      T (K)   dH(Kcal/mol)  dU(Kcal/mol) dS(cal/mol K)      Kc       dG(Kcal/mol)
      300.00    2.903E+01     2.903E+01    -2.580E+00    1.922E-22    2.981E+01
      400.00    2.919E+01     2.919E+01    -2.119E+00    3.847E-17    3.004E+01
      500.00    2.935E+01     2.935E+01    -1.763E+00    6.075E-14    3.023E+01
      600.00    2.951E+01     2.951E+01    -1.472E+00    8.463E-12    3.040E+01
      800.00    2.984E+01     2.984E+01    -1.006E+00    4.251E-09    3.064E+01
     1000.00    3.017E+01     3.017E+01    -6.317E-01    1.850E-07    3.080E+01
```

```
  1200.00    3.052E+01    3.052E+01    -3.114E-01    2.357E-06    3.090E+01
  1500.00    3.107E+01    3.107E+01     9.812E-02    3.115E-05    3.093E+01
  2000.00    3.197E+01    3.197E+01     6.160E-01    4.370E-04    3.074E+01
```

The model fitted is for uni-molecular reaction.

The 3 parameters for the model equation of A(T) = Aprime * T^n * exp(-Ea/RT)
     Aprime = 1.9661E+07   n =   1.84217   Ea =   2.8516E+04

```
Temp(K)        AF(T)            T_K^n          k_calc(T)         k_fit
 300.00      1.706E+12        3.658E+04        1.202E-09       1.205E-09
 400.00      2.869E+12        6.215E+04        3.206E-04       3.200E-04
 500.00      4.290E+12        9.375E+04        6.329E-01       6.310E-01
 600.00      5.961E+12        1.312E+05        1.058E+02       1.056E+02
 800.00      1.005E+13        2.228E+05        7.086E+04       7.090E+04
1000.00      1.516E+13        3.361E+05        3.855E+06       3.867E+06
1200.00      2.138E+13        4.703E+05        5.893E+07       5.916E+07
1500.00      3.284E+13        7.094E+05        9.737E+08       9.757E+08
2000.00      5.682E+13        1.205E+06        1.821E+10       1.812E+10
```

          THERMODYNAMIC ANALYSIS for REACTION
Rx   C2C.CHO   = TS13
Hf {Kcal/mol} -19.160   23.560
S {cal/mol K}   79.120   77.430

```
dHr {kcal/mol}   (298K) =      42.72    dHr avg (298., 1500. K) =        42.94
dU (dE) {kcal/mol} (")  =      42.72    dUr avg (298., 1500. K) =        42.94
dSr {cal/mol K}  ( " )  =      -1.69    dSr avg (298., 1500. K) =        -1.27
dGr {kcal/mol}   ( " )  =      43.22    dGr avg (298., 1500. K) =        44.08
         Kc      ( " )  =   2.058E-32   Kc avg (298., 1500. K ) =     1.926E-11
Fit Af/Ar     : A = 9.961E-03 n =   .69 alpha = 5.731E-04 avg error    1.22 %
Fit Af/Ar w/ddU: A = 6.983E-04 n =  1.19 alpha = 1.136E-03 avg error    2.73 %
```

```
   T (K)  dH(Kcal/mol)  dU(Kcal/mol) dS(cal/mol K)      Kc       dG(Kcal/mol)
   300.00     4.272E+01     4.272E+01   -1.686E+00    3.210E-32     4.323E+01
   400.00     4.280E+01     4.280E+01   -1.453E+00    1.969E-24     4.338E+01
   500.00     4.290E+01     4.290E+01   -1.246E+00    9.474E-20     4.352E+01
   600.00     4.298E+01     4.298E+01   -1.084E+00    1.273E-16     4.363E+01
   800.00     4.312E+01     4.312E+01   -8.917E-01    1.060E-12     4.383E+01
  1000.00     4.317E+01     4.317E+01   -8.330E-01    2.415E-10     4.400E+01
  1200.00     4.315E+01     4.315E+01   -8.481E-01    9.023E-09     4.417E+01
  1500.00     4.306E+01     4.306E+01   -9.124E-01    3.356E-07     4.443E+01
  2000.00     4.287E+01     4.287E+01   -1.020E+00    1.235E-05     4.492E+01
```

The model fitted is for uni-molecular reaction.

The 3 parameters for the model equation of A(T) = Aprime * T^n * exp(-Ea/RT)
     Aprime = 2.5423E+09   n =   1.20614   Ea =   4.2684E+04

```
Temp(K)        AF(T)            T_K^n          k_calc(T)         k_fit
 300.00      2.676E+12        9.722E+02        2.007E-19       1.974E-19
 400.00      4.012E+12        1.375E+03        1.641E-11       1.662E-11
 500.00      5.564E+12        1.800E+03        9.870E-07       1.005E-06
 600.00      7.245E+12        2.243E+03        1.591E-03       1.612E-03
 800.00      1.064E+13        3.173E+03        1.767E+01       1.759E+01
1000.00      1.370E+13        4.154E+03        5.033E+03       4.947E+03
1200.00      1.632E+13        5.175E+03        2.256E+05       2.212E+05
1500.00      1.975E+13        6.773E+03        1.049E+07       1.039E+07
2000.00      2.493E+13        9.583E+03        5.145E+08       5.273E+08
```

Table B.4 Detailed Reaction Mechanism for Model OH Formation [aa]

No.	Reactions	A	n	E_a	ref
1	$C_3CCI \Longleftrightarrow C_3CC \bullet + I$	1.00E+16	0.0	51370	a
2	$C_3CCI + OH \Longleftrightarrow C_3 \bullet CCI + H_2O$	1.08E+07	2.0	2415	a
3	$C_3CCI + H \Longleftrightarrow H_2 + C_3 \bullet CCI$	2.16E+09	1.5	8973	a
4	$C_3 \bullet CCI \Longleftrightarrow C_2C*C + CH_2I$	1.57E+26	-4.2	32137	b
5	$CH_2I + O_2 \Longleftrightarrow CH_2O + IO$	1.00E+13	0.0	29000	a
6	$CH_2I + I \Longleftrightarrow CH_2I_2$	8.00E+13	0.0	0	c
7	$CH_3 + I \Longleftrightarrow CH_3I$	7.05E+12	0.0	0	d
8	$C_3CC \bullet + O_2 \Longleftrightarrow C_3CCOO \bullet$	4.85E+39	-9.1	8039	b
9	$C_3CC \bullet + O_2 \Longleftrightarrow C_3CCHO + OH$	7.09E+25	-4.2	21757	b
10	$C_3CC \bullet + O_2 \Longleftrightarrow C_3 \bullet CCQ$	2.17+166	-50.0	52203	b
11	$C_3CC \bullet + O_2 \Longleftrightarrow C_2CYCCOC + OH$	1.03E+55	-12.7	29656	b
12	$C_3CC \bullet + O_2 \Longleftrightarrow C*C(C)CQ + CH_3$	7.04E+49	-11.2	32249	b
13	$C_3CC \bullet + O_2 \Longleftrightarrow C_2C*C + CH_2O + OH$	2.03E+46	-10.1	32343	b
14	$C_3CC \bullet + O_2 \Longleftrightarrow CCC \bullet (C)COOH$	4.72E+55	-14.1	55712	b
15	$C_3CCOO \bullet \Longleftrightarrow C_3CCHO + OH$	8.33E+35	-7.3	51070	b
16	$C_3CCOO \bullet \Longleftrightarrow C_3 \bullet CCQ$	2.52E+08	1.0	23989	b
17	$C_3 \bullet CCQ \Longleftrightarrow C_2CYCCOC + OH$	4.81E+36	-7.9	23960	b
18	$C_3 \bullet CCQ \Longleftrightarrow C*C(C)CQ + CH_3$	2.04E+56	-14.2	38563	b
19	$C_3 \bullet CCQ \Longleftrightarrow C_2C*C + CH_2O + OH$	1.49E+53	-13.2	38842	b
20	$C_3 \bullet CCQ \Longleftrightarrow CCC \bullet (C)COOH$	1.31+102	-31.1	74604	b
21	$C_2CYCCOC + OH \Longleftrightarrow C_2CYCCOC \bullet + H_2O$	4.80E+06	2.0	-120	a
22	$C_2CYCCOC \bullet \Rightarrow C_3 \bullet CCHO$	4.08E+78	-20.2	45563	b
23	$C_2CYCCOC \bullet \Rightarrow C_2C*COC \bullet$	6.69E+68	-19.0	46097	b
24	$C_3 \bullet CCHO \Longleftrightarrow C_2C*C + HCO$	7.13E+39	-8.8	28753	b
25	$C_3 \bullet CCHO \Longleftrightarrow C*C(C)CHO + CH_3$	3.48E+57	-14.2	42446	b
26	$C_2C*COC \bullet \Longleftrightarrow C_2C*C \bullet + CH_2O$	4.13E+39	-8.2	49345	b
27	$C_2C*C \bullet + O_2 \Longleftrightarrow C_2C*CQ \bullet$	2.83E+62	-15.8	16487	e₁
28	$C_2C*C \bullet + O_2 \Longleftrightarrow C_2C \bullet C*O + O$	7.03E+39	-7.9	16137	e₁
29	$C_2C*C \bullet + O_2 \Longleftrightarrow C_2.C*CQ$	1.02E+32	-12.4	22545	e₁
30	$C_2C*C \bullet + O_2 \Longleftrightarrow C*C(C)C*O + OH$	7.07E+35	-7.5	15904	e₁
31	$C_2C*C \bullet + O_2 \Longleftrightarrow C*C*CQ + CH3$	6.11E-17	6.8	13033	e₁
32	$C_2C*C \bullet + O_2 \Longleftrightarrow C_2C \bullet CYCOO$	1.14E+56	-15.9	13744	e₁
33	$C_2C*C \bullet + O_2 \Longleftrightarrow C_2C*O + HCO$	3.45E+34	-7.0	16395	e₁
34	$C_2C*C \bullet + O_2 \Longleftrightarrow C_2CYCOOC \bullet$	1.69E+52	-16.0	12305	e₁
35	$C_2C*C \bullet + O_2 \Longleftrightarrow C_2C*O + HCO$	1.13E+40	-8.7	15835	e₁
36	$C_2C*CQ \bullet . \Longleftrightarrow C_2C*C*O + O$	2.92E+59	-14.4	50439	e₁
37	$C_2C*CQ \bullet \Longleftrightarrow C_2 \bullet C*CQ$	4.24E+49	-12.2	47059	e₁
38	$C_2C*CQ \bullet \Longleftrightarrow C_2C \bullet CYCOO$	5.36E+32	-6.5	30293	e₁
39	$C_2C*CQ \bullet \Longleftrightarrow C_2CYCOOC \bullet$	6.88E+48	-11.8	44333	e₁
40	$C_2 \bullet C*CQ \Longleftrightarrow C*C(C)C*O + OH$	2.90E+13	-1.1	1416	e₁
41	$C_2 \bullet C*CQ \Longleftrightarrow C*C*CQ + CH_3$	1.93E-32	-0.1	55647	e₁
42	$C_2C \bullet CYCOO \Longleftrightarrow C_2C*O + HCO$	2.43E+39	-11.4	25432	e₁

43	$C_2CYCOOC\bullet <=> C_2C*O+HCO$	3.19E+52	-12.8	26592	e_1
44	$C_3\bullet CCQ+O_2 <=> C_2CCQCQ\bullet$	2.42+124	-35.3	39761	b
45	$C_3\bullet CCQ+O_2 <=> C_2CCQCHO+OH$	1.20E+54	-12.3	25565	b
46	$C_3\bullet CCQ+O_2 <=> C_2CCQCHO+OH$	2.90E+43	-10.1	29722	b
47	$C_3\bullet CCQ+O_2 <=> C_2CCO\bullet CQ\bullet+OH$	3.81E+49	-10.9	29988	b
48	$C_3\bullet CCQ+O_2 <=> C_2\bullet CQCQ$	1.98+236	-72.0	77237	b
49	$C_3\bullet CCQ+O_2 <=> CCQCCOC+OH$	7.38+105	-28.6	53434	b
50	$C_3\bullet CCQ+O_2 <=> C*C(C)CQ+CH_2O+OH$	5.75+107	-28.9	53893	b
51	$C_2CCQCQ\bullet <=> C_2CCQCHO+OH$	2.79E+32	-6.1	31485	b
52	$C_2CCQCQ\bullet <=> C_2CCQCHO+OH$	1.07E+89	-24.4	68021	b
53	$C_2CCQCQ\bullet <=> C_2CCQCHO+OH$	4.12+104	-28.1	72157	b
54	$C_2CCQCQ\bullet <=> C_2\bullet CQCQ$	1.23E+41	-9.4	34718	b
55	$C_2\bullet CQCQ <=> CCQCCOC+OH$	5.93E+31	-6.6	24397	b
56	$C_2\bullet CQCQ <=> C*C(C)CQ+CH_2O+OH$	1.70E+30	-5.9	23280	b
57	$C_2CCQCHO <=> C2CCO\bullet CHO+OH$	2.26E+25	-3.1	48703	b
58	$C_2CCO\bullet CHO <=> C_2C(CHO)_2+H$	5.40E+18	-1.7	32647	b
59	$C_2CCO\bullet CHO <=> C_2C\bullet CHO+CH_2O$	2.32E+11	0.5	4560	b
60	$C_2C\bullet CHO <=> C*C(C)CHO+H$	1.94E+30	-5.4	49854	b
61	$C_2C\bullet CHO <=> C*CC+HCO$	2.40E+30	-5.1	45570	b
62	$C*C(C)COOH <=> C*C(C)CO\bullet+OH$	6.84E+45	-9.6	53480	b
63	$C*C(C)CO\bullet => C*C(C)CHO+H$	1.28E+23	-4.0	13622	b
64	$C_3CC\bullet <=> C_2C*C+CH_3$	5.70E+34	-6.6	38207	b
65	$C_2C*C+OH <=> C_2C\bullet COH$	5.03E+60	-15.1	15552	e_2
66	$C_2C*C+OH <=> C_2CCO\bullet$	4.48E+50	-16.5	13800	e_2
67	$C_2C*C+OH <=> C_2CC*O+H$	1.97E+28	-5.4	18402	e_2
68	$C_2C*C+OH <=> CC\bullet C+CH_2O$	2.56E+33	-6.6	16652	e_2
69	$C_2C*C+OH <=> C_2\bullet CCOH$	6.01E+60	-16.4	29006	e_2
70	$C_2C*C+OH <=> C*CC+C\bullet H_2OH$	2.72E+40	-9.4	28236	e_2
71	$C_2C\bullet COH <=> C_2CCO\bullet$	2.99E+46	-11.3	41056	e_2
72	$C_2CCO\bullet <=> C_2CC*O+H$	4.00E+25	-6.8	17987	e_2
73	$C_2CCO\bullet <=> CC\bullet C+CH_2O$	1.86E+32	-6.8	14390	e_2
74	$C_2\bullet CCOH <=> C*CC+C\bullet H_2OH$	1.93E+41	-8.8	36044	e_2
75	$C_2\bullet CCOH <=> C_2CCO\bullet$	4.33E+25	-4.8	27397	e_2
76	$C_2C*C+OH <=> C_3\bullet COH$	1.08E+63	-15.8	16152	e_2
77	$C_2C*C+OH <=> C_3CO\bullet$	4.63E+42	-15.5	14354	e_2
78	$C_2C*C+OH <=> C_2C*O+CH_3$	4.95E+36	-7.6	16849	e_2
79	$C_3\bullet COH <=> C_3CO\bullet$	1.28E+54	-13.6	43214	e_2
80	$C_3CO\bullet <=> C_2C*O+CH_3$	2.71E+26	-5.1	10840	e
81	$C_2C\bullet COH+O_2 <=> C_2CQ\bullet COH$	4.73E+70	-18.3	20096	b
82	$C_2C\bullet COH+O_2 <=> C*C(C)COH+HO_2$	6.90E+37	-7.5	19851	b
83	$C_2C\bullet COH+O_2 <=> C_2C*COH+HO_2$	2.54E+42	-9.0	20150	b
84	$C_2C\bullet COH+O_2 <=> C_2CQCO\bullet$	5.43E+49	-14.5	13613	b
85	$C_2C\bullet COH+O_2 <=> C_2C*O+CH_2O+OH$	5.14E+41	-8.7	18330	b
86	$C_2C\bullet COH+O_2 <=> C_2\bullet CQCOH$	5.15+115	-32.5	46957	b

87	$C_2C{\bullet}COH+O_2 \Longleftrightarrow C{*}C(C)Q+C{\bullet}H_2OH$	5.91E+63	-15.6	36375	b
88	$C_2C{\bullet}COH+O_2 \Longleftrightarrow C{*}C(C)COH+HO_2$	2.22E+61	-14.9	34645	b
89	$C_2C{\bullet}COH+O_2 \Longleftrightarrow C_2CQC{\bullet}OH$	4.26+158	-46.2	56824	b
90	$C_2C{\bullet}COH+O_2 \Longleftrightarrow C_2C{*}COH+HO_2$	1.59E+65	-15.9	30672	b
91	$C_2CQ{\bullet}COH \Longleftrightarrow C{*}C(C)COH+HO_2$	1.47E+30	-5.4	39896	b
92	$C_2CQ{\bullet}COH \Longleftrightarrow C_2C{*}COH+HO_2$	3.37E+37	-7.8	41899	b
93	$C_2CQ{\bullet}COH \Longleftrightarrow C_2CQCO{\bullet}$	7.46E+14	-1.0	24636	b
94	$C_2CQ{\bullet}COH \Longleftrightarrow C_2{\bullet}CQCOH$	2.65E+44	-10.2	47925	b
95	$C_2CQ{\bullet}COH \Longleftrightarrow C_2CQC{\bullet}OH$	1.98E+29	-5.4	35761	b
96	$C_2CQCO{\bullet} \Longleftrightarrow C_2C{*}O+CH_2O+OH$	6.90E+38	-9.0	16669	b
97	$C_2{\bullet}CQCOH \Longleftrightarrow C{*}C(C)Q+C{\bullet}H_2OH$	1.39E+55	-13.2	40389	b
98	$C_2{\bullet}CQCOH \Longleftrightarrow C{*}C(C)COH+HO_2$	1.49E+48	-11.2	33692	b
99	$C_2CQC{\bullet}OH \Longleftrightarrow C_2C{*}COH+HO_2$	2.42E+38	-8.5	23759	b
100	$C_3{\bullet}COH+O_2 \Longleftrightarrow C_2COHCQ{\bullet}$	4.92E+56	-13.9	15170	b
101	$C_3{\bullet}COH+O_2 \Longleftrightarrow C_2CO{\bullet}CQ$	1.57E+30	-8.3	7340	b
102	$C_3{\bullet}COH+O_2 \Longleftrightarrow C_2C{*}O+CH_2O+OH$	6.98E+38	-8.1	18972	b
103	$C_3{\bullet}COH+O_2 \Longleftrightarrow CH_3+CC{*}OCQ$	6.06E+40	-8.8	21436	b
104	$C_3{\bullet}COH+O_2 \Longleftrightarrow C_2{\bullet}COHCQ$	5.27+174	-50.9	65216	b
105	$C_3{\bullet}COH+O_2 \Longleftrightarrow C{*}C(C)CQ+OH$	1.67E+68	-16.6	40006	b
106	$C_3{\bullet}COH+O_2 \Longleftrightarrow C{*}C(C)OH+CH_2O+OH$	3.78E+59	-14.0	35077	b
107	$C_2COHCQ{\bullet} \Longleftrightarrow C_2CO{\bullet}CQ$	4.61E+14	-1.3	25483	b
108	$C_2COHCQ{\bullet} \Longleftrightarrow C_2{\bullet}COHCQ$	1.34E+20	-2.8	31200	b
109	$C_2CO{\bullet}CQ \Longleftrightarrow C_2C{*}O+CH_2O+OH$	3.48E+47	-11.5	23382	b
110	$C_2CO{\bullet}CQ \Longleftrightarrow CH_3+CC{*}OCQ$	3.47E+46	-11.6	23523	b
111	$C_2{\bullet}COHCQ \Longleftrightarrow C{*}C(C)CQ+OH$	3.33E+64	-15.9	46543	b
112	$C_2{\bullet}COHCQ \Longleftrightarrow C{*}C(C)OH+CH_2O+OH$	6.61E+34	-7.2	29287	b
113	$C_2C{*}C+CH_3 \Longleftrightarrow CCC{\bullet}C_2$	2.51E+11	0.0	6691	f
114	$CCC{\bullet}C_2+O_2 \Longleftrightarrow C_2COO{\bullet}CC$	2.71+109	-30.9	31090	b
115	$CCC{\bullet}C_2+O_2 \Longleftrightarrow CCC{*}(C)C+HO_2$	1.64E+51	-12.3	18955	b
116	$CCC{\bullet}C_2+O_2 \Longleftrightarrow CC{*}CC_2+HO_2$	3.16E+49	-11.9	18285	b
117	$CCC{\bullet}C_2+O_2 \Longleftrightarrow C_2CQCC{\bullet}$	1.07E+79	-24.3	17586	b
118	$CCC{\bullet}C_2+O_2 \Longleftrightarrow C_2CYCCCO+OH$	3.02E+29	-5.9	15794	b
119	$CCC{\bullet}C_2+O_2 \Longleftrightarrow C_2{\bullet}CQCC$	7.01+152	-45.7	52226	b
120	$CCC{\bullet}C_2+O_2 \Longleftrightarrow CCC{*}(C)C+HO_2$	6.70E+54	-13.7	25414	b
121	$CCC{\bullet}C_2+O_2 \Longleftrightarrow C_2CQC{\bullet}C$	2.64E+98	-29.8	27851	b
122	$CCC{\bullet}C_2+O_2 \Longleftrightarrow CC{*}CC_2+HO_2$	1.31E+44	-10.5	17506	b
123	$C_2COO{\bullet}CC \Longleftrightarrow CCC{*}(C)C+HO_2$	6.46E+66	-16.9	48457	b
124	$C_2COO{\bullet}CC \Longleftrightarrow CC{*}CC_2+HO_2$	4.79E+72	-18.8	51113	b
125	$C_2COO{\bullet}CC \Longleftrightarrow C_2CQCC{\bullet}$	3.17E+48	-11.4	37954	b
126	$C_2COO{\bullet}CC \Longleftrightarrow C_2{\bullet}CQCC$	2.22E+78	-21.0	57149	b
127	$C_2COO{\bullet}CC \Longleftrightarrow C_2CQC{\bullet}C$	1.73E+76	-20.2	54123	b
128	$C_2CQCC{\bullet} \Longleftrightarrow C2CYCOCC+OH$	4.60E+37	-9.7	19612	b
129	$C_2{\bullet}CQCC \Longleftrightarrow CCC{*}(C)C+HO_2$	2.08E+75	-19.5	40298	b
130	$C_2CQC{\bullet}C \Longleftrightarrow CC{*}CC_2+HO_2$	9.45E+57	-14.4	28532	b

131	$C_2C^*C+OH \Leftrightarrow C_2 \cdot C^*C+H_2O$	7.80E+12	0.0	0	g
132	$C_2C^*C+O_2 \Leftrightarrow C_2 \cdot C^*C+HO_2$	4.79E+12	0.0	38528	h
133	$C_2C^*C+H \Leftrightarrow C_2 \cdot CC$	6.45E+13	0.0	2700	a
134	$C_2C^*C+H \Leftrightarrow H_2+C_2 \cdot C^*C$	5.50E+13	0.0	7600	a
135	$C_2C^*C+CH_3 \Leftrightarrow CH_4+C_2 \cdot C^*C$	1.86E+06	1.9	1219	a
136	$C_3CC+OH \Leftrightarrow C_3CC \cdot +H_2O$	1.44E+07	2.0	2115	a
137	$C_3CC+O \Leftrightarrow C_3CC \cdot +OH$	9.20E+13	0.0	7154	i
138	$C_3CC+O_2 \Leftrightarrow C_3CC \cdot +HO_2$	1.03E+13	0.0	55640	j
139	$C_3CC+HO_2 \Leftrightarrow C_3CC.+H_2O_2$	3.01E+04	2.5	15500	k
140	$C_3CC \cdot +H \Leftrightarrow C_3CC$	1.00E+14	0.0	0	l
141	$C_3CC \cdot +OH \Leftrightarrow C_3CCOH$	1.00E+13	0.0	0	a
142	$C_3CC \cdot +O \Leftrightarrow C_3CCO \cdot$	1.54E+22	-8.3	8333	b
143	$C_3CC \cdot +O \Leftrightarrow C_3CCHO+H$	6.33E+11	0.1	1084	b
144	$C_3CC \cdot +O \Leftrightarrow C_3C \cdot +CH_2O$	2.04E+14	0.0	0	b
145	$C_3CC \cdot +O \Leftrightarrow C_3 \cdot CCOH$	1.72E-25	4.9	-10668	b
146	$C_3CC \cdot +O \Leftrightarrow C_2C^*C+C \cdot H_2OH$	1.06E+11	0.1	654	b
147	$C_3CC \cdot +O \Leftrightarrow C^*C(C)COH+CH_3$	2.18E+09	0.1	934	b
148	$C_3CC \cdot +O \Leftrightarrow C_3CC \cdot OH$	4.69+106	-32.4	23221	b
149	$C_3CC \cdot +O \Leftrightarrow C_3CCHO+H$	4.06E+11	0.0	1128	b
150	$C_3CCO \cdot \Leftrightarrow C_3CCHO+H$	2.28E+50	-15.3	33867	b
151	$C_3CCO \cdot \Leftrightarrow C_3C \cdot +CH_2O$	3.97E+59	-14.9	29772	b
152	$C_3CCO \cdot \Leftrightarrow C_3 \cdot CCOH$	8.37E+51	-14.9	30488	b
153	$C_3CCO \cdot \Leftrightarrow C_3CC \cdot OH$	2.36E+50	-15.3	33557	b
154	$C_3 \cdot CCOH \Leftrightarrow C_2C^*C+C \cdot H_2OH$	3.83E+88	-23.1	51259	b
155	$C_3 \cdot CCOH \Leftrightarrow C^*C(C)COH+CH_3$	2.58E+86	-23.1	51253	b
156	$C_3CC \cdot OH \Leftrightarrow C_3CCHO+H$	6.03E+14	-0.7	31424	b
157	$C_3CCOO \cdot +C_3CCOO \cdot \Leftrightarrow C_3CCO \cdot +C_3CCO \cdot +O_2$	2.41E+11	0.0	0	m
158	$C_3CCOO \cdot +C_3CCOO \cdot \Leftrightarrow C_3CCHO+C_3CCOH+O_2$	3.61E+11	0.0	0	m
159	$C_3CCOO \cdot +HO_2 \Leftrightarrow C_3CCOOH+ O_2$	8.61E+10	0.0	-2742	n
160	$C_3CCOO \cdot +OH \Leftrightarrow C_3CCO \cdot + HO_2$	2.41E+11	0.0	0	a
161	$C_3CCOOH \Leftrightarrow C_3CCO \cdot +OH$	1.67E+56	-12.8	57175	b
162	$C_3CCOH+H \Leftrightarrow C_3 \cdot CCOH+H_2$	2.16E+09	1.5	7400	a
163	$C_3CCOH+H \Leftrightarrow C_3CC \cdot OH+H_2$	4.80E+08	1.5	3357	a
164	$C_3CCOH+H \Leftrightarrow C_3CCO \cdot +H_2$	2.40E+08	1.5	9324	a
165	$C_3CCOH+O \Leftrightarrow C_3 \cdot CCOH+OH$	1.53E+09	1.5	5410	a
166	$C_3CCOH+O \Leftrightarrow C_3CC \cdot OH+OH$	3.40E+08	1.5	2186	a
167	$C_3CCOH+O \Leftrightarrow C_3CCO \cdot +OH$	1.70E+08	1.5	7630	a
168	$C_3CCOH+OH \Leftrightarrow C_3 \cdot CCOH+H_2O$	1.08E+07	2.0	1205	a
169	$C_3CCOH+OH \Leftrightarrow C_3CC \cdot OH+H_2O$	2.40E+06	2.0	537	a
170	$C_3CCOH+OH \Leftrightarrow C_3CCO \cdot +H_2O$	1.20E+06	2.0	2685	a
171	$C_3CCOH+CH_3 \Leftrightarrow C_3 \cdot CCOH+CH_4$	7.29E+06	1.9	10587	a
172	$C_3CCOH+CH_3 \Leftrightarrow C_3CC \cdot OH+CH_4$	1.62E+06	1.9	6544	a
173	$C_3CCOH+CH_3 \Leftrightarrow C_3CCO \cdot +CH_4$	8.10E+05	1.9	12511	a
174	$C_3CCOH+HO_2 \Leftrightarrow C_3 \cdot CCOH+H_2O_2$	9.64E+10	0.0	12579	a

175	$C_3CCOH+HO_2 <=> C_3CC\bullet OH+H_2O_2$	3.01E+04	2.5	15500	a
176	$C_3CCOH+O_2 <=> C_3\bullet CCOH+HO_2$	9.05E+13	0.0	53800	a
177	$C_3CCOH+O_2 <=> C_3CC\bullet OH+HO_2$	1.37E+13	0.0	47580	a
178	$C_3CCOH+O_2 <=> C_3CCO\bullet+HO_2$	3.10E+08	1.3	57560	a
179	$C_3CCHO+H <=> C_3\bullet CCHO+H_2$	2.16E+09	1.5	7400	a
180	$C_3CCHO+H <=> C_3CC\bullet *O+H_2$	4.00E+13	0.0	4206	a
181	$C_3CCHO+O <=> C_3\bullet CCHO+OH$	1.53E+09	1.5	5410	a
182	$C_3CCHO+O <=> C_3CC\bullet *O+OH$	1.70E+08	1.5	1729	a
183	$C_3CCHO+OH <=> C_3\bullet CCHO+H_2O$	1.08E+07	2.0	1205	a
184	$C_3CCHO+OH <=> C_3CC\bullet *O+H_2O$	9.51E+12	0.0	-622	a
185	$C_3CCHO+CH_3 <=> C_3\bullet CCHO+CH_4$	7.29E+06	1.9	10587	a
186	$C_3CCHO+CH_3 <=> C_3CC\bullet *O+CH_4$	8.10E+05	1.9	2819.5	a
187	$C_3CCHO+O_2 <=> C_3CC\bullet *O+HO_2$	3.01E+13	0.0	41850	a
188	$C_3CCHO+HO_2 <=> C_3\bullet CCHO+H_2O_2$	3.01E+04	2.5	15500	a
189	$C_3CCHO+HO_2 <=> C_3CC\bullet *O+H_2O_2$	3.01E+12	0.0	8000	a
190	$CH_3OO+H <=> CH_3OOH$	9.53E-20	4.1	-6261	b
190	$CH_3OO+H <=> CH_3O+OH$	9.64E+13	0.0	0	b
192	$CH_3OOH <=> CH_3O+OH$	6.22E+45	-10	52063	b
193	$C_3COO\bullet+H<=>C3COOH$	1.19E+67	-17.3	14992	b
194	$C_3COO\bullet+H<=>C3CO\bullet+OH$	1.06E+30	-4.8	8186	b
195	$C_3COOH<=>C3CO\bullet+OH$	5.04E+25	-3.1	51114	b
196	$CH_3OO+CH_3<=>COOC$	1.69E+71	-23.2	8560	b
197	$CH_3OO+CH_3<=>CH3O+CH_3O$	2.42E+13	0	1	b
198	$COOC<=>CH_3O+CH_3O$	2.75E+62	-14.9	53672	b
199	$CH_3OO+CH_3OO=>CH_3O+CH_3O+O_2$	2.47E+11	0.0	0	o
200	$CH_3+HO_2 <=> CH_3OOH$	6.98E+17	-7.5	6281	b
201	$CH_3+HO_2 <=> CH_3O+OH$	1.84E+13	0	2	b
202	$CH_3OOH <=>CH_3O+OH$	5.43E+45	-10	52062	b
203	$CH_3+CH_3<=>C_2H_5+H$	4.14E+32	-6.2	5671	b
204	$CH_3+CH_3<=>C_2H_4+H_2$	4.89E+20	-2.5	12422	b
205	$C_2H_6 <=> C_2H_5+H$	2.22E+16	-1.9	14880	b
206	$C_2H_6 <=> C_2H_4+H_2$	1.51E+42	-8.6	105111	b
207	$CH_3+CH_3 <=> C_2H_6$	5.52E+44	-10.4	109969	b
208	$CH_2O+O <=> OH+HCO$	4.16E+11	0.6	2762	o
209	$CH_2O+H <=> H_2+HCO$	2.29E+10	1.1	3279	o
210	$CH_2O+OH <=> H_2O+HCO$	3.49E+09	1.2	-447	o
211	$CH_2O+HO_2 <=> O_2+C\bullet H_2OH$	3.39E+12	0.0	19121	p
212	$CH_2O+CH_3 <=> HCO + CH_4$	4.09E+12	0.0	8843	o
213	$CH_2O+O2 <=> HO_2 + HCO$	6.03E+13	0.0	40658	o
214	$CH_2O + C\bullet H_2OH <=> CH_3OH+HCO$	5.49E+13	2.8	5862	q
215	$CH_2O + CH_3O <=> CH_3OH+HCO$	3.39E+12	0.0	19121	r
216	$CH_2O + C_3C\bullet <=> C_3C+HCO$	3.01E+11	0.0	6498	s
217	$CH_4+HO_2<=>H_2O_2+CH_3$	9.04E+12	0.0	24641	o
218	$CH_4+O<=>CH_3+OH$	6.92E+08	1.6	8485	o
219	$CH_3+O_2<=>CH_3OO$	8.61E+31	-6.6	4931	b
220	$CH_3+O_2<=>CH_2O+OH$	2.85E+08	1.0	12526	b

221	$CH_3+HO_2=CH_4+O_2$	3.61E+12	0.0	0	r
222	$CH_3O=CH_2O+H$	6.13E+28	-5.7	31351	b
223	$CH_3O+HO_2=CH_2O+H_2O_2$	3.01E+11	0.0	0	r
224	$CH_3+H <=> CH_4$	2.11E+14	0.0	0	m
225	$HCO+O_2 <=> HCQ\bullet{}^*O$	2.89E+28	-9.2	203	b
226	$HCO+O_2 <=> CO+HO_2$	9.32E+09	0.8	-694	b
227	$HCO+O_2 <=> O^*C\bullet{}OOH$	4.10E-02	-2.3	8558	b
228	$HCO+O_2 <=> CO+HO_2$	1.45E-02	3.7	4331	b
229	$HCO+O_2 <=> CO_2+OH$	4.75E+01	2.8	4818	b
230	$HCQ\bullet{}^*O <=> CO+HO_2$	1.22E+36	-7.8	28675	b
231	$HCQ\bullet{}^*O <=> O^*C\bullet{}OOH$	2.54E+24	-9.4	42771	b
232	$O^*C\bullet{}OOH <=> CO+HO_2$	4.69E+27	-6.9	23860	b
233	$O^*C\bullet{}OOH <=> CO_2+OH$	1.36E+32	-6.7	20498	b
234	$OH+HCO<=>CO+H_2O$	1.02E+14	0.0	0	o
235	$HCO <=> H+ CO$	1.57E+14	0.0	15758	t
236	$CO+O <=> CO_2$	6.17E+14	0.0	3001	r
237	$CO+OH<=>CO_2+H$	6.32E+06	1.5	-497	o
238	$CO+HO_2 <=>CO_2+OH$	1.51E+14	0.0	23650	r
239	$CO+O_2 <=> CO_2+O$	2.53E+12	0.0	47693	r
240	$H+O_2+M <=> HO_2+M$	6.17E+17	-0.8	0	t
241	$H+HO_2 <=> H_2+O_2$	1.25E+13	0.0	0	o
242	$H+HO_2 <=> OH+OH$	1.69E+14	0.0	874	o
243	$HO_2+H<=>H_2O+O$	3.01E+13	0.0	1721	o
244	$O+HO_2 <=> O_2+OH$	3.25E+13	0.0	0	o
245	$HO_2+OH<=>O_2+H_2O$	2.89E+13	0.0	-497	o
246	$HO_2+HO_2 <=> O_2+H_2O_2$	1.87E+12	0.0	1540	o
247	$H_2O_2+H <=> H_2+HO_2$	4.82E+13	0.0	7949	r
248	$H_2O_2+H<=>H_2O+OH$	2.41E+13	0.0	3974	r
249	$H_2O_2+O<=>OH+HO_2$	9.63E+06	2.0	3974	r
250	$H_2O_2+OH<=>HO_2+H_2O$	7.83E+12	0.0	1331	o
251	$H+O_2 <=> OH+O$	1.99E+14	0.0	16802	o
252	$H_2+OH <=> H_2O+H$	9.31E+11	1.6	3299	o
253	$OH+OH <=> O+H_2O$	1.51E+09	1.1	99	o
254	$OH+OH+M <=> H_2O_2+M$	2.90E+17	-0.76	0	o
255	$O+H_2 <=>OH+H$	5.11E+04	2.7	6280	o
256	$O+O+M <=> O2+M$	1.89E+13	0.0	-1788	r
257	$H+O+M <=> OH+M$	4.71E+18	-1.0	0	r
258	$OH =>X$	8.80E+01	0.0	0	u

[aa] $k = A\,T^n\,\exp(-E_a/RT)$. Units of s^{-1} for first order reactions, $cm^3\,mol^{-1}\,s^{-1}$ for second order reactions, $cm^6\,mol^{-2}\,s^{-1}$ for third order reactions. Ea in cal mol^{-1}. * Stands for double bond, Q stands for -OOH group, and Y stands for cyclic structure. [a] Estimated in this study by Dean and Bozzelli. [b] From QRRK calculation at P = 0.807 atm and T = 500 ~ 900 K. [c] Hunter, T.F.; Kristjansson, K. S J. Chem. Soc. Faraday Trans. 2: 78, 2067 (1982). [d] Mulenko, S.A. Rev. Roum. Phys. 32, 173 (1987). [e1] The reaction mechanism from reference 51. [e2] The reaction mechanism from reference 5. [f] Seres, L.; Nacsa, A.; Arthur, N.L. Int. J. Chem. Kinet. 26, 227-246 (1994). [g] Baker, R. R.; Baldwin, R. R.; Walker, R. W. J. Chem. Soc. Faraday Trans. 1: 74, 2229 (1978). [h] Ingham,T.; Walker, R.W.; Woolford, R. E. Symp. Int. Combust. Proc. 25, 767-774 (1994). [i] Herron, J.T. J. Phys. Chem. Ref. Data 17, 967 (1988). [j] Estimated from isobutane + O_2 reaction. [k] Estimated from isobutane + HO_2 reaction. [l] Allara D. L.; Shaw R. *J.*

Phys. Chem. Ref. Data 9, 523, (1980). [m] Wallington, T. J.; Andino, J. M.; Potts, A. R. Int. J. Chem. Kinet. 24, 649-663 (1992). [n] Rowley, D. M.; Lesclaux, R.; Lightfoot, P. D.; Hughes, K.; Hurley, M. D.; Rudy, S.; Wallington, T. J. J. Phys. Chem. 96, 7043-7048 (1992). [o] Baulch, D. L.; Cobos, C. J.; Cox, R. A.; Esser, C.; Frank, P.; Just, Th.; Kerr, J. A.; Pilling, M. J.; Troe, J.; Walker, R. W.; Warnatz, J. J. Phys. Chem. Ref. Data 21, 411-429 (1992). [p] Tsuboi, T.; Hashimoto, K. Combust. Flame 42, 61 (1981). [q] Tsang, W. J. Phys. Chem. Ref. Data 16, 471 (1987). [r] Tsang, W.; Hampson, R. F. J. Phys. Chem. Ref. Data 15, 1087 (1986). [s] Tsang, W. J. Phys. Chem. Ref. Data 19, 1-68 (1990). [t] Baulch,D. L.; Cobos, C. J.; Cox, R. A.; Frank, P.; Hayman, G.; Just, Th.; Kerr, J. A.; Murrells, T.; Pilling, M. J.; Troe, J.; Walker, R. W.; Warnatz, J. J. Phys. Chem. Ref. Data 23, 847-1033 (1994). [u] OH Wall reaction from reference 8.

TABLES IN THE THERMOCHEMICAL AND KINETIC ANALYSIS OF REACTIONS OF ISOBUTENE ADDUCTS OXIDATION
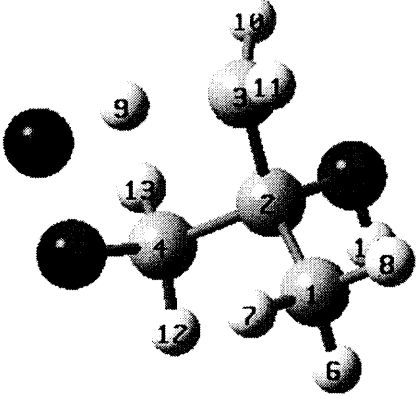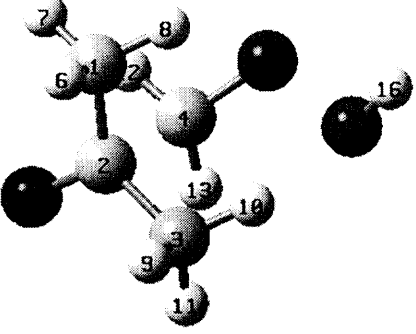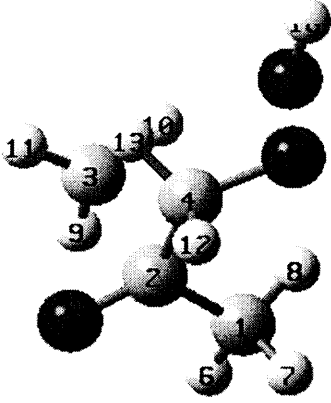
This appendix lists the geometrical parameters, harmonic vibrational frequencies, thermodynamic analysis and detailed reaction mechanism for reactions of isobutene adducts (2-Hydroxy-1,1-Dimethylethyl, 2-Hydroxy-2-Methylpropyl, and 1,1-Dimethylpropyl radicals) oxidation, as discussed in Chapter 5.
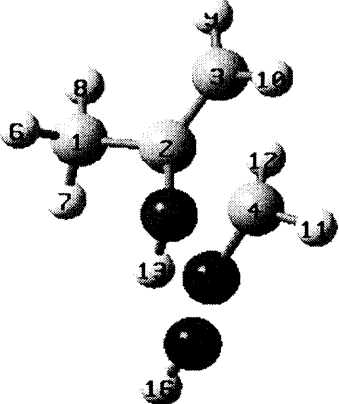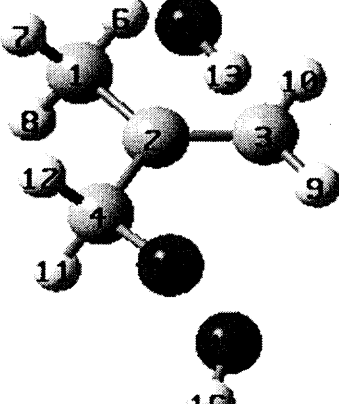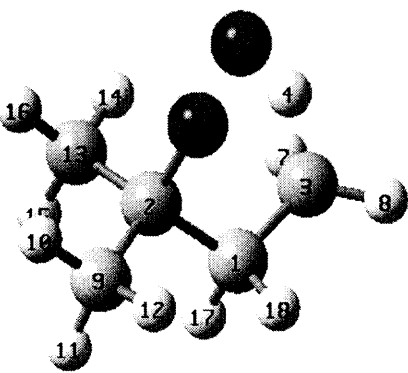
Table C.1 Optimized Geometrical Parameters for Species in Neopentyl Oxidation System
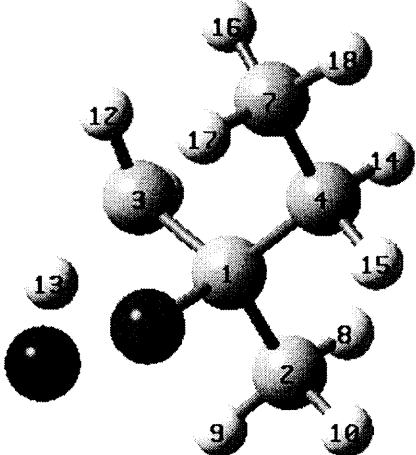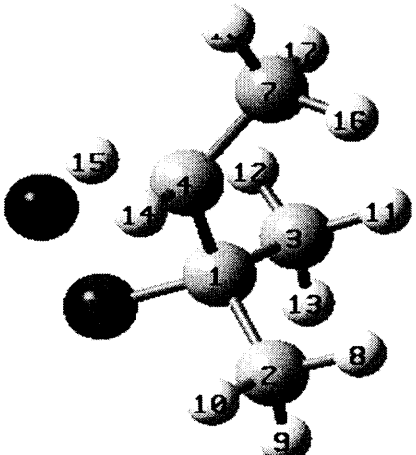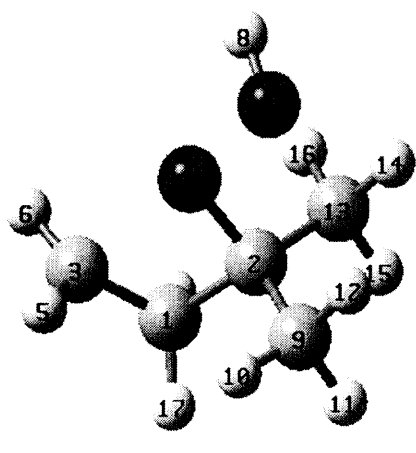
Species	Bond Length Å		Bond Angle Å		Dihedral Angle Degree	
TS14	r21	1.5237	a312	113.88	d4123	235.84
	r31	1.5265	a412	110.06	d5123	124.77
	r41	1.6295	a512	105.57	d6512	182.53
	r51	1.4166	a651	109.90	d7412	191.41
	r65	1.4071	a741	109.42	d8213	65.72
	r74	1.3499	a821	110.00	d9213	306.42
	r82	1.0932	a921	110.13	d10213	186.14
	r92	1.0935	a1021	110.92	d11312	65.71
	r102	1.0927	a1131	109.47	d12312	306.64
	r113	1.0938	a1231	109.63	d13312	186.17
	r123	1.0935	a1331	111.14	d14412	71.61
	r133	1.0889	a1441	103.60	d15412	315.45
	r144	1.1045	a1541	106.30	d16651	310.01
	r154	1.1027	a1665	100.35		
	r166	1.0792				
TS15	r21	1.5253	a312	114.33	d4123	232.32
	r31	1.5361	a412	111.74	d5123	112.57
	r41	1.5406	a512	105.59	d6512	198.57
	r51	1.4589	a651	103.97	d7412	172.16
	r65	1.4308	a741	113.83	d8213	61.94
	r74	1.4125	a821	110.31	d9213	301.79
	r82	1.0939	a921	110.21	d10213	181.77
	r92	1.0925	a1021	110.76	d11312	35.36
	r102	1.0946	a1131	116.16	d12312	253.04
	r113	1.0905	a1231	117.86	d13651	32.74
	r123	1.0873	a1365	94.15	d14412	53.07
	r136	1.2058	a1441	109.20	d15412	296.67
	r144	1.0961	a1541	107.33	d16741	50.47
	r154	1.1015	a1674	106.33		
	r167	0.9704				
TS16	r21	1.5258	a312	112.66	d4123	231.88
	r31	1.5318	a412	113.48	d5123	122.01
	r41	1.5560	a512	106.57	d6512	165.11
	r51	1.4404	a651	104.57	d7412	92.52
	r65	1.4287	a741	119.78	d8213	63.09
	r74	1.3694	a821	110.18	d9213	303.39
	r82	1.0940	a921	110.49	d10213	183.31
	r92	1.0944	a1021	110.49	d11312	56.60
	r102	1.0929	a1131	109.35	d12312	297.78
	r113	1.0929	a1231	111.71	d13312	175.11
	r123	1.0961	a1331	110.43	d14412	319.97
	r133	1.0932	a1441	114.25	d15651	324.44
	r144	1.0926	a1565	92.50	d16741	41.67
	r156	1.2506	a1674	109.08		
	r167	0.9684				

	TS17					

r21	1.5025	a321	119.02	d4213	250.15
r32	1.4992	a421	101.18	d5421	62.54
r42	2.1914	a542	105.14	d6213	140.16
r54	1.2390	a621	108.29	d7621	182.98
r62	1.3749	a762	110.73	d8123	181.87
r76	1.4587	a812	111.09	d9123	62.24
r81	1.0931	a912	108.64	d10123	302.47
r91	1.0927	a1012	111.01	d11321	61.57
r101	1.0983	a1132	110.35	d12321	302.28
r113	1.0996	a1232	108.56	d13321	182.13
r123	1.0920	a1332	111.68	d14421	299.46
r133	1.0901	a1442	90.74	d15421	185.48
r144	1.1094	a1542	89.86	d16762	223.13
r154	1.1081	a1676	98.42		
r167	0.9714				

	TS18					

r21	1.5066	a321	115.89	d4213	204.99
r32	1.5101	a421	118.03	d5213	102.72
r42	1.3914	a521	99.32	d6521	183.13
r52	1.9931	a652	107.25	d7421	185.39
r65	1.4235	a742	123.40	d8123	293.14
r74	1.3481	a812	109.64	d9123	173.37
r81	1.0946	a912	111.82	d10123	51.92
r91	1.0928	a1012	111.06	d11321	50.74
r101	1.0969	a1132	110.59	d12321	291.91
r113	1.0935	a1232	109.61	d13321	173.01
r123	1.0970	a1332	112.46	d14421	357.19
r133	1.0920	a1442	121.91	d15652	88.77
r144	1.0875	a1565	102.67	d16742	34.02
r156	0.9727	a1674	106.57		
r167	0.9815	d4213			

	TS19					

r21	1.4987	a312	121.09	d4123	192.53
r31	1.4006	a412	118.27	d5123	96.82
r41	1.5011	a512	94.15	d6512	232.52
r51	2.2852	a651	97.81	d7412	186.94
r65	1.2817	a741	111.84	d8213	95.00
r74	1.0935	a821	109.55	d9213	335.85
r82	1.1006	a921	111.00	d10213	213.49
r92	1.0907	a1021	111.35	d11312	207.34
r102	1.0930	a1131	117.51	d12651	1.04
r113	1.0961	a1265	97.55	d13412	67.54
r126	1.2670	a1341	109.62	d14412	308.63
r134	1.0993	a1441	111.39	d15312	356.04
r144	1.0932	a1531	120.52	d161531	285.64
r153	1.4090	a16153	108.23		
r1615	0.9666				

TS20					
	r21	1.5026	a312	121.83	d4123	192.92

r21	1.5026	a312	121.83	d4123	192.92
r31	1.3940	a412	115.25	d5123	95.86
r41	1.5140	a512	92.92	d6512	238.26
r51	2.2770	a651	98.32	d7412	173.49
r65	1.2817	a741	115.49	d8213	92.12
r74	1.4135	a821	109.85	d9213	332.72
r82	1.0990	a921	111.37	d10213	211.32
r92	1.0922	a1021	111.66	d11312	348.81
r102	1.0941	a1131	118.11	d12312	201.75
r113	1.0892	a1231	118.11	d13651	359.47
r123	1.0878	a1365	97.94	d14412	48.38
r136	1.2598	a1441	107.47	d15412	293.41
r144	1.1053	a1541	109.22	d16741	287.71
r154	1.0946	a1674	108.01		
r167	0.9658				
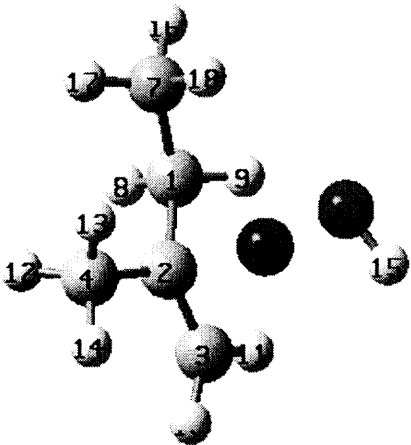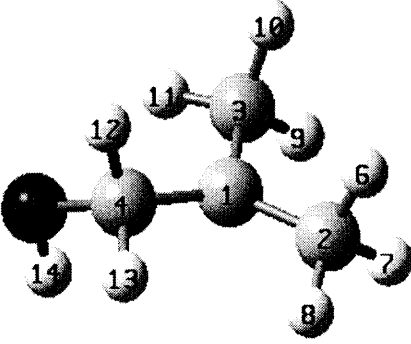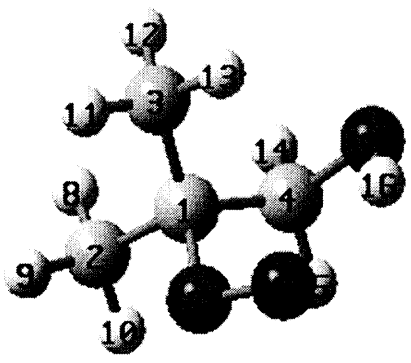
TS21

r21	1.5217	a321	118.68	d4213	205.93
r32	1.3906	a421	116.36	d5213	106.72
r42	1.5092	a521	97.08	d6521	304.65
r52	1.9398	a652	112.22	d7123	199.20
r65	1.4031	a712	113.14	d8123	80.99
r71	1.4102	a812	108.67	d9123	324.14
r81	1.0973	a912	108.53	d10321	193.64
r91	1.1003	a1032	121.20	d11321	18.99
r103	1.0850	a1132	121.03	d12421	71.27
r113	1.0858	a1242	109.56	d13421	312.90
r124	1.0964	a1342	110.51	d14421	191.13
r134	1.0907	a1442	111.27	d15652	257.24
r144	1.0925	a1565	102.39	d16712	51.94
r156	0.9722	a1671	104.84		
r167	0.9703				

TS22

r21	1.5382	a321	112.71	d4213	242.64
r32	1.5432	a421	109.21	d5213	126.42
r42	1.6227	a521	112.33	d6123	294.34
r52	1.3642	a612	109.04	d7123	175.57
r61	1.0936	a712	110.22	d8123	54.19
r71	1.0922	a812	111.91	d9321	59.56
r81	1.0951	a932	108.94	d10321	300.14
r93	1.0935	a1032	111.45	d11321	178.27
r103	1.0946	a1132	110.36	d12421	173.33
r113	1.0926	a1242	107.99	d13421	50.43
r124	1.0931	a1342	109.63	d14521	95.42
r134	1.0926	a1452	106.05	d15421	294.00
r145	1.3527	a1542	108.41	d161452	16.41
r154	1.3934	a16145	154.61		
r1614	1.0846				

TS23

r21	1.5316	a321	111.78	d4213	239.14
r32	1.5116	a421	110.27	d5213	119.79
r42	1.5661	a521	111.30	d6123	181.30
r52	1.4345	a612	110.70	d7123	62.03
r61	1.0967	a712	110.44	d8123	301.27
r71	1.0938	a812	110.45	d9321	259.73
r81	1.0932	a932	99.74	d10321	150.99
r93	1.4256	a1032	114.57	d11321	11.15
r103	1.0888	a1132	117.64	d12421	312.23
r113	1.0889	a1242	110.71	d13421	190.73
r124	1.0963	a1342	109.18	d14521	55.90
r134	1.0952	a1452	107.62	d15421	68.72
r145	0.9681	a1542	110.39	d16932	339.58
r154	1.4172	a1693	153.49		
r169	1.1387				

TS24

r21	1.5321	a321	115.0619	d4213	253.6634
r32	1.5324	a421	99.0851	d5213	151.0871
r42	2.0740	a521	119.2168	d6123	294.5864
r52	1.2584	a612	108.4474	d7123	176.7685
r61	1.0972	a712	109.9508	d8123	53.9382
r71	1.0924	a812	112.6298	d9321	67.7001
r81	1.0937	a932	108.1731	d10321	308.1463
r93	1.0975	a1032	112.9753	d11321	185.3877
r103	1.0924	a1132	109.9412	d12421	293.8213
r113	1.0920	a1242	98.1524	d13421	173.7203
r124	1.0864	a1342	100.1658	d14421	49.2779
r134	1.0859	a1442	115.2497	d151442	90.5122
r144	1.3630	a15144	108.4566	d1615144	210.0241
r1514	1.4564	a161514	99.0019		
r1615	0.9718				

TS25

r21	1.5253	a321	98.4602	d4213	253.04
r32	2.1662	a421	116.3899	d5213	102.15
r42	1.5468	a521	121.3369	d6123	290.98
r52	1.2482	a612	109.4841	d7123	173.45
r61	1.0913	a712	107.9044	d8123	54.84
r71	1.0975	a812	112.8872	d9321	54.44
r81	1.0907	a932	99.3476	d10321	293.38
r93	1.0836	a1032	100.0943	d11321	173.09
r103	1.0830	a1132	99.9516	d12421	265.89
r113	1.0839	a1242	105.7667	d13421	148.72
r124	1.0981	a1342	111.1581	d14421	19.20
r134	1.0947	a1442	116.5535	d151442	78.31
r144	1.4201	a15144	108.3782	d1615144	116.16
r1514	1.4584	a161514	99.6610		
r1615	0.9710				
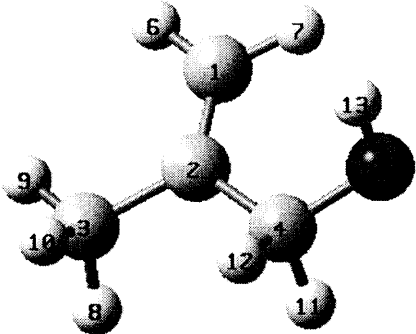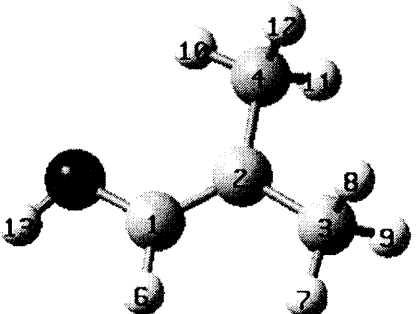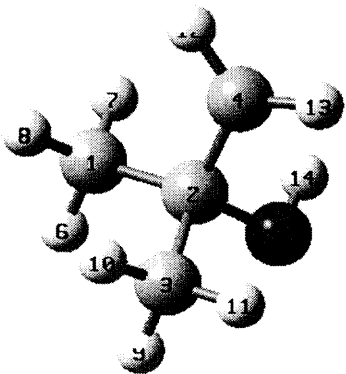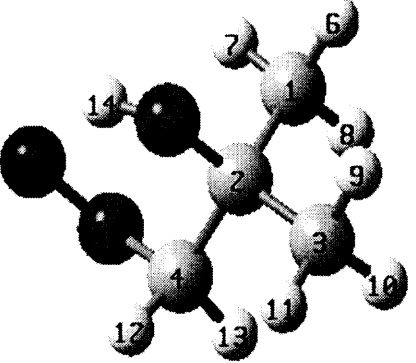
TS26	r21	1.5155	a321	121.51	d4213	252.01
	r32	1.3763	a421	96.82	d5213	149.99
	r42	2.2161	a521	115.22	d6123	270.96
	r52	1.3832	a612	109.18	d7123	151.44
	r61	1.0959	a712	111.76	d8123	30.51
	r71	1.0938	a812	111.04	d9321	340.78
	r81	1.0930	a932	120.67	d10321	165.64
	r93	1.0829	a1032	120.33	d11421	190.51
	r103	1.0834	a1142	100.23	d12421	68.20
	r114	1.0900	a1242	104.73	d13521	52.25
	r124	1.0870	a1352	107.79	d14421	312.80
	r135	0.9698	a1442	111.94	d151442	297.72
	r144	1.3772	a15144	106.93	d161514	179.11
	r1514	1.4808	a161514	98.36	4	
	r1615	0.9709				

TS27	r21	1.5027	a321	122.81	d4213	187.16
	r32	1.3518	a421	114.60	d5213	86.93
	r42	1.5107	a521	97.07	d6123	350.25
	r52	2.2510	a612	111.07	d7123	230.16
	r61	1.0900	a712	110.39	d8123	110.66
	r71	1.0923	a812	110.64	d9321	184.96
	r81	1.0963	a932	121.37	d10321	5.98
	r93	1.0815	a1032	120.58	d11421	64.19
	r103	1.0824	a1142	110.58	d12421	304.81
	r114	1.0973	a1242	108.87	d13521	170.31
	r124	1.0937	a1352	95.63	d14421	188.92
	r135	0.9707	a1442	115.19	d151442	281.42
	r144	1.4195	a15144	107.70	d161514	234.32
	r1514	1.4596	a161514	99.42	4	
	r1615	0.9668				

TS28	r21	1.5662	a312	113.32	d4312	24.60
	r31	1.5066	a431	97.88	d5431	333.74
	r43	1.4223	a543	152.39	d6543	40.51
	r54	1.1398	a654	100.68	d7312	276.96
	r65	1.4171	a731	117.32	d8312	136.37
	r73	1.0898	a831	117.13	d9213	195.65
	r83	1.0888	a921	110.78	d10921	179.89
	r92	1.5284	a1092	110.51	d11921	299.76
	r109	1.0932	a1192	110.21	d12921	59.76
	r119	1.0939	a1292	110.57	d13213	69.72
	r129	1.0935	a1321	112.60	d141321	302.72
	r132	1.5301	a14132	111.49	d151321	63.75
	r1413	1.0905	a15132	110.18	d161321	183.17
	r1513	1.0945	a16132	109.76	d17123	237.10
	r1613	1.0936	a1712	107.47	d18123	121.66
	r171	1.0999	a1812	107.45		
	r181	1.0941				
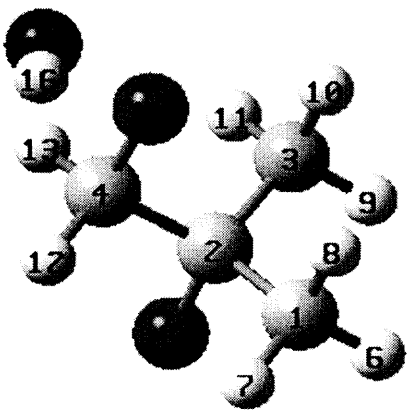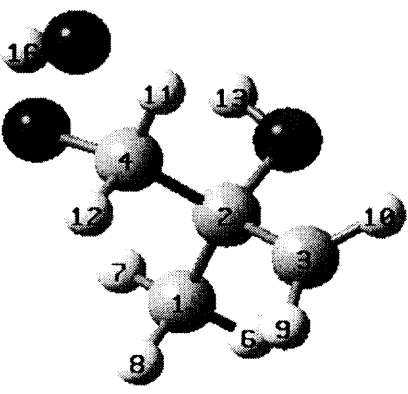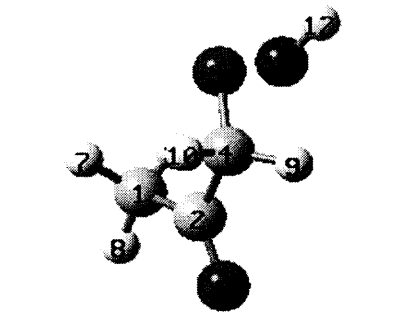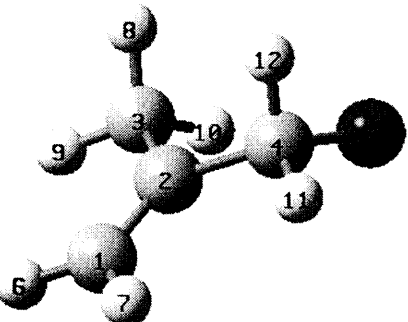
TS29					
r21	1.5316	a312	110.74	d4123	230.06
r31	1.5386	a412	111.63	d5123	112.65
r41	1.5385	a512	110.08	d6512	284.46
r51	1.4567	a651	103.92	d7412	182.17
r65	1.4260	a741	115.85	d8213	64.52
r74	1.5316	a821	110.98	d9213	304.07
r82	1.0946	a921	110.02	d10213	184.64
r92	1.0923	a1021	110.09	d11312	334.42
r102	1.0935	a1131	117.94	d12312	192.26
r113	1.0889	a1231	117.02	d13651	327.95
r123	1.0894	a1365	94.61	d14412	58.19
r136	1.1905	a1441	107.57	d15412	304.55
r144	1.0970	a1541	106.95	d16741	293.39
r154	1.0973	a1674	112.05	d17741	54.22
r167	1.0946	a1774	110.91	d18741	174.04
r177	1.0925	a1874	110.15		
r187	1.0942				

TS30					
r21	1.5277	a312	112.30	d4123	230.36
r31	1.5303	a412	113.12	d5123	120.21
r41	1.5486	a512	105.79	d6512	163.61
r51	1.4528	a651	103.71	d7412	95.77
r65	1.4269	a741	122.04	d8213	63.16
r74	1.5022	a821	110.34	d9213	303.80
r82	1.0943	a921	110.44	d10213	183.63
r92	1.0945	a1021	110.66	d11312	296.57
r102	1.0930	a1131	111.51	d12312	175.23
r113	1.0942	a1231	110.37	d13312	56.22
r123	1.0920	a1331	109.35	d14412	315.43
r133	1.0934	a1441	111.56	d15651	326.03
r144	1.0946	a1565	93.65	d16741	292.46
r156	1.2156	a1674	111.04	d17741	52.57
r167	1.1012	a1774	112.40	d18741	173.99
r177	1.0935	a1874	110.86		
r187	1.0944				

TS31					
r21	1.5489	a312	100.15	d4213	345.78
r31	1.5037	a421	95.48	d5312	272.52
r42	1.4705	a531	120.16	d6312	111.21
r53	1.0840	a631	120.99	d7421	181.09
r63	1.0836	a742	104.38	d8742	129.61
r74	1.6773	a874	93.80	d9213	100.01
r87	.9702	a921	112.85	d10921	310.80
r92	1.5270	a1092	110.60	d11921	70.81
r109	1.0942	a1192	110.38	d12921	191.08
r119	1.0957	a1292	110.23	d13213	229.70
r129	1.0917	a1321	113.78	d141321	173.80
r132	1.5248	a14132	110.66	d151321	294.21
r1413	1.0912	a15132	110.16	d161321	53.60
r1513	1.0958	a16132	110.23	d17123	239.19
r1613	1.0946	a1712	112.46	d18123	117.64
r171	1.0964	a1812	111.10		
r181	1.0937				
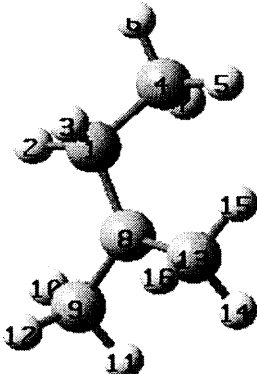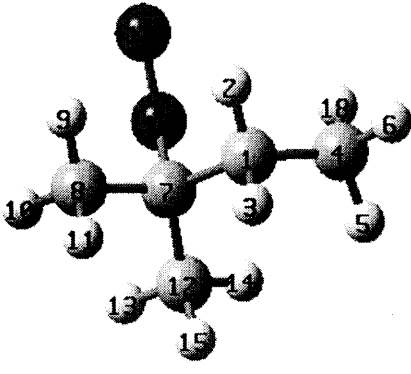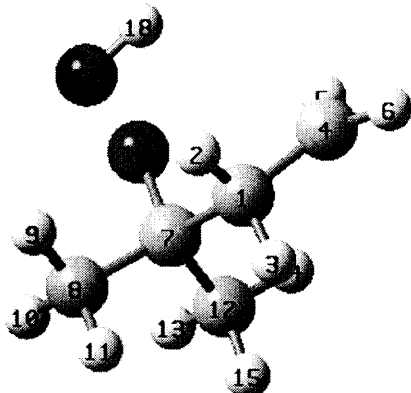
TS32		r21	1.5110	a321	115.53	d4213	205.61
		r32	1.5112	a421	118.69	d5213	102.56
		r42	1.3948	a521	94.42	d6521	187.25
		r52	1.9479	a652	112.42	d7421	173.01
		r65	1.4025	a742	124.72	d8123	301.73
		r74	1.4943	a812	110.34	d9123	181.25
		r81	1.0937	a912	111.38	d10123	60.93
		r91	1.0927	a1012	110.42	d11321	39.13
		r101	1.0969	a1132	110.63	d12321	279.76
		r113	1.0935	a1232	110.65	d13321	160.28
		r123	1.0970	a1332	111.58	d14421	342.21
		r133	1.0932	a1442	116.99	d15652	82.39
		r144	1.0874	a1565	102.95	d16742	310.46
		r156	0.9734	a1674	112.68	d17742	69.43
		r167	1.0962	a1774	109.70	d18742	188.81
		r177	1.1012	a1874	111.44		
		r187	1.0931				
TS33		r21	1.5033	a312	120.79	d4123	191.86
		r31	1.3945	a412	117.53	d5123	96.07
		r41	1.5092	a512	93.44	d6512	239.06
		r51	2.3026	a651	97.47	d7412	197.09
		r65	1.2852	a741	109.22	d8213	95.97
		r74	1.0951	a821	109.85	d9213	336.84
		r82	1.0988	a921	111.55	d10213	215.03
		r92	1.0927	a1021	111.53	d11312	349.07
		r102	1.0935	a1131	118.44	d12312	202.45
		r113	1.0897	a1231	118.23	d13651	359.90
		r123	1.0900	a1365	98.20	d14412	313.98
		r136	1.2491	a1441	109.57	d15412	75.78
		r144	1.0953	a1541	112.29	d161541	59.36
		r154	1.5420	a16154	111.17	d171541	179.13
		r1615	1.0944	a17154	110.24	d181541	298.74
		r1715	1.0942	a18154	111.69		
		r1815	1.0945				
TS34		r21	1.3486	a312	99.64	d4123	241.83
		r31	1.0933	a412	104.19	d5412	303.00
		r41	1.5243	a541	112.24	d6412	182.04
		r54	1.0939	a641	111.77	d7412	62.49
		r64	1.0966	a741	110.41	d8123	115.80
		r74	1.0939	a812	94.52	d9812	267.04
		r81	1.4009	a981	119.92	d10981	20.32
		r98	1.5033	a1098	111.78	d11981	142.34
		r109	1.0929	a1198	111.57	d12981	261.07
		r119	1.0935	a1298	109.49	d13812	99.87
		r129	1.0998	a1381	122.68	d141381	207.93
		r138	1.5024	a14138	111.24	d151381	329.89
		r1413	1.0930	a15138	112.49	d161381	89.23
		r1513	1.0913	a16138	109.46	d17213	239.65
		r1613	1.1001	a1721	115.22	d18213	234.72
		r172	1.9197	a1821	156.68		
		r182	1.2700				

TS35	r21	1.5206	a321	118.157	d4213	206.90
	r32	1.3916	a421	117.685	d5213	105.50
	r42	1.5114	a521	100.865	d6521	315.77
	r52	1.9411	a652	111.606	d7123	194.33
	r65	1.3998	a712	116.262	d8123	71.76
	r71	1.5311	a812	107.055	d9123	317.62
	r81	1.0995	a912	107.772	d10321	191.52
	r91	1.0948	a1032	121.184	d11321	18.17
	r103	1.0848	a1132	121.023	d12421	58.80
	r113	1.0858	a1242	110.006	d13421	299.36
	r124	1.0968	a1342	110.973	d14421	178.57
	r134	1.0920	a1442	111.193	d15652	253.86
	r144	1.0928	a1565	102.343	d16712	177.16
	r156	.9721	a1671	110.029	d17712	296.40
	r167	1.0944	a1771	111.989	d18712	57.40
	r177	1.0947	a1871	110.755		
	r187	1.0918	d4213			
C2C•COH	r21	1.4957	a312	119.18	d4123	199.01
	r31	1.4966	a412	119.37	d5412	207.44
	r41	1.4999	a541	113.70	d6213	73.42
	r54	1.4291	a621	112.08	d7213	314.76
	r62	1.1047	a721	111.52	d8213	193.36
	r72	1.0972	a821	112.02	d9312	49.44
	r82	1.0958	a931	111.74	d10312	290.69
	r93	1.0972	a1031	111.55	d11312	171.08
	r103	1.1046	a1131	110.99	d12412	90.11
	r113	1.0931	a1241	111.28	d13412	332.75
	r124	1.1031	a1341	109.77	d14541	55.82
	r134	1.1027	a1454	106.60		
	r145	0.9672				
$C_2C(OO•)COH$	r21	1.5255	a312	113.2116	d4123	231.37
	r31	1.5239	a412	111.2346	d5123	115.77
	r41	1.5395	a512	102.4045	d6512	171.23
	r51	1.4981	a651	113.5832	d7412	171.45
	r65	1.3217	a741	114.5654	d8213	58.96
	r74	1.4091	a821	109.8530	d9213	299.54
	r82	1.0933	a921	110.5156	d10213	179.15
	r92	1.0932	a1021	111.1949	d11312	54.83
	r102	1.0940	a1131	110.5817	d12312	295.05
	r113	1.0934	a1231	109.6459	d13312	176.09
	r123	1.0939	a1331	110.4902	d14412	52.77
	r133	1.0904	a1441	107.7986	d15412	297.13
	r144	1.0957	a1541	107.8774	d16741	55.60
	r154	1.1020	a1674	105.6181		
	r167	0.9703				

C₂C(OOH)CO•

r21	1.5301	a321	112.07	d4213	235.29
r32	1.5270	a421	110.10	d5421	67.64
r42	1.5502	a542	114.72	d6213	120.44
r54	1.3607	a621	102.75	d7621	177.46
r62	1.4439	a762	109.03	d8123	182.90
r76	1.4571	a812	110.68	d9123	63.37
r81	1.0937	a912	109.15	d10123	303.47
r91	1.0935	a1012	110.82	d11321	52.35
r101	1.0933	a1132	110.70	d12321	292.25
r113	1.0942	a1232	109.72	d13321	173.20
r123	1.0925	a1332	110.64	d14421	184.96
r133	1.0933	a1442	107.64	d15421	298.89
r144	1.1112	a1542	110.57	d16762	107.04
r154	1.1063	a1676	100.32		
r167	0.9710				

C₂C(OOH)C•OH

r21	1.5422	a321	110.97	d4213	233.30
r32	1.5350	a421	111.49	d5213	117.76
r42	1.5076	a521	101.61	d6521	180.45
r52	1.4448	a652	108.78	d7421	84.94
r65	1.4613	a742	120.66	d8123	306.25
r74	1.3721	a812	111.15	d9123	185.72
r81	1.0950	a912	110.15	d10123	66.60
r91	1.0929	a1012	109.34	d11321	58.36
r101	1.0935	a1132	109.60	d12321	300.09
r113	1.0936	a1232	111.40	d13321	178.27
r123	1.0959	a1332	110.78	d14421	299.88
r133	1.0926	a1442	118.47	d15652	119.67
r144	1.0858	a1565	99.17	d16742	38.36
r156	0.9709	a1674	109.08		
r167	0.9667				

C₂•C(OH)COOH

r21	1.5399	a321	111.97	d4213	232.63
r32	1.4898	a421	111.92	d5213	121.97
r42	1.5315	a521	107.61	d6521	297.45
r52	1.4761	a652	109.38	d7123	185.42
r65	1.4556	a712	111.90	d8123	66.78
r71	1.4133	a812	109.35	d9123	309.08
r81	1.0948	a912	108.59	d10321	202.44
r91	1.0994	a1032	120.40	d11321	26.78
r103	1.0851	a1132	121.18	d12421	68.24
r113	1.0849	a1242	109.56	d13421	308.95
r124	1.0935	a1342	109.94	d14421	188.01
r134	1.0912	a1442	110.59	d15652	261.11
r144	1.0933	a1565	100.39	d16712	51.70
r156	0.9711	a1671	105.70		
r167	0.9689				

C=C(C)COH

r21	1.3350	a321	123.22	d4213	179.79
r32	1.5069	a421	121.72	d5421	7.90
r42	1.5155	a542	115.15	d6123	.58
r54	1.4160	a612	121.54	d7123	181.83
r61	1.0858	a712	121.08	d8321	121.39
r71	1.0849	a832	111.12	d9321	.90
r83	1.0979	a932	111.54	d10321	239.93
r93	1.0927	a1032	111.34	d11421	248.91
r103	1.0977	a1142	109.40	d12421	133.64
r114	1.0980	a1242	108.79	d13542	60.21
r124	1.1046	a1354	107.07		
r135	0.9668				

C₂C=COH

r21	1.3406	a321	119.94	d4213	180.00
r32	1.5070	a421	123.97	d5123	179.99
r42	1.5077	a512	128.36	d6123	.00
r51	1.3674	a612	121.49	d7321	.00
r61	1.0860	a732	111.78	d8321	239.41
r73	1.0940	a832	111.44	d9321	120.57
r83	1.0986	a932	111.44	d10421	359.97
r93	1.0986	a1042	113.94	d11421	239.29
r104	1.0962	a1142	111.09	d12421	120.65
r114	1.0978	a1242	111.09	d13512	0.00
r124	1.0978	a1351	109.18		
r135	.9667				

C₃•COH

r21	1.5372	a321	110.7134	a1452	-124.25
r32	1.5382	a421	111.3469	d4213	-245.52
r42	1.4984	a521	109.6840	d5213	-57.99
r52	1.4443	a612	110.0284	d6123	182.30
r61	1.0932	a712	110.7150	d7123	62.47
r71	1.0959	a812	111.2711	d8123	59.77
r81	1.0952	a932	109.6817	d9321	-60.54
r93	1.0950	a1032	110.9394	d10321	-181.08
r103	1.0935	a1132	110.1478	d11321	18.58
r113	1.0931	a1242	121.9550	d12421	191.41
r124	1.0849	a1342	119.0240	d13421	68.23
r134	1.0853	a1452		d14521	
r145	0.9674				

C₂C(OH)COO•

r21	1.5370	a321	111.15	d4213	239.53
r32	1.5326	a421	111.44	d5213	117.24
r42	1.5411	a521	110.54	d6123	301.42
r52	1.4247	a612	109.09	d7123	182.32
r61	1.0929	a712	111.01	d8123	61.49
r71	1.0931	a812	111.72	d9321	63.84
r81	1.0953	a932	108.84	d10321	303.96
r93	1.0931	a1032	111.60	d11321	182.21
r103	1.0940	a1132	110.75	d12421	190.50
r113	1.0940	a1242	110.18	d13421	66.95
r124	1.0932	a1342	112.09	d14521	76.29
r134	1.0927	a1452	106.85	d15421	311.13
r145	0.9708	a1542	113.15	d161542	297.09
r154	1.4606	a16154	112.27		
r1615	1.3255				

C₂C(O•)COOH

r21	1.5571	a321	110.20	d4213	-124.38
r32	1.5428	a421	110.70	d5213	118.29
r42	1.5476	a521	104.87	d6123	-55.84
r52	1.3770	a612	110.02	d7123	183.70
r61	1.0915	a712	110.39	d8123	64.35
r71	1.0928	a812	108.40	d9321	55.93
r81	1.0928	a932	110.07	d10321	-65.14
r93	1.0924	a1032	109.93	d11321	-184.41
r103	1.0927	a1132	110.02	d12421	-59.18
r113	1.0937	a1242	109.35	d13421	181.73
r124	1.0987	a1342	109.54	d14421	61.85
r134	1.0963	a1442	108.09	d151442	-187.83
r144	1.4233	a15144	107.04	d161514	108.48
r1514	1.4550	a161514	100.18	4	
r1615	0.9718				

C₂•C(OH)COOH

r21	1.5423	a321	111.18	d4213	239.83
r32	1.4949	a421	110.33	d5213	118.44
r42	1.5540	a521	110.29	d6123	297.23
r52	1.4289	a612	109.23	d7123	177.56
r61	1.0921	a712	110.34	d8123	57.48
r71	1.0934	a812	111.56	d9321	315.25
r81	1.0953	a932	120.80	d10321	138.10
r93	1.0842	a1032	119.41	d11421	187.12
r103	1.0827	a1142	109.66	d12421	66.63
r114	1.0962	a1242	110.67	d13521	79.66
r124	1.0953	a1352	106.26	d14421	311.57
r135	0.9695	a1442	115.02	d151442	289.14
r144	1.4268	a15144	106.54	d161514	155.27
r1514	1.4734	a161514	98.56	4	
r1615	0.9706				

CC(=O)COOH

r21	1.5101	a321	123.67	d4213	182.07
r32	1.2151	a421	117.63	d5421	341.08
r42	1.5344	a542	115.17	d6123	242.97
r54	1.4170	a612	109.69	d7123	125.83
r61	1.0946	a712	110.52	d8123	4.06
r71	1.0954	a812	109.42	d9421	214.18
r81	1.0905	a942	109.05	d10421	96.48
r94	1.0961	a1042	107.99	d11542	292.34
r104	1.0987	a1154	106.39	d121154	246.66
r115	1.4586	a12115	99.99		
r1211	0.9715				

C=C(C)CO•

r21	1.3349	a321	124.05	d4213	179.63
r32	1.5039	a421	119.99	d5421	136.26
r42	1.5184	a542	115.86	d6123	359.09
r54	1.3688	a612	121.77	d7123	179.10
r61	1.0862	a712	121.64	d8321	118.45
r71	1.0870	a832	111.03	d9321	357.56
r83	1.0980	a932	111.55	d10321	236.26
r93	1.0924	a1032	110.34	d11421	6.13
r103	1.0945	a1142	111.95	d12421	251.37
r114	1.1053	a1242	108.83		
r124	1.1172				

C2C•CC					
r21	1.0968	a312	105.86	d4123	244.13
r31	1.1039	a412	108.78	d5412	178.94
r41	1.5424	a541	111.40	d6412	59.05
r54	1.0948	a641	110.95	d7412	298.80
r64	1.0953	a741	110.95	d8123	118.72
r74	1.0946	a812	109.69	d9812	357.61
r81	1.5046	a981	120.23	d10981	33.83
r98	1.4968	a1098	111.88	d11981	155.17
r109	1.0959	a1198	111.75	d12981	274.19
r119	1.0972	a1298	112.23	d13812	194.40
r129	1.1058	a1381	119.17	d141381	207.70
r138	1.4980	a14138	111.83	d151381	329.07
r1413	1.0971	a15138	112.26	d161381	88.70
r1513	1.0954	a16138	111.80		
r1613	1.1054				

C2C(OO•)CC					
r21	1.0947	a312	106.70	d4123	240.90
r31	1.0970	a412	109.55	d5412	173.71
r41	1.5318	a541	112.23	d6412	54.13
r54	1.0942	a641	110.12	d7123	114.65
r64	1.0941	a712	106.98	d8712	304.47
r71	1.5370	a871	111.49	d9871	57.03
r87	1.5272	a987	110.26	d10871	177.31
r98	1.0921	a1087	110.72	d11871	297.07
r108	1.0938	a1187	110.01	d12712	176.06
r118	1.0940	a1271	114.18	d131271	180.07
r127	1.5265	a13127	110.52	d141271	300.44
r1312	1.0935	a14127	111.40	d151271	60.61
r1412	1.0922	a15127	109.90	d16712	62.65
r1512	1.0940	a1671	108.28	d171671	299.91
r167	1.4996	a17167	112.84	d18412	294.83
r1716	1.3198	a1841	111.08		
r184	1.0936				

C2C(OOH)CC•					
r21	1.1027	a312	104.71	d4123	241.11
r31	1.1001	a412	110.21	d5412	253.39
r41	1.4905	a541	120.99	d6412	69.48
r54	1.0843	a641	120.63	d7123	115.35
r64	1.0843	a712	107.87	d8712	312.54
r71	1.5452	a871	111.11	d9871	62.07
r87	1.5307	a987	110.38	d10871	181.86
r98	1.0921	a1087	110.29	d11871	301.87
r108	1.0936	a1187	110.61	d12712	187.49
r118	1.0949	a1271	111.80	d131271	185.62
r127	1.5329	a13127	110.27	d141271	306.23
r1312	1.0933	a14127	111.24	d151271	66.21
r1412	1.0928	a15127	109.73	d16712	74.80
r1512	1.0940	a1671	110.26	d171671	299.81
r167	1.4491	a17167	109.19	d181716	101.80
r1716	1.4555	a181716	100.11	7	
r1817	0.9720				
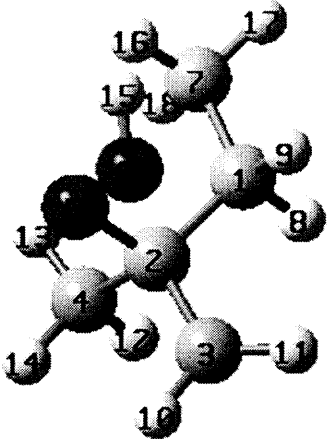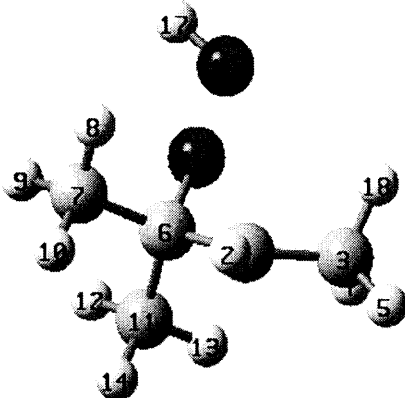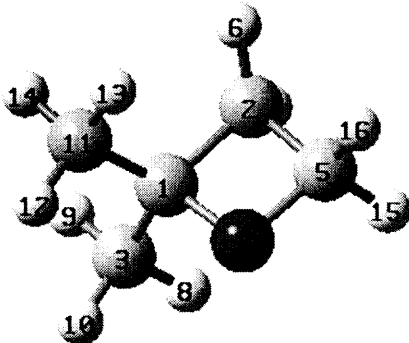
C₂•C(OOH)CC

r21	1.5416	a321	111.08	d4213	234.65
r32	1.4944	a421	113.11	d5213	122.33
r42	1.5389	a521	110.50	d6521	295.59
r52	1.4629	a652	108.69	d7123	180.85
r65	1.4587	a712	115.40	d8123	57.40
r71	1.5309	a812	107.84	d9123	303.28
r81	1.0970	a912	107.12	d10321	178.92
r91	1.0954	a1032	119.23	d11321	8.03
r103	1.0848	a1132	121.59	d12421	57.90
r113	1.0841	a1242	109.82	d13421	297.47
r124	1.0934	a1342	111.05	d14421	177.47
r134	1.0930	a1442	110.17	d15652	114.91
r144	1.0928	a1565	99.67	d16712	52.96
r156	.9708	a1671	111.16	d17712	172.86
r167	1.0946	a1771	110.58	d18712	292.67
r177	1.0943	a1871	112.11		
r187	1.0941				

C₂C(OOH)C•C

r21	1.0868	a312	119.11	d4312	157.96
r31	1.4897	a431	111.96	d5312	36.03
r43	1.0951	a531	111.61	d6123	188.98
r53	1.0956	a612	118.18	d7612	10.32
r61	1.5016	a761	111.75	d8761	60.04
r76	1.5325	a876	110.26	d9761	180.65
r87	1.0926	a976	110.56	d10761	300.53
r97	1.0944	a1076	110.44	d11612	245.10
r107	1.0943	a1161	111.95	d121161	185.33
r116	1.5417	a12116	110.43	d131161	305.63
r1211	1.0946	a13116	110.88	d141161	65.51
r1311	1.0925	a14116	109.64	d15612	133.42
r1411	1.0931	a1561	110.60	d161561	301.05
r156	1.4583	a16156	108.76	d171615	246.85
r1615	1.4589	a171615	99.76	6	276.43
r1716	.9706	a1831	111.11	d18312	
r183	1.1015				

C₂CYCOCC

r21	1.5534	a312	115.55	d4123	113.01
r31	1.5237	a412	90.75	d5412	.00
r41	1.4659	a541	91.91	d6213	131.02
r54	1.4440	a621	114.99	d7213	2.95
r62	1.0927	a721	114.99	d8312	45.91
r72	1.0927	a831	110.70	d9312	285.40
r83	1.0939	a931	110.90	d10312	165.48
r93	1.0958	a1031	110.26	d11123	226.02
r103	1.0949	a1112	115.55	d121112	194.50
r111	1.5237	a12111	110.26	d131112	314.08
r1211	1.0949	a13111	110.70	d141112	74.58
r1311	1.0939	a14111	110.90	d15541	241.11
r1411	1.0958	a1554	111.99	d16541	118.89
r155	1.0975	a1654	111.99		
r165	1.0975				

Table C.2 Harmonic Vibrational Frequencies (cm^{-1}) for Species in Neopentyl Oxidation System

species	Frequencies (Based on B3LYP/6-31g(d,p) level)											moments of inertia (amu-Bohr^2)
TS14	-776.61	165.48	188.15	206.19	269.29	290.53	337.35	391.16	446.09	502.98	534.59	610.79	541.66730
	660.85	813.50	906.77	953.06	961.08	979.07	1029.10	1081.60	1177.30	1211.72	1240.13	1256.81	733.31647
	1284.10	1325.01	1410.91	1428.48	1489.58	1496.17	1506.65	1516.39	1523.67	1870.56	2944.57	3003.81	862.66991
	3061.28	3066.88	3134.38	3140.22	3146.18	3180.42							
TS15	-2170.79	139.14	191.74	208.93	246.98	303.44	357.35	386.73	427.34	525.11	565.10	591.25	587.46774
	636.36	797.92	841.51	888.83	926.49	968.79	1003.14	1022.52	1103.96	1128.97	1140.38	1218.65	685.89141
	1253.22	1266.31	1391.16	1416.57	1450.13	1466.49	1496.72	1506.83	1511.94	1701.18	2997.46	3054.71	906.08543
	3076.91	3119.97	3127.81	3143.55	3223.87	3746.00							
TS16	-1879.45	136.98	187.81	229.07	255.19	274.56	301.53	347.40	432.26	467.31	515.25	575.74	618.66169
	653.17	746.05	862.56	923.68	941.40	954.79	967.58	1025.42	1160.08	1183.22	1215.83	1250.58	725.72391
	1255.04	1316.08	1403.53	1420.27	1434.56	1490.71	1501.83	1510.59	1522.93	1760.77	3044.43	3053.91	928.86352
	3119.28	3123.30	3128.74	3139.61	3141.84	3788.71							
TS17	-166.98	93.81	100.59	139.27	167.22	186.32	217.49	221.32	292.91	339.28	385.39	395.04	560.58426
	532.02	631.94	795.53	911.00	960.66	993.02	1005.06	1075.03	1141.65	1249.67	1269.50	1288.43	970.64327
	1398.02	1414.28	1422.70	1480.11	1487.92	1488.89	1502.81	1509.25	1655.56	2892.87	2945.38	3018.84	1104.13205
	3028.67	3109.51	3123.58	3148.64	3170.40	3769.47							
TS18	-370.95	145.54	152.69	176.66	193.83	225.77	268.59	314.37	318.69	375.31	402.83	456.17	622.32056
	583.74	661.21	768.65	805.53	918.48	972.70	1004.27	1044.34	1083.80	1228.89	1245.05	1326.73	778.14761
	1354.76	1402.56	1421.58	1429.20	1486.92	1499.68	1501.50	1516.13	1580.93	3038.00	3044.07	3103.51	982.89549
	3106.70	3134.57	3142.34	3180.88	3545.29	3709.15							
TS19	-1084.93	125.55	150.84	161.94	197.52	208.22	238.46	255.11	285.54	364.75	419.48	541.69	701.35466
	572.80	636.99	827.77	938.89	972.59	1013.23	1030.97	1098.35	1136.95	1231.29	1268.30	1315.79	773.05938
	1335.96	1367.22	1421.07	1425.54	1479.99	1484.11	1489.56	1508.24	1581.05	1620.14	3013.43	3023.81	1055.28550
	3069.26	3097.76	3103.65	3135.57	3161.31	3795.45							
TS20	-1044.30	68.92	132.90	185.66	200.87	210.73	283.36	324.34	376.14	443.72	520.89	539.23	620.22709
	628.62	654.75	830.69	916.52	983.69	1010.16	1050.74	1064.90	1108.31	1215.82	1267.50	1308.93	891.49241
	1340.46	1396.31	1406.91	1419.89	1436.08	1486.33	1491.43	1502.59	1580.13	1621.83	2953.46	3025.75	1091.90899
	3089.68	3098.49	3120.48	3141.79	3206.73	3816.85							
TS21	-444.47	92.45	140.36	165.52	172.39	237.31	277.78	322.04	379.09	406.63	431.31	496.11	662.30445
	523.03	573.23	786.88	792.16	921.01	940.50	973.29	1036.44	1059.93	1112.57	1222.89	1307.12	741.77636
	1344.87	1376.92	1404.77	1430.82	1447.49	1487.15	1503.39	1505.25	1536.65	3007.46	3052.16	3066.33	986.96888
	3123.27	3155.88	3161.36	3253.41	3719.92	3759.19							

TS22	-862.96	109.00	206.01	232.00	261.11	311.22	359.28	425.38	458.25	494.71	548.92	600.38	433.02091
	686.90	805.85	918.89	922.98	954.75	987.66	1023.12	1061.61	1107.86	1158.75	1200.43	1238.88	912.79366
	1299.60	1314.46	1395.96	1420.30	1471.67	1489.84	1498.58	1507.01	1516.15	1853.24	3048.59	3053.40	939.12601
	3071.39	3123.61	3130.51	3142.55	3146.49	3155.67							
TS23	-1555.19	97.65	240.24	271.82	293.03	325.89	336.33	398.75	446.70	464.85	494.75	538.92	443.88667
	654.05	766.28	900.17	920.62	953.05	967.22	986.27	1015.42	1054.73	1107.70	1151.61	1184.19	922.24501
	1227.69	1270.16	1339.89	1382.59	1415.09	1459.74	1479.79	1505.12	1512.75	1596.19	3039.29	3047.19	971.51846
	3111.55	3114.33	3120.59	3139.34	3218.04	3785.61							
TS24	-344.82	42.86	111.48	131.99	177.39	197.08	214.48	226.76	320.43	393.20	428.42	470.51	466.37029
	498.92	697.45	766.96	881.95	894.06	955.13	1003.26	1073.70	1099.03	1155.16	1196.72	1220.87	1118.81473
	1390.69	1401.36	1420.27	1444.07	1471.00	1482.98	1488.04	1503.31	1550.26	3036.35	3041.80	3108.01	1175.06671
	3116.39	3133.86	3145.69	3153.61	3260.33	3767.57							
TS25	-439.69	55.10	129.81	167.66	177.04	205.92	219.84	238.39	261.32	386.96	428.28	466.92	518.74301
	546.92	612.03	624.98	755.30	860.81	927.55	948.84	1003.50	1042.54	1079.11	1212.12	1275.39	975.78742
	1351.22	1375.46	1400.60	1431.61	1442.40	1451.33	1482.81	1490.99	1572.58	3043.27	3045.96	3105.08	1077.96484
	3120.13	3125.79	3171.12	3284.16	3301.16	3761.68							
TS26	-528.42	68.50	139.62	154.16	189.44	211.88	245.55	286.30	380.81	405.48	427.30	487.48	470.71667
	545.85	608.83	630.56	722.91	797.02	824.95	944.39	965.19	1031.01	1058.52	1072.60	1198.21	1053.75330
	1268.66	1317.72	1389.25	1416.07	1432.80	1440.40	1496.43	1507.14	1572.35	3045.81	3098.10	3112.96	1108.50657
	3136.03	3179.42	3231.13	3279.02	3751.02	3778.86							
TS27	-79.90	41.58	132.98	144.90	158.51	189.76	206.42	267.90	352.56	362.84	380.60	436.10	494.47096
	574.11	673.41	679.31	838.45	865.34	910.26	958.22	982.25	1022.63	1051.41	1079.38	1269.59	1070.02016
	1297.67	1369.51	1403.58	1409.24	1438.94	1439.51	1480.63	1492.94	1641.94	3010.21	3021.82	3079.22	1158.26576
	3085.38	3122.78	3157.69	3253.21	3748.80	3778.49							
TS28	-1507.76	146.51	192.12	221.35	261.36	283.50	346.12	391.75	408.54	463.35	501.62	539.41	555.63902
	638.46	730.89	825.08	854.98	930.64	943.83	985.18	1011.80	1020.11	1067.16	1076.54	1131.44	759.55005
	1192.35	1231.67	1247.70	1269.19	1356.25	1413.00	1428.04	1464.32	1487.09	1494.97	1503.17	1505.65	895.42886
	1526.03	1590.51	3012.97	3055.61	3061.11	3096.82	3115.92	3128.15	3134.92	3137.93	3159.15	3204.49	
TS29	-2191.00	86.35	165.36	226.39	238.05	265.27	294.25	345.98	405.13	433.17	537.17	562.09	515.14009
	632.32	758.68	785.02	859.24	917.01	928.19	944.22	999.98	1011.44	1068.10	1074.81	1107.90	856.28738
	1180.52	1214.53	1259.33	1321.71	1382.52	1414.58	1427.19	1466.44	1485.76	1504.46	1513.24	1514.71	995.21417
	1524.87	1719.05	3038.36	3054.92	3055.38	3075.73	3117.43	3122.02	3128.36	3142.88	3146.42	3213.23	
TS30	-2106.41	122.42	171.67	189.23	240.80	243.44	271.22	308.37	347.75	450.13	495.27	531.54	628.98505
	645.26	719.74	799.11	848.80	922.21	938.98	941.58	1003.60	1051.08	1062.27	1122.01	1167.46	747.35410
	1179.67	1245.75	1257.34	1371.36	1408.26	1419.34	1424.36	1485.64	1491.51	1497.95	1501.58	1510.82	955.77916

	1520.90	1729.04	3003.23	3050.49	3058.23	3086.64	3095.20	3122.28	3128.60	3132.05	3137.53	3147.91	
TS31	-789.67	66.52	149.68	201.33	222.07	246.87	257.64	327.32	338.01	384.42	443.98	462.56	585.80013
	543.92	591.92	752.56	791.47	812.00	900.78	933.63	973.35	995.52	1046.56	1054.85	1073.07	768.57659
	1176.60	1224.52	1254.80	1284.38	1318.72	1408.08	1421.11	1481.49	1486.89	1503.59	1504.99	1507.47	935.31001
	1526.99	3043.99	3044.45	3051.71	3104.25	3112.54	3118.15	3148.80	3153.01	3171.30	3274.19	3793.74	
TS32	-445.83	90.06	114.40	131.26	171.52	190.66	227.48	260.39	278.36	319.49	386.08	411.63	724.43943
	447.78	529.01	705.63	767.11	944.58	961.53	975.26	1009.84	1020.79	1079.38	1082.80	1132.72	748.90072
	1245.77	1354.93	1371.80	1410.99	1419.11	1425.73	1477.53	1489.74	1495.93	1503.03	1503.72	1524.37	1040.89366
	1547.90	3002.99	3039.55	3043.48	3069.84	3105.39	3108.87	3122.16	3133.86	3138.79	3173.95	3691.77	
TS33	-1047.23	76.88	116.45	162.84	179.20	195.57	230.05	261.09	388.18	425.27	469.81	602.41	476.86830
	610.72	666.13	781.43	807.48	945.33	1005.41	1010.48	1027.04	1045.82	1091.13	1112.17	1267.07	1160.72481
	1288.60	1321.39	1330.93	1362.23	1418.05	1421.50	1443.48	1490.63	1491.76	1508.95	1513.92	1524.78	1210.57056
	1578.71	1622.59	3029.01	3048.57	3054.91	3095.35	3100.48	3108.76	3122.60	3126.46	3140.06	3190.94	
TS34	-1016.99	112.31	139.41	159.87	168.69	197.32	205.25	228.39	291.49	385.77	421.81	520.26	726.51330
	538.98	630.12	782.12	870.84	950.53	977.49	1008.79	1066.08	1088.92	1098.23	1120.22	1252.29	788.64732
	1286.81	1329.24	1364.48	1420.25	1428.83	1435.22	1480.72	1485.13	1491.30	1504.83	1512.70	1516.65	1086.76603
	1578.35	1618.93	3017.90	3022.68	3040.70	3096.32	3099.13	3104.34	3105.09	3125.77	3137.97	3151.39	
TS35	-455.08	88.17	122.64	161.59	181.92	222.85	266.19	275.44	321.91	384.74	413.40	432.98	694.13142
	498.12	535.31	756.46	774.58	782.26	927.89	958.67	1009.24	1015.24	1055.95	1095.75	1109.49	757.19334
	1289.40	1317.26	1340.78	1373.38	1411.17	1428.13	1436.44	1481.10	1492.57	1507.40	1519.26	1528.60	1023.77418
	1537.80	3023.24	3046.27	3054.70	3088.04	3116.05	3117.58	3146.76	3150.73	3154.81	3251.71	3714.93	
C2C•COH	84.24	126.26	145.49	238.07	300.03	357.89	378.99	504.09	773.48	918.06	944.23	976.88	240.17783
	1002.57	1052.45	1063.68	1190.42	1268.72	1304.17	1380.02	1401.26	1414.89	1432.96	1483.42	1486.39	509.37807
	1501.02	1504.09	1509.29	2956.74	2960.23	2968.69	2992.52	3046.14	3053.80	3096.81	3126.81	3795.31	686.37155
$C_2C(OO\bullet)COH$	100.45	168.96	200.85	234.63	255.65	282.14	345.31	372.94	422.75	459.28	560.66	584.64	601.35747
	746.49	817.41	897.23	952.25	1002.89	1037.66	1111.59	1158.19	1210.33	1241.78	1260.83	1278.57	719.05489
	1395.57	1417.78	1430.49	1454.68	1491.85	1496.63	1507.08	1510.59	1521.90	2993.16	3058.10	3064.58	912.22639
	3083.34	3133.91	3134.92	3141.84	3166.34	3751.83							
$C_2C(OOH)CO\bullet$	149.37	187.07	208.26	227.47	272.81	286.07	345.40	376.74	409.63	434.83	497.30	573.17	577.22072
	637.28	812.23	847.96	947.64	949.55	976.91	1017.24	1067.04	1200.24	1221.51	1236.89	1276.16	719.06446
	1310.13	1408.99	1425.82	1484.19	1489.13	1494.95	1505.07	1517.07	1537.60	2939.11	3003.55	3062.09	883.39998
	3067.23	3134.03	3141.73	3147.93	3185.75	3323.72							
$C_2C(OOH)C\bullet OH$	33.79	137.47	208.42	215.83	236.63	251.50	264.61	312.28	347.21	392.59	444.35	489.07	562.97230
	567.96	657.52	753.94	871.82	922.22	936.11	973.43	1015.71	1150.25	1182.43	1197.53	1273.82	853.90607

1308.93	1363.92	1395.46	1410.25	1433.84	1491.35	1501.05	1513.93	1524.93	3045.77	3050.24	3115.57	1002.43359
3126.51	3141.50	3143.21	3200.04	3758.51	3809.77							

$C_2 \bullet C(OH)COOH$	80.18	106.77	172.13	204.63	220.34	257.50	289.48	323.50	356.37	379.71	436.71	490.50	625.58632
	568.56	603.99	758.34	843.67	894.20	925.53	963.85	994.13	1084.81	1132.90	1227.76	1247.11	707.82806
	1285.99	1361.79	1391.95	1414.44	1435.73	1472.81	1498.46	1508.48	1515.27	3019.35	3062.20	3093.83	934.23151
	3135.97	3155.38	3159.00	3263.79	3751.35	3780.59							
$C=C(C)COH$	121.45	172.72	281.07	353.09	387.08	433.24	538.10	722.86	840.37	928.88	959.20	984.67	203.01225
	1020.02	1076.41	1105.54	1220.36	1274.76	1388.12	1421.10	1425.49	1448.22	1493.70	1501.43	1510.18	492.55125
	1737.96	2958.88	3025.44	3050.84	3073.37	3129.49	3160.89	3247.56	3804.26				666.42133
$C_2C=COH$	102.80	199.95	282.78	288.27	345.91	365.43	486.46	576.90	807.50	891.50	979.94	1021.79	219.96658
	1049.92	1102.10	1181.35	1213.77	1319.92	1414.05	1431.90	1443.54	1480.55	1496.73	1509.76	1517.83	485.51161
	1761.63	3012.07	3018.84	3055.95	3069.82	3084.92	3113.11	3201.37	3808.93				683.14805
$C_3 \bullet COH$	114.89	226.45	269.93	319.94	333.18	351.79	404.43	444.88	463.86	546.37	762.46	903.65	368.40326
	924.93	943.57	989.44	1022.43	1133.43	1221.43	1267.90	1348.00	1404.18	1421.73	1466.94	1491.70	380.18490
	1496.85	1511.46	1520.11	3039.92	3049.34	3108.11	3124.17	3133.32	3138.25	3155.65	3266.64	3794.13	391.15873
$C_2C(OH)COO \bullet$	79.17	179.32	224.21	237.38	261.78	312.61	352.48	399.41	445.72	458.67	487.57	609.17	432.88110
	765.39	873.81	928.94	941.51	950.95	1014.09	1032.43	1156.47	1167.43	1225.98	1249.68	1312.97	955.27980
	1355.45	1405.58	1421.19	1434.47	1474.97	1492.47	1503.92	1515.28	1524.16	3050.25	3055.47	3080.39	980.57601
	3124.98	3130.66	3138.24	3141.89	3149.88	3734.28							
$C_2C(O \bullet)COOH$	82.00	106.60	177.64	200.03	215.91	229.27	248.32	331.66	340.57	358.79	454.67	520.50	396.63418
	752.03	893.41	918.55	930.41	946.22	968.22	996.09	1075.91	1134.32	1185.66	1239.81	1259.17	1185.78468
	1364.24	1378.23	1382.90	1412.21	1483.05	1494.61	1500.32	1518.78	1534.94	3021.56	3057.70	3061.79	1199.40993
	3080.57	3137.74	3145.62	3150.80	3158.67	3746.23							
$C_2 \bullet C(OH)COOH$	68.58	156.70	180.53	200.30	243.66	255.58	295.36	372.18	390.93	405.95	453.71	494.92	440.31437
	541.40	602.77	766.03	860.03	906.74	919.05	972.67	1002.99	1018.87	1134.64	1180.87	1221.59	960.11607
	1300.26	1367.58	1392.95	1407.15	1416.82	1452.43	1464.39	1505.07	1508.17	3047.69	3051.11	3111.89	1002.80513
	3122.31	3145.75	3171.31	3289.29	3755.54	3780.26							
$CC(=O)COOH$	64.30	130.52	153.41	194.18	261.38	389.18	466.31	498.89	570.48	770.24	852.63	908.50	64.30
	1003.84	1057.91	1109.81	1236.07	1280.35	1347.05	1379.13	1399.16	1442.82	1473.69	1484.43	1822.40	1003.84
	3037.36	3055.08	3095.03	3120.90	3170.04	3754.34							3037.36
$C=C(C)CO \bullet$	75.73	178.33	262.51	390.12	409.93	559.03	702.51	795.48	818.46	932.43	971.58	1024.45	226.76715
	1063.65	1087.45	1142.01	1284.00	1332.24	1359.31	1420.83	1463.34	1488.94	1508.48	1736.55	2834.95	441.77374
	2962.50	3034.40	3097.76	3138.62	3149.64	3232.57							617.94217
$C_2C \bullet CC$	33.35	105.73	122.26	199.27	233.99	343.21	380.14	428.88	736.93	783.93	938.43	946.14	262.47640

	985.46	1013.55	1027.81	1061.18	1085.71	1254.93	1287.12	1325.55	1373.68	1412.04	1419.21	1430.64	531.23194
	1484.71	1486.89	1493.50	1499.78	1506.49	1515.45	1520.60	2942.12	2950.31	2964.90	3041.63	3045.02	695.62378
	3049.36	3058.64	3095.71	3099.87	3111.59	3118.69							
$C_2C(OO\bullet)CC$	76.79	137.78	188.00	206.83	230.56	263.25	300.67	334.30	368.51	399.06	507.82	541.71	627.14289
	716.00	772.14	810.14	927.09	941.30	1010.98	1014.77	1074.94	1085.33	1178.77	1220.99	1230.12	750.12716
	1280.74	1336.83	1384.34	1409.22	1427.24	1429.98	1484.20	1496.29	1501.12	1507.68	1516.75	1520.24	957.38786
	1529.24	3048.08	3053.52	3056.79	3062.47	3095.41	3121.53	3128.28	3132.16	3135.14	3145.82	3149.40	
$C_2C(OOH)CC\bullet$	48.54	174.60	194.75	201.23	222.49	239.06	293.43	323.27	337.24	364.96	404.26	450.55	657.63453
	519.86	547.01	725.96	838.08	867.56	927.39	948.47	955.47	1003.48	1028.22	1103.57	1135.91	700.81277
	1219.36	1249.70	1301.58	1363.62	1373.64	1410.00	1426.26	1464.50	1471.10	1493.27	1501.33	1507.53	939.25691
	1524.80	2978.35	3021.52	3053.35	3059.56	3124.82	3134.70	3141.45	3146.76	3165.47	3270.42	3736.66	
$C_2\bullet C(OOH)CC$	78.52	92.49	152.33	192.72	216.42	229.24	257.60	283.30	330.33	362.17	397.56	485.80	631.60489
	530.84	583.05	733.37	780.39	843.04	925.49	939.35	979.28	1011.31	1018.23	1080.56	1167.74	751.21860
	1236.48	1261.67	1319.97	1360.34	1383.27	1413.59	1424.47	1470.49	1492.93	1497.62	1508.32	1516.30	969.18555
	1526.88	3046.90	3049.53	3060.10	3086.68	3118.81	3121.85	3139.44	3140.77	3160.56	3271.29	3757.94	
$C_2C(OOH)C\bullet C$	81.03	85.97	141.09	203.14	216.45	228.33	261.56	280.24	303.35	343.72	399.86	422.50	658.15366
	533.69	566.01	746.41	844.61	919.51	927.42	942.40	992.66	1015.05	1047.16	1128.68	1169.52	720.77823
	1215.59	1267.36	1357.45	1387.43	1403.54	1418.42	1420.31	1481.38	1489.74	1497.03	1501.52	1510.79	963.37973
	1525.06	2993.86	3050.31	3055.06	3064.78	3109.43	3123.03	3130.95	3139.26	3143.57	3181.03	3762.66	
$C_2CYCOCC$	71.55	207.36	252.21	315.84	346.81	398.31	436.66	650.81	792.47	856.61	865.99	922.72	354.33387
	967.10	970.85	1007.63	1030.34	1036.60	1165.38	1182.66	1216.78	1245.22	1291.60	1294.60	1361.17	549.78273
	1414.39	1425.38	1488.28	1496.01	1502.98	1508.78	1520.26	1549.93	3022.48	3038.61	3044.45	3060.27	608.23003
	3080.97	3110.85	3117.78	3122.38	3125.60	3136.01							

Table C.3 Calculated $\Delta H_f{}^{\circ}{}_{298}$ Values [a]

Reaction Series	B3LYP /6-31G(d,p)		B3LYP /6-311++G(3df,2p)		CBSQ//B3LYP /6-31G(d,p)	
	$\Delta H^{\circ}{}_{rxn}$	$\Delta H_f{}^{\circ}{}_{298}$	$\Delta H^{\circ}{}_{rxn}$	$\Delta H_f{}^{\circ}{}_{298}$	$\Delta H^{\circ}{}_{rxn}$	$\Delta H_f{}^{\circ}{}_{298}$
$C_2C{\cdot}COH + CH_4 \rightarrow C_3COH + CH_3$	6.08	-28.09	5.15	-27.16	0.21	-22.22
$C_2C{\cdot}COH + C_2H_6 \rightarrow C_3COH + C_2H_5$	1.32	-27.00	0.46	-26.14	-3.45	-22.23
						-22.22
$C_3{\cdot}COH + CH_4 \rightarrow C_2COH + C_2H_5$	3.79	-22.29	3.48	-21.98	6.65	-25.15
$C_3{\cdot}COH + C_2H_6 \rightarrow C_3COH + C_2H_5$	-0.80	-24.88	-1.11	-24.57	-1.56	-24.12
						-24.64
$C_2C(OO{\cdot})COH + CH_4 \rightarrow COO{\cdot} + C_3COH$	13.73	-68.41	11.08	-65.76	8.03	-62.71
$C_2C(OO{\cdot})COH + C_2H_6 \rightarrow CCOO{\cdot} + C_3COH$	8.33	-69.61	5.68	-66.96	1.92	-63.20
						-62.96
$C_2C(OH)COO{\cdot} + CH_4 \rightarrow COO{\cdot} + C_3COH$	6.76	-61.44	4.48	-59.16	6.83	-61.51
$C_2C(OH)COO{\cdot} + C_2H_6 \rightarrow CCOO{\cdot} + C_3COH$	1.36	-62.64	-0.91	-60.37	0.72	-62.00
						-61.76
$C_2C(O{\cdot})COOH + C_2H_6 \rightarrow C_3CO{\cdot} + CCOOH$	-0.96	-41.64	-2.11	-40.49	-1.38	-41.22
$C_2C(O{\cdot})COOH + C_3H_8 \rightarrow C_3CO{\cdot} + CCCOOH$	-0.65	-42.24	-1.63	-41.26	-1.52	-41.37
						-41.30
$C_2{\cdot}C(OOH)COH + CH_4 \rightarrow C_2{\cdot}COH + CCOOH$	5.19	-41.95	2.47	-39.23	7.50	-44.26
$C_2{\cdot}C(OOH)COH + CH_4 \rightarrow C_2{\cdot}COH + CCCOOH$	3.89	-43.37	1.24	-40.72	4.59	-44.07
						-44.16
$C_2{\cdot}C(OH)COOH + CH_4 \rightarrow C{\cdot}COOH + CCCOH$	6.59	-42.93	4.16	-40.50	10.34	-46.68
$C_2{\cdot}C(OH)COOH + CH_4 \rightarrow C{\cdot}CCOOH + CCOH$	2.00	-45.52	-0.42	-43.10	2.13	-45.65
						-46.17
$C_2C(OOH)C{\cdot}OH + CH_4 \rightarrow C_2COOH + CC{\cdot}OH$	1.17	-45.58	-0.16	-44.25	4.75	-49.16
$C_2C(OOH)C{\cdot}OH \rightarrow C_2{\cdot}C(OH)COOH$	4.47	-48.74	4.86	-49.13	4.36	-48.63
						-48.90
$C_2C(OO{\cdot})CC + CH_4 \rightarrow C_2COO{\cdot} + C_3H_8$	3.65	-27.98	2.92	-27.25	9.51	-33.84
$C_2C(OO{\cdot})CC + CH_3OH \rightarrow CCCOO{\cdot} + i\text{-}C_3OH$	-1.01	-28.34	-1.29	-28.06	4.51	-33.86
						-33.58
$C_2C(OOH)CC{\cdot} \rightarrow C_3{\cdot}CCOOH$	5.99	-15.42	5.19	-14.62	2.04	-14.34
$C_2C(OOH)CC{\cdot} + CH_4 \rightarrow C_3CCOOH + CH_3{\cdot}$	10.24	-16.13	9.24	-15.13	8.73	-14.62
						-14.48
$C_2{\cdot}C(OOH)CC \rightarrow C_3{\cdot}CCOOH$	3.67	-13.10	2.87	-12.30	3.14	-12.57
$C_2{\cdot}C(OOH)CC + CH_4 \rightarrow C_3CCOOH + CH_3{\cdot}$	7.91	-13.80	6.92	-12.81	6.69	-12.58
						-12.58
$C_2C(OOH)C{\cdot}C \rightarrow C_3{\cdot}CCOOH$	8.90	-18.33	8.07	-17.50	7.19	-16.62
$C_2C(OOH)C{\cdot}C + CH_4 \rightarrow C_3CCOOH + CH_3{\cdot}$	13.14	-19.03	12.12	-18.01	10.74	-16.63
						-16.63
$C_2CYCOCC \rightarrow C_2CYCCOC$	5.81	-41.24	5.45	-40.88	4.34	-39.77
$C_2CYCOCC + CH_3OOH \rightarrow CCQCYCOCC + CH_4$	1.11	-39.95	2.03	-40.87		

[a] Units in kcal mol^{-1}.

Table C.4 Calculated Ideal Gas Phase Thermodynamic Properties[a]

Species	$\Delta H_f{}^\circ{}_{298}$[b]	$S^\circ{}_{298}$[c]	C_p300[c]	C_p400	C_p500	C_p600	C_p800	C_p1000	C_p1500
TS14	-40.83	86.63	32.89	40.87	47.65	53.2	61.51	67.35	75.97
TS15	-27.25	89.32	32.15	39.96	46.52	51.85	59.78	65.44	74.10
TS16	-34.3	89.09	32.34	39.9	46.32	51.56	59.5	65.19	73.96
TS17	-37.37	94.07	34.28	40.97	46.84	51.8	59.54	65.29	74.35
TS18	-37.51	88.65	33.63	40.79	46.85	51.84	59.48	65.13	74.11
TS19	-30.78	82.75	27.74	34.8	41.03	46.26	54.26	60.05	68.92
TS20	-30.73	88.09	30.36	37.86	44.46	49.97	58.35	64.38	73.56
TS21	-31.01	92.64	34.00	41.36	47.48	52.43	59.92	65.41	74.20
TS22	-38.95	85.15	31.10	39.16	45.97	51.54	59.92	65.90	74.97
TS23	-35.03	87.89	31.64	39.64	46.42	51.92	60.13	65.95	74.84
TS24	-31.99	94.60	34.21	41.24	47.24	52.19	59.78	65.39	74.30
TS25	-28.36	95.56	34.92	41.73	47.55	52.35	59.69	65.09	73.68
TS26	-20.26	97.60	35.60	42.52	48.30	53.01	60.19	65.51	74.15
TS28	-9.10	85.78	33.26	42.46	50.33	56.78	66.54	73.57	84.34
TS29	2.36	88.38	33.72	42.73	50.46	56.83	66.52	73.53	84.32
TS30	-0.50	88.78	34.22	43.00	50.52	56.73	66.17	73.03	83.60
TS31	5.00	91.45	35.65	44.21	51.43	57.32	66.34	73.00	83.64
TS32	-4.65	93.85	36.33	44.18	50.99	56.68	65.56	72.20	82.81
TS33	-4.04	91.96	34.02	42.47	49.98	56.30	66.08	73.20	84.15
TS34	-3.76	91.39	34.76	42.95	50.21	56.33	65.81	72.75	83.46
TS35	1.03	92.47	35.76	43.90	50.93	56.79	65.89	72.67	83.49
$C_2C \bullet COH$	-22.22	86.95	25.21	30.47	35.62	40.22	47.71	53.40	62.47
$C_2C(OO\bullet)COH$	-62.71	96.31	32.88	40.05	46.21	51.26	58.87	64.38	73.01
$C_2 \bullet C(OOH)COH$	-46.68	103.72	34.91	41.62	47.29	51.92	58.95	64.09	72.29
$C_2C(OOH)C \bullet OH$	-49.16	100.02	35.27	42.32	48.23	52.99	60.05	65.07	72.90
$C_2C(OOH)CO \bullet$	-43.52	95.94	34.35	41.71	47.89	52.90	60.41	65.77	73.95
$C_2C=COH$	-49.50	80.02	25.98	31.14	35.75	39.73	46.12	51.01	58.89
$C=C(C)COH$	-39.81	83.04	24.68	29.78	34.45	38.49	44.97	49.91	57.83
$C(C=O)COOH$	-68.21	90.1	27.6	32.56	36.75	40.15	45.18	48.7	54.05
$C_3 \bullet COH$	-24.12	85.52	27.71	33.73	38.84	43.07	49.69	54.73	62.97
$C_2C(OH)COO \bullet$	-61.76	98.71	32.63	39.89	46.08	51.11	58.59	63.97	72.33
$C_2C(O\bullet)CQ$	-41.30	99.14	34.46	41.64	47.77	52.76	60.15	65.35	73.27
$C_2 \bullet C(OH)CQ$	-44.27	102.41	35.39	42.44	48.27	52.95	59.90	64.90	72.74
$C_2C(OO\bullet)CC$	-33.58	91.05	34.81	43.26	50.65	56.82	66.39	73.47	84.58
$C_2C(OOH)CC \bullet$	-12.58	96.27	37.49	45.84	52.99	58.89	67.99	74.74	85.51
$C_2 \bullet C(OOH)CC$	-14.48	93.80	37.33	45.79	53.00	58.94	68.07	74.83	85.58
$C_2C(OOH)C \bullet C$	-16.63	93.22	37.40	45.61	52.73	58.67	67.86	74.68	85.52
$C_2CYCOCC$	-39.77	80.17	27.29	35.27	42.39	48.35	57.56	64.32	74.78

[a] Thermodynamic properties are referred to a standard state of an ideal gas of pure enantiometer at 1 atm. [b] Units in kcal mol^{-1}. [c] Units in cal mol^{-1} K^{-1}. [d] Furuyama, S.; Golden, D. M.; Benson, S. W. Int. J. Chem. Kinet. **1969**, 1(3), 283. [e] Bedjanian, Y.; Bras, G. L.; Poulet, G. J. Phys. Chem. **1997**, 101, 4088.

Table C.5 Input and Output Kinetic Parameters for QRRK and Master Equation Analysis in C_2C•COH + O_2 System

adducts	QRRK input parameters		
	Frequency / degeneracy		
$C_2C(OO•)COH$	411.0 / 15.756	1351.1 / 16.037	3514.5 / 7.708
$C_2C(OOH)CO•$	433.0 / 17.630	1399.0 / 15.199	3558.2 / 6.672
$C_2•C(OOH)COH$	396.7 / 17.060	1377.8 / 14.362	3572.1 / 7.577
$C_2C(OOH)C•OH$	402.6 / 17.340	1360.3 / 14.855	3667.9 / 6.805
Lennard-Jones parameter	σ (Å)	ε/k (K)	
	5.86	632	

reaction	A (s^{-1} or cm^3 mol^{-1} s^{-1})	n	E_a (kcal mol^{-1})
$C_2C•COH + O_2 \rightarrow C_2C(OO•)COH$	3.60×10^{12} [a]	0.0	0.0
$C_2C(OO•)COH \rightarrow C_2C•COH + O_2$	$3.95E \times 10^{15}$ [b]	0.0	38.44
$C_2C(OO•)COH \rightarrow C_2C(OOH)CH_2O•$	4.24×10^4	2.17256	20.94
$C_2C(OO•)COH \rightarrow C_2•C(OOH)COH$	3.85×10^7	1.38130	35.09
$C_2C(OO•)COH \rightarrow C_2C(OOH)C•OH$	7.82×10^7	1.26442	28.14
$C_2C(OO•)COH \rightarrow C=C(C)COH+HO_2$	6.17×10^3	2.89780	30.56
$C_2C(OO•)COH \rightarrow C_2C=COH+HO_2$	4.39×10^8	1.29524	31.71
$C_2C(OOH)CH_2O• \rightarrow C_2•C(OOH)COH$	6.96×10^6	0.71821	25.82
$C_2C(OOH)CH_2O• \rightarrow C_2C=O+CH_2O+OH$	6.87×10^{10}	0.67733	8.34
$C_2•C(OOH)COH \rightarrow C_2C(OO•)COH$	1.58×10^6	1.25308	18.92
$C_2•C(OOH)COH \rightarrow C=C(C)COH+HO_2$	2.95×10^6	1.44470	15.21
$C_2C(OOH)C•OH \rightarrow C_2C(OO•)COH$	5.06×10^8	0.66570	14.76
$C_2C(OOH)C•OH \rightarrow C_2C=COH+HO_2$	2.42×10^8	0.76676	11.59

	QRRK output parameters		
	A (s^{-1} or cm^3 mol^{-1} s^{-1})	n	E_a (kcal mol^{-1})
			P(atm)
$C_2C•COH + O_2 \rightarrow C_2C(OO•)COH$	7.60+101	-28.30	29731	0.1
$C_2C•COH + O_2 \rightarrow C_2C(OO•)COH$	7.86E+66	-17.09	18836	1.0
$C_2C•COH + O_2 \rightarrow C_2C(OO•)COH$	1.30E+37	-7.69	8744	10.0
$C_2C•COH + O_2 \rightarrow C=C(C)COH+HO_2$	9.27E+45	-10.20	19843	0.1
$C_2C•COH + O_2 \rightarrow C=C(C)COH+HO_2$	5.65E+35	-6.82	19362	1.0
$C_2C•COH + O_2 \rightarrow C=C(C)COH+HO_2$	1.84E+10	1.14	12397	10.0
$C_2C•COH + O_2 \rightarrow C_2C=COH+HO_2$	2.11E+49	-11.40	19669	0.1
$C_2C•COH + O_2 \rightarrow C_2C=COH+HO_2$	2.99E+40	-8.43	19725	1.0
$C_2C•COH + O_2 \rightarrow C_2C=COH+HO_2$	4.78E+15	-0.68	13083	10.0
$C_2C•COH + O_2 \rightarrow C_2C(OOH)CH_2O•$	5.04E+87	-26.49	27289	0.1
$C_2C•COH + O_2 \rightarrow C_2C(OOH)CH_2O•$	5.82E+44	-12.95	11660	1.0
$C_2C•COH + O_2 \rightarrow C_2C(OOH)CH_2O•$	9.04E-04	1.71	-9261	10.0
$C_2C•COH + O_2 \rightarrow C_2C=O+CH_2O+OH$	4.61E+56	-13.51	21067	0.1
$C_2C•COH + O_2 \rightarrow C_2C=O+CH_2O+OH$	7.73E+38	-7.83	17534	1.0
$C_2C•COH + O_2 \rightarrow C_2C=O+CH_2O+OH$	1.17E+11	0.78	9346	10.0
$C_2C•COH + O_2 \rightarrow C_2•C(OOH)COH$	6.68+153	-44.95	55999	0.1
$C_2C•COH + O_2 \rightarrow C_2•C(OOH)COH$	2.05+102	-28.22	43136	1.0
$C_2C•COH + O_2 \rightarrow C_2•C(OOH)COH$	9.82E+32	-6.44	21177	10.0
$C_2C•COH + O_2 \rightarrow C=C(C)COH+HO_2$	7.11E+68	-17.47	32786	0.1
$C_2C•COH + O_2 \rightarrow C=C(C)COH+HO_2$	1.11E+47	-10.27	30997	1.0
$C_2C•COH + O_2 \rightarrow C=C(C)COH+HO_2$	2.72E-02	4.86	17486	10.0
$C_2C•COH + O_2 \rightarrow C_2C(OOH)C•OH$	6.17+143	-42.53	44713	0.1
$C_2C•COH + O_2 \rightarrow C_2C(OOH)C•OH$	4.75+156	-45.48	56816	1.0
$C_2C•COH + O_2 \rightarrow C_2C(OOH)C•OH$	2.05E+92	-24.84	39018	10.0
$C_2C•COH + O_2 \rightarrow C_2C=COH+HO_2$	2.53E+60	-14.88	23529	0.1

$C_2C \cdot COH + O_2 \rightarrow C_2C=COH+HO_2$	5.43E+63	-15.45	30741	1.0
$C_2C \cdot COH + O_2 \rightarrow C_2C=COH+HO_2$	2.10E+17	-0.80	19224	10.0
$C_2C(OO \cdot)COH \rightarrow C=C(C)COH+HO_2$	4.21E+52	-12.48	47354	0.1
$C_2C(OO \cdot)COH \rightarrow C=C(C)COH+HO_2$	2.00E+28	-4.78	39256	1.0
$C_2C(OO \cdot)COH \rightarrow C=C(C)COH+HO_2$	1.68E+12	0.27	33611	10.0
$C_2C(OO \cdot)COH \rightarrow C_2C=COH+HO_2$	6.38E+60	-15.15	49549	0.1
$C_2C(OO \cdot)COH \rightarrow C_2C=COH+HO_2$	3.62E+35	-7.14	41228	1.0
$C_2C(OO \cdot)COH \rightarrow C_2C=COH+HO_2$	1.59E+18	-1.69	35161	10.0
$C_2C(OO \cdot)COH \rightarrow C_2C(OOH)CH_2O \cdot$	1.69E+28	-5.22	29320	0.1
$C_2C(OO \cdot)COH \rightarrow C_2C(OOH)CH_2O \cdot$	8.49E+13	-0.73	24300	1.0
$C_2C(OO \cdot)COH \rightarrow C_2C(OOH)CH_2O \cdot$	1.17E+07	1.41	21827	10.0
$C_2C(OO \cdot)COH \rightarrow C_2 \cdot C(OOH)COH$	3.06E+69	-18.20	55850	0.1
$C_2C(OO \cdot)COH \rightarrow C_2 \cdot C(OOH)COH$	1.55E+42	-9.49	47186	1.0
$C_2C(OO \cdot)COH \rightarrow C_2 \cdot C(OOH)COH$	1.19E+21	-2.83	39925	10.0
$C_2C(OO \cdot)COH \rightarrow C_2C(OOH)C \cdot OH$	5.71E+49	-11.90	42683	0.1
$C_2C(OO \cdot)COH \rightarrow C_2C(OOH)C \cdot OH$	4.60E+27	-4.92	35193	1.0
$C_2C(OO \cdot)COH \rightarrow C_2C(OOH)C \cdot OH$	1.67E+14	-0.71	30433	10.0
$C_2C(OOH)CH_2O \cdot \rightarrow C_2C=O+CH_2O+OH$	1.98E+37	-8.81	16178	0.1
$C_2C(OOH)CH_2O \cdot \rightarrow C_2C=O+CH_2O+OH$	1.05E+39	-9.01	16753	1.0
$C_2C(OOH)CH_2O \cdot \rightarrow C_2C=O+CH_2O+OH$	1.06E+41	-9.29	18012	10.0
$C_2 \cdot C(OOH)COH \rightarrow C=C(C)COH+HO_2$	1.18E+61	-15.39	37591	0.1
$C_2 \cdot C(OOH)COH \rightarrow C=C(C)COH+HO_2$	9.98E+39	-8.64	31028	1.0
$C_2 \cdot C(OOH)COH \rightarrow C=C(C)COH+HO_2$	1.79E+32	-6.22	28209	10.0
$C_2C(OOH)C \cdot OH \rightarrow C_2C=COH+HO_2$	2.60E+45	-10.97	24741	0.1
$C_2C(OOH)C \cdot OH \rightarrow C_2C=COH+HO_2$	8.21E+37	-8.33	23716	1.0
$C_2C(OOH)C \cdot OH \rightarrow C_2C=COH+HO_2$	1.19E+25	-4.22	19661	10.0

[a] Estimated from $CCC \cdot + O_2$, Atkinson, R.; Baulch, D. L.; Cox, R. A.; R. F. Hampson, J.; Kerr, J. A.; Troe, J. *J. Chem. Ref. Data* **1989**, *18*, 881. [b] From the principle of microscopic reversibility, and $E_a = \Delta H^o_{rxn} - RT$.

Table C.6 Input and Output Kinetic Parameters for QRRK and Master Equation Analysis in $C_3 \cdot COH + O_2$ System

adducts	QRRK input parameters		
	frequency / degeneracy		
$C_2C(OH)COO\cdot$	443.9 / 16.724	1417.3 / 15.592	3870.7 / 7.184
$C_2C(O\cdot)CQ$	425.0 / 17.563	1427.6 / 15.683	3961.0 / 6.254
$C_2\cdot C(OH)CQ$	414.0 / 17.846	1375.5 / 14.157	3664.1 / 6.996
Lennard-Jones parameter	σ (Å)	ε/k (K)	
	5.86	632	

reaction	A (s^{-1} or cm^3 mol^{-1} s^{-1})	n	E_a(kcal mol^{-1})
$C_3\cdot COH + O_2 \rightarrow C_2C(OH)COO\cdot$	3.60×10^{12} [a]	0.0	0.0
$C_2C(OH)COO\cdot \rightarrow C_3\cdot COH + O_2$	130×10^{15} [b]	0.0	36.15
$C_2C(OH)COO\cdot \rightarrow C_2C(O\cdot)CQ$	3.09×10^5	1.56863	22.16
$C_2C(OH)COO\cdot \rightarrow C_2\cdot C(OH)CQ$	6.70×10^5	1.67050	26.07
$C_2C(O\cdot)CQ \rightarrow C_2C(OH)COO\cdot$	1.70×10^7	0.82262	0.21
$C_2C(O\cdot)CQ \rightarrow C_2C=O+CH_2O+OH$	1.52×10^9	0.93149	9.28
$C_2C(O\cdot)CQ \rightarrow CH_3+C(C=O)CQ$	3.52×10^9	0.89989	13.72
$C_2\cdot C(OH)CQ \rightarrow C_2C(OH)COO\cdot$	4.77×10^6	0.95527	8.82
$C_2\cdot C(OH)CQ \rightarrow C=C(C)CQ+OH$	1.96×10^{14} [c]	0.0	30.0 [c]
$C_2\cdot C(OH)CQ \rightarrow C=C(C)OH+CH_2O+OH$	1.95×10^8	1.21702	20.17

	QRRK output parameters			
	A (s^{-1} or cm^3 mol^{-1} s^{-1})	n	E_a(kcal mol^{-1})	P(atm)
$C_3\cdot COH + O_2 \rightarrow C_2C(OH)COO\cdot$	9.11E+79	-21.38	22278	0.1
$C_3\cdot COH + O_2 \rightarrow C_2C(OH)COO\cdot$	1.96E+55	-13.45	14760	1.0
$C_3\cdot COH + O_2 \rightarrow C_2C(OH)COO\cdot$	1.12E+30	-5.48	6213	10.0
$C_3\cdot COH + O_2 \rightarrow C_2C(O\cdot)CQ$	6.40E+66	-19.77	21496	0.1
$C_3\cdot COH + O_2 \rightarrow C_2C(O\cdot)CQ$	3.67E+25	-6.94	5206	1.0
$C_3\cdot COH + O_2 \rightarrow C_2C(O\cdot)CQ$	5.72E+06	-1.44	-7320	10.0
$C_3\cdot COH + O_2 \rightarrow C_2C=O+CH_2O+OH$	4.21E+50	-11.91	20586	0.1
$C_3\cdot COH + O_2 \rightarrow C_2C=O+CH_2O+OH$	8.37E+37	-7.82	18895	1.0
$C_3\cdot COH + O_2 \rightarrow C_2C=O+CH_2O+OH$	2.24E+20	-2.30	15331	10.0
$C_3\cdot COH + O_2 \rightarrow CH_3+C(C=O)CQ$	2.85E+47	-11.11	20992	0.1
$C_3\cdot COH + O_2 \rightarrow CH_3+C(C=O)CQ$	8.57E+39	-8.57	21419	1.0
$C_3\cdot COH + O_2 \rightarrow CH_3+C(C=O)CQ$	4.98E+24	-3.73	19084	10.0
$C_3\cdot COH + O_2 \rightarrow C_2\cdot C(OH)CQ$	6.19+166	-49.32	55465	0.1
$C_3\cdot COH + O_2 \rightarrow C_2\cdot C(OH)CQ$	1.55+172	-50.08	64926	1.0
$C_3\cdot COH + O_2 \rightarrow C_2\cdot C(OH)CQ$	4.98E+93	-25.31	40470	10.0
$C_3\cdot COH + O_2 \rightarrow C=C(C)CQ+OH$	1.40E+56	-13.36	31637	0.1
$C_3\cdot COH + O_2 \rightarrow C=C(C)CQ+OH$	2.75E+66	-16.05	41285	1.0
$C_3\cdot COH + O_2 \rightarrow C=C(C)CQ+OH$	1.48E+16	-0.27	27657	10.0
$C_3\cdot COH + O_2 \rightarrow C=C(C)OH+CH_2O+OH$	7.30E+63	-15.73	30966	0.1
$C_3\cdot COH + O_2 \rightarrow C=C(C)OH+CH_2O+OH$	1.57E+55	-12.56	34233	1.0
$C_3\cdot COH + O_2 \rightarrow C=C(C)OH+CH_2O+OH$	5.01E-12	8.18	14467	10.0
$C_2C(OH)COO\cdot \rightarrow C_2C(O\cdot)CQ$	5.15E+25	-4.76	29348	0.1
$C_2C(OH)COO\cdot \rightarrow C_2C(O\cdot)CQ$	2.62E+13	-0.90	25037	1.0
$C_2C(OH)COO\cdot \rightarrow C_2C(O\cdot)CQ$	1.10E+08	0.78	23100	10.0
$C_2C(OH)COO\cdot \rightarrow C_2\cdot C(OH)CQ$	5.69E+34	-7.41	36195	0.1
$C_2C(OH)COO\cdot \rightarrow C_2\cdot C(OH)CQ$	2.29E+18	-2.25	30576	1.0
$C_2C(OH)COO\cdot \rightarrow C_2\cdot C(OH)CQ$	3.33E+10	0.21	27784	10.0
$C_2C(O\cdot)CQ \rightarrow C_2C=O+CH_2O+OH$	5.23E+45	-11.23	22445	0.1
$C_2C(O\cdot)CQ \rightarrow C_2C=O+CH_2O+OH$	5.97E+47	-11.53	23528	1.0

$C_2C(O\bullet)CQ \rightarrow C_2C=O+CH_2O+OH$	7.25E+50	-12.13	25820	10.0
$C_2C(O\bullet)CQ \rightarrow CH_3+C(C=O)CQ$	2.13E+44	-11.24	22449	0.1
$C_2C(O\bullet)CQ \rightarrow CH_3+C(C=O)CQ$	7.19E+46	-11.68	23705	1.0
$C_2C(O\bullet)CQ \rightarrow CH_3+C(C=O)CQ$	8.23E+49	-12.18	26352	10.0
$C_2\bullet C(OH)CQ \rightarrow C=C(C)CQ+OH$	1.37E+62	-16.28	41988	0.1
$C_2\bullet C(OH)CQ \rightarrow C=C(C)CQ+OH$	8.58E+64	-16.02	49015	1.0
$C_2\bullet C(OH)CQ \rightarrow C=C(C)CQ+OH$	6.83E+36	-7.06	40010	10.0
$C_2\bullet C(OH)CQ \rightarrow C=C(C)OH+CH_2O+OH$	3.59E+37	-8.49	27453	0.1
$C_2\bullet C(OH)CQ \rightarrow C=C(C)OH+CH_2O+OH$	1.27E+31	-5.95	28130	1.0
$C_2\bullet C(OH)CQ \rightarrow C=C(C)OH+CH_2O+OH$	7.35E+13	-0.51	22271	10.0

[a] Estimated from CCC•+ O_2, Atkinson, R.; Baulch, D. L.; Cox, R. A.; R. F. Hampson, J.; Kerr, J. A.; Troe, J. *J. Chem. Ref. Data* **1989**, *18*, 881. [b] From the principle of microscopic reversibility, and $E_a=\Delta H^o_{rxn} - RT$. . [c] Chen, C.-J.; Bozzelli, J. W. *J. Phys. Chem. A* **1999**, *103*, 9731.

Table C.7 Input and Output Kinetic Parameters for QRRK and Master Equation Analysis in $C_2C•C + O_2$ System

adducts	QRRK input parameters		
	frequency / degeneracy		
$C_2C(OO•)CC$	481.5 / 19.682	1533.1 / 19.160	3900.0 / 9.159
$C_2C(OOH)CC•$	452.8 / 20.449	1467.6 / 18.005	3711.9 / 9.546
$C_2•C(OOH)C•C$	437.4 / 19.987	1471.3 / 18.509	3709.6 / 9.504
$C_2•C(OOH)CC$	445.6 / 20.315	1464.9 / 18.046	3708.0 / 9.639
Lennard-Jones parameter	σ (Å)	ε/k (K)	
	5.86	632	

reaction	A (s^{-1} or cm^3 mol^{-1} s^{-1})	n	E_a (kcal mol^{-1})
$C_2C•CC + O_2 \rightarrow C_2C(OO•)CC$	3.60×10^{12} [a]	0.0	0.0
$C_2C(OO•)CC \rightarrow C_2C•CC + O_2$	3.49×10^{16} [b]	0.0	38.06
$C_2C(OO•)CC \rightarrow C_2C(OOH)CC•$	1.90×10^7	1.57887	23.83
$C_2C(OO•)CC \rightarrow C_2•C(OOH)CC$	1.03×10^8	1.53572	35.38
$C_2C(OO•)CC \rightarrow C_2C(OOH)C•C$	2.30×10^{10}	0.81833	33.21
$C_2C(OO•)CC \rightarrow C=C(C)CC+HO_2$	3.46×10^9	1.28816	29.62
$C_2C(OO•)CC \rightarrow C_2C=CC+HO_2$	2.23×10^{11}	0.68558	31.24
$C_2C(OOH)CC• \rightarrow C_2C(OO•)CC$	3.31×10^8	0.72840	3.20
$C_2C(OOH)CC• \rightarrow C_2CYCOCC+OH$	1.89×10^9	0.94503	17.39
$C_2C(OOH)C•C \rightarrow C_2C(OO•)CC$	1.20×10^{12}	0.03464	16.59
$C_2C(OOH)C•C \rightarrow CC=CC_2+HO_2$	5.75×10^{13}	-0.10708	12.76
$C_2•C(OOH)CC \rightarrow C_2C(OO•)COH$	1.78×10^9	0.68525	14.74
$C_2•C(OOH)CC \rightarrow C=C(C)COH+HO_2$	2.84×10^{10}	0.62675	13.65

	QRRK output parameters			
	A (s^{-1} or cm^3 mol^{-1} s^{-1})	n	E_a (kcal mol^{-1})	P(atm)
$C_2C•CC + O_2 \rightarrow C_2C(OO•)CC$	6.97+118	-34.24	32313	0.1
$C_2C•CC + O_2 \rightarrow C_2C(OO•)CC$	1.06+108	-30.42	30797	1.0
$C_2C•CC + O_2 \rightarrow C_2C(OO•)CC$	5.27E+86	-23.42	25145	10.0
$C_2C•CC + O_2 \rightarrow C=C(C)CC+HO_2$	2.10E+42	-9.75	13187	0.1
$C_2C•CC + O_2 \rightarrow C=C(C)CC+HO_2$	6.96E+51	-12.46	19474	1.0
$C_2C•CC + O_2 \rightarrow C=C(C)CC+HO_2$	1.18E+52	-12.28	22853	10.0
$C_2C•CC + O_2 \rightarrow C_2C=CC+HO_2$	2.02E+39	-8.94	12132	0.1
$C_2C•CC + O_2 \rightarrow C_2C=CC+HO_2$	2.02E+50	-12.11	18864	1.0
$C_2C•CC + O_2 \rightarrow C_2C=CC+HO_2$	5.24E+52	-12.60	23042	10.0
$C_2C•CC + O_2 \rightarrow C_2C(OOH)CC•$	1.95+102	-31.63	27090	0.1
$C_2C•CC + O_2 \rightarrow C_2C(OOH)CC•$	5.97E+75	-23.26	16121	1.0
$C_2C•CC + O_2 \rightarrow C_2C(OOH)CC•$	2.00E+69	-21.20	11178	10.0
$C_2C•CC + O_2 \rightarrow C_2CyCOCC+OH$	1.55E+16	-1.97	9133	0.1
$C_2C•CC + O_2 \rightarrow C_2CyCOCC+OH$	1.27E+31	-6.40	16648	1.0
$C_2C•CC + O_2 \rightarrow C_2CyCOCC+OH$	2.33E+49	-11.70	27392	10.0
$C_2C•CC + O_2 \rightarrow C_2•C(OOH)CC$	1.85+127	-38.46	38402	0.1
$C_2C•CC + O_2 \rightarrow C_2•C(OOH)CC$	2.52+155	-46.39	53726	1.0
$C_2C•CC + O_2 \rightarrow C_2•C(OOH)CC$	1.09+166	-48.79	64364	10.0
$C_2C•CC + O_2 \rightarrow C=C(C)CC+HO_2$	8.41E+30	-6.65	13140	0.1
$C_2C•CC + O_2 \rightarrow C=C(C)CC+HO_2$	2.91E+57	-14.51	26862	1.0
$C_2C•CC + O_2 \rightarrow C=C(C)CC+HO_2$	1.40E+73	-18.83	38853	10.0
$C_2C•CC + O_2 \rightarrow C_2C(OOH)C•C$	1.19E+96	-29.60	25599	0.1
$C_2C•CC + O_2 \rightarrow C_2C(OOH)C•C$	1.54E+99	-30.00	28320	1.0
$C_2C•CC + O_2 \rightarrow C_2C(OOH)C•C$	2.63+118	-35.27	38576	10.0

$C_2C \cdot CC + O_2 \rightarrow C_2C{=}CC{+}HO_2$	3.19E+32	-7.10	10964	0.1
$C_2C \cdot CC + O_2 \rightarrow C_2C{=}CC{+}HO_2$	1.48E+45	-10.79	18170	1.0
$C_2C \cdot CC + O_2 \rightarrow C_2C{=}CC{+}HO_2$	9.97E+52	-12.93	24568	10.0
$C_2C(OO \cdot)CC \rightarrow C{=}C(C)CC{+}HO_2$	9.21E+74	-19.68	49994	0.1
$C_2C(OO \cdot)CC \rightarrow C{=}C(C)CC{+}HO_2$	4.37E+65	-16.50	48163	1.0
$C_2C(OO \cdot)CC \rightarrow C{=}C(C)CC{+}HO_2$	5.75E+49	-11.37	43513	10.0
$C_2C(OO \cdot)CC \rightarrow C_2C{=}CC{+}HO_2$	9.40E+79	-21.39	52146	0.1
$C_2C(OO \cdot)CC \rightarrow C_2C{=}CC{+}HO_2$	3.77E+71	-18.46	50864	1.0
$C_2C(OO \cdot)CC \rightarrow C_2C{=}CC{+}HO_2$	6.48E+55	-13.33	46470	10.0
$C_2C(OO \cdot)CC \rightarrow C_2C(OOH)CC \cdot$	1.73E+58	-14.58	40698	0.1
$C_2C(OO \cdot)CC \rightarrow C_2C(OOH)CC \cdot$	2.00E+47	-11.03	37584	1.0
$C_2C(OO \cdot)CC \rightarrow C_2C(OOH)CC \cdot$	1.65E+33	-6.55	32996	10.0
$C_2C(OO \cdot)CC \rightarrow C_2 \cdot C(OOH)CC$	1.17E+83	-22.90	56781	0.1
$C_2C(OO \cdot)CC \rightarrow C_2 \cdot C(OOH)CC$	3.09E+77	-20.73	57045	1.0
$C_2C(OO \cdot)CC \rightarrow C_2 \cdot C(OOH)CC$	1.71E+63	-15.95	53812	10.0
$C_2C(OO \cdot)CC \rightarrow C_2C(OOH)C \cdot C$	2.22E+82	-22.46	54497	0.1
$C_2C(OO \cdot)CC \rightarrow C_2C(OOH)C \cdot C$	1.74E+75	-19.88	53938	1.0
$C_2C(OO \cdot)CC \rightarrow C_2C(OOH)C \cdot C$	9.76E+59	-14.85	50013	10.0
$C_2C(OOH)CC \cdot \rightarrow C_2CyCOCC{+}OH$	1.85E+34	-9.03	18124	0.1
$C_2C(OOH)CC \cdot \rightarrow C_2CyCOCC{+}OH$	1.48E+38	-9.83	19889	1.0
$C_2C(OOH)CC \cdot \rightarrow C_2CyCOCC{+}OH$	1.58E+38	-9.08	22656	10.0
$C_2 \cdot C(OOH)CC \rightarrow C{=}C(C)CC{+}HO_2$	1.29E+72	-18.80	38219	0.1
$C_2 \cdot C(OOH)CC \rightarrow C{=}C(C)CC{+}HO_2$	4.41E+75	-19.59	40547	1.0
$C_2 \cdot C(OOH)CC \rightarrow C{=}C(C)CC{+}HO_2$	4.81E+66	-16.47	38956	10.0
$C_2 \cdot C(OOH)CC \rightarrow C_2C{=}CC{+}HO_2$	5.07E+56	-14.30	27993	0.1
$C_2 \cdot C(OOH)CC \rightarrow C_2C{=}CC{+}HO_2$	1.48E+58	-14.46	28633	1.0
$C_2 \cdot C(OOH)CC \rightarrow C_2C{=}CC{+}HO_2$	2.19E+61	-15.16	30483	10.0

[a] Estimated from $CCC \cdot + O_2$, Atkinson, R.; Baulch, D. L.; Cox, R. A.; R. F. Hampson, J.; Kerr, J. A.; Troe, J. *J. Chem. Ref. Data* **1989**, *18*, 881. [b] From the principle of microscopic reversibility, and $E_a{=}\Delta H^{o}{}_{rxn} - RT$.

Table C.8 Detailed Reaction Mechanism [aa]

No.	Reactions	A	n	E_a	ref
1	$Cl+Cl+M=>Cl_2+M$	2.00E+15	0.0	0	a
2	$Cl+C_3CC<=>C_3CC.+HCl$	7.96E+13	0.0	70	a
3	$OH+Cl<=>O+HCl$	5.90E+12	0.0	5683	a
4	$OH+Cl<=>ClO+H$	1.25E+17	-0.7	38017	b
5	$OH+Cl_2<=>HOCl+Cl$	8.43E+11	0.0	1788	a
6	$HO_2+Cl<=>ClO+OH$	2.47E+13	0.0	894	c
7	$Cl+HO_2<=>HCl+O_2$	1.08E+13	0.0	-340	d
8	$C_3CC•+O_2 <=> C_3CCOO•$	9.07E+77	-21.1	21221	b
9	$C_3CC•+O_2 <=> C_3CCHO+OH$	5.19E+47	-11.2	26797	b
10	$C_3CC•+O_2 <=> C_3•CCQ$	3.83E+95	-28.8	20237	b
11	$C_3CC•+O_2 <=> C_2CYCCOC+OH$	1.22E+63	-15.5	27359	b
12	$C_3CC•+O_2 <=> C*C(C)CQ+CH_3$	3.89E+59	-14.6	30830	b
13	$C_3CC•+O_2 <=> C_2C*C+CH_2O+OH$	8.68E+55	-13.4	30887	b
14	$C_3CC•+O_2 <=> CCC•(C)COOH$	8.40E+41	-10.0	48579	b
15	$C_3CCOO• <=> C_3CCHO+OH$	2.29E+68	-17.5	61948	b
16	$C_3CCOO• <=> C_3•CCQ$	4.34E+21	-3.2	28736	b
17	$C_3•CCQ <=> C_2CYCCOC+OH$	1.98E+13	-1.2	12419	b
18	$C_3•CCQ <=> C*C(C)CQ+CH_3$	2.24E+12	-1.6	17148	b
19	$C_3•CCQ <=> C_2C*C+CH_2O+OH$	7.47E+08	-0.5	17263	b
20	$C_3•CCQ <=> CCC•(C)COOH$	3.42E+16	-8.3	34105	b
21	$C_2CyCCOC + H <=> C_2CyCCOC• +H_2$	9.60E+08	1.5	5677.5	a
22	$C_2CyCCOC + OH <=> C_2CyCCOC• + H_2O$	4.80E+06	2.0	-120	a
23	$C_2CyCCOC + O <=> C_2CyCCOC• + OH$	6.80E+08	1.5	3422.5	a
24	$C_2CyCCOC + CH_3 <=> C_2CyCCOC• +CH_4$	3.24E+06	1.9	8864.5	a
25	$C_2CyCCOC + O_2 <=> C_2CyCCOC• + HO_2$	1.81E+13	0.0	51150	a
26	$C_2CyCCOC + Cl <=> C_2CyCCOC• + HCl$	2.56E+13	0.0	825	a
27	$C_2CyCCOC• <=>C_3•CCHO$	2.75E+77	-20.2	45152	b
28	$C_2CyCCOC• <=>C2C*COC•$	3.30E+66	-18.6	45287	b
29	$C_3•CCHO <=> C_2C*C + HCO$	3.14E+50	-12.4	30888	b
30	$C_3•CCHO <=> C*C(C)CHO + CH_3$	1.02E+65	-17.2	41717	b
31	$C_2C*COC• <=> C_2C*C• + CH_2O$	5.36E+42	-9.1	50471	b
32	$C_2C*C•+O_2 <=>C_2C*CQ•.$	5.49E+68	-18	17646	e
33	$C_2C*C•+O_2 <=> C_2C•C*O+O$	4.81E+38	-7.7	13996	e
34	$C_2C*C•+O_2 <=> C_2•C*CQ$	1.33E+33	-8.5	14202	e
35	$C_2C*C•+O_2 <=> C*C(C)C*O+OH$	1.34E+36	-7.8	14337	e
36	$C_2C*C•+O_2 <=> C*C*CQ+CH_3$	1.78E-20	7.8	11502	e
37	$C_2C*C•+O_2 <=> C_2C•CyCOO$	5.56E+39	-9.5	10274	e
38	$C_2C*C•+O_2 <=> C_2C*O+HCO$	5.67E+29	-5.7	12936	e
39	$C_2C*C•+O_2 <=> C_2CyCOOC•$	4.40E+40	-10.6	11402	e
40	$C_2C*C•+O_2 <=> C_2C*O+HCO$	2.85E+41	-9.3	14739	e
41	$C_2C*CQ• <=> C_2C•C*O+O$	1.81E+60	-14.5	51298	e
42	$C_2C*CQ• <=> C_2•C*CQ$	3.89E+45	-12.5	47086	e
43	$C_2C*CQ• <=> C*C(C)C*O+OH$	1.36E+49	-11.9	47445	e

49	$C_2 \bullet C^*CQ <=> C^*C(C)C^*O+OH$	8.71E+10	-0.8	-260	e
50	$C_2 \bullet C^*CQ <=> C^*C^*CQ+CH_3$	1.99E+11	-0.9	55475	e
51	$C_2C \bullet CyCOO <=> C_2C^*O+HCO$	2.92E+24	-4.7	27440	e
52	$C2CyCOOC \bullet <=> C_2C^*O+HCO$	4.92E+37	-9.2	14037	e
53	$C_3 \bullet CCQ+O_2 <=> C_2CCQCQ \bullet$	1.66+182	-53.8	57762	b
54	$C_3 \bullet CCQ+O_2 <=> C_2CCQCHO+OH$	4.45E+67	-16.8	26666	b
55	$C_3 \bullet CCQ+O_2 <=> C_2CCQCHO+OH$	1.94E+27	-5.4	20161	b
56	$C_3 \bullet CCQ+O_2 <=> C_2CCO \bullet CQ \bullet +OH$	3.83E+31	-5.6	19977	b
57	$C_3 \bullet CCQ+O_2 <=> C_2 \bullet CQCQ$	1.66+182	-56.5	48589	b
58	$C_3 \bullet CCQ+O_2 <=> CCQCCOC+OH$	4.64E+79	-21.1	35592	b
59	$C_3 \bullet CCQ+O_2 <=> C^*C(C)CQ+CH_2O+OH$	1.23E+81	-21.4	35856	b
60	$C_2CCQCQ \bullet <=> C_2CCQCHO+OH$	8.38E+58	-14.5	40254	b
61	$C_2CCQCQ \bullet <=> C_2CCQCHO+OH$	6.72+124	-36.3	76763	b
62	$C_2CCQCQ \bullet <=> C_2CCQCHO+OH$	5.28+139	-40.0	80134	b
63	$C_2CCQCQ \bullet <=> C_2 \bullet CQCQ$	3.41E+69	-18.5	44021	b
64	$C_2 \bullet CQCQ <=> CCQCCOC+OH$	1.22E+23	-4.3	18833	b
65	$C_2 \bullet CQCQ <=> C^*C(C)CQ+CH_2O+OH$	8.67E+21	-3.7	18025	b
66	$C_2CCQCHO <=> C2CCO \bullet CHO+OH$	2.43E+46	-9.7	56013	b
67	$C_2CCO \bullet CHO <=> C_2C(CHO)_2+H$	1.55E+41	-8.8	40453	b
68	$C_2CCO \bullet CHO <=> C_2C \bullet CHO+CH_2O$	2.32E+11	0.5	4560	b
69	$C_2C \bullet CHO <=> C^*C(C)CHO+H$	6.81E+46	-10.7	54756	b
70	$C_2C \bullet CHO <=> C^*CC+HCO$	1.04E+46	-10.1	50497	b
71	$C^*C(C)COOH <=> C^*C(C)CO \bullet +OH$	1.14E+63	-15.1	58663	b
72	$C^*C(C)CO \bullet => C^*C(C)CHO+H$	1.58E+04	1.5	5284	b
73	$C_3CC \bullet <=> C_2C^*C+CH_3$	3.96E+57	-13.9	45563	b
74	$C_2C^*C+OH <=> C_2C \bullet COH$	1.05E+72	-19.0	17695	b
75	$C_2C^*C+OH <=> C_2CCO \bullet$	4.12E+53	-18.3	15666	b
76	$C_2C^*C+OH <=> C_2CC^*O+H$	7.59E+16	-2.1	11681	b
77	$C_2C^*C+OH <=> CC \bullet C+CH_2O$	7.49E+26	-4.8	11342	b
78	$C_2C^*C+OH <=> C_2 \bullet CCOH$	9.82E+73	-21.0	29435	b
79	$C_2C^*C+OH <=> C^*CC+C \bullet H_2OH$	2.16E+35	-8.1	21861	b
80	$C_2C \bullet COH <=> C_2CCO \bullet$	1.52E+55	-14.4	42269	b
81	$C_2CCO \bullet <=> C_2CC^*O+H$	1.61E+20	-5.6	18324	b
82	$C_2CCO \bullet <=> CC \bullet C+CH_2O$	9.73E+30	-6.8	13834	b
83	$C_2 \bullet CCOH <=> C^*CC+C \bullet H_2OH$	4.03E+20	-6.0	16959	b
84	$C_2 \bullet CCOH <=> C_2CCO \bullet$	1.15E+58	-14.3	40597	b
85	$C_2C^*C+OH <=> C_3 \bullet COH$	2.33E+73	-19.4	17833	b
86	$C_2C^*C+OH <=> C_3CO \bullet$	4.94E+49	-18.2	16679	b
87	$C_2C^*C+OH <=> C_2C^*O+CH_3$	1.20E+28	-5.2	10863	b
88	$C_3 \bullet COH <=> C_3CO \bullet$	3.73E+60	-16.0	43448	b
89	$C_3CO \bullet <=> C_2C^*O+CH_3$	1.99E+25	-5.1	10510	b
90	$C_2C \bullet COH+O_2 <=> C_2CQ \bullet COH$	4.24+105	-29.5	30813	b
91	$C_2C \bullet COH+O_2 <=> C^*C(C)COH+HO_2$	8.29E+45	-10.2	19453	b
92	$C_2C \bullet COH+O_2 <=> C_2C^*COH+HO_2$	3.15E+49	-11.5	19361	b

93	$C_2C \bullet COH + O_2 \Longleftrightarrow C_2CQCO \bullet$	2.94E+92	-28.0	28851	b
94	$C_2C \bullet COH + O_2 \Longleftrightarrow C_2C*O + CH_2O + OH$	1.17E+58	-14.0	21219	b
95	$C_2C \bullet COH + O_2 \Longleftrightarrow C_2 \bullet CQCOH$	7.01+153	-45.1	54916	b
96	$C_2C \bullet COH + O_2 \Longleftrightarrow C*C(C)Q + C \bullet H_2OH$	1.27E+57	-14.0	28025	b
97	$C_2C \bullet COH + O_2 \Longleftrightarrow C*C(C)COH + HO_2$	1.58E+75	-19.7	33538	b
98	$C_2C \bullet COH + O_2 \Longleftrightarrow C_2CQC \bullet OH$	5.53+141	-42.0	43302	b
99	$C_2C \bullet COH + O_2 \Longleftrightarrow C_2C*COH + HO_2$	6.25E+59	-14.7	22783	b
100	$C_2CQ \bullet COH \Longleftrightarrow C*C(C)COH + HO_2$	5.17E+55	-13.5	48335	b
101	$C_2CQ \bullet COH \Longleftrightarrow C_2C*COH + HO_2$	9.04E+63	-16.2	50534	b
102	$C_2CQ \bullet COH \Longleftrightarrow C_2CQCO \bullet$	2.19E+30	-5.9	30046	b
103	$C_2CQ \bullet COH \Longleftrightarrow C_2 \bullet CQCOH$	5.40E+72	-19.3	56810	b
104	$C_2CQ \bullet COH \Longleftrightarrow C_2CQC \bullet OH$	4.70E+52	-12.8	43633	b
105	$C_2CQCO \bullet \Longleftrightarrow C_2C*O + CH_2O + OH$	1.43E+37	-8.8	16154	b
106	$C_2 \bullet CQCOH \Longleftrightarrow C*C(C)Q + C \bullet H_2OH$	1.02E+74	-19.5	44429	b
107	$C_2 \bullet CQCOH \Longleftrightarrow C*C(C)COH + HO_2$	1.13E+62	-15.7	37694	b
108	$C_2CQC \bullet OH \Longleftrightarrow C_2C*COH + HO_2$	2.13E+47	-11.6	25252	b
109	$C_3 \bullet COH + O_2 \Longleftrightarrow C_2COHCQ \bullet$	1.14E+81	-21.8	22474	b
110	$C_3 \bullet COH + O_2 \Longleftrightarrow C_2CO \bullet CQ$	1.97E+68	-20.3	21900	b
111	$C_3 \bullet COH + O_2 \Longleftrightarrow C_2C*O + CH_2O + OH$	2.25E+50	-11.9	20157	b
112	$C_3 \bullet COH + O_2 \Longleftrightarrow CH_3 + CC*OCQ$	7.34E+46	-10.9	20439	b
113	$C_3 \bullet COH + O_2 \Longleftrightarrow C_2 \bullet COHCQ$	2.53+160	-47.5	52291	b
114	$C_3 \bullet COH + O_2 \Longleftrightarrow C*C(C)CQ + OH$	1.46E+57	-13.7	30033	b
115	$C_3 \bullet COH + O_2 \Longleftrightarrow C*C(C)OH + CH_2O + OH$	1.69E+63	-15.6	29954	b
116	$C_2COHCQ \bullet \Longleftrightarrow C_2CO \bullet CQ$	9.72E+26	-5.2	29781	b
117	$C_2COHCQ \bullet \Longleftrightarrow C_2 \bullet COHCQ$	2.10E+36	-7.9	36705	b
118	$C_2CO \bullet CQ \Longleftrightarrow C_2C*O + CH_2O + OH$	3.41E+45	-11.2	22380	b
119	$C_2CO \bullet CQ \Longleftrightarrow CH_3 + CC*OCQ$	1.35E+44	-11.2	22381	b
120	$C_2 \bullet COHCQ \Longleftrightarrow C*C(C)CQ + OH$	2.46E+58	-15.1	38598	b
121	$C_2 \bullet COHCQ \Longleftrightarrow C*C(C)OH + CH_2O + OH$	7.77E+38	-9.0	27493	b
122	$C_2C*C + CH_3 \Longleftrightarrow CCC \bullet C_2$	2.51E+11	0.0	6691	f
123	$CCC \bullet C_2 + O_2 \Longleftrightarrow C_2COO \bullet CC$	3.34+119	-34.5	32301	b
124	$CCC \bullet C_2 + O_2 \Longleftrightarrow CCC*(C)C + HO_2$	1.17E+41	-9.4	12471	b
125	$CCC \bullet C_2 + O_2 \Longleftrightarrow CC*CC_2 + HO_2$	9.10E+37	-8.5	11396	b
126	$CCC \bullet C_2 + O_2 \Longleftrightarrow C_2CQCC \bullet$	8.01+103	-32.2	27639	b
127	$CCC \bullet C_2 + O_2 \Longleftrightarrow C_2CYCCCO + OH$	9.39E+14	-1.6	8547	b
128	$CCC \bullet C_2 + O_2 \Longleftrightarrow C_2 \bullet CQCC$	3.95+124	-37.7	37019	b
129	$CCC \bullet C_2 + O_2 \Longleftrightarrow CCC*(C)C + HO_2$	4.18E+28	-6.0	12008	b
130	$CCC \bullet C_2 + O_2 \Longleftrightarrow C_2CQC \bullet C$	1.34E+96	-29.7	25479	b
131	$CCC \bullet C_2 + O_2 \Longleftrightarrow CC*CC_2 + HO_2$	1.24E+31	-6.7	10227	b
132	$C_2COO \bullet CC \Longleftrightarrow CCC*(C)C + HO_2$	4.22E+75	-19.9	50055	b
133	$C_2COO \bullet CC \Longleftrightarrow CC*CC_2 + HO_2$	3.43E+80	-21.6	52151	b
134	$C_2COO \bullet CC \Longleftrightarrow C_2CQCC \bullet$	1.45E+59	-14.9	40925	b
135	$C_2COO \bullet CC \Longleftrightarrow C_2 \bullet CQCC$	2.43E+83	-23.0	56656	b
136	$C_2COO \bullet CC \Longleftrightarrow C_2CQC \bullet C$	6.14E+82	-22.6	54438	b

137	$C_2CQCC\bullet <=> C_2CyCOCC+OH$	1.06E+34	-9.0	18050	b
138	$C_2\bullet CQCC <=> CCC^*(C)C+HO_2$	7.10E+71	-18.8	38055	b
139	$C_2CQC\bullet C <=> CC^*CC_2+HO_2$	3.86E+56	-14.3	27964	b
140	$C_2C^*C+OH<=>C_2\bullet C^*C+H_2O$	7.80E+12	0.0	0	g
141	$C_2C^*C+O_2<=>C_2\bullet C^*C+HO_2$	4.79E+12	0.0	38528	h
142	$C_2C^*C+H<=>C_2\bullet CC$	6.45E+13	0.0	2700	a
143	$C_2C^*C+H<=>H_2+C_2\bullet C^*C$	5.50E+13	0.0	7600	a
144	$C_2C^*C+CH_3<=>CH_4+C_2\bullet C^*C$	1.86E+06	1.9	1219	a
145	$C_2\bullet C^*C+O_2<=>C^*C(C)CQ\bullet$	1.35E+86	-23.9	25535	e
146	$C_2\bullet C^*C+O_2<=>C^*C(C)CO\bullet+O$	2.27E+18	-1.9	41733	e
147	$C_2\bullet C^*C+O_2<=>C^*CICC^*O+OH$	7.17E+07	0.8	18587	e
148	$C_2\bullet C^*C+O_2<=>C^*C(C\bullet)CQ$	3.23E+51	-12.7	21132	e
149	$C_2\bullet C^*C+O_2<=>C^*CyCCOC+OH$	2.10E+40	-9.3	35411	e
150	$C_2\bullet C^*C+O_2<=>C^*C(C\bullet)CO\bullet+OH$	3.08E+43	-9.3	36490	e
151	$C_2\bullet C^*C+O_2<=>C^*C^*C+C\bullet H_2OOH$	1.29E+39	-8.4	41307	e
152	$C_2\bullet C^*C+O_2<=>C^*C(C)C^*O+OH$	8.34E+29	-6.6	40938	e
153	$C_2\bullet C^*C+O_2<=>CCYC.COOC$	2.87E+79	-25.3	23912	e
154	$C_2\bullet C^*C+O_2<=>CC.C^*O+CH_2O$	4.01E-04	3.2	15802	e
155	$C_2\bullet C^*C+O_2<=>CCyC\bullet CO+CH_2O$	1.07E+16	-2.1	11712	e
156	$C_2\bullet C^*C+O_2<=>C_2\bullet C^*O+CH_2O$	7.10E+04	1.3	14567	e
157	$C_2\bullet C^*C+O_2<=>CCYC\bullet CO+CH_2O$	1.05E+03	2.0	15823	e
158	$C^*C(C)CQ\bullet<=>C^*C(C)CO\bullet+O$	1.97E+61	-20.9	65742	e
159	$C^*C(C)CQ\bullet<=>C^*C(C)C^*O+OH$	1.35E+72	-21.5	50937	e
160	$C^*C(C)CQ\bullet<=>C^*C(C\bullet)CQ$	9.79E+50	-12.9	33778	e
161	$C^*C(C)CQ\bullet<=>CCyC\bullet COOC$	7.17E+66	-18.7	43243	e
162	$C^*C(C)CQ\bullet<=>C2.CYCCOO$	4.48E+68	-19.4	44814	e
163	$C^*C(C\bullet)CQ<=>C^*CYCCOC+OH$	5.02E+66	-17.5	59429	e
164	$C^*C(C\bullet)CQ<=>C^*C(C\bullet)CO\bullet+OH$	1.11E+71	-17.9	61056	e
165	$C^*C(C\bullet)CQ<=>C^*C^*C+C\bullet H_2OOH$	2.55E+80	-21.4	71001	e
166	$CCyC\bullet COOC<=>CC\bullet C^*O+CH_2O$	2.36E+35	-11.8	35866	e
167	$CCyC\bullet COOC<=>CCyC\bullet CO+CH_2O$	1.35E+45	-11.0	23306	e
168	$C_2\bullet CYCCOO<=>C_2.C^*O+CH_2O$	5.22E+56	-15.0	31984	e
169	$C_2\bullet CYCCOO<=>CCYC.CO+CH_2O$	1.97E+55	-14.6	31962	e
170	$C^*C(C\bullet)CO\bullet<=>C^*C^*C+CH2O$	9.89E+13	-1.6	6589	e
171	$C^*C(C\bullet)CO\bullet<=>C^*C(C\bullet)C^*O+H$	5.86E+13	-1.3	16907	e
172	$CCyC\bullet CO<=> C_2\bullet C^*O$	4.90E+40	-8.6	14883	e
173	$CCyC\bullet CO<=> C^*C^*O+CH_3$	1.41E+29	-4.4	17943	e
174	$C_2\bullet C^*O <=> C^*C^*O+CH_3$	4.12E+38	-8.1	47640	e
175	$C_2CyC_2O <=>CCyC\bullet CO+CH_3$	7.32E+18	-0.2	88879	e
176	$C_3CC+OH<=>C_3CC\bullet+H_2O$	1.44E+07	2.0	2115	a
177	$C_3CC+O <=> C_3CC\bullet+OH$	9.20E+13	0.0	7154	i
178	$C_3CC+O_2 <=>C_3CC\bullet+HO_2$	1.03E+13	0.0	55640	j
179	$C_3CC+HO_2<=>C_3CC\bullet+H_2O_2$	3.01E+04	2.5	15500	k
180	$C_3CC\bullet +H <=> C_3CC$	1.00E+14	0.0	0	l

181	$C_3CC\bullet +OH<=>C_3CCOH$	1.00E+13	0.0	0	a
182	$C_3CC\bullet+O <=> C_3CCO\bullet$	1.48E+21	-8.3	8332	b
183	$C_3CC\bullet+O <=> C_3CCHO+H$	6.32E+11	0.1	1083	b
184	$C_3CC\bullet+O<=>C_3C\bullet+CH_2O$	2.04E+14	0.0	0	b
185	$C_3CC\bullet+O <=> C_3\bullet CCOH$	1.44E+19	-8.7	9606	b
186	$C_3CC\bullet+O <=> C_2C*C+C\bullet H_2OH$	1.06E+11	0.1	654	b
187	$C_3CC\bullet+O <=> C*C(C)COH+CH_3$	2.17E+09	0.1	933	b
188	$C_3CC\bullet+O <=> C_3CC\bullet OH$	2.42+101	-34.9	12130	b
189	$C_3CC\bullet+O <=> C_3CCHO+H$	2.39E+11	0.1	1024	b
190	$C_3CCO\bullet <=> C_3CCHO+H$	2.06E+46	-14.5	34560	b
190	$C_3CCO\bullet <=> C_3C\bullet+CH_2O$	2.73E+58	-14.8	29436	b
192	$C_3CCO\bullet <=> C_3\bullet CCOH$	4.59E+49	-14.6	29985	b
193	$C_3CCO\bullet <=> C_3CC\bullet OH$	2.82E+46	-14.5	34157	b
194	$C_3\bullet CCOH <=> C_2C*C+C\bullet H_2OH$	3.62E+87	-23.1	51238	b
195	$C_3\bullet CCOH <=> C*C(C)COH+CH_3$	2.44E+85	-23.1	51232	b
196	$C_3CC\bullet OH <=> C_3CCHO+H$	7.13E+29	-5.4	36736	b
197	$C_3CCOO\bullet+C_3CCOO\bullet <=> C_3CCO\bullet+C_3CCO\bullet+O_2$	2.41E+11	0.0	0	m
198	$C_3CCOO\bullet+C_3CCOO\bullet <=> C_3CCHO+C_3CCOH+O_2$	3.61E+11	0.0	0	m
199	$C_3CCOO\bullet+HO_2 <=> C_3CCOOH+ O_2$	8.61E+10	0.0	-2742	n
200	$C_3CCOO\bullet+OH <=> C_3CCO\bullet + HO_2$	2.40E+11	0.0	0	a
201	$C_3C\bullet+O_2 <=> C_3COO\bullet$	8.54E+92	-25.9	23848	e_1
202	$C_3C\bullet+O_2 <=> C_3CO\bullet+O$	4.07E+12	-0.1	25661	e_1
203	$C_3C\bullet+O_2 <=> C_2C*C+HO_2$	1.73E+40	-8.8	11464	e_1
204	$C_3C\bullet+O_2 <=> C_3\bullet COOH$	1.74E+95	-27.7	27734	e_1
205	$C_3C\bullet+O_2 <=> C_2C*C+HO_2$	2.62E+29	-5.9	10469	e_1
206	$C_3C\bullet+O_2 <=> C_2CyC_2O+OH$	1.39E+27	-5.4	10278	e_1
207	$C_3C\bullet+O_2 <=> C*C(C)Q+CH_3$	5.75E+07	1.0	19576	e_1
208	$C_3COO\bullet<=> C_3CO\bullet+O$	1.41E+77	-25.1	69290	e_1
209	$C_3COO\bullet<=>C_2C*C+HO_2$	1.14E+61	-15.3	43307	e_1
210	$C_3COO\bullet<=>C_3\bullet COOH$	2.17E+69	-18.5	49811	e_1
211	$C_3\bullet COOH<=>C_2C*C+HO_2$	8.31E+66	-17.2	37206	e_1
212	$C_3\bullet COOH<=>C_2CyC_2O+OH$	3.24E+65	-17.1	37199	e_1
213	$C_3\bullet COOH<=>C*C(C)Q+CH_3$	1.94E+59	-17.7	41599	e_1
214	$C_3C\bullet+HO_2<=>C_3COOH$	1.01+108	-33.4	21083	e_1
215	$C_3C\bullet+HO_2<=>C_3CO\bullet+OH$	3.67E+12	0.0	3	e_1
216	$C_3COOH<=>C_3CO\bullet+OH$	5.02E+65	-15.8	59047	e_1
217	$C_3CCOOH <=> C_3CCO\bullet+OH$	1.67E+56	-12.8	57175	b
218	$C_3CCOH+H <=> C_3\bullet CCOH+H_2$	2.16E+09	1.5	7400	a
219	$C_3CCOH+H <=> C_3CC\bullet OH+H_2$	4.80E+08	1.5	3357	a
220	$C_3CCOH+H <=> C_3CCO\bullet+H_2$	2.40E+08	1.5	9324	a
221	$C_3CCOH+O <=> C_3\bullet CCOH+OH$	1.53E+09	1.5	5410	a
222	$C_3CCOH+O <=>C_3CC\bullet OH+OH$	3.40E+08	1.5	2186	a
223	$C_3CCOH+O <=> C_3CCO\bullet+OH$	1.70E+08	1.5	7630	a
224	$C_3CCOH+OH <=> C_3\bullet CCOH+H_2O$	1.08E+07	2.0	1205	a

225	$C_3CCOH+OH <=> C_3CC{\bullet}OH+H_2O$	2.40E+06	2.0	537	a
226	$C_3CCOH+OH <=>C_3CCO{\bullet}+H_2O$	1.20E+06	2.0	2685	a
227	$C_3CCOH+CH_3 <=> C_3{\bullet}CCOH+CH_4$	7.29E+06	1.9	10587	a
228	$C_3CCOH+CH_3 <=> C_3CC{\bullet}OH+CH_4$	1.62E+06	1.9	6544	a
229	$C_3CCOH+CH_3 <=> C_3CCO{\bullet}+CH_4$	8.10E+05	1.9	12511	a
230	$C_3CCOH+HO_2 <=> C_3{\bullet}CCOH+H_2O_2$	9.64E+10	0.0	12579	a
231	$C_3CCOH+HO_2 <=> C_3CC{\bullet}OH+H_2O_2$	3.01E+04	2.5	15500	a
232	$C_3CCOH+O_2 <=> C_3{\bullet}CCOH+HO_2$	9.05E+13	0.0	53800	a
233	$C_3CCOH+O_2 <=> C_3CC{\bullet}OH+HO_2$	1.37E+13	0.0	47580	a
234	$C_3CCOH+O_2 <=> C_3CCO{\bullet}+HO_2$	3.10E+08	1.3	57560	a
235	$C_3CCHO+H <=> C_3{\bullet}CCHO+H_2$	2.16E+09	1.5	7400	a
236	$C_3CCHO+H <=> C_3CC{\bullet}*O+H_2$	4.00E+13	0.0	4206	a
237	$C_3CCHO+O <=> C_3{\bullet}CCHO+OH$	1.53E+09	1.5	5410	a
238	$C_3CCHO+O <=> C_3CC{\bullet}*O+OH$	1.70E+08	1.5	1729	a
239	$C_3CCHO+OH <=> C_3{\bullet}CCHO+H_2O$	1.08E+07	2.0	1205	a
240	$C_3CCHO+OH <=> C_3CC{\bullet}*O+H_2O$	9.51E+12	0.0	-622	a
241	$C_3CCHO+CH_3 <=> C_3{\bullet}CCHO+CH_4$	7.29E+06	1.9	10587	a
242	$C_3CCHO+CH_3 <=> C_3CC{\bullet}*O+CH_4$	8.10E+05	1.9	2819.5	a
243	$C_3CCHO+O_2 <=> C_3CC{\bullet}*O+HO_2$	3.01E+13	0.0	41850	a
244	$C_3CCHO+HO_2 <=> C_3{\bullet}CCHO+H_2O_2$	3.01E+04	2.5	15500	a
245	$C_3CCHO+HO_2 <=> C_3CC{\bullet}*O+H_2O_2$	3.01E+12	0.0	8000	a
246	$CH_3OO+H <=> CH_3OOH$	9.08E-21	4.1	-6264	b
247	$CH_3OO+H <=> CH_3O+OH$	9.64E+13	0.0	0	b
248	$CH_3OOH <=> CH_3O+OH$	4.84E+44	-10.0	50869	b
249	$C_3COO{\bullet}+H<=>C3COOH$	5.75E+85	-24.4	16400	b
250	$C_3COO{\bullet}+H<=>C3CO{\bullet}+OH$	2.23E+16	-0.7	1092	b
251	$C_3COOH<=> C3CO{\bullet}+OH$	1.11E+44	-8.9	57560	b
252	$CH_3OO+CH_3 <=> COOC$	5.74E+50	-18.6	3865	b
253	$CH_3OO+CH_3 <=> CH3O+CH_3O$	2.42E+13	0.0	1	b
254	$COOC <=> CH_3O+CH_3O$	1.55E+69	-17.3	54398	b
255	$CH_3OO+CH_3OO <=>CH_3O+CH_3O+O_2$	2.47E+11	0.0	0	o
256	$CH_3+HO_2 <=> CH_3OOH$	1.51E+40	-14.5	17430	b
257	$CH_3+HO_2 <=> CH_3O+OH$	1.84E+13	0.0	2	b
258	$CH_3OOH <=>CH_3O+OH$	4.71E+44	-10.0	50868	b
259	$CH_3+CH_3<=>C_2H_5+H$	2.51E+40	-8.8	7596	b
260	$CH_3+CH_3<=>C_2H_4+H_2$	6.68E+16	-1.4	9461	b
261	$C_2H_6 <=> C_2H_5+H$	3.68E+13	-1.1	13326	b
262	$C_2H_6 <=> C_2H_4+H_2$	6.00E+46	-10.6	104822	b
263	$CH_3+CH_3 <=> C_2H_6$	2.87E+46	-12.0	108550	b
264	$CH_2O+O <=> OH+HCO$	4.16E+11	0.6	2762	o
265	$CH_2O+H <=> H_2+HCO$	2.29E+10	1.1	3279	o
266	$CH_2O+OH <=> H_2O+HCO$	3.49E+09	1.2	-447	o
267	$CH_2O+HO_2 <=> O_2+C{\bullet}H_2OH$	3.39E+12	0.0	19121	p
268	$CH_2O+CH_3 <=> HCO + CH_4$	4.09E+12	0.0	8843	o
269	$CH_2O+O_2 <=> HO_2 + HCO$	6.03E+13	0.0	40658	o

270	$CH_2O + C\bullet H_2OH <=> CH_3OH+HCO$	5.49E+13	2.8	5862	q
271	$CH_2O + CH_3O <=> CH_3OH+HCO$	1.02E+11	0.0	2981	r
272	$CH_2O + C_3C\bullet <=> C_3C+HCO$	3.01E+11	0.0	6498	s
273	$CH_4+HO_2<=>H_2O_2+CH_3$	9.04E+12	0.0	24641	o
274	$CH_4+O<=>CH_3+OH$	6.92E+08	1.6	8485	o
275	$CH_3+O_2<=>CH_3OO$	8.61E+31	-6.6	4931	b
276	$CH_3+O_2<=>CH_2O+OH$	2.85E+08	1.0	12526	b
277	$CH_3+HO_2=CH_4+O_2$	3.61E+12	0.0	0	r
278	$CH_3O=CH_2O+H$	6.13E+28	-5.7	31351	b
279	$CH_3O+HO_2=CH_2O+H_2O_2$	3.01E+11	0.0	0	r
280	$CH_3+H <=> CH_4$	2.11E+14	0.0	0	m
281	$HCO+O_2 <=> HCQ\bullet*O$	2.21E+20	-7.2	914	b
282	$HCO+O_2 <=> CO+HO_2$	9.37E+09	0.8	-693	b
283	$HCO+O_2 <=> O*C\bullet OOH$	2.54E-01	-2.8	9430	b
284	$HCO+O_2 <=> CO+HO_2$	1.43E-02	3.7	4329	b
285	$HCO+O_2 <=> CO_2+OH$	4.70E+01	2.8	4816	b
286	$HCQ\bullet*O <=> CO+HO_2$	1.03E+34	-7.5	27407	b
287	$HCQ\bullet*O <=> O*C\bullet OOH$	3.37E+16	-7.6	43943	b
288	$O*C\bullet OOH <=> CO+HO_2$	5.31E+26	-6.9	24018	b
289	$O*C\bullet OOH <=> CO_2+OH$	1.25E+31	-6.7	20473	b
290	$OH+HCO<=>CO+H_2O$	1.02E+14	0.0	0	o
291	$HCO <=> H+ CO$	1.57E+14	0.0	15758	t
292	$CO+O <=> CO_2$	6.17E+14	0.0	3001	r
293	$CO+OH<=>CO_2+H$	6.32E+06	1.5	-497	o
294	$CO+HO_2 <=>CO_2+OH$	1.51E+14	0.0	23650	r
295	$CO+O_2 <=> CO_2+O$	2.53E+12	0.0	47693	r
296	$H+O_2+M <=> HO_2+M$	2.11E+18	-0.8	0	t
297	$H+HO_2 <=> H_2+O_2$	4.28E+13	0.0	1411	o
298	$H+HO_2 <=> OH+OH$	3.01E+13	0.0	1721	o
299	$HO_2+H<=>H_2O+O$	1.69E+14	0.0	874	o
300	$O+HO_2 <=> O_2+OH$	3.25E+13	0.0	0	o
301	$HO_2+OH<=>O_2+H_2O$	2.89E+13	0.0	-497	o
302	$HO_2+HO_2 <=> O_2+H_2O_2$	1.87E+12	0.0	1540	o
303	$H_2O_2+H <=> H_2+HO_2$	4.82E+13	0.0	7949	r
304	$H_2O_2+H<=>H_2O+OH$	2.41E+13	0.0	3974	r
305	$H_2O_2+O<=>OH+HO_2$	9.63E+06	2.0	3974	r
306	$H_2O_2+OH<=>HO_2+H_2O$	7.83E+12	0.0	1331	o
307	$H+O_2 <=> OH+O$	1.99E+14	0.0	16802	o
308	$H_2+OH <=> H_2O+H$	9.31E+11	1.6	3299	o
309	$OH+OH <=> O+H_2O$	1.51E+09	1.1	99	o
310	$OH+OH+M<=>H_2O_2+M$	2.90E+17	-0.8	0	o
311	$O+H_2<=>OH+H$	5.11E+04	2.7	6280	o
312	$O+O+M<=>O2+M$	1.89E+13	0.0	-1788	r
313	$H+O+M<=>OH+M$	4.71E+18	-1.0	0	r
314	$OH =>X$	8.80E+01	0.0	0	u
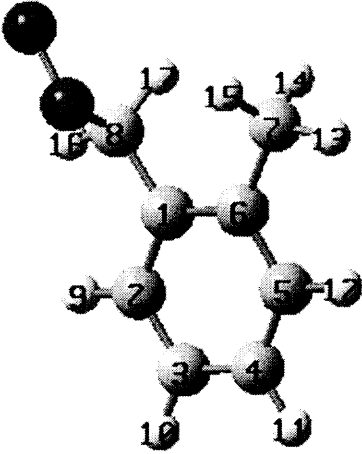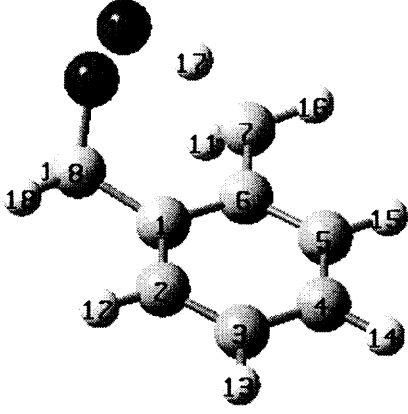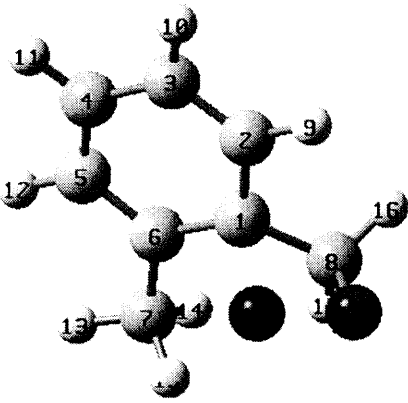
[aa] $k = A$ T^n $\exp(-E_a/RT)$. Units of s^{-1} for first order reactions, cm^3 mol^{-1} s^{-1} for second order reactions, cm^6 mol^{-2} s^{-1} for third order reactions. Ea in cal mol^{-1}. * Stands for double bond, Q stands for -OOH group, and Y stands for cyclic structure. [a] Estimated in this study by Dean and Bozzelli. * stand for double bond, and Q stand for -OOH group. [b] From QRRK calculation at P = 0.807 atm and T = 500 ~ 900 K. [c] Hunter, T.F.; Kristjansson, K. S J. Chem. Soc. Faraday Trans. 2: 78, 2067 (1982). [d] Mulenko, S.A. Rev. Roum. Phys. 32, 173 (1987). [e] The mechanism from Chen, C-J; Bozzelli, J.W. J. Phys. Chem. A 2000, 104, 9715. [e1] The mechanism from Chen, C.-J.; Bozzelli, J. W. *J. Phys. Chem. A* **1999**, *103*, 9731. [f] Seres, L.; Nacsa, A.; Arthur, N.L. Int. J. Chem. Kinet. 26, 227-246 (1994). [g] Baker, R. R.; Baldwin, R. R.; Walker, R. W. J. Chem. Soc. Faraday Trans. 1: 74, 2229 (1978). [h] Ingham,T.; Walker, R.W.; Woolford, R. E. Symp. Int. Combust. Proc. 25, 767-774 (1994). [i] Herron, J.T. J. Phys. Chem. Ref. Data 17, 967 (1988). [j] Estimated from isobutane + O$_2$ reaction.). [k] Estimated from isobutane + HO$_2$ reaction. [l] Allara D. L.; Shaw R. *J. Phys. Chem. Ref. Data* 9, 523, (1980). [m] Wallington, T. J.; Andino, J. M.; Potts, A. R. Int. J. Chem. Kinet. 24, 649-663 (1992). [n] Rowley, D. M.; Lesclaux, R.; Lightfoot, P. D.; Hughes, K.; Hurley, M. D.; Rudy, S.; Wallington, T. J. J. Phys. Chem. 96, 7043-7048 (1992). [o] Baulch, D. L.; Cobos, C. J.; Cox, R. A.; Esser, C.; Frank, P.; Just, Th.; Kerr, J. A.; Pilling, M. J.; Troe, J.; Walker, R. W.; Warnatz, J. J. Phys. Chem. Ref. Data 21, 411-429 (1992). [p] Tsuboi, T.; Hashimoto, K. Combust. Flame 42, 61 (1981). [q] Tsang, W. J. Phys. Chem. Ref. Data 16, 471 (1987). [r] Tsang, W.; Hampson, R. F. J. Phys. Chem. Ref. Data 15, 1087 (1986). [s] Tsang, W. J. Phys. Chem. Ref. Data 19, 1-68 (1990). [t] Baulch,D. L.; Cobos, C. J.; Cox, R. A.; Frank, P.; Hayman, G.; Just, Th.; Kerr, J. A.; Murrells, T.; Pilling, M. J.; Troe, J.; Walker, R. W.; Warnatz, J. J. Phys. Chem. Ref. Data 23, 847-1033 (1994). [u] OH Wall reaction by Hughes, K. J.; Lightfoot, P. D.; Pilling, M. J. *Chemical Physics Letters* 1992, *191*, 581.

APPENDIX D

TABLES IN THE THERMOCHEMICAL AND KINETIC ANALYSIS
ON REACTION OF 2-METHYLBENZYL RADICAL OXIDATION

This appendix lists the geometrical parameters, harmonic vibrational frequencies,

isodesmic reaction analysis for calculation of enthalpy values on reaction of 2-

methylbenzyl radical oxidation, as discussed in Chapter 6.

Table D.1 Geometrical Parameters for Species in Ortho-Xylene Oxidation System

Species	Bond Length Å		Bond Angle degree		Dihedral Angle degree	
ortho-C5H4(CH3)CH2OO•	r21	1.3990	a321	121.10	d4321	0.35
	r32	1.3941	a432	119.25	d5432	359.96
	r43	1.3932	a543	119.97	d6543	359.82
	r54	1.3957	a654	121.49	d7654	180.04
	r65	1.3986	a765	120.27	d8123	179.89
	r76	1.5109	a812	119.24	d9213	180.14
	r81	1.5000	a921	119.09	d10321	180.20
	r92	1.0870	a1032	120.18	d11432	179.89
	r103	1.0856	a1143	120.24	d12543	179.83
	r114	1.0861	a1254	119.54	d13765	357.41
	r125	1.0867	a1376	110.90	d14765	117.19
	r137	1.0926	a1476	111.58	d15765	236.83
	r147	1.0971	a1576	111.51	d16812	348.23
	r157	1.0942	a1681	112.13	d17812	223.92
	r168	1.0927	a1781	113.59	d18812	106.02
	r178	1.0927	a1881	108.70	d191881	172.96
	r188	1.4780	a19188	110.84		
	r1918	1.3209				
TS1	r21	1.3965	a321	121.22	d4321	2.18
	r32	1.3949	a432	119.62	d5432	358.69
	r43	1.3976	a543	119.94	d6543	358.32
	r54	1.3901	a654	121.26	d7654	182.04
	r65	1.4094	a765	120.59	d8123	187.57
	r76	1.4631	a812	119.95	d9812	111.34
	r81	1.5095	a981	108.33	d10981	92.79
	r98	1.4474	a1098	109.28	d11765	126.08
	r109	1.4055	a1176	116.34	d12213	179.25
	r117	1.0916	a1221	119.07	d13321	180.87
	r122	1.0870	a1332	120.06	d14432	178.68
	r133	1.0857	a1443	120.16	d15543	180.07
	r144	1.0859	a1554	119.96	d16765	349.76
	r155	1.0865	a1676	115.95	d171098	297.58
	r167	1.0894	a17109	103.89	d18812	355.97
	r1710	1.1770	a1881	110.66	d19812	232.16
	r188	1.0942	a1981	114.58		
	r198	1.0950				
TS2	r21	1.4455	a321	121.65	d4321	357.08
	r32	1.3766	a432	119.73	d5432	0.16
	r43	1.4056	a543	120.09	d6543	359.90
	r54	1.4052	a654	122.01	d7654	178.38
	r65	1.3850	a765	121.13	d8123	163.24
	r76	1.5037	a812	116.39	d9213	177.00
	r81	1.5362	a921	117.25	d10321	177.55
	r92	1.0855	a1032	120.16	d11432	180.23
	r103	1.0857	a1143	120.18	d12543	180.02
	r114	1.0855	a1254	119.14	d13765	354.25
	r125	1.0867	a1376	110.95	d14765	114.65
	r137	1.0927	a1476	112.26	d15765	234.00
	r147	1.0970	a1576	110.06	d16812	325.09
	r157	1.0954	a1681	114.24	d17812	199.51
	r168	1.0960	a1781	112.53	d18812	81.93
	r178	1.0966	a1881	97.69	d191881	20.84
	r188	1.4236	a19188	93.07		
	r1918	1.4722				

—

TS3
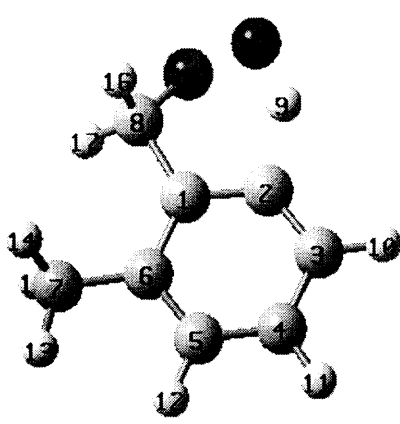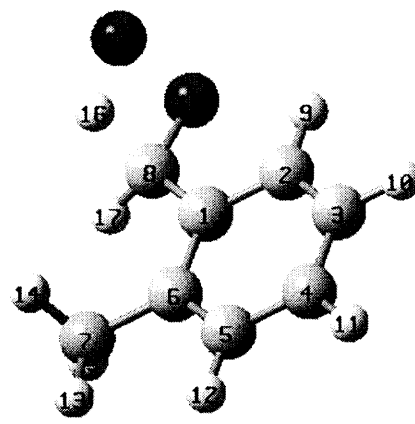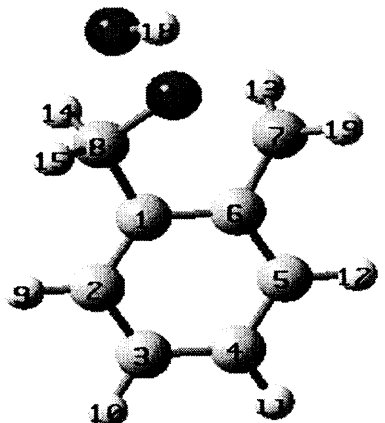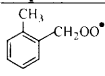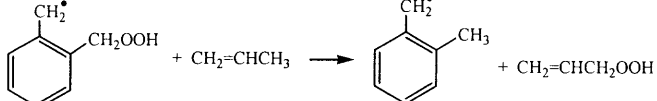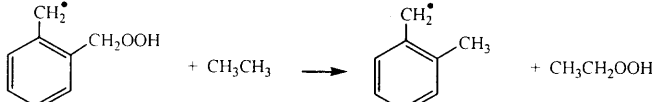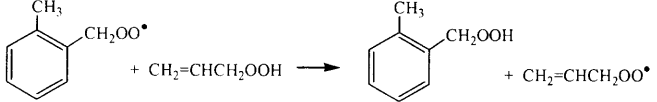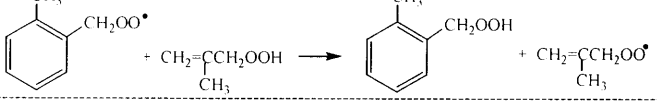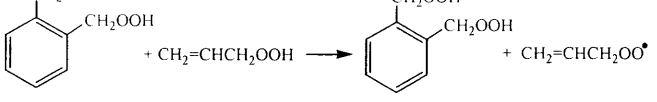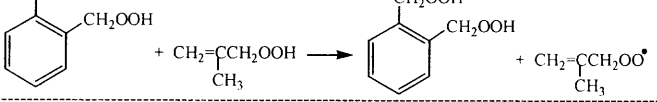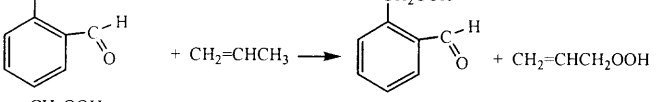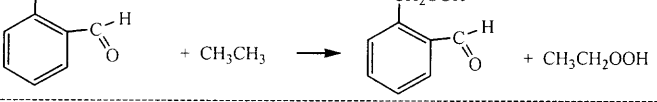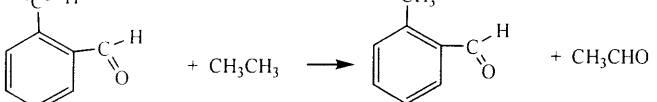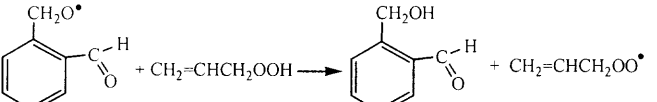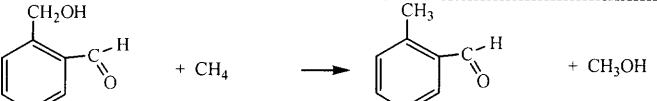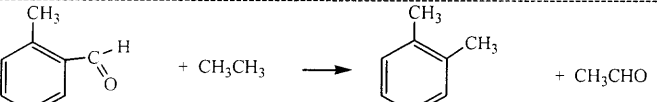
r21	1.3816	a321	125.71	d4321	0.67
r32	1.3790	a432	116.16	d5432	359.45
r43	1.4016	a543	120.27	d6543	0.21
r54	1.3957	a654	122.11	d7654	180.49
r65	1.4018	a765	120.79	d8123	178.82
r76	1.5111	a812	118.42	d9213	178.49
r81	1.5213	a921	101.94	d10321	180.21
r92	1.4951	a1032	122.53	d11432	179.35
r103	1.0852	a1143	119.74	d12543	180.22
r114	1.0866	a1254	119.18	d13765	0.69
r125	1.0866	a1376	110.92	d14765	120.78
r137	1.0928	a1476	111.81	d15765	240.73
r147	1.0961	a1576	111.65	d16812	268.97
r157	1.0966	a1681	110.99	d17812	146.70
r168	1.0991	a1781	112.26	d18812	30.90
r178	1.0940	a1881	109.91	d19921	13.54
r188	1.4252	a1992	144.59		
r199	1.0937				

TS4

r21	1.4067	a321	120.63	d4321	359.28
r32	1.3900	a432	119.63	d5432	359.92
r43	1.3962	a543	119.98	d6543	0.21
r54	1.3970	a654	121.52	d7654	180.45
r65	1.3961	a765	120.22	d8123	179.86
r76	1.5105	a812	119.56	d9213	179.41
r81	1.4684	a921	118.28	d10321	179.46
r92	1.0840	a1032	120.00	d11432	180.21
r103	1.0856	a1143	120.25	d12543	180.28
r114	1.0859	a1254	119.55	d13765	2.05
r125	1.0867	a1376	110.74	d14765	122.15
r137	1.0925	a1476	111.84	d15765	242.18
r147	1.0960	a1576	111.85	d16812	271.52
r157	1.0967	a1681	114.01	d17812	151.31
r168	1.2993	a1781	118.38	d18812	10.26
r178	1.0941	a1881	117.40	d191681	123.31
r188	1.3946	a19168	101.85		
r1916	1.3336				

TS5

r21	1.3939	a321	119.88	d4321	1.22
r32	1.3967	a432	120.09	d5432	359.03
r43	1.3966	a543	120.17	d6543	359.10
r54	1.3950	a654	120.03	d7654	181.22
r65	1.4021	a765	124.65	d8123	183.75
r76	1.4656	a812	123.81	d9213	178.62
r81	1.5097	a921	120.00	d10321	179.73
r92	1.0870	a1032	119.83	d11432	178.74
r103	1.0859	a1143	120.02	d12543	180.26
r114	1.0859	a1254	120.21	d13765	107.13
r125	1.0863	a1376	119.81	d14812	276.65
r137	1.0850	a1481	111.74	d15812	37.04
r148	1.1013	a1581	111.03	d16812	156.00
r158	1.0942	a1681	107.92	d171681	194.00
r168	1.4363	a17168	100.63	d1817168	143.60
r1716	1.6663	a181716	94.07	d19765	311.16
r1817	0.9709	a1976	120.23		
r197	1.0863				

TS6	r21	1.3995	a321	121.77	d4321	359.38
	r32	1.3924	a432	119.51	d5432	0.19
	r43	1.3953	a543	119.71	d6543	0.45
	r54	1.3900	a654	121.23	d7654	181.13
	r65	1.4075	a765	119.98	d8123	179.73
	r76	1.4869	a812	115.76	d9812	181.55
	r81	1.5234	a981	117.04	d10981	63.29
	r98	1.4236	a1098	108.67	d11213	180.05
	r109	1.4103	a1121	118.84	d12321	179.52
	r112	1.0878	a1232	119.98	d13432	180.04
	r123	1.0858	a1343	120.42	d14543	179.86
	r134	1.0857	a1454	120.05	d15765	241.82
	r145	1.0837	a1576	116.62	d161098	274.87
	r157	1.0950	a16109	98.54	d17812	64.27
	r1610	1.2429	a1781	109.90	d18812	305.98
	r178	1.0971	a1881	109.14	d19765	13.19
	r188	1.0980	a1976	111.80	d201976	195.91
	r197	1.3890	a20197	107.93	d2120197	249.32
	r2019	1.4469	a212019	100.14		
	r2120	0.9727				

TS7	r21	1.3843	a321	125.86	d4321	0.58
	r32	1.3778	a432	116.56	d5432	359.22
	r43	1.4032	a543	119.88	d6543	0.21
	r54	1.3934	a654	122.01	d7654	179.45
	r65	1.4037	a765	118.84	d8123	179.81
	r76	1.5152	a812	118.21	d9213	178.01
	r81	1.5255	a921	102.22	d10321	180.33
	r92	1.5049	a1032	122.32	d11432	179.53
	r103	1.0855	a1143	119.88	d12543	180.39
	r114	1.0863	a1254	119.39	d13765	34.93
	r125	1.0868	a1376	110.19	d14765	155.65
	r137	1.0957	a1476	112.54	d15812	269.12
	r147	1.0948	a1581	110.99	d16812	145.88
	r158	1.0984	a1681	111.64	d17812	30.72
	r168	1.0919	a1781	109.51	d18921	12.54
	r178	1.4249	a1892	144.17	d19765	280.71
	r189	1.0877	a1976	113.36	d201976	288.80
	r197	1.4309	a20197	107.21	d2120197	101.93
	r2019	1.4529	a212019	100.84		
	r2120	0.9724				

TS8	r21	1.4017	a321	120.74	d4321	0.00
	r32	1.3909	a432	120.05	d5432	359.85
	r43	1.3993	a543	119.84	d6543	359.97
	r54	1.3903	a654	120.80	d7654	181.22
	r65	1.4029	a765	117.14	d8123	182.04
	r76	1.4886	a812	116.84	d9213	179.46
	r81	1.5007	a921	117.91	d10321	179.82
	r92	1.0845	a1032	119.86	d11432	179.93
	r103	1.0858	a1143	120.14	d12543	180.28
	r114	1.0857	a1254	121.37	d13765	357.22
	r125	1.0847	a1376	123.27	d14765	176.61
	r137	1.2169	a1476	116.95	d15812	168.31
	r147	1.1064	a1581	116.92	d16812	252.98
	r158	1.1065	a1681	94.82	d17812	359.91
	r168	1.8398	a1781	122.53		
	r178	1.2306				

Table D.2 Harmonic Vibrational Frequencies and Moments of Inertia

species	frequencies (cm^{-1})								moments of inertia (amu-Bohr^2)
	42.44	80.38	112.89	131.44	198.37	298.92	325.71	362.21	694.61878
	426.73	463.20	527.57	554.05	633.88	733.93	764.10	772.65	2015.78601
	859.45	883.13	924.02	952.79	977.44	994.06	1014.46	1065.32	2560.57186
	1080.04	1143.08	1192.48	1193.02	1209.28	1217.28	1253.88	1322.26	
	1353.59	1377.68	1427.95	1484.78	1497.92	1507.41	1515.89	1536.99	
	1634.90	1664.92	3040.16	3077.87	3102.38	3134.41	3136.77	3175.79	
	3180.22	3193.83	3208.29						
TS1	-1765.45	105.90	148.43	253.49	311.25	335.12	347.28	451.02	688.81149
	480.01	507.39	525.93	590.86	600.16	642.85	749.81	759.22	1725.23316
	775.76	862.93	884.14	900.80	951.39	992.10	1003.33	1014.70	2242.90001
	1023.34	1073.04	1080.29	1147.89	1190.24	1201.25	1215.41	1251.36	
	1274.17	1318.02	1348.17	1365.68	1469.52	1489.01	1495.27	1510.77	
	1530.95	1610.75	1647.17	3056.34	3097.92	3115.55	3176.43	3181.79	
	3185.30	3195.22	3209.01						
TS2	-551.11	106.16	111.41	185.18	201.44	220.19	315.07	362.97	837.83035
	413.63	463.49	485.26	548.27	651.44	663.02	744.81	782.19	1402.53256
	833.22	855.38	884.40	938.70	977.52	994.15	1005.56	1040.90	1946.39862
	1054.69	1061.55	1138.19	1175.05	1179.90	1197.95	1214.75	1310.89	
	1341.04	1368.19	1418.49	1453.01	1481.01	1492.29	1507.75	1534.27	
	1564.20	1617.50	3032.39	3039.08	3085.89	3094.12	3132.59	3180.52	
	3190.87	3203.28	3212.68						
TS3	-1107.07	89.26	134.21	154.11	230.40	237.71	345.17	382.82	860.78963
	436.38	478.45	489.73	496.67	558.22	660.84	683.71	761.88	1578.74509
	788.67	824.00	894.79	913.08	966.81	974.82	1010.84	1041.00	2380.69828
	1066.15	1082.04	1097.67	1183.86	1196.74	1242.85	1266.96	1279.34	
	1323.73	1371.18	1427.40	1447.58	1477.25	1498.93	1500.29	1507.13	
	1580.10	1649.12	1670.03	3023.04	3037.10	3090.66	3110.00	3128.95	
	3177.77	3192.85	3206.61						
TS4	-1755.52	77.79	94.76	157.39	174.13	212.57	262.84	320.87	800.66118
	446.47	455.91	507.80	527.09	600.72	646.66	721.38	769.93	1849.88356
	794.75	854.34	859.32	885.95	925.96	968.25	998.42	1010.26	2523.69901
	1061.70	1072.53	1085.90	1143.23	1180.87	1189.82	1213.94	1250.62	
	1312.73	1340.82	1386.69	1428.57	1481.60	1499.68	1513.47	1521.33	
	1617.31	1646.95	1968.82	3037.24	3089.75	3092.63	3131.64	3179.25	
	3192.82	3206.38	3225.72						
TS5	-733.12	45.16	121.02	141.13	153.67	223.54	243.43	322.49	580.08551
	400.61	424.98	478.58	500.38	521.05	565.38	631.72	718.62	2095.79765
	757.74	788.73	823.77	867.07	881.17	940.67	986.79	1005.60	2599.48124
	1016.41	1037.71	1063.61	1115.21	1135.06	1187.62	1213.18	1220.30	
	1265.80	1300.00	1337.13	1373.93	1477.36	1494.53	1519.28	1526.46	
	1626.00	1652.12	2995.77	3087.09	3151.17	3176.72	3183.30	3194.84	
	3206.99	3244.36	3787.19						
TS6	-1656.85	57.77	71.58	114.12	165.80	170.29	223.64	258.47	1503.01847
	301.03	313.13	386.10	414.59	451.72	479.62	510.34	605.84	2249.12767

	633.51	652.00	715.29	764.67	794.59	861.53	882.36	931.39	3600.90293
	633.51	652.00	715.29	764.67	794.59	861.53	882.36	931.39	
	945.17	953.63	990.44	996.84	1028.64	1058.64	1084.54	1107.81	
	1166.86	1194.17	1206.26	1222.60	1246.79	1294.27	1305.25	1324.47	
	1353.30	1391.07	1394.24	1469.05	1485.36	1528.39	1620.71	1649.16	
	1654.10	3028.27	3077.89	3086.94	3167.40	3189.71	3205.22	3225.24	
	3743.66								
TS7	-1043.73	53.42	78.46	109.43	140.42	191.29	233.66	279.21	1574.83997
	295.49	357.93	384.60	442.88	455.20	477.03	493.69	528.66	2184.96227
	605.79	660.72	732.12	776.30	794.49	829.83	879.21	909.13	3422.65907
	913.86	970.82	973.68	989.00	1027.10	1051.04	1083.64	1098.96	
	1185.84	1199.13	1244.65	1254.81	1277.83	1290.10	1338.52	1365.09	
	1373.19	1383.66	1450.45	1478.90	1491.36	1497.28	1579.62	1645.93	
	1689.31	3029.81	3056.51	3106.47	3139.60	3179.69	3193.19	3205.97	
	3741.97								
TS8	-820.88	92.74	100.67	125.09	210.80	233.87	258.09	352.33	1073.20552
	411.23	434.22	456.43	469.63	504.38	629.10	700.07	728.31	1404.42516
	785.82	823.73	840.24	917.45	989.87	1013.08	1018.52	1023.44	2455.33346
	1066.69	1104.73	1186.09	1207.76	1221.26	1294.11	1360.82	1406.12	
	1455.58	1486.98	1518.63	1619.23	1641.13	1681.43	1788.59	2937.62	
	2973.58	3190.20	3204.36	3219.49	3222.16				

Table D.3 Calculated $\Delta H_f{}^\circ{}_{298}$ from Isodesmic Reaction Analysis [a]

reaction	B3LYP/6-31G(d,p)		B3LYP/6311+G(3df,2p)	
	ΔH_{rxn}	$\Delta H_{f,298}$	ΔH_{rxn}	$\Delta H_{f,298}$
(·CH_2)(CH_2OOH)benzene + $CH_2=CHCH_3$ → (·CH_2)(CH_3)benzene + $CH_2=CHCH_2OOH$	-0.12	23.21	-0.63	23.72
(·CH_2)(CH_2OOH)benzene + CH_3CH_3 → (·CH_2)(CH_3)benzene + CH_3CH_2OOH	-2.09	23.89	-2.75	24.55
(CH_3)($CH_2OO·$)benzene + $CH_2=CHCH_2OOH$ → (CH_3)(CH_2OOH)benzene + $CH_2=CHCH_2OO·$	-0.43	20.50	0.36	19.71
(CH_3)($CH_2OO·$)benzene + $CH_2=C(CH_3)CH_2OOH$ → (CH_3)(CH_2OOH)benzene + $CH_2=C(CH_3)CH_2OO·$	0.55	20.60	1.20	19.95
($CH_2OO·$)(CH_2OOH)benzene + $CH_2=CHCH_2OOH$ → (CH_2OOH)(CH_2OOH)benzene + $CH_2=CHCH_2OO·$	-3.08	5.97	-3.34	6.23
($CH_2OO·$)(CH_2OOH)benzene + $CH_2=C(CH_3)CH_2OOH$ → (CH_2OOH)(CH_2OOH)benzene + $CH_2=C(CH_3)CH_2OO·$	-2.10	4.99	-2.50	5.39
(CH_2OOH)(CHO)benzene + $CH_2=CHCH_3$ → (CH_2OOH)(CHO)benzene + $CH_2=CHCH_2OOH$	-1.91	-34.70	-2.05	-34.56
(CH_2OOH)(CHO)benzene + CH_3CH_3 → (CH_2OOH)(CHO)benzene + CH_3CH_2OOH	-3.87	-34.03	-4.17	-33.73
(O=CH)(CHO)benzene + CH_3CH_3 → (CH_3)(CHO)benzene + CH_3CHO	0.37	-39.17	-1.66	-37.14
($CH_2O·$)(CHO)benzene + $CH_2=CHCH_2OOH$ → (CH_2OH)(CHO)benzene + $CH_2=CHCH_2OO·$	-18.94	-3.76	-19.04	3.86
(CH_2OH)(CHO)benzene + CH_4 → (CH_3)(CHO)benzene + CH_3OH	2.88	-51.30	1.27	-49.69
(CH_3)(CHO)benzene + CH_3CH_3 → (CH_3)(CH_3)benzene + CH_3CHO	3.99	-19.99	2.24	-18.24

[a] Units: kcal/mol

REFERENCES

1. Hehre, W.; Radom, L.; Schleyer, P. R.; Pople, J. A. *Ab Initio Molecular Orbital Theory*; John Wiley & Sons: New York, 1986.

2. Foresman, J. B.; Frisch, A. *Exploring Chemistry with Electronic Structure Methods*, 2nd ed.; Gaussian, Inc.: Pittsburgh, PA, 1996.

3. Levine, l. N. *Quantum Chemistry*, 5th ed.; Prentice Hall: Upper Saddle River, NJ 07485, 2000.

4. Becke, A. D. *Physical Review A: Atomic, Molecular, and Optical Physics* **1988**, *38*, 3098.

5. Pople, J. A.; Head-Gordon, M.; Raghavachari, K. *J. Chem. Phys.* **1987**, *87*, 5968.

6. Ochterski, J. W.; Petersson, G. A.; Montgomery, J. A. *J. Chem. Phys.* **1996**, *104*, 2598.

7. Hehre, W. J. *A Guide to Molecular Mechanics and Quantum Chemical Calculations*; Wavefunction, Inc.: Irvine, CA 92612, 2003.

8. Lindemann, F. A. *Trans. Faraday Soc.* **1922**, *17*, 598.

9. Hinshelwood, C. N. *Proc. Roy. Soc. A* **1927**, *114*, 84.

10. Rice, O. K.; Ramsperger, H. C. *J. Am. Chem. Soc.* **1927**, *49*, 1617.

11. Kassel, L. S. *J. Phys. Chem.* **1928**, 225.

12. Steinfeld, J. I.; Francisco, J. S.; Hase, W. L. *Chemical Kinetics and Dynamics*; Prentice-Hall, Inc.: Englewood Cliffs, New Jersey 07632, 1989.

13. Marcus, R. A. *J. Chem. Phys.* **1952**, *20*, 359.

14. Marcus, R. A. *J. Chem. Phys.* **1965**, *43*, 2658.

15. Marcus, R. A. **1970**, *52*, 1018.

16. Robinson, P. J.; Holbrook, K. A. *Unimolecular Reactions*; Wiley-Interscience, 1971.

17. Chang, A. Y.; Bozzelli, J. W.; Dean, A. M. *Zeitschrift fuer Physikalische Chemie (Muenchen)* **2000**, *214*, 1533.

18. Dean, A. M.; Bozzelli, J. W.; Ritter, E. R. *Combustion Science and Technology* **1991**, *80*, 63.

19. Dean, A. M. *J. Phys. Chem.* **1985**, *89*, 4600.

20. Gilbert, R. G.; Smith, S. C. *Theory of Unimolecular and Recombination Reactions.*; Blackwell Scientific Publ., Oxford, UK, 1990.

21. Gilbert, R. G.; Smith, S. C.; M. J. T. Jordan. UNIMOL Program Suite (Calculation of Fall-off Curve for Unimolecular and Recombination Reactions); Sidney, 1993.

22. Ritter, E. R. *Journal of Chemical Information and Computer Sciences* **1991**, *31*, 400.

23. Bozzelli, J. W.; Chang, A. Y.; Dean, A. M. *International Journal of Chemical Kinetics* **1997**, *29*, 161.

24. Hirschfelder, J. O.; Curtiss, C. F.; Bird, R. B. *Molecular Theory of Gases and Liquids*; Wiley, London, 1963.

25. Reid, R. C.; Prausnitz, J. M.; Polling, B. E. *Properties of Gases and Liquids*; McGraw-Hill, New York, 1989.

26. Sheng, C. Y.; Bozzelli, J. W.; Dean, A. M.; Chang, A. Y. *Journal of Physical Chemistry A* **2002**, *106*, 7276.

27. Heymann, M.; Hippler, H.; Troe, J. *Journal of Chemical Physics* **1984**, *80*, 1853.

28. Hahn, D. K.; Klippenstein, S. J.; Miller, J. A. *Faraday Discussions Combustion Chemistry: Elementary Reactions to Macroscopic Processes* **2001**, *119*, 79.

29. Knyazev, V. D.; Slagle, I. R. *Journal of Physical Chemistry* **1996**, *100*, 5318.

30. Atkinson, R.; Baulch, D. L.; Cox, R. A.; R. F. Hampson, J.; Kerr, J. A.; Troe, J. *J. Chem. Ref. Data* **1989**, *18*, 881.

31. Frisch, M. J.; Trucks, G. W.; Schlegel, H. B.; Gill, P. M. W.; Johnson, B. G.; Robb, M. A.; Cheeseman, J. R.; Keith, T.; Petersson, G. A.; Montgomery, J. A.; Raghavachari, K.; Al-Laham, M. A.; Zakrzewski, V. G.; Ortiz, J. V.; Foresman, J. B.; Cioslowski, J.; Stefanov, B. B.; Nanayakkara, A.; Challacombe, M.; Peng, C. Y.; Ayala, P. Y.; Chen, W.; Wong, M. W.; Andres, J. L.; Replogle, E. S.; Gomperts, R.; Martin, R. L.; Fox, D. J.; Binkley, J. S.; Defrees, D. J.; Baker, J.; Stewart, J. P.; Head-Gordon, M.;

Gonzalez, C.; Pople, J. A. *Gaussian 94*; Revision D.4 ed.; Gaussian, Inc.: Pittsburgh, 1995.

32.   Frisch, M. J.; Trucks, G. W.; Schlegel, H. B.; Scuseria, G. E.; Robb, M. A.; Cheeseman, J. R.; Zakrzewski, V. G.; J. A. Montgomery, J.; Stratmann, R. E.; Burant, J. C.; Dapprich, S.; Millam, J. M.; Danies, A. D.; Kudin, K. N.; Strain, M. C.; Farkas, O.; Tomasi, J.; Barone, V.; Cossi, M.; Cammi, R.; Mennucci, B.; Pomelli, C.; Adamo, C.; Clifford, S.; Ochterski, J.; Petersson, G. A.; Ayala, P. Y.; Cui, Q.; Morokuma, K.; Malick, D. K.; A. D. Rabuck; Raghavachari, K.; Foresman, J. B.; Cioslowski, J.; Ortiz, J. V.; Baboul, A. G.; Stefanov, B. B.; G. Liu, A. L.; Piskorz, P.; Komaromi, I.; Gomperts, R.; Martin, R. L.; Fox, D. J.; Keith, T.; M. A. Al-Laham; Peng, C. Y.; Nanayakkara, A.; Challacombe, M.; Gill, P. M. W.; Johnson, B.; Chen, W.; Wong, M. W.; Andres, J. L.; Gonzalez, C.; Head-Gordon, M.; Replogle, E. S.; Pople, J. A. Gaussian 98; Revision A.9 ed.; Gaussian, Inc.: Pittsburgh, 1998.

33.   Curtiss, L. A.; Raghavachari, K.; Redfern, P. C.; Pople, J. A. *J. Chem. Phys.* **1997**, *106*, 1063.

34.   Durant, J. L.; Rohlfing, C. M. *J. Chem. Phys.* **1993**, *98*, 8031.

35.   Durant, J. L. *Chem. Phys. Lett.* **1996**, *256*, 595.

36.   Petersson, G. A.; Malick, D. K.; Wilson, W. G. *J. Chem. Phys.* **1998**, *109*, 10570.

37.   Andino, J. M.; Smith, J. N.; Flagan, R. C.; Goddard, W. A.; Seinfield, J. H. *J. Phys. Chem.* **1996**, *100*, 10967.

38.   Wong, M. W.; Radom, L. *J. Phys. Chem. A* **1998**, *102*, 2237.

39.   Cioslowski, J.; Liu, G.; Moncrieff, D. *J. Phys. Chem. A* **1998**, *102*, 9965.

40.   Montgomery, J. A.; Ochterski, J. W.; Petersson, G. A. *J. Chem. Phys.* **1994**, *101*, 5900.

41.   Petersson, G. A.; Al-Laham, M. A. *J. Chem. Phys.* **1991**, *94*, 6081.

42.   Scott, A. P.; Radom, L. *J. Phys. Chem.* **1996**, *100*, 16502.

43.   Lay, T. H.; Krasnoperov, L. N.; Venanzi, C. A.; Bozzelli, J. W.; Shokhirev, N. V. *J. Phys. Chem.* **1996**, *100*, 8240

44.   Schneider, W. F.; Nance, B. I.; Wallington, T. J. *J. Am. Chem. Soc.* **1995**, *117*, 478

45.   Omoto, K.; Marusaki, K.; Hirao, H.; Imade, M.; Fujimoto, H. *J. Phys. Chem. A* **2000**, *104*, 6499

46.   Sun, H.; Bozzelli, J. W. *J. Phys. Chem. A* **2001**, *105*, 4504.

47.   Pauling, L. *The Nature of the Chemical Bond*; Cornell University Press: USA, 1947.

48.   Henry, D. J.; Parkinson, C. J.; Mayer, P. M.; Radom, L. *J. Phys. Chem. A* **2001**, *105*, 6750.

49.   Chase, M. W., Jr. *J. Phys. Chem. Ref. Data* **1998**, *Monograph 9*.

50.   Frenkel, M.; Kabo, G. J.; Marsh, K. N. *Thermodynamics of Organic Compounds in the Gas State*; Thermodynamic Research Center, Texas A&M university: College Station,TX., 1994.

51.   Stull, D. R.; Prophet, H. *JANAF Thermochemical Tables*, 2nd ed.; U.S. Government Printing Office: Washington D.C., 1970.

52.   Stull, D. R.; Westrum, E. F.; Sinke, G. C. *The Chemical Thermodynamic of Organic Compounds*; Robert E. Kireger Publishing Company: Malabar, FL, 1987.

53.   Holmes, J. L.; Lossing, F. P. *J. Am. Chem. Soc.* **1988**, *110*, 7343.

54.   Mayer, P. M.; Glukhovtsev, b. M. N.; Gauld, c. J. W.; Radom, L. *J. Am. Chem. Soc.* **1997**, *119*, 12889.

55.   Tsang, W.; Martinho Simoes, J. A.; Greenberg, A.; Liebman, J. F., Eds *Heats of Formation of Organic Free Radicals by Kinetic Methods in Energetics of Organic Free Radicals*; Blackie Academic and Professional: London, 1996.

56.   Pedley, J. B.; Naylor, R. D.; Kirby, S. P. *Thermochemical Data of Organic Compounds*, 2nd ed; Chapman and Hall: London: New York, 1986.

57.   Cioslowski, J.; Liu, G.; Moncrieff, D. *J. Am. Chem. Soc.* **1997**, *119*, 11452.

58.   Shevtsova, L. A.; Rozhnov, A. M.; Andreevskii, D. N. *Russ. J. Phys. Chem.* (Engl. Transl.) **1970**, *44*, 852.

59.   Sun, H.; Bozzelli, J. W. *J. Phys. Chem. A* **2001**, *105*, 9543.

60.   Cox, J. D.; Pilcher, G. *Thermochemistry of Organic & Organometallic Compounds*; Academic Press: London, New York, 1970.

61.   Sekuak, S.; Liedl, K. R.; Sablji, A. *J. Phys. Chem. A* **1998**, *102*, 1583.

62.   Shi, J.; Wallington, T. J.; Kaiser, E. W. *J. Phys. Chem.* **1993**, *97*, 6184.

63.   Hou, H.; Wang, B.; Gu, Y. *J. Phys. Chem. A* **2000**, *104*, 1570.

64.   Benson, S. W. *Thermochemical Kinetics*, 2nd ed.; Wiley Inter-science: New York, 1976.

65.   Cohen, N. *J. Phys. Chem. Ref. Data* **1996**, *25*, 1411.

66.   Lay, T. H.; Bozzelli, J. W.; Dean, A. M.; Ritter, E. R. *J. Phys. Chem.* **1995**, *99*, 14514.

67.   Barckholtz, T. A.; Miller, T. A. *Int. Rev. Phys. Chem.* **1998**, *17*, 435.

68.   Ramond, T. M.; Davico, G. E.; Schwartz, R. L.; Lineberger, W. C. *J. Chem. Phys.* **2000**, *112*, 1158.

69.   Atkinson, R. B., D. L.; Cox, R. A.; Hampson, R. F., Jr.; Kerr, J. A.; Rossi, M. J.; Troe, J. *J. Phys. Chem. Ref. Data* **1997**, *26*, 1329.

70.   Snelson, A.; Skinner, H. A. *Trans. Faraday Soc.* **1961**, *57*, 2125.

71.   Cohen, N. *J. Phys. Chem. Ref. Data* **1995**, *25*, 141.

72.   Sheng, C. Representative Hydrocarbon Oxidation Model and Detailed Mechanism for Combustion of a Complex Solid Fuel in a Pilot Scale Incinerator. Ph.D. Dissertation, New Jersey Institute of Technology, 2002.

73.   Shokhirev, N. V.; Krasnoperov, L. N. ROTATOR; http://www.chem.arizona.edu/faculty/walk/nikolai/programs, 1999.

74.   Wu, F.; Carr, R. W. *J. Phys. Chem. A* **2001**, *105*, 1423.

75.   Wu, F.; Carr, R. W. *Chem. Phys. Lett.* **1999**, *305*, 44.

76.   Khachkuruzov, G. A.; Przheval'skii, I. N. *Opt. Spektrosk.* **1974**, *36*, 299.

77.   Sun, H.; Chen, C.-J.; Bozzelli, J. W. *J. Phys. Chem. A* **2000**, *104*, 8270.

78.   Seetula, J. A. *Phys. Chem. Chem. Phys.* **2000**, *2*, 3807.

79.   Manion, J. A. *Journal of Physical and Chemical Reference Data* **2002**, *31*, 123.

80.   Chen, C.-J.; Wong, D.; Bozzelli, J. W. *J. Phys. Chem. A* **1998**, *102*, 4551.

81.   Wallington, T. J.; Schneider, W. F.; Barnes, I.; Becker, K. H.; Sehested, J.; Nielsen, O. J. *Chem. Phys. Lett.* **2000**, *322*, 97

82.   Wang, S.-K.; Zhang, Q.-Z.; Hou, H.; Wang, B.; Liu, F.-X.; Gu, Y.-S. *Chinese Journal of Chemistry* **2001**, *19*, 729.

83.   Schnell, M.; Muhlhauser, M.; Peyerimhoff, S. D. *Chemical Physics Letters* **2001**, *344*, 519.

84.   Stewart, J. J. P. MOPAC 6.0; Frank J. Seiler Research Lab, U.S. Air Force Academy: Colorado, 1990.

85.   Wardlaw, D. M.; Marcus, R. A. *Chemical Physics Letters* **1984**, *110*, 230.

86.   Wardlaw, D. M.; Marcus, R. A. *Journal of Chemical Physics* **1985**, *83*, 3462.

87.   Klippenstein, S. J.; Marcus, R. A. *Journal of Chemical Physics* **1987**, *87*, 3410.

88.   Klippenstein, S. J.; Wagner, A. F.; Dunbar, R. C.; Wardlaw, D. M.; Robertson, S. H. VARIFLEX; VERSION 1.00 ed.; Argonne National Laboratory: Argonne, IL 60439, 1999.

89.   Varshni, Y. P. *Reviews of Modern Physics* **1957**, *29*, 664.

90.   Ben-Amotz, D.; Herschbach, D. R. *Journal of Physical Chemistry* **1990**, *94*, 1038.

91.   Humpfer, R.; Oser, H.; Grotheer, H.-H.; Just, T. *Proc. Combust. Inst.*, **1994**, 721.

92.   Baulch, D. L.; Cobos, C. J.; Cox, R. A.; Frank, P.; Hayman, G.; Just, T.; Kerr, J. A.; Murrells, T.; Pilling, M. J. *Combustion and Flame* **1994**, *98*, 59.

93.   Fagerstroem, K.; Lund, A.; Mahmoud, G.; Jodkowski, J. T.; Ratajczak, E. *Chemical Physics Letters* **1993**, *208*, 321.

94.   Jungkamp, T. P. W.; Kukui, A.; Schindler, R. N. *Berichte der Bunsen-Gesellschaft* **1995**, *99*, 1057.

95.   Daele, V. L., Gerard; Poulet, Gilles. *International Journal of Chemical Kinetics* **1996**, *28*, 589.

96.   Lim, K. P.; Michael, J. V. *Symp. Int. Combust. Proc.* **1994**, *25*, 809.

97.   Dobe, S.; Berces, T.; Temps, F.; Wagner, H. G.; Ziemer, H. *J. Phys. Chem.* **1994**, *98*, 9792.

98.	Bozzelli, J. W.; Dean, A. M. *Journal of Physical Chemistry* **1990**, *94*, 3313.

99.	Bozzelli, J. W.; Pitz, W. J. *Symp. Int. Combust. Proc.* **1994**, 25, 783.

100.	Norton, T. S.; Dryer, F. L. *International Journal of Chemical Kinetics* **1992**, *24*, 319.

101.	Warnatz, J. *Proc. Combust. Inst.*, **1985**, *20*, 845.

102.	Chen, C.-J.; Bozzelli, J. W. *J. Phys. Chem. A* **1999**, *103*, 9731.

103.	DeSain, J. D.; Klippenstein, S. J.; Taatjes, C. A. *Physical Chemistry Chemical Physics* **2003**, *5*, 1584.

104.	Hughes, K. J.; Lightfoot, P. D.; Pilling, M. J. *Chemical Physics Letters* **1992**, *191*, 581.

105.	Hughes, K. J.; Halford-Maw, P. A.; Lightfood, P. D.; Turanyi, T.; Pilling, M. J. *Symp. Int. Combust. Proc.* **1992**, 24, 645.

106.	Baldwin, R. R.; Hisham, M. W. M.; Walker, R. W. *J. Chem. Soc. Faraday Trans.* **1982**, *78*, 1615.

107.	Wu, D. B., Kyle D. *International Journal of Chemical Kinetics* **1986**, *18*, 547.

108.	Xi, Z.; Han, W. J.; Bayes, K. D. *Journal of Physical Chemistry* **1988**, *92*, 3450.

109.	Baker, R. R.; Baldwin, R. R.; Everett, C. J.; Walker, R. W. *Combust. Flame* **1975**, *25*, 285.

110.	Baker, R. R.; Baldwin, R. R.; Walker, R. W. *Combust. Flame* **1976**, *27*, 147.

111.	Dagaut, P.; Cathonnet, M. *Combustion and Flame* **1999**, *118*, 191.

112.	Tsuzuki, S.; Uchimaru, T.; Tanabe, K.; Hirano, T. *J. Phys. Chem.* **1993**, *97*, 1346.

113.	Wang, S. M., David L.; Cernansky, Nicholas P.; Curran, Henry J.; Pitz, William J.; Westbrook, Charles K. *Combustion and Flame* **1999**, *118*, 415.

114.	Curran, H. J.; Pitz, W. J.; Westbrook, C. K.; Hisham, M. W. M.; Walker, R. W. *Symp. Int. Combust. Proc.* **1996**, 26,641.

115.	Ritter, E. R.; Bozzelli, J. W. *International Journal of Chemical Kinetics* **1991**, *23*, 767.

116. Westmoreland, P. R. *Combustion Science and Technology* **1992**, *82*, 151.

117. Dean, A. M.; Westmoreland, P. R. *International Journal of Chemical Kinetics* **1987**, *19*, 207.

118. Bozzelli, J. W.; Dean, A. M. *Journal of Physical Chemistry* **1993**, *97*, 4427.

119. McGrath, M. P.; Radom, L. *Journal of Chemical Physics* **1991**, *94*, 511.

120. Glukhovtsev, M. N.; Pross, A.; McGrath, M. P.; Radom, L. *Journal of Chemical Physics* **1995**, *103*, 1878.

121. GaussView; 2.1 ed.; Gaussian, Inc.: Pittsburgh, 1998.

122. Gilbert, R. G.; Luther, K.; Troe, J. *Ber. Bunsenges. Phys. Chem.* **1983**, *87*, 169.

123. Good, W. D. *J. Chem. Thermodynamics* **1970**, *2*, 237.

124. Sumathi, R.; Carstensen, H.-H.; Green, W. H., Jr. *Journal of Physical Chemistry A* **2001**, *105*, 6910.

125. Holmes, J. L.; Lossing, F. P.; Maccoll, A. *Journal of the American Chemical Society* **1988**, *110*, 7339.

126. Knyazev, V. D.; Slagle, I. R. *J. Phys. Chem.* **1998**, *102*, 1770.

127. Clifford, E. P.; Wenthold, P. G.; Gareyev, R.; Lingberger, W. C.; Depuy, C. H.; Bierbaum, V. M.; Ellison, G. B. *J. Chem. Phys* **1998**, *109*, 10293.

128. Chen, C.-J.; Bozzelli, J. W. *J. Phys. Chem. A* **2000**, *104*, 4997.

129. Ervin, K. M. G., Scott; Barlow, S. E.; Gilles, Mary K.; Harrison, Alex G.; Bierbaum, Veronica M.; DePuy, Charles H.; Lineberger, W. C.; Ellison, G. Barney. *J. Am. Chem. Soc.* **1990**, *112*, 5750.

130. Blanksby, S. J.; Ramond, T. M.; Davico, G. E.; Nimlos, M. R.; Kato, S.; Bierbaum, V. M.; Lineberger, W. C.; Ellison, G. B.; Okumura, M. *J. Am. Chem. Soc.* **2001**, *123*, 9585

131. Holmes, J. L.; Lossing, F. P.; Mayer, P. M. *J. Am. Chem. Soc.* **1991**, *113*, 9723.

132. Curtiss, L. A.; Lucas, D. J.; Pople, J. A. *J. Chem. Phys.* **1995**, *102*, 3292.

133. Ruscic, B.; Berkowitz, J. *J. Phys. Chem.* **1993**, *97*, 11451.

134. Dobe, S. B., T. ; Turanyi, T. M., F. ; Grussdorf, J.; Temps, F.; Wagner, H. G. *J. Phys. Chem.* **1996**, *100*, 19864.

135. Sun, H.; Bozzelli, J. W. *J. Phys. Chem. A* **2003**, *107*, 1018.

136. Furuyama, S.; Golden, D. M.; Benson, S. W. *Int. J. Chem. Kinet.* **1969**, *1*, 283.

137. Bedjanian, Y.; Bras, G. L.; Poulet, G. *J. Phys. Chem.* **1997**, *101*, 4088.

138. Chen, C.-J.; Bozzelli, J. W. *J. Phys. Chem. A* **2000**, *104*, 9715.

139. Slagle, I. R.; Batt, L.; Gmurczyk, G. W.; Gutman, D.; Tsang, W. *Journal of Physical Chemistry* **1991**, *95*, 7732.

140. Chemkin II; version 3.1 ed.; Sandia National Labs, Combustion Research Facility: Livermore,CA, 1990.

141. Dean, A. M.; Bozzelli, J. W. *In Gas-Phase Combustion Chemistry II, Chapter 2: Combustion Chemistry of Nitrogen*; Springer-Verlag: New York, 1999.

142. Sun, H.; Bozzelli, J. W. *Submitted to J. Phys. Chem.* **2003**.

143. Marshall, P. *J. Phys. Chem. A* **1999**, *103*, 4560.

144. Chen, C.-J.; Bozzelli, J. W. *Unpublished Data.*

145. Sun, H.; Bozzelli, J. W. *Journal of Physical Chemistry A* **2002**, *106*, 3947.

146. Wiberg, K. B.; Hao, S. *J. Org. Chem* **1991**, *56*, 5108.

147. Ringner, B.; Sunner, S.; Watanabe, H. *Acta Chem. Scand.* **1971**, *25*, 141.

148. Chemkin III; version 3.6.2 ed.; Reaction Design, Inc: San Diego, CA, 92121, 2001.

149. Hsu, C.-C.; Mebel, A. M.; Lin, M. C. *Journal of Chemical Physics* **1996**, *105*, 2346.

150. Leone, J. A.; Flagan, R. C.; Grosjean, D.; Seinfeld, J. H. *International Journal of Chemical Kinetics* **1985**, *17*, 177.

151. Atkinson, R. C., William P. L.; Darnall, Karen R.; Winer, Arthur M.; Pitts, James N., Jr. *International Journal of Chemical Kinetics* **1980**, *12*, 779.

152. Atkinson, R. L., Alan C. *Journal of Physical and Chemical Reference Data* **1984**, *13*, 315.

153. Emdee, J. L. B., K.; Glassman, I. *Symp. Int. Combust. Proc.* **1990**, *23*, 77.

154. Kang, J. K.; Musgrave, C. B. *Journal of Chemical Physics* **2001**, *115*, 11040.

155. Becke, A. D. *Journal of Chemical Physics* **1993**, *98*, 5648.

156. Curtiss, L. A.; Raghavachari, K.; Trucks, G. W.; Pople, J. A. *Journal of Chemical Physics* **1991**, *94*, 7221.